

UNIVERSIDAD DE BARCELONA

Facultad de Biología

Departamento de Nutrición y Bromatología

**CATABOLISMO DE LA GLUCOSA Y LOS
AMINOÁCIDOS EN EL ÓRGANO ADIPOSO DE LA
RATA**

SOFÍA ARRIARÁN GERMÁN-PALACIOS

Barcelona, Noviembre de 2015

UNIVERSIDAD DE BARCELONA
FACULTAD DE BIOLOGÍA
DEPARTAMENTO DE NUTRICIÓN Y BROMATOLOGÍA
PROGRAMA DE DOCTORADO DE NUTRICIÓN Y METABOLISMO

CATABOLISMO DE LA GLUCOSA Y LOS AMINOÁCIDOS EN EL ÓRGANO ADIPOSO DE LA RATA

Memoria presentada por Sofía Arriarán Germán-Palacios para optar por el título de doctor por la Universidad de Barcelona

Los codirectores

Dr. Marià Alemany Lamana

Dr. Jose Antonio Fernández López

Catedrático de Nutrición y Bromatología

Profesor Titular de Nutrición y Bromatología

Índice

Resumen	7
Abstract	8
1. Introducción	13
1.1. La obesidad en el contexto del síndrome metabólico	13
1.1.1. Causas de la obesidad	16
1.1.2. El concepto de ponderostato: la obesidad como alteración del mecanismo del control del peso corporal	18
1.2. El tejido adiposo	20
1.2.1. Estructura del tejido adiposo	20
1.2.2. Funciones del tejido adiposo	22
1.2.3. Alteraciones del tejido adiposo en la obesidad	24
1.3. Metabolismo del tejido adiposo blanco	27
1.3.1. Metabolismo del tejido adiposo en el ayuno	29
1.3.2. Metabolismo del tejido adiposo en el estado postprandial	36
2. Justificación y objetivos	43
3. Resultados	49
3.1. Producción basal de lactato en el tejido adiposo	49
* <i>Cultured 3T3L1 adipocytes dispose of excess medium glucose as lactate under abundant oxygen availability</i>	51
* <i>Evidence of basal lactate production in the main white adipose tissue sites of rats. Effects of sex and a cafeteria diet</i>	73
3.2. Adaptación y desarrollo de métodos para la valoración de la actividad de las enzimas del ciclo de la urea en tejido adiposo blanco	92
* <i>A radiochemical method for carbamoyl-phosphate synthetase-I: Application to rats fed a hyperproteic diet</i>	95
* <i>Notas sobre el desarrollo de metodología adaptada para la valoración en el tejido adiposo blanco de la actividad de las enzimas del ciclo de la urea</i>	101
3.3. Estudio del metabolismo de los aminoácidos en el tejido adiposo blanco	117
* <i>The urea cycle of rat white adipose tissue</i>	119
* <i>Effects of sex and site on amino acid metabolism enzyme gene expression and activity in rat white adipose tissue</i>	131
* <i>Overall white adipose tissue urea cycle activity remains unchanged in female rats after one-month treatment with a hyperlipidic diet.</i>	161
4. Discusión general	195
4.1. Producción basal de lactato en el tejido adiposo blanco	195
4.2. Estudio del metabolismo de los aminoácidos en el tejido adiposo blanco	199
5. Conclusiones	207
6. Bibliografía citada	211

Catabolismo de la glucosa y los aminoácidos en el órgano adiposo de la rata

Departamento de Nutrición y Bromatología, Facultad de Biología, Universidad de Barcelona

Sofía Arriarán Germán-Palacios

Resumen

En los últimos años, la trascendencia fisiológica del tejido adiposo blanco ha crecido considerablemente, en especial desde que se conocieron sus funciones endocrinas. Sin embargo, y a pesar de estos grandes avances, nuestro conocimiento en lo que respecta al metabolismo del nitrógeno y los aspectos cuantitativos de su función glucolítica, incluyendo la producción de lactato y glicerol, sigue siendo muy limitado. Esta tesis doctoral se ha centrado en el metabolismo energético del tejido adiposo blanco, estudiando, en especial, aspectos bioquímicos básicos del metabolismo de los aminoácidos y de la modulación de la utilización de la glucosa, con la producción de lactato como alternativa a la lipogénesis. Para ello, iniciamos un estudio *in vitro* con adipocitos 3T3L1 y, posteriormente, analizamos y comparamos las principales vías metabólicas de partición de energía en las cuatro localizaciones de mayor tamaño de tejido adiposo blanco (subcutáneo, retroperitoneal, mesentérico y perigonadal) de ratas Wistar adultas, tanto machos como hembras con normopeso, comparándolas con una situación de obesidad en fase de desarrollo inducida por la dieta.

Los resultados obtenidos nos indican que el tejido adiposo blanco participa directamente en el mantenimiento de la glucemia al metabolizar la glucosa a lactato en grandes cantidades mediante la vía glucolítica. Este hallazgo contradice la idea generalizada de utilización de la glucosa sólo para promover la lipogénesis. La producción de lactato se mantiene en condiciones de normoxia y es proporcional a la disponibilidad de glucosa. Por tanto, hemos establecido que en condiciones normales pero con exceso de glucosa disponible, el tejido adiposo blanco, específicamente sus adipocitos, es esencialmente anaerobio, con independencia de la disponibilidad de oxígeno.

Por otro lado, pudimos comprobar, por primera vez, que el tejido adiposo blanco cuenta con un ciclo de la urea completo, activo y funcional. Es probable que este ciclo funcione según demanda, aunque creemos que su principal objetivo podría ser el de controlar la disponibilidad de arginina. La uniformidad del comportamiento del ciclo, en buena medida independiente de la localización estudiada, del sexo o de la dieta, sugiere que las diferentes masas del tejido adiposo blanco funcionan de manera coordinada, como un único órgano disperso. En paralelo al funcionamiento del ciclo de la urea, hemos comprobado que el tejido adiposo blanco está muy implicado en el metabolismo de los aminoácidos. En este caso, sin embargo, se observan importantes diferencias, en especial en lo que respecta a la producción y destoxicificación de amonio, que están relacionadas con la dieta, y especialmente por el sexo.

En conclusión, podemos afirmar que el potencial metabólico y de control del tejido adiposo blanco sobre el metabolismo energético global (y, en especial en cuanto al metabolismo de los aminoácidos) es más importante de lo que habitualmente se supone. En este sentido cuando consideramos toda la masa del órgano adiposo sólo sería comparable con el hígado.

Amino acid and glucose catabolism in the rat adipose organ

Departamento de Nutrición y Bromatología, Facultad de Biología, Universidad de Barcelona

Sofía Arriarán Germán-Palacios

Abstract

In recent years, the physiological significance of white adipose tissue has increasingly grown, especially since its endocrine functions were uncovered. However, in spite of the impressive advances achieved, our knowledge of the tissue's nitrogen metabolism, and quantitative aspects of its glycolytic function, including the production of lactate and glycerol, is yet painstakingly limited. This thesis has been focused on the energy metabolism of white adipose tissue, mainly analysing so far ill-known basic biochemical aspects of amino acid metabolism and its modulation of glucose utilization for lactate production as an alternative to lipogenesis. To carry out this study, we started with an *in vitro* study using 3T3L1 adipocytes to analyse and compare the main metabolic pathways of energy partition. Later we studied them in the four larger locations of white adipose tissue (subcutaneous, retroperitoneal, mesenteric and perigonadal) of adult Wistar rats, both males and females, with normal weight, comparing this basal situation condition with animals in which diet-induced obesity was developing.

The results obtained hint that white adipose tissue is directly involved in the maintenance of blood glucose, through its massive conversion of glucose to lactate through the glycolytic pathway. This finding contradicts the widespread idea of the use of glucose only to promote lipogenesis. Lactate production was proportional to glucose availability and maintained under normoxic conditions. Consequently, we postulate that under normal conditions, but with excess glucose available, white adipose tissue (specifically its adipocytes), is essentially anaerobic, regardless of oxygen availability.

On the other hand, for the first time, we proved that white adipose tissue contains a full, active and functional urea cycle. The cycle is likely to work on demand, although we believe that its main objective may be to help control the arginine availability. The uniformity of the cycle behaviour (gene expressions, enzyme activities) was largely independent of the location studied, and of sex and diet, suggesting that the different masses of white adipose tissue work and are regulated in a coordinated way, as corresponds to a single dispersed organ. In parallel to the operation of the urea cycle, we found that white adipose tissue is markedly involved in the metabolism of amino acids. In this aspect, however, there were deep differences between groups and sites. The main differences were observed in the paths for production and detoxification of ammonia, which were found to be related to diet, and, especially, to sex. In conclusion, we can state that the white adipose tissue metabolic potential and its control on global energy metabolism (especially with respect to amino acid metabolism) is more important than usually assumed. In this regard, when we take into account the whole body fat mass the tissue metabolic potential could be comparable only to the liver.

Publicaciones directamente relacionadas con la tesis doctoral:

Arriarán, S., Agnelli, S., Fernández-López, JA., Remesar, X., Alemany, M. A radiochemical method for carbamoyl-phosphate synthetase-I: application to rats fed a hyperproteic diet. *Journal of Enzyme Research* **3**, 29-33 (2012)

Sabater, D., Arriarán, S., Romero, MM., Agnelli, S., Remesar, X., Fernández-López, JA., Alemany, M. Cultured 3T3L1 adipocytes dispose of excess medium glucose as lactate under abundant oxygen availability. *Scientific Reports* **4**, 3663 (2014)

Arriarán, S., Agnelli, S., Sabater, D., Remesar, X., Fernández-López, JA., Alemany, M. Evidences of basal lactate production in the main white adipose tissue sites of rats. Effects of sex and a cafeteria diet. *PLoS ONE* **10**, e0119572 (2015)

Arriarán, S., Agnelli, S., Remesar, X., Fernández-López, JA., Alemany, M. The urea cycle of rat white adipose tissue. *RSC Advances* **5**, 93403-14 (2015)

Arriarán, S., Agnelli, S., Remesar, X., Fernández-López, JA., Alemany, M. Effects of sex and site on amino acid metabolism enzyme gene expression and activity in rat white adipose tissue. *Peer J* **3**, e1399 (2015)

Arriarán, S., Agnelli, S., Remesar, X., Fernández-López, JA., Alemany, M. Overall white adipose tissue urea cycle activity remains unchanged in female rats after one-month treatment with a hyperlipidic diet. Manuscrito enviado a la revista *British Journal of Nutrition*

INTRODUCCIÓN

1. Introducción

1.1. La obesidad en el contexto del síndrome metabólico

La obesidad es considerada, hoy en día, la pandemia del siglo XXI, su creciente prevalencia y las complicaciones asociadas con ella en el contexto del síndrome metabólico la convierten en uno de los mayores problemas de salud pública global¹. De acuerdo a la Organización Mundial de la Salud (OMS), en el año 2011 unos 500 millones de personas en el mundo eran obesos, y se estima que estos números se duplicarán para el año 2030². El principal problema sanitario de la obesidad radica en sus enfermedades asociadas (diabetes, hipertensión, otras alteraciones cardiovasculares y problemas psicológicos y de autoestima entre otras), las cuales dan lugar a la mayor parte de las alteraciones metabólicas de la obesidad, y que, en conjunto representan un elevado porcentaje de la morbilidad y mortalidad de todo el mundo. Solo la combinación de cáncer, enfermedades infecciosas y muertes asociadas a violencia y/o accidentes supera a las enfermedades metabólicas en términos de mortalidad, aunque no en años de morbilidad o en su incidencia sobre aspectos socioeconómicos y de calidad de vida³. Las alteraciones asociadas al sobrepeso y la obesidad han sido reunidas, junto con sus co-morbilidades, bajo el concepto genérico de “síndrome metabólico”⁴.

En la última década se ha producido una fuerte controversia entre algunas sociedades científicas relacionadas con la salud y asociaciones médicas para definir en términos diagnósticos cuantitativos el concepto de síndrome metabólico y qué aspectos incluye⁵. Casi todas las definiciones describen a este síndrome como un conjunto de alteraciones metabólicas que predisponen a quien las padece a desarrollar un mayor riesgo de padecer enfermedades cardiovasculares y diabetes de tipo 2⁶. Dentro de este conjunto se incluyen la resistencia a la insulina/ intolerancia a la glucosa, hipertensión arterial, obesidad y dislipidemias (incluyendo hipertriaciglicerolemia, incremento plasmático de ácidos grasos libres y disminución de los valores circulantes de lipoproteínas de alta densidad). Además de las enfermedades cardiovasculares y la diabetes, este cuadro dismetabólico ha sido asociado a otras manifestaciones clínicas como el síndrome de ovario poliquístico, la ateroesclerosis, el estado pro-inflamatorio, el estrés oxidativo, la depresión, el hipercortisolismo, la hiperuricemia y la esteatosis hepática de origen no alcohólico⁷.

En la actualidad, todavía no se ha podido establecer el mecanismo patogénico que asocie todas las anomalías funcionales reunidas en el síndrome metabólico. Sin embargo, muchos de los componentes del síndrome tienen un origen compartido en la exposición crónica a dietas ricas en energía, con altas proporciones de grasas, proteínas de origen animal, sal y azúcares de bajo peso molecular ⁸. Cada día crece más el convencimiento de la implicación directa y clave del tejido adiposo, y sus mecanismos de defensa, en el comienzo de las diversas facetas del síndrome metabólico ⁹. En este sentido, diversos estudios han postulado la asociación del origen del síndrome con los efectos de la obesidad y la dieta materna sobre su descendencia, destacando la influencia especial de la dieta durante la gestación ^{10,11}. Sin embargo, estos factores epigenéticos también se manifiestan por vía paterna ¹², observándose su persistencia a lo largo de generaciones, por lo que se confirma una predisposición hereditaria adquirida a desarrollar el síndrome metabólico ¹³.

Debido a su compleja etiología, que incluye la herencia, el ambiente intrauterino, los patrones anormales de acumulación de grasas, la sobrecarga crónica de energía y la inactividad física, el síndrome metabólico podría considerarse una alteración de base endocrina, compleja y multifactorial que no comparte uno, sino varios mecanismos patogénicos entrecruzados e interdependientes en su desarrollo ^{3,7}.

La resistencia a la insulina ha sido considerada a menudo como el elemento que posiblemente mejor define el síndrome metabólico ¹⁴; se caracteriza por una menor sensibilidad a la acción de la insulina, que, a su vez, conlleva una reducción de la captación periférica de glucosa ¹⁵.

Sin embargo, se ha señalado que la resistencia a la insulina es un mecanismo evolutivo de adaptación, desarrollado y afinado mediante selección natural, que protege, y ha protegido a lo largo de todo el proceso evolutivo a los humanos (igual que al resto de mamíferos y sus ancestros) en situaciones de escasez o baja disponibilidad de alimento ⁸. Este mecanismo maximiza la utilización de la energía proveniente de los alimentos, almacenando parte de la energía "sobrante" en el tejido adiposo en forma de triacilgliceroles de reserva ¹⁶, para poder hacer frente a los previsibles períodos de escasez. No obstante, los mecanismos de supervivencia, incluyendo la resistencia a la insulina, no están preparados para las situaciones de exposición a un exceso continuo de energía, como las que caracterizan buena parte de nuestra sociedad actual. No hay

precedentes evolutivos para ello, por lo que sólo disponemos de recursos metabólicos y funcionales para hacer frente a la escasez; el exceso de nutrientes complica nuestra supervivencia al no poderse aplicar los recursos previstos y desarrollados para hacer frente a un reto que nunca se había producido antes. En períodos de inanición, la resistencia a la insulina induce al músculo a utilizar como fuente de energía los ácidos grasos provenientes de la hidrólisis de los triacilgliceroles del tejido adiposo, conservando así la proteína muscular¹⁷, y reservando la glucosa (disponible en cantidades limitadas) para los tejidos glucolíticos obligatorios⁸. En contraposición, bajo condiciones de elevada disponibilidad de energía y lípidos, los triacilgliceroles de la dieta evitan la utilización de la glucosa (resistencia a la insulina), y los aminoácidos no pueden ser degradados con fines gluconeogénicos por existir demasiada glucosa disponible dando lugar a un incremento de la disponibilidad de 2-amino nitrógeno¹⁸, y a un importante aumento de los niveles circulantes de glucosa⁸. La hiperglucemia induce una mayor secreción de insulina por el páncreas, provocando un ambiente hiperinsulinémico que intenta contrarrestar los efectos de la resistencia a la insulina forzando (sin demasiado éxito) su captación por todos los tejidos. Así, la combinación de hiperinsulinemia y resistencia a la insulina inducen al hígado (y otros tejidos) a captar glucosa de la sangre para regular su exceso, convirtiéndola mayoritariamente en triacilgliceroles que luego empaca e intenta secretar como lipoproteínas de muy baja densidad (VLDL)¹⁹. Finalmente, y como consecuencia de su limitada capacidad de almacenamiento, el hígado pronto alcanza la máxima acumulación posible de reservas de lípidos y de glucosa (glucógeno), interrumriendo su capacidad efectiva de tamponamiento energético. Por ello, y ante la continuidad del exceso de disponibilidad de energía, aparece una esteatosis que daña el parénquima hepático en un proceso mediado por el sistema inmune²⁰. Bajo estas condiciones, la capacidad del hígado para regular la glucemia y la extracción de insulina se deteriora rápidamente²¹, con lo que parte de estas tareas recaen en el tejido adiposo, no tan bien preparado para desarrollar un papel central en el control del exceso de energía.

La abundancia de energía a la que hace frente el organismo en la obesidad activa los pocos mecanismos de defensa disponibles, como el incremento del gasto energético (termogénesis) y un aumento del recambio proteico (favorecido por la mayor disponibilidad de aminoácidos)¹⁶ para paliar la situación. Sin embargo, cuando el exceso de nutrientes se mantiene indefinidamente, el tejido adiposo responde

almacenando buena parte de esta energía, esencialmente en forma de triacilgliceroles²² y convirtiendo la glucosa en lactato²³ y otros metabolitos de tres carbonos para hacer frente a los efectos deletéreos de la hiperglucemia. La excesiva acumulación de triacilgliceroles en el adipocito genera, a su vez, nuevas señales de alarma por daño del propio tejido (hipertrofia, hipoxia, y acidosis) que activan al sistema inmune en un intento de frenar el desaforado crecimiento de los depósitos de grasa del tejido adiposo.

1.1.1 Causas de la obesidad

Aunque la resistencia a la insulina podría ser una pieza fundamental del síndrome metabólico, es probable que la obesidad sea uno de los principales factores desencadenantes. La obesidad es una enfermedad crónica multifactorial, caracterizada por un exceso de reservas de grasa corporal, que se encuentra directamente relacionada con daños metabólicos y endocrinos, alteraciones cardiovasculares y respiratorias, estados depresivos, problemas articulares y alteraciones de la piel entre otras patologías²⁴.

En el desarrollo de la obesidad convergen factores genéticos y epigenéticos, pero también ambientales. Así las elevadas tasas actuales de obesidad son un reflejo de las profundas modificaciones de la dieta y el estilo de vida. Los últimos dos siglos han sido fundamentales en la transformación de la dieta, tanto en cantidad como en tipo de alimentos disponibles, gracias a la llegada de la revolución agro-industrial del siglo diecinueve y la modernización de la producción y procesamiento industrial de los alimentos en el siglo veinte (*la revolución verde*)²⁵. En menos de cinco décadas, la Organización de las Naciones Unidas para la Alimentación y la Agricultura (FAO) ha registrado un incremento global de la ingesta energética asociado a un cambio en la composición de la dieta, en la que aumenta la presencia de proteínas de origen animal, grasas saturadas, colesterol, y azúcares²⁶. A esta situación se añade un estilo de vida cada vez más sedentario, caracterizado por hábitos laborales y de transporte que disminuyen notablemente la actividad física, unido a alteraciones del sueño y ritmos circadianos²⁷. Otro factor importante es el mantenimiento de un nivel continuado de estrés, a menudo ligado a la sensación de inseguridad, inadaptación y presión social²⁸.

En los modelos epidemiológicos, diversos agentes ambientales actúan sobre el huésped, desencadenando la aparición de una enfermedad; su intensidad y gravedad

están en función de la virulencia de los agentes y de la susceptibilidad del huésped ²⁹. En la obesidad, los agentes ambientales no solo incluyen las dietas ricas en energía, el estrés y la inactividad física, citados más arriba, sino también otros factores de acción más temprana: intrauterinos, neonatales, y toxicológicos o farmacológicos ³⁰. Entre los dos primeros, cabe destacar la diabetes gestacional ³¹, la desnutrición intrauterina ³² y la corta duración de la lactancia materna ³³ (menos de tres meses) como factores que incrementan el riesgo de un individuo de padecer obesidad y/o diabetes en la vida adulta. La susceptibilidad del individuo a padecer obesidad se asocia, también, indiscutiblemente a perfiles genéticos determinados ³⁴ y a factores epigenéticos ³⁵. Se han identificado más de noventa alteraciones genéticas implicadas en el desarrollo de obesidad en determinados grupos humanos ³⁶, entre las que destacan las de los genes implicados en el control del apetito y el balance energético como los son los genes de la leptina ³⁷, propiomelanocortina (POMC), el receptor de melanocortina-4, y el gen *AGOUTI* ³⁰. Sin embargo, a pesar de haberse identificado una gran cantidad de variaciones alélicas asociadas a la obesidad, no se debe perder de vista que la epidemia de obesidad discurre en un trasfondo genético que no se modifica tan rápidamente como los agentes ambientales, siendo, por consiguiente, estos últimos esenciales para que la enfermedad se manifieste ²⁹. Cabe señalar, que buena parte de estos estudios se han hecho con poblaciones pequeñas, y utilizando un fuerte componente de interpretación estadística no siempre reproducible. Precisamente, los análisis genómicos a gran escala han demostrado que no existen genes que determinen la obesidad de un modo global ³⁸. Hasta el momento, sólo el gen *FTO* ha sido relacionado claramente con la obesidad con estudios poblacionales masivos ³⁹, aunque no se conoce aún, plenamente, la relación entre las alteraciones de este gen y la obesidad.

1.1.2 El concepto de ponderostato: la obesidad como alteración del mecanismo del control del peso corporal

El ponderostato, análogo al lipostato o el glucostato, no es más que una traslación al control de una variable fisiológica (el peso corporal como indicador de la masa de reservas grasas del cuerpo) formado por un típico modelo homeostático (Figura 1).

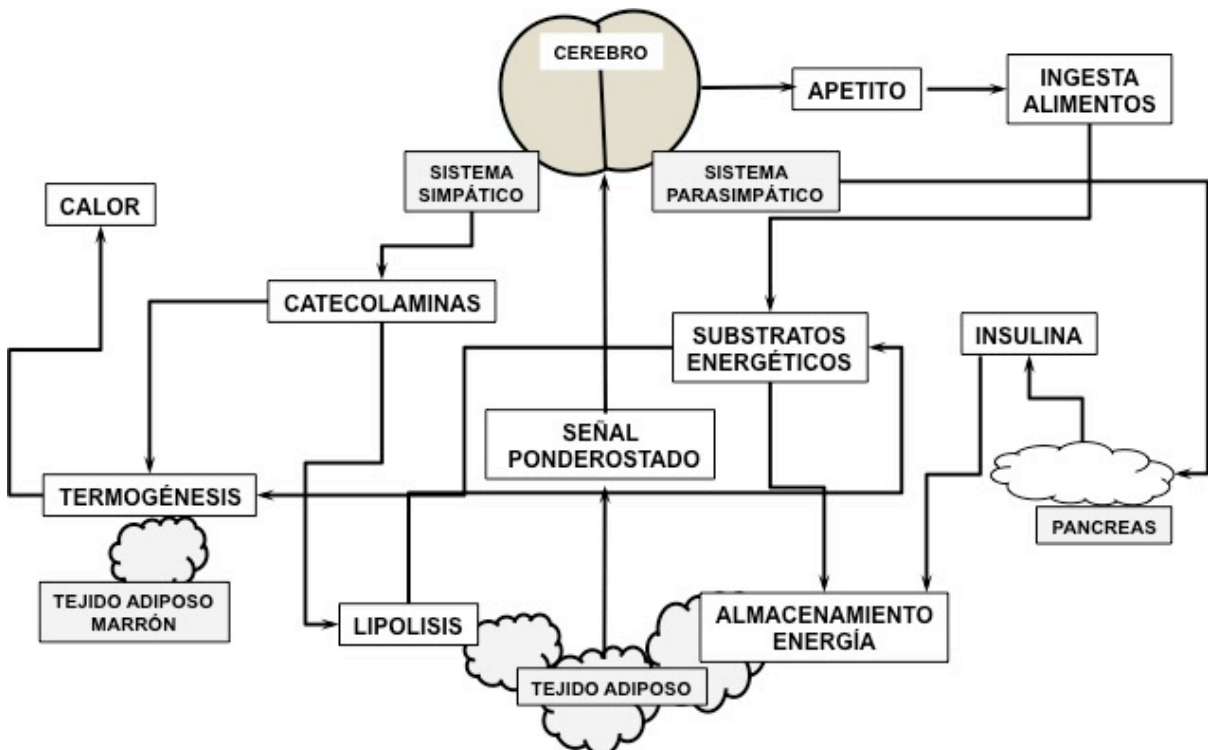


Figura 1. Esquema del modelo homeostático del ponderostato

El cerebro (esencialmente varios núcleos hipotalámicos relacionados) controla la ingesta en buena medida regulando el apetito y el tránsito intestinal (en el que está implicado el sistema nervioso autónomo parasimpático). Pero también controla la lipólisis del tejido adiposo y la termogénesis, que permiten la pérdida de reservas y su oxidación para la simple generación de calor. Estas variables se complementan con el papel de la insulina, que favorece la acumulación de reservas y que, indirectamente, está controlada por el cerebro y la disponibilidad de substratos. En este sistema, el cerebro mantiene la masa de reservas mediante la estimulación de la ingesta y deposición (aumento) o lipólisis y termogénesis (disminución), con la inhibición del apetito durante la termogénesis y la de ésta cuando conviene aumentar las reservas⁴⁰. Así, de acuerdo a un patrón de peso establecido por influencias genéticas, ambientales y del desarrollo, el organismo intenta mantener constante la cantidad apropiada de reservas grasas⁴¹. El

punto clave es cómo conoce el cerebro los niveles de reservas grasas del cuerpo, es decir cuál es la señal de ponderostato. Para esta función se han postulado metabolitos como la glucosa (glucostato) ⁴², los lípidos circulantes (lipostato) ⁴³, la leptina ⁴⁴ y la oleoil-estrona ⁴⁵ entre otros. No hay consenso sobre cómo se transmite la información, pero conceptualmente el modelo del ponderostato explica el mantenimiento (y defensa) del peso corporal. La obesidad sería entonces el resultado de un desajuste en este sistema, que impide mantener un peso corporal adecuado y constante frente situaciones de elevada disponibilidad de nutrientes y bajo gasto energético ⁴⁶. Los desajustes en el sistema del ponderostato en la obesidad podrían tener su origen en las alteraciones del tejido adiposo producidas por una hipertrofia que los mecanismos del ponderostato no han sido capaces de frenar; se ha comprobado, que en personas genéticamente susceptibles, el mantenimiento de un constante balance energético positivo, suscitado por el consumo de dietas sobrecargadas de energía y ricas en grasa, acaba alterando, al alza, los valores de masa de reservas pre establecidos ⁴⁷.

La investigación sobre las interrelaciones entre la función endocrina del tejido adiposo y el perfil neuroquímico de la obesidad ha crecido de manera considerable desde el descubrimiento de la leptina en 1994 ⁴⁴ y su subsiguiente descripción como una hormona esencial en la regulación del peso corporal ⁴⁸. La leptina es una proteína pequeña, sintetizada principalmente en el tejido adiposo. Esta hormona es responsable, en el cerebro, de la acción recíproca de cuatro mediadores neuronales de la ingesta y el gasto energético, incluyendo el neuropéptido Y (NPY) rico en tirosina, el péptido relacionado con la coloración del agouti, la proopiomelanocortina, y el transcripto relacionado con cocaína y anfetaminas (CART) ⁴⁴.

Dada la fuerte implicación en los circuitos neuroquímicos en la obesidad, es razonable reconocer que la patofisiología de la obesidad está muy relacionada con el tejido adiposo blanco; por lo que el amplio estudio de su morfología, fisiología, metabolismo y regulación es un aspecto fundamental para comprender las bases moleculares y bioquímicas de la obesidad.

1.2. El tejido adiposo

1.2.1. Estructura del tejido adiposo

Hay muchas indicaciones que apuntan a la existencia de una organización unitaria de las diferentes masas de tejido adiposo formando un gran órgano, de anatomía dispersa, pero con suministro vascular y nervioso específicos, de citología compleja, y con una elevada plasticidad fisiológica ⁴⁹. Este órgano está conformado por varias localizaciones anatómicas, que en los mamíferos pequeños están principalmente representadas por dos depósitos subcutáneos (anterior y posterior), y varios depósitos viscerales: mediastínico, mesentérico, retroperitoneal, y abdomino-pélvico (perirrenal, periovárico/epididimal, parametrial, y perivesical) ⁵⁰. Estas localizaciones lipídicas, así como otras presentes dentro y alrededor de órganos y tejidos ⁵¹, comparten un mecanismo de regulación común, aunque difieren en parte en su funcionamiento y metabolismo ⁵².

En animales sometidos a condiciones de termoneutralidad, el órgano adiposo es predominantemente blanco, con algunas áreas amarronadas en el depósito subcutáneo anterior y visceral. Las áreas amarronadas son aquellas en las que los adipocitos marrones predominan como célula parenquimal y representan al tejido adiposo marrón (TAM), el cual se encuentra altamente inervado y vascularizado. Las áreas blancas están principalmente compuestas por adipocitos blancos y corresponden al tejido adiposo blanco (TAB), con una menor irrigación e inervación ⁴⁹.

Las cantidades relativas de tejido adiposo blanco y marrón en el organismo son variables, y dependen de varios factores, entre los que destacan la edad, la dieta, y la temperatura ambiental ⁵⁰. Se ha demostrado que en todos los depósitos adiposos convergen el tejido adiposo blanco y marrón, y que en las áreas comprendidas entre estos tejidos existen adipocitos con una morfología intermedia entre los adipocitos blancos y marrones; a este tipo celular se le ha denominado adipocitos “beige” o “pauciloculares” ⁵³, también llamados “*brite*” (*brown-in-white*) cuando la mezcla de marrones y blancos es patente. Cabe resaltar, que las células parenquimales de los diferentes depósitos lipídicos tienen la increíble capacidad de transdiferenciarse; es así como el tejido adiposo blanco puede aumentar su contenido de células marrones (“amarronarse”) durante la exposición crónica al frío. El proceso de amarronamiento se inicia con la activación de las fibras nerviosas noradrenérgicas del órgano adiposo, lo

cual induce la conversión reversible de adipocitos blancos a adipocitos marrones con plena capacidad termogénica ⁵⁴. A la inversa, el tejido adiposo marrón puede “blanquearse” cuando no se requiere su actividad termogénica debido a factores como la edad avanzada, la obesidad y temperaturas cálidas. La presencia de estos factores modifica el perfil de expresión génica de los adipocitos marrones presentes en los depósitos blancos del tejido adiposo. Estas modificaciones génicas acercan la morfología de los adipocitos marrones a la de los adipocitos beige ⁵⁵.

El “amarronamiento” del tejido adiposo es un proceso de marcado interés fisiológico y terapéutico, ya que, en principio, podría ser utilizado para el tratamiento de la obesidad y el síndrome metabólico mediante el incremento de la capacidad termogénica ⁵⁶. Así, la expresión en adipocitos blancos de moléculas implicadas en la diferenciación de adipocitos marrones, como es el caso del gen *PRDM16*, induce a resistencia a la obesidad, mejorando la sensibilidad a la insulina ⁵⁷.

Durante la gestación y la lactancia, algunos depósitos lipídicos del tejido adiposo subcutáneo anterior y posterior participan en la producción y secreción de leche a través de la glándula mamaria con la que está anatómicamente entremezclado ⁵⁸. Esta transformación, conocida como alveologénesis, involucra la aparición de células epiteliales provistas de gotas lipídicas, las cuales se cree derivan de la transdiferenciación de adipocitos del tejido subcutáneo. Para estas células productoras de leche, derivadas de adipocitos, se ha propuesto el nombre de adipocitos “rosados” ⁵⁹.

Los diversos tipos de adipocitos se pueden diferenciar de modo simplificado por su coloración, pero ésta responde a claras diferencias en la estructura celular, vías metabólicas activas, función especializada, y localización anatómica. Los adipocitos blancos son células que tienen cerca del 90% de su volumen ocupado por una única vacuola lipídica, su tamaño, generalmente muy grande, hace parecer el núcleo pequeño. Son células principalmente glucolíticas, con un bajo consumo de oxígeno ⁶⁰ y un número limitado de mitocondrias ⁶¹. Los adipocitos marrones son células más pequeñas, con un núcleo redondeado, varias vacuolas lipídicas citoplasmáticas, y se caracterizan por contener numerosas mitocondrias (que le dan el color característico debido a la presencia de citocromo C). Los adipocitos beige son células con una morfología intermedia entre la de los adipocitos blancos y marrones ⁴⁹

La estructura del tejido adiposo es más compleja de lo que se suele suponer, y a pesar que ocupan la mayor parte del espacio en este órgano, los adipocitos no son el único tipo celular que lo compone. Aproximadamente la mitad de las células nucleadas del tejido adiposo constituyen la heterogénea “fracción vascular-estromal”, que incluye células madre, pre-adipocitos, células endoteliales y macrófagos⁶². A ello habría que añadir otros tipos celulares como los fibroblastos, histiocitos, linfocitos, granulocitos, mastocitos y terminales nerviosas⁶¹.

Recientemente se han identificado a las células madre de pericitos vasculares como las progenitoras de los adipocitos blancos⁶³. Sin embargo, hay estudios que señalan un origen polifilético de los adipocitos blancos a partir de distintas líneas celulares que se diferencian dando diversas poblaciones de adipocitos que coexisten en un mismo espacio⁶⁴. En cuanto a los adipocitos marrones, e independientemente del proceso de amarronamiento, se ha comprobado que derivan de células madre musculares⁵⁷. Aún continúa en debate si las células beige derivan de un conjunto de progenitores de adipocitos blancos, o si su origen es también independiente, como sugiere la bibliografía publicada en los últimos años⁶⁵.

1.2.2. Funciones del tejido adiposo

La principal función del tejido adiposo blanco es la de almacenar energía para mantener las demandas metabólicas del organismo en caso de necesidad. En condiciones de falta de aporte de nutrientes en cantidad suficiente para sostener las necesidades energéticas, el tejido adiposo moviliza rápidamente sus reservas. El principal agente desencadenante es la secreción de catecolaminas y otras hormonas lipolíticas⁶⁶. Por el contrario, en situaciones de balance energético positivo, el tejido adiposo acumula el exceso de energía en reservas de triacilgliceroles, esencialmente bajo el control de la insulina⁶⁷.

Además de su función como tejido de reserva energética, el tejido adiposo blanco presenta un perfil metabólico activo, en el que destaca la glucolisis, participando en los ciclos de Cori⁶⁸, de la glucosa-alanina⁶⁹ y de Randle (glucosa-ácidos grasos)⁷⁰, lo que define claramente su función interactiva con el lecho esplácnico en cuanto al control del flujo de substratos energéticos y el control de los niveles de los mismos⁷¹. El tejido adiposo también puede utilizar aminoácidos como fuente de energía⁷², en especial el

TAM⁷³. Asimismo, hemos demostrado que el exceso de glucosa se puede convertir masivamente en lactato y glicerol (fragmentos de 3C) para disminuir la carga glucémica del organismo⁷⁴.

Por otro lado, el tejido adiposo marrón se caracteriza por la expresión de la proteína desacopladora 1 (UCP1), una proteína de la membrana mitocondrial interna que permite el desacoplamiento de la fosforilación oxidativa de la síntesis de ATP, dando así lugar a la producción de calor (termogénesis)⁴⁹ al permeabilizar la membrana mitocondrial a los protones y deshacer su gradiente.

La actividad metabólica relacionada con el almacenamiento energético y la termogénesis han sido las funciones globales más estudiadas del tejido adiposo hasta la última década. Sin embargo, años después de la identificación de la leptina⁴⁴, se ha llegado a establecer que el tejido adiposo es un órgano multifuncional con un importante número de funciones añadidas⁶⁷. Entre éstas cabe destacar las de protección pasiva, secreción⁷⁵, defensa activa (como parte del sistema inmune)⁷⁶, reparación de tejidos y estructuras⁷⁷, señalización endocrina⁷⁸ y regulación del balance energético^{67,79}. Es tal la plasticidad y funcionalidad del tejido adiposo, que actualmente se utiliza como fuente de células madre para terapia celular, reconstrucción quirúrgica e ingeniería de tejidos⁸⁰.

La función secretora del tejido adiposo es bastante amplia y abarca funciones como la endocrina, paracrina, inmune y de señalización⁸¹. Su amplio secretoma incluye ácidos grasos, lactato, pequeñas proteínas de señalización (conocidas como adipocitoquinas), péptidos reguladores del flujo sanguíneo, eicosanoides, hormonas esteroideas y posiblemente muchos otros componentes, de bajo peso molecular, que pueden contribuir a la compleja interacción entre las células del tejido adiposo y las de otros órganos⁶⁷.

Las moléculas reguladoras segregadas por las células del tejido adiposo actúan de manera autocrina, paracrina y/o endocrina, y se encuentran involucradas en una gran variedad de procesos y mecanismos como la diferenciación de los adipocitos, el metabolismo energético, la captación y transporte de lípidos, la respuesta inmune y la inflamación, la reparación celular de estructuras, el desarrollo (y control) vascular y neuronal, y la remodelación de la matriz extracelular⁷⁵. Las adipocitoquinas ya

identificadas incluyen proteínas asociadas al control del balance energético como la leptina y la adiponectina⁸², así como citoquinas/ quimiocinas, como la interleucina 6 (IL-6) y el factor de necrosis tumoral alfa (TNFα) implicadas en procesos de apoptosis, regulación y remodelación celular⁸³. También incluye todos los componentes del sistema renina-angiotensina⁸⁴, miembros de la vía alternativa del complemento, el factor de crecimiento insulínico tipo 1 (IGF-1) y sus proteínas de unión⁸⁵, así como otros factores con funciones aún no definidas o en proceso de definición⁶⁷.

En resumen, el órgano adiposo, y el tejido adiposo blanco en particular, debido a su amplio tamaño y distribución dispersa, tiene un enorme potencial metabólico, inmune y regulador, que probablemente se activa bajo demanda, dependiendo de las necesidades específicas del organismo.

1.2.3. Alteraciones del tejido adiposo blanco en la obesidad

En la obesidad, el tejido adiposo está patológicamente expandido. En los obesos, los depósitos grados presentan un crecimiento excesivo, que puede comprometer su funcionamiento, y también la supervivencia del sujeto afectado⁹. La obesidad se caracteriza por la hipertrofia de los adipocitos⁸⁶, una vascularización insuficiente que puede dar lugar a hipoxia celular en determinadas circunstancias⁸⁷, la sobreproducción de componentes de la matriz extracelular⁸⁸ y la infiltración masiva de macrófagos, que segregan grandes cantidades de citoquinas inflamatorias⁸⁹. Esta remodelación patológica del tejido ejerce además efectos nocivos sobre su funcionalidad, disminuyendo, paradójicamente, su capacidad de almacenamiento de lípidos, en paralelo a la acumulación de grasa en localizaciones “ectópicas” como el hígado, el músculo y el páncreas⁹⁰.

Bajo condiciones constantes de balance energético positivo, se activa una respuesta inflamatoria de los órganos clave, desde el punto de vista metabólico, como el tejido adiposo y el hígado. El resultado es una inflamación crónica sistémica, que generalmente es de baja intensidad, característica de la obesidad, y responsable del desarrollo de muchos de los desequilibrios metabólicos y funcionales que se observan en el síndrome metabólico^{91,92}.

El mantenimiento prolongado de la hipertrofia de los adipocitos, producida, por ejemplo, como respuesta a una dieta hiperenergética especialmente rica en grasas, administrada de forma continuada, provoca una reacción defensiva del tejido adiposo en un intento por conservar su integridad y función⁹. Esta reacción se lleva a cabo a través de tres mecanismos clave: el primero se asocia a la disminución del metabolismo celular para limitar la incorporación de más energía⁶⁵; el segundo involucra la secreción de citoquinas y otras señales metabólicas para corregir la hipoxia presente, reducir el tamaño excesivo de los adipocitos (incluyendo la apoptosis), y disminuir la respuesta del tejido a señales hormonales que facilitan el depósito de grasa⁹⁰. Por último, el tercer mecanismo se asocia al incremento de la diapédesis, y con ella la infiltración masiva de células del sistema inmune que luchan contra la agresión a través de la depresión del metabolismo celular, la alteración de la señalización hormonal y la ralentización del crecimiento y la diferenciación celular⁹³.

En la obesidad, el tejido adiposo incrementa su contenido de células inmunitarias, con una mayor actividad funcional. Específicamente, hay un incremento en el número y actividad de las que tienen una función pro-inflamatoria (principalmente macrófagos, mastocitos, neutrófilos, y linfocitos T y B)⁹⁴, mientras que se reduce la presencia de los subtipos con perfil anti-inflamatorio como los eosinófilos y varios subtipos de linfocitos T (T colaborador 2 (Th2), T regulador, y T citolítico natural (iNKT))⁹³.

La hipertrofia de los adipocitos en el tejido adiposo en expansión induce la infiltración masiva de macrófagos, que muestran una polarización hacia el genotipo pro-inflamatorio M1⁹⁵. En condiciones de normopeso, los macrófagos del tejido adiposo presentan un genotipo predominantemente M2⁹⁶, caracterizado por producir citoquinas anti-inflamatorias como las interleucinas IL4 e IL13 implicadas en la remodelación y homeostasis del tejido⁹³. Los macrófagos que infiltran el tejido adiposo durante la obesidad son los principales secretores de citoquinas inflamatorias, como el factor de necrosis tumoral α, la interleucina 6, y la proteína quimio-atrayente de monocitos (MCP-1), capaces de interferir en la fosforilación del receptor de insulina y del sustrato 1 del receptor de insulina (IRS-1)⁹⁷. La inadecuada fosforilación del IRS-1 conlleva la alteración de la vía de transducción de la insulina y el desarrollo de resistencia a su acción⁹⁰.

El estrés del retículo endoplasmático del adipocito es un fenómeno que enlaza la disfunción celular con la activación de la respuesta inmune e inflamatoria del tejido adiposo en situación de abundancia energética. Cuando los nutrientes están en un exceso de efectos patológicos, el retículo endoplasmático del adipocito debe hacer frente a un fuerte incremento en la demanda de síntesis proteica; esta situación altera su función en el plegado de las cadenas de proteínas, e induce la activación de un mecanismo de defensa conocido como respuesta a las proteínas desplegadas (*unfolded protein response*, UPR) ⁹⁸. Este mecanismo de defensa inhibe la síntesis de proteínas y elimina las cadenas defectuosas ya sintetizadas (vía ubiquitina-proteasomas) ⁹⁹, pero también activa vías de señalización implicadas en la secreción de citoquinas inflamatorias, producción de radicales libres de oxígeno altamente reactivos, y la muerte celular ¹⁰⁰. De esta manera, el estrés del retículo endoplasmático contribuye activamente al estado inflamatorio (y se potencia con él) y de resistencia a la insulina en el que se encuentra el tejido adiposo en la obesidad ⁹².

La disfunción del adipocito en la obesidad se traduce en su incapacidad para seguir almacenando el elevado flujo de ácidos grasos provenientes de la dieta y de la lipogénesis esplácnica. Además, la resistencia a la insulina impide la inhibición de la lipasa sensible a hormonas, enzima importante para la movilización de los ácidos grasos del tejido adiposo por estimulación adrenérgica ¹⁰¹. El resultado es una capacidad limitada de almacenamiento y retención de lípidos, lo que provoca el mantenimiento de los elevados niveles circulantes de ácidos grasos retroalimentando la resistencia a la insulina, generando una situación de lipotoxicidad por el depósito crónico de triacilgliceroles en prácticamente todos los tejidos por encima de su capacidad biológica funcional ¹⁰².

La distribución del tejido adiposo está influenciada por el sexo. El patrón androide, con predominancia de la grasa visceral sobre la subcutánea, suele dar lugar, con la hipertrofia, a cambios metabólicos más graves para la salud que el patrón ginoide, que se caracteriza por la acumulación de grasa en depósitos subcutáneos, preferentemente en la mitad inferior del cuerpo ⁹. Los depósitos adiposos viscerales tienden a ser más pro-inflamatorios que los depósitos grases de otras localizaciones, como los subcutáneos ⁹⁰. La expresión de marcadores inflamatorios como la IL-6, MCP-1, y el inhibidor del activador del plasminógeno-1 (PAI-1), se encuentra en niveles más

elevados en el tejido adiposo visceral en comparación con los depósitos subcutáneos¹⁰³. Por consiguiente, la presencia de depósitos grases de tamaños variables en diferentes zonas del cuerpo da lugar a una marcada disparidad de consecuencias metabólicas⁹⁰.

1.3. Metabolismo del tejido adiposo blanco

En los últimos años, la apreciación de la trascendencia fisiológica del tejido adiposo está creciendo en paralelo al descubrimiento del alcance de sus funciones. El punto de inicio fue el conocimiento de que el tejido adiposo se comporta globalmente como un órgano endocrino⁷⁸, aunque sus diversas localizaciones puedan llevar a cabo diferentes funciones, compartiendo algunas pero no todas las posibilidades de un tejido muy maleable⁶⁷. A pesar de estos grandes avances, el metabolismo del tejido adiposo, y en especial el del tejido adiposo blanco, ha sido poco estudiado, siendo el metabolismo nitrogenado el menos investigado: sólo hay unos pocos estudios (realizados en las últimas décadas del siglo pasado) sobre la actividad de algunas enzimas del metabolismo de aminoácidos^{72,104}. Esto explica, en parte, que la posible implicación del tejido adiposo blanco en el metabolismo global de los aminoácidos del organismo no haya sido analizada en la práctica. A pesar de esta brecha en lo referente al conocimiento del metabolismo del tejido adiposo, pasaremos a continuación, a desarrollar los principales aspectos del metabolismo del tejido adiposo que actualmente conocemos.

En condiciones normales de disponibilidad de alimentos y de gasto energético global, nuestro organismo cumple los siguientes objetivos: almacenar substratos energéticos para maximizar la duración de las reservas del organismo, mantener la glucemia, por lo menos para permitir el uso de la glucosa por el sistema nervioso central y los eritrocitos, y preservar el nitrógeno 2-amínico y, en especial, los aminoácidos esenciales para sustentar el recambio proteico y la síntesis de otros compuestos de nitrógeno (ADN, ATP, porfirinas), y reponer las pérdidas obligatorias. La utilización de substratos sirve fundamentalmente para cumplir los objetivos antes mencionados, de manera que después de cada ciclo prandial-postprandial la composición del cuerpo se mantenga sin modificaciones, y toda la energía ingerida, incluyendo todos los tipos de nutrientes, se elimine a mediano plazo en forma de calor y productos de excreción^{8,105}.

Una de las principales funciones del tejido adiposo blanco es, precisamente, la de contribuir a regular la disponibilidad de energía. Para ello, almacena los nutrientes que se encuentran en exceso en la circulación durante el periodo postprandial (especialmente lípidos y glucosa) en forma de triacilgliceroles¹⁰⁶. También, en situaciones de ayuno o elevada demanda energética, libera al resto del organismo ácidos grasos¹⁰⁷, lactato¹⁰⁸, y aminoácidos¹⁰⁴ para su utilización energética. Cabe resaltar, que estos mecanismos se encuentran activamente regulados por vías hormonales y nerviosas; la insulina es un potente inductor del almacenamiento de lípidos, de la síntesis proteica y del metabolismo de la glucosa en el tejido adiposo¹⁰⁹, mientras que la movilización de sus reservas se encuentra principalmente bajo el control del sistema nervioso simpático, específicamente a través de la activación adrenérgica estimulada por la adrenalina y noradrenalina¹¹⁰.

La glucosa y los ácidos grasos libres están considerados como los principales substratos metabólicos encargados de cubrir las necesidades energéticas del organismo⁷¹. Muchos estudios sobre la contribución energética de estos nutrientes han determinado también los valores plasmáticos, y en algunos casos tisulares (hígado, músculo, y tejido adiposo) de aminoácidos y lactato. Sin embargo, el rol que cumplen estos metabolitos en el metabolismo en general, y en el energético en especial, aún no ha sido suficientemente clarificado²³. El lactato es el principal precursor de la gluconeogénesis hepática en el ayuno (y el post-ejercicio), pero no conocemos en profundidad, como en el caso de la glucosa, tanto su origen como su destino específico en el cuerpo¹¹¹. Los aspectos del metabolismo del lactato que han recibido considerable atención han sido su participación en el ciclo de Cori⁶⁸, definido como la circulación cíclica de la glucosa y el lactato entre el hígado y el músculo; su presencia en la contracción muscular como producto de la glucolisis anaeróbica en el ejercicio¹¹²; y su contribución como sustrato extra-hepático en la síntesis hepática de glucógeno¹¹³. Hace más de dos décadas, Di Girolamo *et al.*²³ confirmaron que el tejido adiposo es un productor activo de lactato tanto en el ayuno crónico como en el estado postprandial. La magnitud de la conversión de glucosa a lactato, y su modulación por concentraciones variables de substratos y hormonas sugieren que la producción de lactato a partir de glucosa es una función del tejido adiposo que debería ser añadida a sus clásicas funciones de lipogénesis y lipólisis¹¹⁴.

Curiosamente, y como se ha comentado anteriormente, el estudio del metabolismo nitrogenado ha sido frecuentemente descuidado, a pesar de que las proteínas son una fuente clave de energía nutricional. Probablemente, este descuido se deba a que el metabolismo de las proteínas involucra un amplio número de especies moleculares de fácil interconversión, así como múltiples vías catabólicas, presenta dificultades metodológicas para determinar el destino del nitrógeno, existe una enorme multiplicidad de potenciales reservorios funcionales de aminoácidos (de hecho todas las proteínas), asociados con un activo metabolismo inter-órganos, y finalmente, al hecho que tenemos un pobre conocimiento de sus vías catabólicas y de su regulación en el humano (y en mamíferos)¹¹⁵. La implicación del tejido adiposo en el metabolismo nitrogenado ha sido aún menos estudiada; sin embargo, se ha comprobado que este tejido cuenta con la actividad de muchas enzimas propias del metabolismo de los aminoácidos como la glutamina sintetasa¹¹⁶, la glutaminasa¹¹⁷, las transaminasas de aminoácidos de cadena ramificada¹¹⁸ y la AMP desaminasa¹¹⁹, entre otras. Además, el tejido adiposo es capaz de utilizar aminoácidos como substratos energéticos y/o lipogénicos y, dependiendo del estado nutricional del organismo y de las necesidades específicas de diversos tejidos, segregá a la circulación cantidades significativas de glutamina, alanina, tirosina y serina⁷². Todo ello apunta al tejido adiposo como un órgano con probablemente intensa, aunque desconocida, implicación en el metabolismo de los aminoácidos y su regulación.

1.3.1. Metabolismo del tejido adiposo en el ayuno

El ayuno ha sido un componente de la vida humana a lo largo de todo el proceso evolutivo. Por tanto, la adaptación a esta situación temporal ha sido un prerrequisito básico para la supervivencia de la especie. Hoy en día, el ayuno es relevante sólo para algunos grupos de personas; muchas religiones, por ejemplo, incorporan períodos de ayuno a sus rituales incluyendo a los musulmanes, quienes ayunan desde el amanecer hasta el anochecer en el mes de Ramadán, y a los cristianos, judíos, hindúes, y budistas, quienes tradicionalmente ayunan en días específicos del año¹²⁰. En los humanos, el ayuno de corto plazo (fisiológico) se encuentra típicamente representado por el estado nutricional del organismo después de al menos una noche sin ingerir alimentos⁷¹.

En el ayuno o estado postabsortivo las concentraciones plasmáticas de los diferentes metabolitos y reguladores energéticos varían; la glucosa e insulina caen a valores

mínimos, y los ácidos grasos libres alcanzan valores máximos ¹²⁰. Se ha establecido que el ayuno es un potente inductor de resistencia a la insulina; condición que induce al músculo a utilizar como fuente de energía los ácidos grasos circulantes, provenientes de los triacilgliceroles del tejido adiposo, conservando así la proteína muscular ¹⁷, y reservando la glucosa plasmática (presente en cantidades limitadas) para tejidos glucolíticos obligatorios ⁸. Ante esta situación, el hígado mantiene la glucemia al activar la movilización del glucógeno y la gluconeogénesis a partir de lactato ¹¹⁴ y aminoácidos ¹²¹. Se estima que la glucogenolisis contribuye sólo a apenas con un tercio de las necesidades de glucosa, recayendo el mantenimiento de la glucosa plasmática sobre todo en la gluconeogénesis hepática ⁷¹. El tejido adiposo juega un papel esencial en este proceso ya que provee al hígado de algunos de los substratos principales (glicerol y lactato) ¹²² y la energía necesaria (ácidos grasos) ¹²³ para mantener activa la gluconeogénesis. El lactato es el substrato gluconeogénico de preferencia ya que contribuye a cerca del 50% de la gluconeogénesis hepática ⁷¹, y además de ser producido en el tejido adiposo, es también sintetizado por tejidos principalmente glucolíticos (cerebro y eritrocitos) y por el músculo ¹¹¹. El músculo aporta lactato poniendo en marcha el ciclo de Cori (unidireccional, ya que no "recupera" la glucosa), que funciona a partir de la glucolisis de la glucosa que proviene del glucógeno muscular almacenado; debido a que el músculo carece de glucosa-6 fosfatasa y, por tanto, no puede liberar glucosa directamente como hace el hígado. Así, el músculo libera lactato al plasma con la finalidad de servir de substrato gluconeogénico en el hígado ⁶⁸. En el ayuno, el músculo utiliza muy poca glucosa, ya de por sí escasa, y opta por obtener la mayor parte de la energía que necesita de la oxidación de ácidos grasos circulantes ¹²⁴ (libres o en forma de lipoproteínas) inicialmente procedentes del tejido adiposo, que en esta situación se encuentran en concentraciones elevadas en plasma. Además de los ácidos grasos, el músculo es también capaz de utilizar aminoácidos como fuente de energía, especialmente los aminoácidos de cadena ramificada ¹²⁵, los cuales aprovecha a partir de la degradación proteica que ocurre, en parte, como respuesta a las bajas concentraciones plasmáticas de insulina y la escasez generalizada de energía para mantener el recambio proteico. El grupo amino de estos aminoácidos acaba siendo transaminado al piruvato (en buena medida proveniente de la degradación del glucógeno muscular) para formar alanina, que se libera al plasma y que finalmente es captada por el hígado que puede utilizar el esqueleto hidrocarbonado (piruvato) para gluconeogénesis y el grupo amino acaba formando parte de la urea ¹²⁶. A esta

interacción entre el metabolismo de la glucosa y el metabolismo de los aminoácidos se le conoce como ciclo de la glucosa-alanina⁶⁹, por analogía con el ciclo de Cori. El principal objetivo de este ciclo es doble, exportar el nitrógeno amínico liberado de los aminoácidos cuyos 2-ceto-ácidos han sido oxidados en el músculo y a su vez aprovechar la glucosa del glucógeno muscular.

En el estado postabsortivo hay una elevada liberación de ácidos grasos desde el tejido adiposo debido a la falta de inhibición por insulina de la lipasa sensible a hormonas¹¹⁰. Pero también por la activación de la triacilglicerol lipasa del tejido adiposo¹²⁷. Los ácidos grasos no esterificados son captados y oxidados, como se ha indicado más arriba, sobre todo en el músculo (como fuente de energía alternativa a la glucosa) y en el hígado. En este órgano, la oxidación de los ácidos grasos se produce en mayor medida de la necesaria para sostener sus necesidades energéticas, por lo que se acompaña de la formación de cuerpos cetónicos, que contribuyen a suplir parte de las necesidades energéticas de muchos tejidos, al aportar substratos que no requieren de la β-oxidación para generar acetil-CoA como fuente rápida y fiable de energía oxidativa para el ciclo de Krebs¹²⁸. En términos energéticos, la oxidación de los cuerpos cetónicos puede contribuir con un promedio aproximado del 8% del gasto energético en reposo, aunque esta contribución incrementa considerablemente si el ayuno se prolonga¹²⁹. Durante el ayuno voluntario o la restricción forzada de alimentos, los mamíferos desarrollan mecanismos eficientes de conservación de nitrógeno¹³⁰. Para ello, las actividades de las enzimas clave del metabolismo de los aminoácidos experimentan cambios importantes en el hígado y tejidos periféricos, incluido el tejido adiposo, en el cual se observa un descenso del catabolismo de aminoácidos¹⁰⁴. Esta reducción origina una disminución de los niveles plasmáticos (y excreción urinaria) de urea por la ausencia de suministro exógeno, y a pesar del incremento endógeno de la proteólisis y la utilización de aminoácidos¹³¹. Por los resultados obtenidos en los pocos estudios disponibles, al parecer el tejido adiposo previene la pérdida de nitrógeno amínico y refuerza su conservación con la finalidad de incentivar su reutilización por otros tejidos¹³².

* Movilización de los lípidos en el tejido adiposo

En condiciones como el ayuno y el ejercicio, cuando se requiere la movilización de reservas energéticas endógenas, los triacilgliceroles almacenados en el tejido adiposo son hidrolizados mediante la lipólisis y los productos resultantes, glicerol y ácidos grasos

son liberados a la circulación¹⁰⁷. El glicerol es captado esencialmente por el hígado como substrato gluconeogénico (o para la reesterificación)¹³³ y los ácidos grasos libres, algo tóxicos, son utilizados como substratos energéticos por los tejidos periféricos (como el músculo), donde pueden servir como substratos para la β-oxidación y la producción de ATP⁶⁶. Sin embargo, buena parte de estos ácidos grasos son captados por el hígado que los utiliza también como substrato energético¹²³, para la formación de lipoproteínas para la exportación de energía a los tejidos periféricos¹¹⁰ o para la formación de cuerpos cetónicos¹²⁸ explicada más arriba.

Los adipocitos son las únicas células que pueden liberar ácidos grasos procedentes de la lipólisis endógena a la circulación, aunque muchos otros tipos celulares realizan la lipólisis de triacilgliceroles de lipoproteínas en su superficie, mediante la lipoproteína lipasa¹³⁴, en gran medida captando los ácidos grasos como substrato energético también en condiciones postabsortivas¹³⁵, aunque no modifican significativamente los niveles de ácidos grasos no esterificados circulantes. En consecuencia, en el estado postabsortivo, la mayor parte de los ácidos grasos sistémicos se originan en el tejido adiposo¹³⁶. En los mamíferos, la hidrólisis de los triacilgliceroles se logra gracias al efecto secuencial de tres lipasas; la lipasa de triacilgliceroles del tejido adiposo¹³⁷, enzima limitante del proceso de lipólisis que convierte los triacilgliceroles en diacilgliceroles. La lipasa sensible a hormonas, que hidroliza los diacilgliceroles a monoacilgliceroles, y la monoacilglicerol lipasa, enzima que rompe los monoacilgliceroles en ácidos grasos y glicerol¹³⁸. En el ayuno, la movilización de los ácidos grasos se promueve por los efectos combinados de la reducción plasmática de insulina y el aumento de la secreción de adrenalina y noradrenalina. Además, se ha demostrado que la lipólisis en el tejido adiposo se refuerza en el ayuno como resultado de la resistencia a la insulina y del incremento en la sensibilidad β-adrenérgica¹⁰⁷. Estos cambios en la sensibilidad hormonal están mediados, al menos en parte, por la hormona de crecimiento, que se encuentra elevada en el ayuno prolongado¹³⁹. La lipasa de triacilgliceroles del tejido adiposo y la lipasa sensible a hormonas constituyen la principal maquinaria enzimática de la lipólisis. Ambas enzimas se encuentran reguladas a corto y largo plazo; la regulación a largo plazo involucra controles transcripcionales, y la de medio y corto plazo se asocia a procesos de fosforilación dependiente de AMP cíclico. La fosforilación y activación de la lipasa de triacilgliceroles del tejido adiposo y de la lipasa sensible a hormonas se inicia por procesos mediados por catecolaminas,

habiéndose identificado diversas moléculas capaces de estimularlas⁶⁶. Entre estas moléculas cabe destacar los péptidos natriuréticos (factor natriurético atrial y factor natriurético cerebral)¹⁴⁰, los glucocorticoides¹⁴¹, y el factor de necrosis tumoral alfa¹⁴².

* Metabolismo de la glucosa: énfasis en la producción de lactato por el tejido adiposo en el ayuno

En el ayuno, el organismo requiere energía metabólica para sus necesidades energéticas así como substratos para mantener la gluconeogénesis hepática. Durante el periodo postabsortivo, el lactato es el substrato responsable de aproximadamente el 60-70% de la gluconeogénesis hepática²³. Los estudios realizados en ratas han demostrado que el adipocito es capaz de incrementar su producción de lactato del 5-15% de la glucosa metabolizada en condiciones basales al 50-60% en la restricción parcial de alimentos o ayuno a corto plazo¹⁴³. La cuestión es ¿de dónde procede todo este lactato? En condiciones basales, el sistema nervioso y los eritrocitos justifican buena parte de este lactato, pero en el ayuno, la contribución del glucógeno muscular no cubre la diferencia¹²⁶, y aunque el glucógeno del tejido adiposo puede hacer una contribución significativa, sigue habiendo una importante diferencia que aún no ha sido suficientemente explicada.

La síntesis (y utilización) de lactato en el tejido adiposo¹⁰⁸, puede ser significativa para la economía de la escases (ayuno), ya que podría contribuir con lactato, además de ácidos grasos y glicerol, a las necesidades metabólicas del organismo durante este estado¹¹⁴. El incremento selectivo de la conversión de glucosa a lactato en el ayuno, en paralelo a la disminución de los demás productos del metabolismo de la glucosa, sugiere que esta función del tejido adiposo se encuentra íntimamente relacionada con la provisión hepática de substratos gluconeogénicos²³.

La síntesis de lactato en el tejido adiposo blanco depende de varios factores, entre los que destacan el tamaño de los adipocitos, la sensibilidad del tejido a la insulina, y la localización anatómica del tejido adiposo¹⁴³. Cuando se analizó el impacto del tamaño y el número de adipocitos en la síntesis de lactato, se observó que, en condiciones basales, los adipocitos pequeños de ratas alimentadas *ad libitum* convierten el 5-15% de la glucosa captada del plasma en lactato, mientras que los adipocitos más grandes de ratas obesas convierten hasta el 40-50%²³. En comparación, los adipocitos de humanos

obesos convierten en condiciones basales el 60-70% de la glucosa en lactato¹⁰⁸. Asimismo, varios grupos de investigación han hallado mayores niveles circulantes de lactato, en ayuno, en personas con obesidad cuando se comparan con controles con normopeso^{144,145}. Debido a que la resistencia a la insulina es una alteración metabólica muy común en la obesidad, Lovejoy, J. *et al.*¹⁴⁶ investigaron la posible relación entre la sensibilidad a la insulina y la concentración basal de lactato, encontrando una relación inversa entre ambos factores. Además, estimaron que la sensibilidad a la insulina es responsable de un 34% de la variabilidad de las concentraciones basales de lactato, mientras que la obesidad colabora solo con un 10% a dicha variabilidad. Se han observado diferencias metabólicas entre diferentes localizaciones anatómicas de tejido adiposo⁶⁷; el patrón del metabolismo de la glucosa no es particularmente distinto entre las diversas localizaciones, aunque si se observan grandes diferencias en la tasa de metabolización de la glucosa¹⁴⁷. Así, los adipocitos del tejido adiposo mesentérico convierten 2-3 veces más glucosa en lactato que los adipocitos de otras localizaciones, a pesar de ser significativamente más pequeños. Esta diferencia regional se mantiene tanto en el ayuno como en el estado postprandial¹⁴⁸, y podría explicarse por la conexión del sistema venoso mesentérico con la vena porta. De esta manera, los productos metabólicos (como lactato, ácidos grasos y glicerol) producidos por las células adiposas mesentéricas son transportados directamente al hígado, lugar donde son procesados dependiendo de las condiciones locales y sistémicas. Un claro ejemplo es el efecto de los ácidos grasos libres sobre la extracción y sensibilidad hepática a la insulina²³.

* Metabolismo de los aminoácidos en el tejido adiposo en el ayuno

Los cambios en el metabolismo de los aminoácidos observados en el tejido adiposo en el ayuno han sido estudiados sólo mediante el análisis de algunas de sus actividades enzimáticas. Aun siendo los resultados válidos, es importante no perder de vista que el efecto del ayuno en las actividades enzimáticas de un tejido que contiene grandes cantidades de lípidos puede tener diversas interpretaciones dependiendo de las unidades que se utilicen para estudiar y presentar la información¹⁰⁴. En el periodo postabsortivo, la proporción relativa de proteínas y agua del tejido adiposo incrementa en paralelo a la reducción de su contenido lipídico, como consecuencia de las mayores demandas energéticas que exige este periodo¹⁴⁹.

La información disponible en la actualidad sobre el metabolismo de los aminoácidos en el tejido adiposo blanco en ayuno proviene de estudios de casi 30 años de antigüedad realizados en ratas¹⁰⁴. La única excepción la representan los aminoácidos de cadena ramificada, que han sido activamente estudiados en este tejido por su relación con la obesidad^{150,151}.

Del metabolismo de los aminoácidos en el tejido adiposo blanco cabe destacar la oxidación con fines energéticos de los aminoácidos de cadena ramificada, en especial de la leucina, que es uno de los más utilizados por el tejido¹⁵². La leucina se incorpora sin dificultad a las proteínas y a los lípidos, a la vez que se oxida fácilmente a CO₂ debido a la elevada actividad de las transaminasas de cadena ramificada del tejido adiposo¹¹⁸. En el ayuno, la degradación de la leucina disminuye en el tejido adiposo pero incrementa en el músculo¹⁵³; es probable que el incremento muscular de la oxidación de aminoácidos de cadena ramificada sea compensado por la disminución de este proceso en el tejido adiposo. Como resultado de esta traslación del punto principal de catabolismo, la tasa total de descarboxilación de leucina se mantiene constante en el periodo postabsortivo¹⁵⁴. Se cree que la rápida caída de la capacidad del tejido adiposo para oxidar los aminoácidos de cadena ramificada en el ayuno se asocia a la conservación de estos aminoácidos principalmente para la cetogénesis¹⁵⁵. Al parecer, la disminución de la oxidación de aminoácidos de cadena ramificada por el tejido adiposo en ayunas se debe a la caída en las concentraciones de insulina y glucosa, principales estimuladores de este proceso¹⁵⁶.

Los estudios en rata demuestran que la secreción de alanina por el tejido adiposo en el estado postprandial está disminuida en el ayuno¹³¹, en paralelo a la menor presencia de alanina transaminasa en el tejido. La misma situación se observa con las enzimas glutamato deshidrogenasa y AMP desaminasa¹¹⁹, lo que sugiere que el ayuno disminuye el catabolismo de los aminoácidos en el tejido adiposo blanco de rata¹⁰⁴. Por el contrario, la actividad de la glutamina sintetasa se incrementa significativamente en el ayuno¹¹⁶, lo que podría indicar la necesidad del tejido de deshacerse del exceso de amonio producido a expensas de los aminoácidos.

1.3.2. Metabolismo del tejido adiposo en el estado postprandial

El estado postprandial que se describirá a continuación, corresponde a la situación metabólica en el que se encuentra el organismo después de la ingesta de comida que contiene glúcidos, lípidos, y proteínas. Una vez ingeridos, estos nutrientes son absorbidos y entran a la circulación a diferentes tiempos ⁷¹. Ante el incremento de la glucemia y de los aminoácidos plasmáticos, el páncreas responde rápidamente elevando la concentración plasmática de insulina de manera paralela a la de glucosa ¹⁵⁷. El incremento de la insulinemia inhibe la movilización de lípidos (liberación de ácidos grasos del tejido adiposo) ¹⁵⁸, por lo que la concentración plasmática de ácidos grasos libres cae en respuesta a concentraciones elevadas de glucosa (e insulina) plasmática ¹⁰⁷. En el músculo, la tasa de oxidación de ácidos grasos es casi enteramente dependiente de su concentración plasmática ¹¹⁰. Por ende, cuando la glucosa en plasma aumenta el músculo la utiliza como substrato energético sustituyendo a los ácidos grasos libres; este mecanismo, descrito en 1963 por Randle y colegas ⁷⁰, favorece la captación de glucosa inducida por la insulina e inhibe la oxidación muscular de ácidos grasos al estimular su desaparición en plasma.

El tejido adiposo contribuye de manera significativa al metabolismo de los aminoácidos en el estado postprandial ¹⁵⁴. Bajo estas condiciones, el tejido adiposo oxida aminoácidos de cadena ramificada y, a diferencia del músculo que los oxida a CO₂ como fuente alternativa de energía ¹⁵³, el tejido adiposo puede utilizar el acetil-coenzima A derivado de esta degradación para la síntesis de ácidos grasos de cadena larga y colesterol ¹⁵⁹. También se ha descrito que el destino del grupo amino de estos aminoácidos en el tejido adiposo, en el periodo postprandial, se concreta en la producción de alanina ¹⁶⁰ y, mediante la mineralización a amonio de parte de estos grupos amino mediante el ciclo del purín-nucleótido ¹⁶¹, se sintetiza glutamina ¹⁶². Debido a que el tejido adiposo representa un porcentaje significativo del peso corporal (especialmente en humanos), se ha postulado que sus diversas localizaciones anatómicas podrían actuar como reguladores importantes de las concentraciones circulantes de alanina, glutamina y aminoácidos de cadena ramificada según el estado nutricional en el que se encuentre el organismo ¹⁵⁴.

El almacenamiento de lípidos en el tejido adiposo varía ampliamente entre individuos. La mujer adulta estándar tiene, en promedio, cerca de un 30% de su peso corporal total en

forma de grasa, y el hombre un promedio del 20% ¹⁶³. En respuesta a la ingesta de alimentos, el tejido adiposo almacena triacilgliceroles a partir de los ácidos grasos captados de las lipoproteínas plasmáticas, y de la lipogénesis *de novo* ¹⁶⁴, a partir de otras fuentes, principalmente glucosa. Se ha debatido durante bastante tiempo cuál era la contribución real de la lipogénesis *de novo* a la acumulación de lípidos de reserva del tejido adiposo. En roedores, esta contribución es mucho mayor que en humanos ¹⁶⁵, en los que esta vía solo opera cuando la ingesta de lípidos es baja y la de glúcidos excede los requerimientos energéticos ¹⁶⁶. Estudios con técnicas isotópicas han indicado que aproximadamente el 10% de los ácidos grasos de los triacilgliceroles del tejido adiposo provienen de la lipogénesis *de novo* ¹⁶⁷, aunque queda por comprobar si esta síntesis se produce realmente en el propio tejido adiposo. La mayoría de los ácidos grasos del tejido adiposo en humanos provienen del plasma, principalmente de la fracción de triacilgliceroles de las lipoproteínas plasmáticas, con una pequeña contribución de la captación directa de ácidos grasos no esterificados ¹²⁴.

* Almacenamiento de lípidos en el tejido adiposo

En los mamíferos, los triacilgliceroles se almacenan principalmente en el tejido adiposo, actuando como reservorios de energía, pero también de ácidos grasos esenciales y de precursores de fosfolípidos ¹⁶⁸. Después de una comida, los lípidos de la dieta aparecen en gran medida en el plasma en forma de triacilgliceroles reconstituidos en el intestino y transportados (vía linfa y circulación sistémica) como constituyentes de los quilomicra y lipoproteínas de muy baja densidad (VLDL) nacientes ¹⁶⁹. Estas moléculas, y las VLDL sintetizadas masivamente en el hígado ¹⁷⁰, reparten sus triacilgliceroles a aquellos tejidos que expresan la lipoproteína lipasa. En el estado postprandial la lipoproteína lipasa del tejido adiposo se activa por procesos post-traslacionales en respuesta a la elevación de los niveles de insulina ¹⁷¹. Una vez activa, la lipoproteína lipasa es exportada a su lugar de acción, la zona luminal de las células endoteliales capilares, donde actúa sobre los triacilgliceroles de las lipoproteínas circulantes liberando ácidos grasos ¹¹⁰ que migran a través de la pared endotelial hacia los adipocitos por medio de transportadores de ácidos grasos dependientes de insulina, entre los que destacan la proteína transportadora de ácidos grasos 1 (FATP1), y la proteína CD36 ¹⁷². Una vez dentro de los adipocitos, los ácidos grasos se activan a acil-CoA y esterifican al glicerol-3P para formar triacilgliceroles, que se unen a una vacuola lipídica para su

almacenamiento. Las vacuolas lipídicas son “gotas de lípido” rodeadas por una monocapa de fosfolípidos y proteínas específicas, como la perilipina¹⁷³ y la proteína relacionada con la diferenciación adiposa (ADRP)¹⁷⁴, que probablemente regulan su formación, crecimiento, y disolución. Aún no conocemos bien cómo se regula la esterificación de estos ácidos grasos, aunque la insulina probablemente juega un rol esencial en este proceso¹⁶⁸. Esta hormona cobra además un papel protagonista en este contexto al estimular la captación de glucosa y promover la glucólisis, que aporta el glicerol 3-fosfato necesario para la formación de los triacilgliceroles¹⁷⁵. Probablemente, el principal punto de control de la incorporación de ácidos grasos al propio tejido adiposo sea su transporte desde el exterior de la célula, tanto para los ácidos grasos procedentes de la acción de la lipoproteína lipasa como de los ácidos grasos libres en plasma; el papel de las proteínas transportadoras de ácidos grasos cada vez tiene más adeptos como principal factor de control¹⁷⁶.

La lipogénesis *de novo* es la vía metabólica que sintetiza ácidos grasos a partir del exceso de hidratos de carbono, aunque los aminoácidos también pueden actuar como substratos, en el periodo postprandial⁷¹. En los humanos, se ha demostrado que la lipogénesis *de novo* se activa en el hígado ante la ingesta elevada de glúcidos¹⁷⁷; sin embargo, este mismo estímulo produce una respuesta casi nula en el tejido adiposo. Por el contrario, en algunas otras especies de mamíferos, como las ratas por ejemplo¹⁷⁸, la lipogénesis del tejido adiposo es mas activa y esta regulada por la proteína de unión al elemento regulador de esteroles (SREBP-1c)¹⁷⁹; esta proteína es un factor de transcripción estimulado por concentraciones elevadas de insulina y glucosa. Se ha propuesto que la posible baja expresión del SREBP-1c en el tejido adiposo de humanos podría justificar las diferencias existentes en la lipogénesis *de novo* con otras especies¹⁶⁵.

* Metabolismo de la glucosa: producción de lactato por el tejido adiposo en el periodo postprandial

La visión convencional de la utilización de glucosa por el adipocito establece que los principales productos resultantes de su metabolización son el CO₂, el glucógeno (aunque la síntesis de glucógeno en el tejido adiposo es bastante limitada, usualmente menos del 2-3% de la glucosa metabolizada) y los triacilgliceroles¹⁸⁰. Con el avance en las técnicas de estimación de la desaparición de glucosa en medios de incubación de

adipocitos, se pudo comprobar que el tejido adiposo también era capaz de producir lactato a partir de glucosa bajo condiciones postprandiales¹⁴³. Los niveles de lactato liberado fluctúan a lo largo del día, siguiendo una pauta relacionada con las comidas²³. El lactato plasmático postprandial aumenta (2-3 veces su valor basal) unos 20 minutos después de producirse el incremento de glucosa e insulina; este lactato es producido por el lecho esplácnico, el músculo y, principalmente, el tejido adiposo¹⁴⁶.

Ante niveles elevados de glucosa e insulina, el adipocito responde reduciendo la movilización de las grasas y acelerando el transporte y metabolismo de la glucosa¹¹⁰. La conversión de glucosa a lactato en estas condiciones parece estar sensiblemente influenciada por los efectos de la insulina¹⁸¹. Por ello, es posible que el tejido adiposo, expuesto a elevadas concentraciones de glucosa e insulina después de una comida, pueda sintetizar lactato en cantidades suficientes como para incrementar significativamente los valores circulantes y contribuir así a la reposición del glucógeno hepático²³. Incluso, se ha observado que la producción de lactato en adipocitos aislados de ratas realimentadas *ad libitum* tras un ayuno de 6-8 horas se mantiene elevada hasta 12-24 horas después del periodo de recuperación de la ingesta (que es cuando se acelera la síntesis de glucógeno)¹⁴⁸. Estos datos refuerzan la hipótesis que la producción de lactato en el tejido adiposo puede jugar un rol metabólico significativo en el periodo postprandial. En lo referente al papel que juega la insulina en este proceso, varios autores han descrito que las concentraciones de lactato en tejido adiposo después de una comida o de la ingesta de glucosa son más altas en individuos con resistencia a la insulina y diabetes *mellitus* de tipo 2 que en individuos sanos^{182,183}. Sin embargo, otros estudios afirman que hay una relación inversa entre la producción aguda de lactato tras la ingesta de glucosa y la obesidad, a pesar de tener los obesos una glucemia más elevada, lo que podría indicar una capacidad limitada del tejido adiposo para captar y convertir glucosa a lactato como consecuencia de la resistencia a la insulina^{146,184}. Por otro lado, la cantidad y la calidad de la dieta tienen, también, un papel importante en la capacidad del adipocito para convertir glucosa a lactato²³. Cuando se compararon los adipocitos de ratas alimentadas con pienso normal con los de ratas alimentadas con dieta hiperlipídica, se comprobó que los adipocitos del grupo hiperlipídico mostraban una mayor tasa de conversión de glucosa a lactato. El efecto de la composición de la dieta se observó en unas dos semanas, y estuvo acompañado de resistencia a la insulina, tanto local (en el adipocito) como sistémica¹⁸⁵.

* Metabolismo de los aminoácidos en el tejido adiposo en el estado postprandial

Como hemos indicado más arriba, el tejido adiposo en condiciones postprandiales es capaz de sintetizar alanina, glutamato y glutamina¹⁶². También puede oxidar leucina, isoleucina y valina¹⁵⁴. Basándose en mediciones *ex vivo* del flujo de leucina en tejidos de rata, Rosenthal *et al.*¹⁵⁹ sugirieron que el tejido adiposo es sólo inferior al músculo en su capacidad para catabolizar aminoácidos de cadena ramificada, y que la capacidad de ambos es de 6-7 veces mayor que la del hígado cuando se tienen en cuenta las masas relativas de estos tejidos. Este mismo estudio, demostró que durante el periodo postprandial el tejido adiposo puede sintetizar triacilgliceroles a partir de leucina en presencia de insulina y glucosa. Al parecer, la insulina estimula a la deshidrogenasa del complejo 2-cetoácido de cadena ramificada, factor limitante de la oxidación de la leucina, al inducir modificaciones post-translacionales en la estructura de la enzima¹⁸⁶. Por su parte, la glucosa podría ejercer su efectos sobre la oxidación de la leucina al incrementar la disponibilidad de los cofactores necesarios para su desaminación y/o descarboxilación¹⁵⁶, así como actuar como fuente de glicerol3-P. Al igual que en el músculo¹⁸⁷, y en el corazón¹⁴⁰, se ha observado que en el tejido adiposo en estado postprandial la leucina evita la oxidación de glucosa al comportarse como una fuente alternativa de acetil-CoA para la lipogénesis¹⁵⁴. El N del grupo amino de los aminoácidos de cadena ramificada se transamina con 2-cetoglutarato para dar glutamato, fuente final del N de la glutamina y la alanina¹⁶⁰. Sin embargo, la síntesis de alanina se encuentra limitada por la disponibilidad de piruvato, por lo que en ausencia de glucosa exógena, sólo el glucógeno podría aportar el esqueleto hidrocarbonado para la síntesis de este aminoácido¹⁵⁴. A partir de estos resultados se concluye que el tejido adiposo contribuye de manera significativa, principalmente en el periodo postprandial, a mantener los niveles circulantes de glutamina¹⁶² y alanina¹⁴⁹, principales aminoácidos de producción periférica que son utilizados por el intestino (glutamina)¹⁸⁸ e hígado (alanina)⁶⁹. Además, su capacidad para modular los niveles circulantes de aminoácidos de cadena ramificada ha sido confirmada en un estudio *in vivo* en el cual el trasplante de tejido adiposo a ratones con defectos globales en el metabolismo periférico de aminoácidos de cadena ramificada redujo las concentraciones de estos últimos en un 30% en ayunas y en un 50% en el periodo postprandial¹¹⁸.

JUSTIFICACIÓN Y OBJETIVOS

2. Justificación y objetivos

En los últimos años se han producido grandes avances en el reconocimiento de la heterogénea anatomía y funcionalidad del tejido adiposo. Desde el descubrimiento de la leptina, podemos encontrar muchas publicaciones sobre la función reguladora del tejido adiposo; se han descrito cientos de adiponectinas, y se ha ahondado en el papel regulador que ejerce este tejido sobre el metabolismo de los glucocorticoides, las hormonas sexuales, y otros agentes reguladores de los que depende en buena parte el mantenimiento de la homeostasis de todo el organismo. Sin embargo, y a pesar estos progresos, nuestro conocimiento de la implicación cuantitativa real del tejido adiposo, y específicamente la del tejido adiposo blanco, en el funcionamiento y regulación de las vías metabólicas de los principales nutrientes energéticos (glúcidos, lípidos y proteínas) sigue siendo muy escaso e incompleto. Se ha observado que el tejido adiposo presenta un perfil metabólico activo, en el que destacan la glucólisis y la síntesis de glucógeno, pero también se ha comprobado su participación en el ciclo de la glucosa-alanina, y la utilización ocasional de aminoácidos como fuente de energía. A pesar de ello, existen grandes agujeros en nuestro conocimiento, especialmente por lo que respecta al metabolismo nitrogenado y a los aspectos cuantitativos de las relaciones glucométabólicas con la producción de moléculas de 3 carbonos (lactato/ piruvato y glicerol).

Los pocos estudios disponibles sobre el metabolismo de los aminoácidos en el tejido adiposo blanco han sido realizados en su mayor parte por el grupo Nitrógeno-Obesidad (a finales del siglo pasado), dentro del cual también se ha realizado el presente trabajo. Aunque estos trabajos iniciales son los únicos disponibles y que presentan datos relevantes, son bastante antiguos y de difícil adaptación y aplicación a las técnicas y amplio conocimiento actuales de otras facetas del tejido adiposo. Las investigaciones actuales sobre el metabolismo energético del tejido adiposo se centran sobre todo en estudiar la expresión de los genes implicados, alejándose cada vez más de los aspectos cuantitativos. Mayoritariamente, se ha perdido de vista que el estudio del metabolismo energético en un tejido tan versátil como lo es el tejido adiposo necesita también de análisis dinámicos, del funcionamiento de enzimas, reguladores metabólicos, metabolitos tisulares e incluso flujos sanguíneos. Dada la escasa --y limitada-- información disponible sobre el metabolismo energético en el tejido adiposo blanco, para el desarrollo de esta tesis doctoral decidimos investigar algunos de los aspectos menos

estudiados de este metabolismo (pero de una considerable importancia global); la regulación, síntesis y secreción de lactato, y las bases de su metabolismo nitrogenado. Para ello, intentamos empezar el estudio del metabolismo nitrogenado en cultivos de células 3T3L1, con la sorpresa de encontrarnos elevadas cantidades de lactato en los medios de cultivo, que inicialmente contenían cantidades fisiológicas de glucosa. Este hecho era conocido, pero al contrastar los datos cuantitativos, comprobamos que la glucolización era excesiva para condiciones de normoxia, es decir, el lactato era un producto final fisiológico y no accidental. Teniendo estos resultados como referencia, comprobamos posteriormente la producción *in vivo* de lactato por diferentes localizaciones de tejido adiposo blanco de rata. Debido a que existe una estrecha relación (inversa) entre el metabolismo de la glucosa y la utilización de aminoácidos como substrato energético, decidimos reorientar nuestros estudios hacia la investigación *in vivo* del metabolismo nitrogenado, partiendo de la base que el tejido adiposo no está formado únicamente por adipocitos sino que contiene una amplia gama de células estromales. En consecuencia, dejamos de lado los estudios en células 3T3L1 y nos centramos en un análisis mucho más primario (a nivel bioquímico, algo que aún no se había completado) del metabolismo de los aminoácidos en el tejido adiposo blanco. Para ello, utilizamos a la rata como modelo.

El **objetivo** de este estudio ha sido investigar el metabolismo energético del tejido adiposo blanco desde la perspectiva del tejido como un gran órgano adiposo formado por diferentes localizaciones específicas que comparten un mecanismo de regulación común. Para ello se han analizado y comparado las principales vías metabólicas de partición de energía en 4 localizaciones de tejido adiposo blanco (subcutáneo SC, retroperitoneal RP, mesentérico ME y epididimal EP o perigonadal en hembras PG) de ratas en condiciones fisiológicas y de obesidad inducida por la dieta. Este objetivo general se ha desarrollado a lo largo de los siguientes objetivos específicos:

- Analizar las bases bioquímicas del metabolismo nitrogenado del tejido adiposo blanco, ahondando en el funcionamiento de su eje central, el ciclo de la urea. El primer paso era, simplemente, comprobar si este ciclo estaba completo y funcional en el tejido adiposo, ya que estas características han sido descritas al completo sólo en el hígado. Para este estudio, así como para los siguientes, se

utilizaron ratas Wistar hembra y macho alimentadas durante 4 semanas con dieta estándar o dieta “de cafetería”, con la finalidad de describir y comparar los procesos metabólicos que ocurren con los aminoácidos en el tejido adiposo blanco bajo condiciones fisiológicas y de inicio del desarrollo del síndrome metabólico por dieta hiperlipídica.

- Desarrollar una metodología adecuada a un tejido con escaso citoplasma y mucha grasa, disperso y formado por varios tipos de células, basada en la adaptación de técnicas de cuantificación enzimática y de análisis de expresión génica (PCR en tiempo real) que nos permitiera analizar la presencia y funcionalidad de las enzimas del ciclo de la urea (y vías relacionadas en las cuatro localizaciones estudiadas de tejido adiposo blanco de rata).
- Determinar cómo se modula la utilización de la glucosa en el tejido adiposo blanco, centrándonos en su capacidad de síntesis y secreción de lactato, principalmente mediante el estudio del lactato tisular, de flujos sanguíneos, y de la expresión génica y actividad enzimática de las proteínas involucradas; realizando además un análisis paralelo de un grupo de animales con sobrepeso inducido por la dieta para empezar --también-- un análisis más profundo de las relaciones entre el metabolismo del lactato y el tejido adiposo en la inflamación que caracteriza el síndrome metabólico.

RESULTADOS

3. Resultados

3.1. Producción basal de lactato en el tejido adiposo blanco

* *Cultured 3T3L1 adipocytes dispose of excess medium glucose as lactate under abundant oxygen availability*

* *Evidence of basal lactate production in the main white adipose tissue sites of rats. Effects of sex and a cafeteria diet*

En este apartado se analizó la capacidad del tejido adiposo blanco para producir lactato a partir de glucosa, facilitando de esta manera la partición de energía a través de la distribución de substratos de 3 carbonos. Pero sobre todo ayudando al control de la glucemia al convertir grandes cantidades de glucosa en lactato. Este trabajo se desarrolló a partir de dos tipos de análisis: el primero, *in vitro* con adipocitos murinos 3T3L1 incubados en condiciones de alta disponibilidad de oxígeno y expuestos a concentraciones variables de glucosa en el medio, y el segundo, *in vivo* analizando diferentes localizaciones de tejido adiposo blanco en ratas.

Para el estudio *in vitro* se cultivaron y desarrollaron fibroblastos 3T3L1 en condiciones estándar durante 9 días. Las células y los medios de cultivo se recolectaron en los días 0, 2, 4, 6 y 9 después del inicio de la diferenciación de los fibroblastos con la finalidad de determinar los efectos de la diferenciación celular sobre la utilización de substratos y el perfil de expresión génica. Al mismo tiempo, para analizar los efectos de la concentración de glucosa, se cultivaron adipocitos 3T3L1 maduros en medios conteniendo diferentes concentraciones de glucosa (de 0 a 30 mM) durante 3 días. En ambos estudios, se analizaron las concentraciones de glucosa, lactato, pH y pO₂ en los medios de cultivo. Las células recolectadas se contaron y su ARN se extrajo para determinar la expresión de genes relevantes del metabolismo glucídico y lipídico. En paralelo al estudio *in vitro*, y para poder desarrollar el estudio *in vivo*, se alimentaron ratas Wistar adultas, tanto hembras como machos, con pienso estándar o con una dieta “de cafetería” simplificada a lo largo de un mes. Posteriormente, los animales se sacrificaron y se tomaron muestras de cuatro localizaciones de tejido adiposo blanco: perigonadal (periovárico/ epididimal), subcutáneo inguinal, mesentérico y retroperitoneal. Se analizó la expresión de los genes clave del metabolismo glucídico y lipídico, así como los niveles de lactato plasmático y tisular, y la actividad de la enzima lactato deshidrogenasa. Se determinó también la influencia del sexo y la dieta en los niveles

tisulares de lactato y su relación con la actividad de la lactato deshidrogenasa y la expresión de genes.

El análisis *in vitro* demostró que bajo condiciones de normoxia las células 3T3L1 secretan grandes cantidades de lactato al medio con un fuerte consumo de glucosa, de forma proporcional a los niveles de ésta. Durante todo el proceso de diferenciación y crecimiento, solo una fracción de la glucosa disponible fue convertida a triacilgliceroles, mientras que una gran proporción de la glucosa fue transformada a lactato en un proceso netamente anaeróbico. Los resultados del análisis *in vivo* confirmaron las conclusiones observadas *in vitro*, al demostrar que el tejido adiposo blanco produce lactato en grandes cantidades, independientemente de su localización, pero también de la dieta o el sexo. Además, la producción de lactato era proporcional a la actividad de la lactato deshidrogenasa. En conclusión, la producción de lactato por el tejido adiposo no depende de la disponibilidad de oxígeno (en los adipocitos) o de su estado metabólico. Creemos que, en el tejido adiposo, la producción masiva de lactato es parte de un mecanismo de defensa dirigido a convertir el exceso de glucosa circulante en fragmentos de 3 carbonos, como un modo de limitar su utilización como substrato (e hipertrofiar aún más el tejido adiposo, por ejemplo), para ayudar a controlar la glucemia y/o proveer substratos de cadena corta para su uso como fuente de energía en otros tejidos.



OPEN

Cultured 3T3L1 adipocytes dispose of excess medium glucose as lactate under abundant oxygen availability

SUBJECT AREAS:
METABOLIC DISORDERS
INFLAMMATION
OXIDOREDUCTASES

Received
21 October 2013

Accepted
16 December 2013

Published
13 January 2014

Correspondence and requests for materials should be addressed to
M.A. (malemany@ub.edu)

David Sabater^{1,2,3}, Sofía Arriarán^{1,2,3}, María del Mar Romero^{1,2,3}, Silvia Agnelli^{1,2,3}, Xavier Remesar^{1,2,3}, José Antonio Fernández-López^{1,2,3} & Marià Alemany^{1,2,3}

¹Department of Nutrition and Food Science, Faculty of Biology, University of Barcelona, Barcelona 08028, Spain, ²Institute of Biomedicine, University of Barcelona, Barcelona 08028, Spain, ³CIBER Obesity and Nutrition, Institute of Health Carlos III, Spain.

White adipose tissue (WAT) produces lactate in significant amount from circulating glucose, especially in obesity. Under normoxia, 3T3L1 cells secrete large quantities of lactate to the medium, again at the expense of glucose and proportionally to its levels. Most of the glucose was converted to lactate with only part of it being used to synthesize fat. Cultured adipocytes were largely anaerobic, but this was not a Warburg-like process. It is speculated that the massive production of lactate, is a process of defense of the adipocyte, used to dispose of excess glucose. This way, the adipocyte exports glucose carbon (and reduces the problem of excess substrate availability) to the liver, but the process may be also a mechanism of short-term control of hyperglycemia. The *in vivo* data obtained from adipose tissue of male rats agree with this interpretation.

White adipose tissue (WAT) main substrate is glucose^{1,2}, which uses in part to synthesize fatty acids for its triacylglycerol (TAG) stores³. WAT also takes up unesterified fatty acids⁴ or those in lipoproteins, released by gut and liver^{5,6}. WAT produces lactate from glucose^{7,8}, in proportions that may account for up to 30% of all body glucose metabolism, as reviewed by DiGirolamo *et al.*⁹. Production of lactate is also increased in primary cultures of adipocytes from obese or diabetic humans, accounting for up to 50–70% of all glucose taken up¹⁰, in a process dependent, at least in part, on insulin^{10,11}. Lactate release by WAT has been related to obesity and insulin resistance¹², since cells from diabetic humans produce more lactate than those of healthy subjects¹³. Small adipocytes, during the process of increasing fat storage, produce less lactate from glucose than larger cells, containing more TAG¹⁴.

WAT lactate production has been assumed to be part of a Cori cycle¹⁵ between WAT –as peripheral organ producing lactate from glucose– and liver. The result of such large production of lactate may be an increase in liver gluconeogenesis and/or hepatic glycogen storage¹⁶. However, this explanation could not be quantitatively sustained under conditions of excess glucose availability, since it blocks gluconeogenesis and glycogen storage.

WAT lactate release has been often considered a telltale of hypoxia¹⁷, correlated with acidosis¹⁸, tissue stress¹⁹, mitochondrial function disturbances²⁰, endothelial inflammation²¹ and altered cytokine release pattern²². The paradigm of lactate release as indication of hypoxia has been challenged by direct analysis of *in vivo* oxygen levels and consumption by adipose tissue^{23,24}, which is relatively low. WAT blood flow is diminished in obesity²⁵, but the tissue could not be considered hypoxic because direct measurement of pO₂ proved that the tissue receives sufficient oxygen to sustain its metabolism given the limited needs of the tissue²⁴. Low blood flow may be partly compensated by lactate release, decreasing blood pH, but freeing more oxygen from oxyhemoglobin to counter hypoxia through the Bohr effect²⁶. The decrease in WAT blood flow may be a defensive mechanism, under conditions of insulin resistance, to limit the entry of blood-carried energy substrates, which the tissue has to take up as end-of-the-line dumping place²⁷.

Adipocyte lactate efflux in the presence of high glucose is levels may be due to:

- a simple defense strategy to survive under hyperglycemia, limiting substrate availability to prevent unwanted hyperthrophia through decreased blood flow at the expense of lower oxygen supply. There is no hypoxia because oxygen needs may be minimized using glucose massively through anaerobic glycolysis. This may also help reduce substrate availability, or

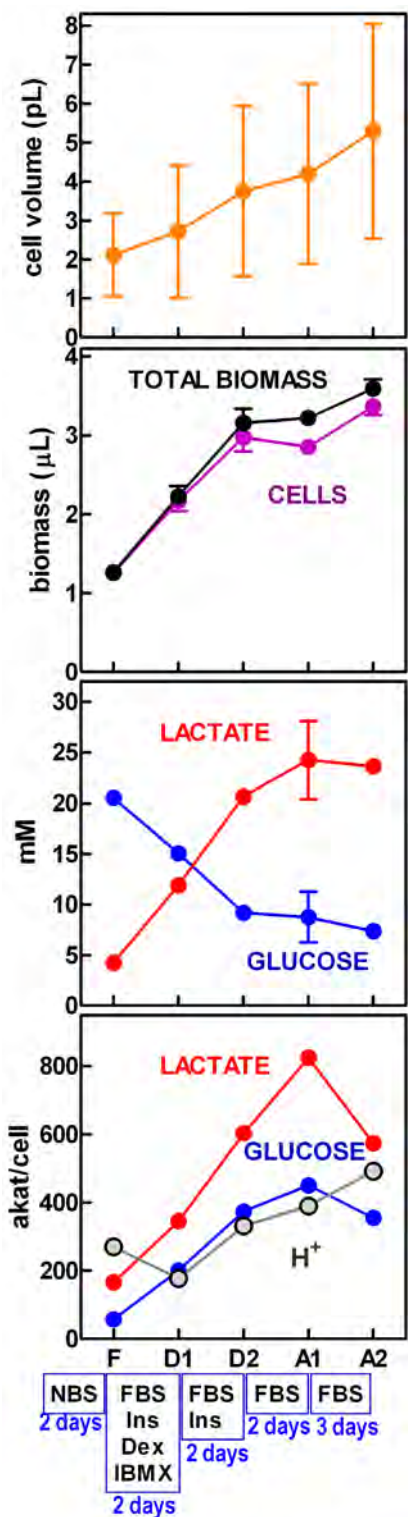


Figure 1 | Changes in cell volume, culture biomass, glucose uptake and lactate release of 3T3L1 cells along the differentiation process from fibroblasts (at confluence) to mature adipocytes. F = fibroblasts at confluence; D1 = end of the treatment with the first differentiation medium; D2 = end of the treatment with the second differentiation medium; A1 = mature adipocytes on day 6; A2 = mature adipocytes on day 9. The composition of the incubation media used in the transitions from one stage to the other are indicated at the bottom, as well as the duration of the process. NBS = neonatal bovine serum; FBS = fetal bovine serum; Ins = insulin; Dex = dexamethasone; IBMX = 3-isobutyl-1-methylxanthine, a phosphodiesterase inhibitor. The upper panel shows the mean cell volumes (\pm SD) for cells at the different stages of differentiation

and growth in size. Since cell volume includes thousands of individual measurements we used the SD instead of SEM values to give a better idea of cell size variability. The second panel shows the data for biomass (mean \pm SEM) in the culture wells; purple corresponds to cells, and black to total biomass, i.e. cells and other smaller particles (largely debris formed during harvesting). The third panel shows the lactate and glucose concentrations (mean \pm SEM) in the culture medium (initially lactate 0 mM, glucose 22 mM). The fourth panel presents the mean rates (in attokatals per cell) for lactate production, glucose uptake and proton release into the medium calculated (see text for information) using mean parameter values.

- b) the recourse to anaerobic glycolysis is a Warburg-like²⁸ effect, such as that observed in fast-growing tumor cells²⁹; the cells forsake oxidative phosphorylation to obtain the ATP they need by using large amounts of glucose in glycolysis to lactate³⁰.

In order to discern between these alternatives to justify high lactate production, we used murine 3T3L1 adipocytes exposed to varying glucose concentrations in the medium, under full oxygen availability, and determining how these conditions modulate fat deposition, lactate production and oxygen consumption.

Results

Substrate utilization during 3T3L1 adipocytes differentiation. Figure 1 shows the changes in cell volume and biomass (i.e. the sum of cells and debris produced during harvesting) accumulation in 3T3L1 cell cultures, from fibroblasts at confluence to mature adipocytes. Medium glucose (22 mM when fresh), decreased steadily with differentiation in spent media, in parallel to increasing lactate, which arrived at a plateau in the 25 mM range. These trends were maintained when the data were expressed as mean rates per cell. Proton release/leakage increased during differentiation with rates similar to those of glucose uptake.

Energy balance and glucose fate during the differentiation of 3T3L1 adipocytes. For the sake of calculations, we assumed that the cell components of a fibroblast and a mature adipocyte were similar, and the differences in size between them were largely due to accumulation of TAG.

The mean biomass of a confluent fibroblast culture was 1.27 µL/well, and that of mature adipocytes obtained from the same stock and number of fibroblasts was 3.59 µL/well at the end of the 9-day process. The difference in volume, assumed to be mainly fat, translated to about 2.07 mg/well, i.e. 2.3 µmol TAG, synthesized using 36 µmol glucose (for details see Supplemental Methods). On the other hand, the 9-day process of differentiation and growth of adipocytes consumed 196 ± 36 µmol glucose, producing 339 ± 4 µmol lactate. The amount of glucose converted to lactate was about 169 µmol, leaving only 27 µmol glucose for TAG synthesis and other uses, including oxidative energy production. Even assuming a wide margin of error in our assumptions, these values were in the same range than those calculated from biomass changes. These data suggest that practically all available glucose was used for lactate production and lipid synthesis.

In the process analyzed, 45% glucose (of the initial 22 mM) was taken up from the medium; about 80–86% of the incorporated glucose was converted to lactate, and 15–18% was used for TAG synthesis. From these data we can assume that ATP was mainly obtained from glycolysis: 339 µmol, 36 µmol were excess ATP produced from TAG synthesis, and the equivalent of 16 µmol was lost as H^+ leakage (assuming 3 protons per ATP). Thus, aerobic glucose oxidation was necessarily very low, since only the pyruvate dehydrogenase step in the lipogenic process was aerobic, and anaerobic pathways practically justified the entire glucose uptake. In consequence, 3T3L1 cells showed a markedly anaerobic metabolism under high glucose, even during differentiation and TAG storage.

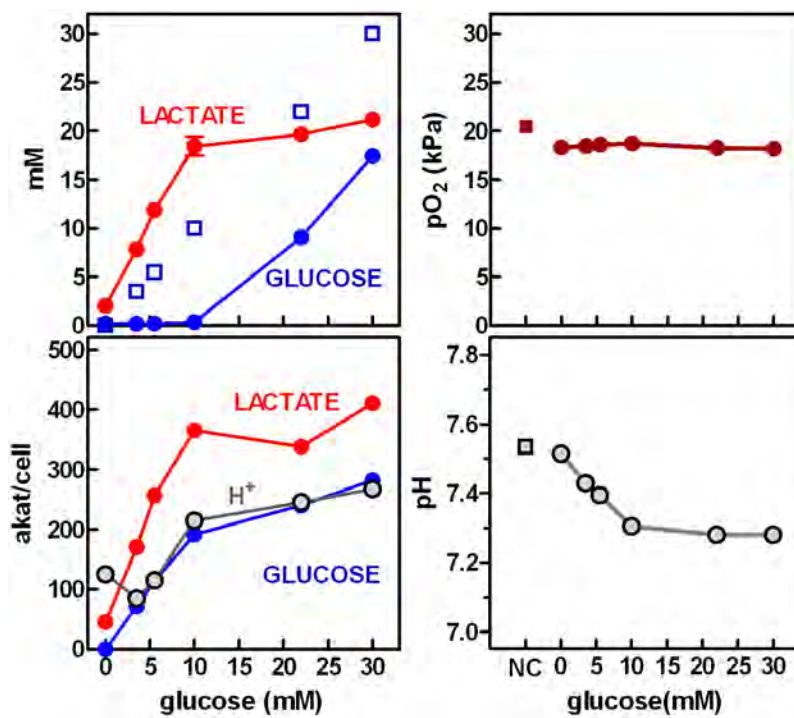


Figure 2 | Effects on glucose uptake, lactate efflux, pO_2 and pH of the concentration of glucose in the medium of 3T3L1 mature adipocytes. Left upper panel: medium glucose and lactate (mean \pm SEM) after 3 days of incubation of the cells at the given glucose concentration. The left bottom panel shows the same data presented as rates (attokatals per cell, mean values only); proton release into the medium has been also included (mean \pm SEM). The right panels represent the pO_2 and pH vs. initial medium glucose concentration (mean \pm SEM). NC correspond to a well incubated under the same conditions (i.e. [Glc] = 22 mM) but containing no cells.

Figure 2 presents the medium lactate and glucose concentrations after incubation of mature 3T3L1 cells (from days 6 to 9). Glucose levels were practically zero in the spent media from initial values of 0 to 10 mM, reaching up to 17 mM for the 22–30 mM range. The zero values observed below 10 mM suggest that total removal of glucose under these conditions could have gone beyond these values if more glucose were initially available. On the other hand, lactate levels increased up to 20 mM but then leveled off irrespective of glucose availability. The adjustment of medium concentrations to rates per cell repeated the same pattern. There was a significant release of protons, parallel to glucose uptake.

Effect of medium glucose concentration on adipocyte uptake of glucose and lactate production. No morphological differences between adipocytes exposed to different glucose concentrations were observed (Supplemental Figure 1) and no fibroblasts were observed in any glucose-concentration group. Biomass and cell size/counts were not significantly different either, but there were slight differences in total cell mass and biomass (Supplemental Figure 2). In our calculations, the changes in biomass were equilibrated by cell counts, and resulted in a net production (in 3 days) of -0.13 mg (at glucose 0 mM) to 0.34 mg (at glucose 22 mM). At concentrations of glucose 10–30 mM, the percentage of glucose uptake used for lipid synthesis was in the range of 11–12%, with smaller percentages for lower initial glucose levels (Supplemental Table 1). Lactate was produced ($4.2 \mu\text{mol}$) even at 0 mM glucose; it was probably formed from alanine or residual glucose from previous medium change. Glucose uptake (with respect to medium glucose) decreased from a maximal 94% at 3.5 mM to 42% at 30 mM. Conversion of glucose taken up to lactate decreased from 120% at 3.5 mM to 76% at 22 mM. The mean proportion of glucose conversion to lactate was 98% and the leakage of protons was equivalent to about 5% of the ATP obtained from lactate.

Figure 2 also presents the values of pH and pO_2 in the medium of 3T3L1 cells exposed to different glucose concentrations. The pO_2 of wells with no cells was 20.5 kPa, a figure close to that calculated from incubator atmosphere gas composition (20 kPa). The presence of cells resulted in a slight decrease of pO_2 , in a range of 18.2 kPa to 18.7 kPa, with no differences between the groups, but all of them being lower than the no-cell control well ($p < 0.05$, Student's *t* test). The high pO_2 values showed that the cells were not under hypoxic conditions.

The medium pH in the no-cell control well was 7.54, and decreased in those with cells, the lowest value, 7.28 corresponding to the highest initial glucose concentrations ($p < 0.001$ for initial glucose; one way ANOVA). The acidification was due to proton leakage from the cells, proportional to glucose concentration.

Gene expression during the differentiation of 3T3L1 cells to adipocytes. Since the use of Transwells eliminated the presence of non-differentiated fibroblasts in wells containing only adipocytes³¹, we were able to refer the gene expression data to cell numbers, since the semiquantitative method used for gene expression analysis allowed this type of comparisons³². The results were presented as mean number of copies of the corresponding mRNA per cell. This is only an approximation, but given the homogeneous origin of the samples, they allow comparisons of the expression data between different groups.

Figure 3 shows the expressions of a number of representative genes of glucose metabolism, lipid synthesis, handling and storage and a few regulatory genes controlling these processes or used as signals to other tissues. All genes studied showed a significant effect of differentiation/growth on their expressions, but followed different patterns. The number of copies for lactate dehydrogenase a (muscle type), and fatty acid transporter protein Ap2 were more than three orders of magnitude higher than those with the smallest number of copies: leptin and carnitine palmitoleoyl-transferase. Hexokinase



Table 1 | Lactate dehydrogenase activity and gene expressions in liver and adipose tissue of adult male Wistar rats

parameter	units	liver	subcutaneuos WAT	epididymal WAT
lactate dehydrogenase (EC 1.1.1.27)				
tissue activity	µkat/g protein	31.2 ± 1.5 ^A	3.11 ± 0.55 ^B	1.88 ± 0.14 ^B
<i>Ldha</i> expression	pmol/g protein	12890 ± 1150 ^A	1.51 ± 0.48 ^B	0.728 ± 0.051 ^B
<i>Ldhb</i> expression	pmol/g protein	5.85 ± 0.74 ^A	1.33 ± 0.40 ^B	0.678 ± 0.101 ^B
<i>Ldha/Ldhb</i> expression ratio		2203	1.13	1.07
expression of genes for enzymes controlling fatty acid synthesis/pyruvate oxidation				
<i>Acc1</i> (acetyl-CoA carboxylase 1)	fmol/g protein	2360 ± 245 ^A	175 ± 63 ^B	109 ± 19 ^B
<i>Fas</i> (fatty acid synthase)	pmol/g protein	7.22 ± 0.70 ^A	10.84 ± 4.38 ^{AB}	1.24 ± 0.28 ^B
<i>Pdk4</i> (pyruvate dehydrogenase kinase 4)	fmol/g protein	866 ± 105 ^A	174 ± 63 ^B	13 ± 4 ^C

Non-individual values are the mean ± sem of 6 different animals. Groups with different superscript letter are significantly different ($p < 0.05$, one-way ANOVA).

and pyruvate dehydrogenase kinase 4 showed a similar pattern: increased expression during the development period followed by a drop in the largest adipocytes. Preadipocyte factor 1, as expected, showed a reverse pattern, high on fibroblasts and lower in all adipocytes. The rest of genes studied followed a similar time-related pattern, increasing their expression during the different stages of differentiation from fibroblasts to a maximum in 9-day mature adipocytes.

Gene expression modulation during exposure to changing glucose concentration in the medium. In Figure 4, the effects of medium glucose on gene expression are shown. Here, the significance of differences between groups was limited to hexokinase, phosphofructokinase (muscle type), lactate dehydrogenase a (muscle type), carnitine palmitoleoyl-transferase, hormone-sensitive lipase, adipose TAG lipase, PPAR γ , 11 β -hydroxysteroid dehydrogenase type 1 and leptin. Most patterns showed slight changes only, with lowest expression values at 30 mM glucose; the typical pattern, better exemplified by hexokinase showed a slight rise from 0 mM to 3.5 mM glucose followed by a progressive decrease in expression with increasing medium glucose. There was a lack of significant changes in all genes coding for enzymes implicated in lipid synthesis in spite of the actual increase in TAG synthesis (i.e. fat stores grew) in parallel to medium glucose. The expression of the main lactate dehydrogenase (muscle type) isoform decreased in spite of increasing lactate production with high medium glucose.

The ratio of transcripts per cell between total lactate dehydrogenase and muscle type enzyme gave a mean of $94.3 \pm 0.3\%$ of transcripts for muscle type enzyme, i.e. practically all (ratio in the range of 19/20). Thus, 3T3L1 cell lactate dehydrogenase belongs to the muscle type isozyme.

In vivo analysis of rat tissue lactate and lactate dehydrogenase. Table 1 shows the lactate dehydrogenase activity in the rat tissues tested, as well as the expressions of lactate dehydrogenases and a genes controlling fatty acid synthesis. Liver lactate dehydrogenase activity was one order of magnitude higher per g of protein than that of WAT. However, the differences in expression of the genes for this enzyme were much higher, between 3 and 4 orders of magnitude larger: i.e. WAT lactate dehydrogenase activity was related to a much lower amount of copies of both mRNA^{Ldha} and mRNA^{Ldhb} than liver in spite of the latter higher specific activity.

WAT locations showed similar expressions of both genes coding for lactate dehydrogenases, which suggests that in adult male rats half of the transcripts were of the muscle subtype and the other half of the heart isoform, whilst the liver was overwhelmingly of the muscle type as has been previously established³³. All gene expressions investigated showed that subcutaneous WAT had higher expression levels than epididymal WAT, the differences being, however, not significant, in part because of high individual variation. The expression of *Acc1* and *Pdk4* were one order of magnitude lower in WAT than

those of *Ldha* and *Ldhb*, but not than that of *Fas*, which also showed the highest variability.

Table 2 presents the plasma levels of lactate and glucose in blood plasma, and the concentrations of lactate in tissue (per g of tissue and as molality fraction), as well as the molality quotients between tissues and plasma. Glycemia was relatively high for normal rats (they were under isoflurane anesthesia, which increases glycemia, when killed), but was maintained within the range of normalcy for this stock. The levels of tissue lactate in liver (µmol/g) were four-fold higher than the circulating plasma levels, but those of WAT were lower. However, when only water space was taken into account (i.e. discarding the mass of TAG), the molality ratios of tissue lactate to plasma showed that in both WAT sites and liver, tissue lactate concentration was higher than in plasma.

Discussion

A key finding of this study is that lactate production by 3T3L1 adipocytes is not a consequence of hypoxia. Direct measurement of pO₂ showed that cultured cells had higher oxygen availability than that of blood plasma. Along the whole process of differentiation and growth, only a fraction of the widely available medium glucose was converted to TAG, whilst a larger proportion of the available glucose was converted to lactate through a fully anaerobic pathway.

Why was so much glucose metabolized anaerobically (i.e. wasted from the point of view of carbon or energy utilization) in the presence of sufficient oxygen to sustain a more efficient aerobic glucose oxidation? Did the cells show a Warburg effect^{28,30}? It is plausible that a Warburg-like mechanism may suffice to cover the cell energy needs under conditions of rapid growth and abundance of energy substrates, since the ATP yield of glycolysis may be enough for rapid cell buildup, as in tumors²⁹. However, the results we obtained do not support a Warburg-like effect for adipocytes, since the ability to use glucose through glycolysis to lactate as end-product was parallel to cell differentiation and lipid accrual. It may be expected to find a maximal Warburg effect at the earlier stages of differentiation, i.e. fibroblasts, but we observed just the reverse. In addition, we found no cell proliferation (cells' numbers did not increase; adipocytes only grew larger), another factor for active glycolysis in the presence of oxygen³⁰.

Lactate production in the presence of varying proportions of glucose suggests that the adipocyte is probably a "obligatory glycolytic" cell. In fact, mature adipocytes produced lactate even at glucose 0 mM (probably from alanine and/or remnants of previous medium). Glycolysis, apparently, took precedence upon lipid synthesis and storage (as shown by the different accrual of biomass). Medium glucose did not affect the expression of enzymes implied in the synthesis of fat, but modified those affecting its degradation and the incorporation of exogenous fatty acids. The strictest control was apparently directed, in fact to limit the entry of glucose into the cells (i.e. hexokinase³⁴) and to lower the expression of lactic acid dehydrogenases, perhaps to regulate glucose wasting. Nevertheless, the

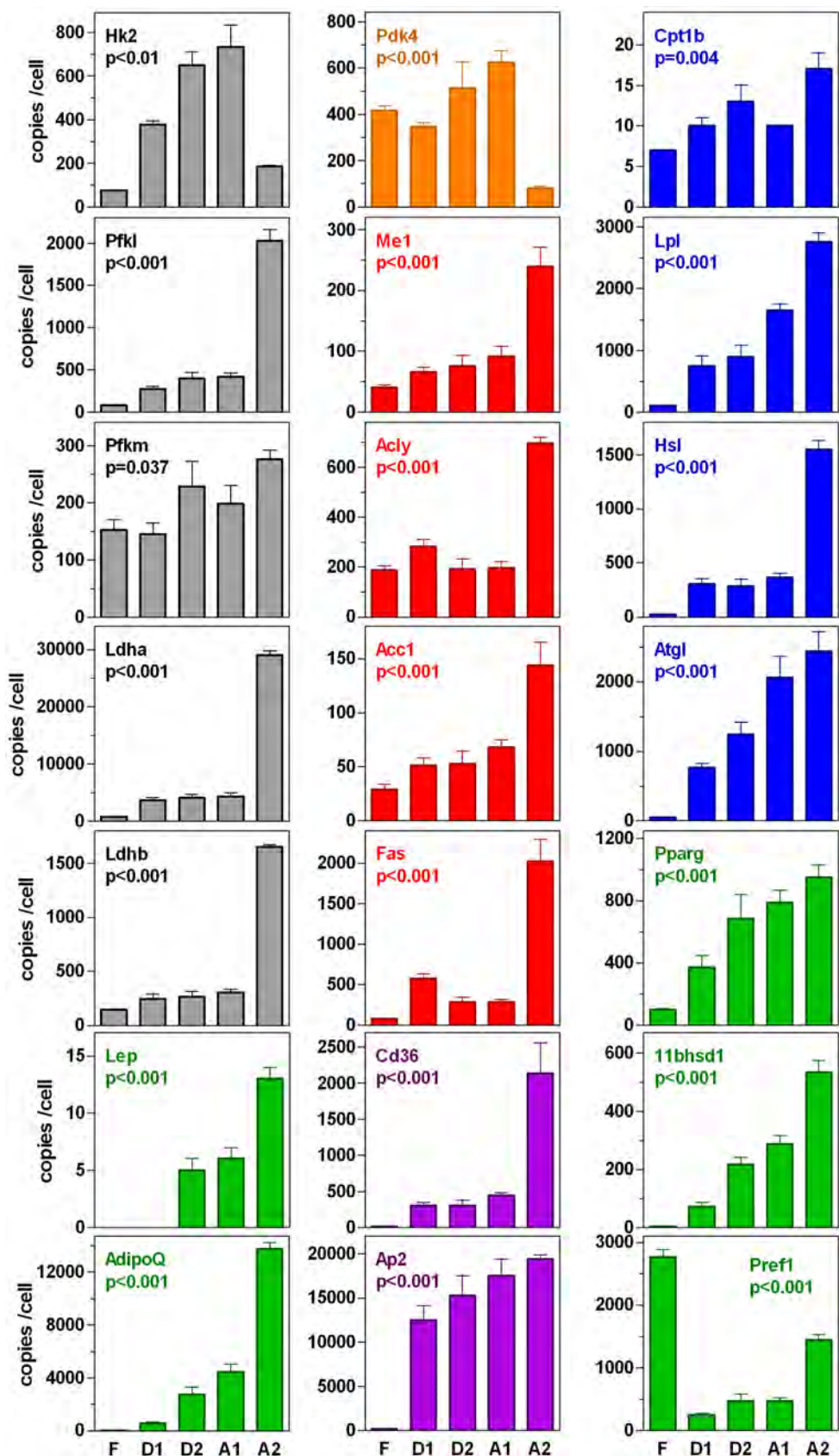


Figure 3 | Levels of expression of key genes in 3T3L1 cells during the differentiation process from fibroblasts (at confluence) to mature adipocytes. F = fibroblasts at confluence; D1 = end of the treatment with the first differentiation medium; D2 = end of the treatment with the second differentiation medium; A1 = mature adipocytes (day 6); A2 = mature adipocytes (day 9). The columns represent the mean (\pm sem) number of copies of the corresponding mRNA per cell at the different stages of differentiation. The statistical significance of changes along the process (one-way ANOVA) is given within each panel. Grey: carbohydrate catabolism pathways; Orange: 3C to 2C conversion; Red: lipogenesis; Blue: TAG catabolism; Purple: fatty acid transport; Green: regulatory agents.

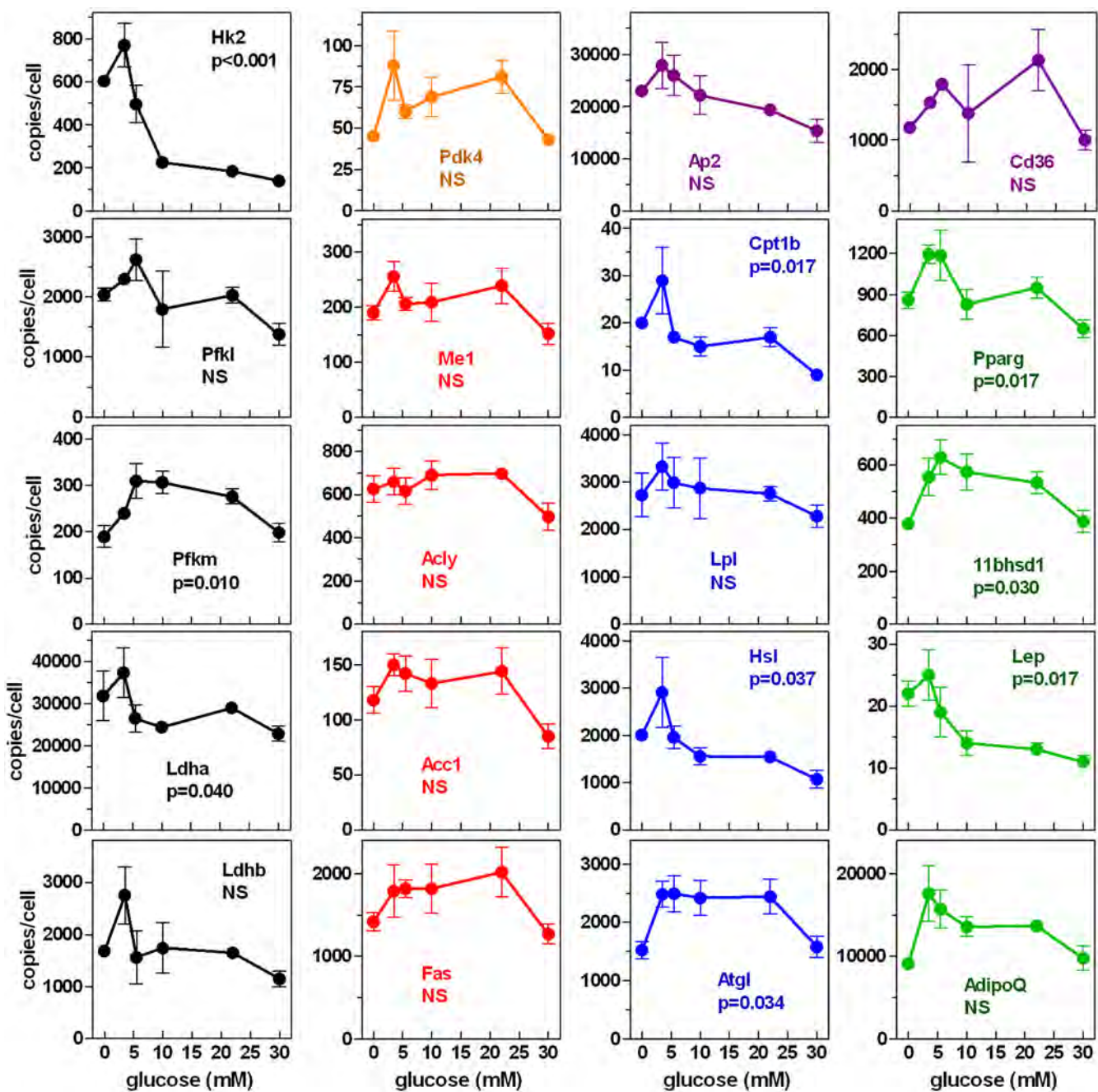


Figure 4 | Levels of expression of key genes in mature 3T3L1 adipocytes incubated during three days at different glucose concentrations in the medium. Points represent the mean (\pm sem) number of copies of the corresponding mRNA per cell. The statistical significance of the effect of medium glucose concentration (one-way ANOVA) is given within each panel. Grey: carbohydrate catabolism pathways; Orange: 3C to 2C conversion; Red: lipogenesis; Blue: TAG catabolism; Purple: fatty acid transport; Green: regulatory agents.

amount of glucose broken up to lactate was sustained at high rates even at the highest glucose concentrations.

Uncoupling of mitochondrial oxidative phosphorylation in 3T3L1 cells increases glycolysis to lactate at the expense of lipogenesis³⁵. The sum of the largely anaerobic processes of synthesis of TAG and glycolysis to lactate accounted for practically all glucose. When the protons released (i.e. not used by the mitochondria for energy) were taken into account as their energy equivalent, the conclusion was that 3T3L1 cells had practically nil needs (and, consequently, consumption) of oxygen under the conditions tested.

The lack of changes in pO_2 with increasing medium glucose levels also hints at the lack of relationship between the abundance of the cells' main substrate and oxidative metabolism. The data we present

here suggest that 3T3L1 adipocytes are essentially anaerobic even during lipogenesis and TAG storage. However, it must be taken into account that WAT contains other types of fully aerobic cells (stromal) in addition to adipocytes, and thus WAT as a whole may be more susceptible to hypoxia than its main constituent, adipocytes alone. Our results using 3T3L1 cells can be safely attributed solely to adipocytes³¹.

Our *in vivo* data show that WAT lactate dehydrogenase activity was relatively high in comparison with other enzyme activities of the tissue. Lactate molality ratios vs. plasma were always positive, thus, rat WAT produced lactate under standard conditions, in agreement with the existence of lactate gradients in animal and human models^{14,16}. Circulating lactate is increased in the immediate postprandial

**Table 2 | Lactate concentrations in plasma, liver and adipose tissue of adult male Wistar rats**

tissue lactate	parameter	units	liver	subcutaneous WAT	epididymal WAT	blood plasma
plasma glucose		mM				9.84 ± 0.42
tissue water content		g water/g tissue	0.77	0.36	0.17	0.91
tissue lactate concentration	μmol/g tissue (mM in plasma)	14.6 ± 0.75 ^A		2.08 ± 0.71 ^{BC}	1.68 ± 0.23 ^B	3.10 ± 0.29 ^C
	μmol/g water (molality)	19.0		5.8	10.1	3.4
tissue/plasma molality ratio			5.6	1.7	3.0	1.0

Non-individual values are the mean ± sem of 6 different animals. Groups with different superscript letter are significantly different ($p < 0.05$, one-way ANOVA).

state, rising later than glucose and insulin³⁶. The process is quantitatively important, since, in insulin-resistant humans, WAT converts to lactate up to 2/3 of all glucose taken up¹³. The rapid conversion of glucose to lactate has been also observed *in vivo*, in human subcutaneous WAT^{16,37}, at rates that exceed the relatively low needs for energy of WAT itself. High liver lactate molality ratios reflect its role as lactate receptor in the Cori cycle, since lactate is a prime substrate for gluconeogenesis¹⁵.

Adipocytes, by massively breaking up glucose to lactate (especially when WAT mass is large), lower glycemia, thus contributing to maintain glucose homeostasis. The process is mainly sustained by large adipocytes⁹, thus we can assume that WAT glucose removal (and overall lactate production) are increased in obesity³⁸, in spite of locally reduced blood flow and access to substrates.

High glucose levels tend to decrease the relative ability of 3T3L1 cells to produce lactate from glucose (lower gene expressions); but, in absolute terms, this was not translated into decreased lactate production. We can speculate that the limit of glucose uptake and lactate production may, rather, depend on the ability to use the ATP generated, since the net ATP consumption of lipogenesis is small (Supplemental Figures 3 and 4), and its needs for adipocyte maintenance are limited.

From the data presented we can postulate an additional role for adipocytes in energy homoeostatic regulation: WAT helps decrease plasma glucose, especially under hyperglycemia, and thus indirectly improving insulin resistance³⁹. As indicated above, WAT is the last dumping site for glucose under insulin resistance-induced hyperglycemia^{27,40}. In WAT, excess glucose is used, in part, to build up TAG stores, but most of the glucose, unwanted elsewhere, is converted to lactate, which could be used as substrate by a number of tissues^{41,42}. Most of circulating lactate, however, is taken up by the liver⁴³ and oxidized to pyruvate. Under conditions of excess glucose, in the liver, the gluconeogenic pathway remains inhibited⁴⁴, and the excess 3C is oxidized to acetyl-CoA via pyruvate dehydrogenase, followed by oxidation in the Krebs cycle (if not already saturated), or its utilization in other pathways. Since ketogenesis is also inhibited by glucose⁴⁵, practically the only path open is lipogenesis, fully operational for lactate in the liver⁴⁶. Accumulation of newly formed lipid may hamper liver function (steatosis), but liver TAG may be exported (via lipoproteins) to other tissues, including WAT, which thus receives the “unwanted glucose carbon” as lipoprotein-carried TAG fatty acids, aggravating the WAT problem of TAG storage.

In the long term, the process outlined may help extend the damages caused by excess nutrients, but on the short term may help limit the effects of sustained glucose peaks, facilitate energy partition via distribution of 3C substrates and the centralization (and control) of fat synthesis in the liver rather than in disperse WAT sites. The process we postulate is a bidirectional transposition of the well known glucose-fatty acid (or Randall) cycle⁴⁷.

In conclusion, cultured adipocytes are largely anaerobic, and produce huge amounts of lactate from glucose in normoxic conditions. It is speculated that the massive production of lactate, directly related to glucose availability, is a process of defense of the adipocyte, exporting

glucose carbon (and the problem) to the liver as lactate, but it may be also a mechanism of control of hyperglycemia. The *in vivo* data obtained from male rats agree with this interpretation.

Methods

Effects of differentiation of 3T3L1 cells on gene expression and substrate utilization.

A batch of 3T3L1 fibroblasts was allowed to grow and differentiate under standard conditions, as described in the Supplemental Procedures, using Transwell™ inserts (Corning Life Sciences)³¹. Cells were harvested at 0, 2, 4, 6 and 9 days after the beginning of fibroblast differentiation (i.e., day 0 cultures contained only confluent fibroblasts, and days 6–9 only mature adipocytes). Cells were harvested, counted and their total RNA extracted using the GenElute™ (RTN10, RTN70 and RTN350, from Sigma-Aldrich) isolation procedure, following the instructions of the provider. RNA was used for the gene expression analysis. Media were used for the analysis of glucose, lactate and proton leakage (as described in the Supplemental Procedures).

Cultured 3T3L1 cells exposure to different medium glucose concentrations.

Mature 3T3L1 adipocytes (i.e., on day 6 after fibroblast confluence as described above) were used for the analysis of the effect of medium glucose concentration. The medium was prepared omitting glucose, which was added to final concentrations of 0, 3.5, 5.5, 10, 22 or 30 mM. These media were used the last three days of incubation, substituting the standard 22 mM glucose medium. Spent media were used for the analysis of pH, glucose and lactate concentrations. The cells were harvested, counted and used for the extraction of total RNA for gene expression analysis.

pO₂ in the medium during incubation conditions. During the cells' exposure to different glucose concentrations, on day 9 (i.e., before harvesting), the medium pO₂ was measured using 1 mL syringes equilibrated at 37°C, which were filled with medium and resealed. Measurements of pH and pO₂ were done within 15 min, using an ABL-5 gas analyzer (Radiometer; Copenhagen Denmark). Control wells contained fresh medium and were incubated with no cells.

Analysis of gene expression in cultured 3T3L1 cells. Total RNA from harvested cells in different experiments was quantified using a ND-100 spectrophotometer (Nanodrop Technologies, Wilmington DE USA). RNA samples were reverse transcribed using the MMLV reverse transcriptase (Promega, Madison, WI USA) and oligo-dT primers.

Real-time PCR amplification was carried out using 10 μL amplification mixtures containing Power SYBR Green PCR Master Mix (Applied Biosystems, Foster City, CA USA), equivalent to 4 ng of reverse-transcribed RNA and 150 nM primers. Reactions were run on an ABI PRISM 7900 HT detection system (Applied Biosystems) using a fluorescent threshold manually set to OD 0.150 for all runs. The primers used for the estimation of murine (3T3L1 cells) gene expression are presented in Supplemental Table 2.

A semiquantitative approach for the estimation of the concentration of specific gene mRNAs per cell or unit of tissue weight was used³². *Rpl32* was used as charge control gene. The data were presented as the number of transcript copies per cell, allowing for direct comparisons independently of the number of cells in a given well.

In vivo study. Animals and housing conditions. Nine week old male Wistar rats (Harlan Laboratories Models, Sant Feliu de Codines, Spain) were used. The rats (N = 6) were housed in two 3-rat cages, had free access to water and were kept in a controlled environment (lights on from 08:00 to 20:00; 21.5–22.5°C; 50–60% humidity), and were fed standard rat chow (2014, Harlan).

The rats were kept, handled and killed following the procedures specifically approved by the University of Barcelona Animal Welfare and Ethics Committee, in accordance with the Rules set by the European Union and the Governments of Spain and Catalonia.

The animals were killed by exsanguination through the aorta under isoflurane anesthesia; samples of liver and WAT at the inguinal subcutaneous and epididymal fat pads were sampled, frozen in liquid nitrogen, and stored at -80°C. Blood plasma was separated from (heparinized) blood and kept frozen at -80°C.



Tissue lactate. Frozen tissue samples were weighed and homogenized in about 20 volumes of chilled water: acetone, to a final proportion of 1 : 1.2⁴⁸. The samples were centrifuged at 0°C for 20 min at 4000 × g. Supernatants were delipidated (when needed) with finely powdered solid MgO, and used for the measurement of lactate (in parallel to plasma glucose and lactate) using the same procedures described (Supplemental Procedures) for cultured cell media.

Tissue and plasma lactate concentrations were expressed in molar units per g of fresh tissue weight, but also, as an estimate, per g of tissue water (molality). Adipose tissues contain about 70–80% of fat, which reduces considerably their water (and lactate) space¹⁹. The tissue (and plasma) water (i.e., lactate space) was estimated as shown in Supplemental Table 3. Calculation of theoretical tissue lactate concentration in these volumes of water was used to estimate the mean tissue vs. plasma lactate molality concentration ratios.

Measurement of lactate dehydrogenase activity. Frozen samples of liver were homogenized using a tissue disruptor (IKA-T10 basic Ultra-Turrax, IKA, Stauffen Germany) in 10 volumes of chilled Krebs-Ringer bicarbonate solution, pH 7.8 containing 5 mM dithiothreitol, 0.5% bovine serum albumin, 1% dextran (MW 200,000), 0.1% Triton X-100, and 1 mM EDTA⁵⁰. Adipose tissue samples were homogenized in the same way as liver, but the homogenates were left standing for 5 min at 4°C. Sediments and floating fat-cakes were discarded, and only the intermediate layer was pipetted for lactate dehydrogenase activity. Homogenate protein was also estimated⁵¹, using homogenization medium for blanks.

Total lactate dehydrogenase (EC 1.1.1.27) activity was measured in liver and WAT homogenates, using a standard kinetic NADH-oxidation UV method⁵² to determine V_i values. Activity was expressed as nmkat/g of wet tissue and μkat/g of protein.

Analysis of gene expression in rat liver and WAT. Tissue total RNA was extracted from frozen tissue samples (about 30 mg) using the GenElute™ procedure. Gene expression was estimated as described for cultured cells, using a different set of primers; the list is presented in Supplemental Table 2. The semiquantitative approach described above was used for the estimation of the number of specific mRNA copies for each gene per unit of tissue weight and per g of protein. The genes studied coded for lactic acid dehydrogenases (muscle and heart), two key enzymes of fatty acid synthesis: acetyl-CoA carboxylase and fatty acid synthetase; and pyruvate kinase 4, which controls the use of pyruvate for oxidation to Acetyl-CoA. The *Ppia* gene was used as control of charge.

Statistical analyses. Comparisons between groups were done using one-way ANOVA analyses and the Bonferroni post-hoc test with the Prism 5 (GraphPad Software, San Diego CA USA) graphics/statistics package. Analysis of correlations and curve fitting were done using the same program. The Student's *t* test was also used for comparison between isolated data groups.

- Weber, G., Banerjee, G. & Ashmore, J. Activities of enzymes involved in glycolysis, gluconeogenesis and hexosemonophosphate shunt in rat adipose tissue. *Biochem. Biophys. Res. Commun.* **3**, 182–186 (1960).
- Atsumi, T. *et al.* Expression of inducible 6-phosphofructo-2-kinase/fructose-2,6-bisphosphatase/PFKB3 isoforms in adipocytes and their potential role in glycolytic regulation. *Diabetes* **54**, 3349–3357 (2005).
- Acheson, K. J. *et al.* Glycogen storage capacity and de novo lipogenesis during massive carbohydrate overfeeding in man. *Am. J. Clin. Nutr.* **48**, 240–247 (1988).
- Shadid, S., Koutsari, C. & Jensen, M. D. Direct free fatty acid uptake into human adipocytes in vivo. Relation to body fat distribution. *Diabetes* **56**, 1369–1375 (2007).
- Lasunción, M. A. & Herrera, E. “In vitro” utilization of labelled esterified fatty acids and glyceride glycerol from triglyceride-rich lipoproteins in rat adipose tissue. *Horm. Metabol. Res.* **13**, 335–339 (1981).
- Weinstock, P. H. *et al.* Lipoprotein lipase controls fatty acid entry into adipose tissue, but fat mass is preserved by endogenous synthesis in mice deficient in adipose tissue lipoprotein lipase. *Proc. Natl. Acad. Sci. USA* **94**, 10261–10266 (1997).
- Thacker, S. V., Nickel, M. & DiGirolamo, M. Effects of food restriction on lactate production from glucose by rat adipocytes. *Am. J. Physiol.* **233**, E336–E342 (1977).
- Jansson, P. A., Smith, U. & Lonnroth, P. Evidence for lactate production by human adipose tissue in vivo. *Diabetologia* **33**, 253–256 (1990).
- DiGirolamo, M., Newby, F. D. & Lovejoy, J. Lactate production in adipose tissue: a regulated function with extra-adipose implications. *FASEB J.* **6**, 2405–2412 (1992).
- Newby, F. D., Wilson, L. K., Thacker, S. V. & DiGirolamo, M. Adipocyte lactate production remains elevated during refeeding after fasting. *Am. J. Physiol.* **259**, E865–E871 (1990).
- King, J. L. & DiGirolamo, M. Lactate production from glucose and response to insulin in perfused adipocytes from mesenteric and epididymal regions of lean and obese rats. *Obesity Res.* **6**, 69–75 (2001).
- Nellemann, B., Gormsen, L. C., Sørensen, L. P., Christiansen, J. S. & Nielsen, S. Impaired insulin-mediated antilipolysis and lactate release in adipose tissue of upper-body obese women. *Obesity* **20**, 57–64 (2012).
- Kashivagi, A. *et al.* In vitro insulin resistance of human adipocytes isolated from subjects with noninsulin-dependent diabetes mellitus. *J. Clin. Invest.* **72**, 1246–1254 (1983).
- Newby, F. D., Sykes, M. N. & DiGirolamo, M. Regional differences in adipocyte lactate production from glucose. *Am. J. Physiol.* **255**, E716–E722 (1988).
- Cori, C. F. The glucose-lactic acid cycle and gluconeogenesis. *Curr. Top. Cell. Regulat.* **18**, 377–387 (1981).
- Hagström, E., Arner, P., Ungerstedt, U. & Bolinder, J. Subcutaneous adipose tissue: a source of lactate production after glucose ingestion in humans. *Am. J. Physiol.* **258**, E888–E893 (1990).
- Sahlin, K. Lactate formation and tissue hypoxia. *J. Appl. Physiol.* **67**, 2640 (1989).
- Sestoft, L., Bartels, P. D. & Folke, M. Pathophysiology of metabolic acidosis: effects of low pH on the hepatic uptake of lactate, pyruvate and alanine. *Clin. Physiol.* **2**, 51–58 (1982).
- Soares, A. F. *et al.* Effects of oxidative stress on adiponectin secretion and lactate production in 3T3-L1 adipocytes. *Free Radic. Biol. Med.* **38**, 882–889 (2005).
- Carrière, A. *et al.* Mitochondrial reactive oxygen species control the transcription factor CHOP-10/GADD153 and adipocyte differentiation - A mechanism for hypoxia-dependent effect. *J. Biol. Chem.* **279**, 40462–40469 (2004).
- del Rio, R., Moya, E. A. & Iturriaga, R. Differential expression of pro-inflammatory cytokines, endothelin-1 and nitric oxide synthases in the rat carotid body exposed to intermittent hypoxia. *Brain Res.* **1395**, 74–85 (2011).
- Hosogai, N. *et al.* Adipose tissue hypoxia in obesity and its impact on adipocytokine dysregulation. *Diabetes* **56**, 901–911 (2007).
- Goossens, G. H. *et al.* Increased adipose tissue oxygen tension in obese compared with lean men is accompanied by insulin resistance, impaired adipose tissue capillarization, and inflammation. *Circulation* **124**, 67–76 (2011).
- Hodson, L., Humphreys, S. M., Karpe, F. & Frayn, K. N. Metabolic signatures of human adipose tissue hypoxia in obesity. *Diabetes* **62**, 1417–1425 (2013).
- McQuaid, S. E. *et al.* Downregulation of adipose tissue fatty acid trafficking in obesity. A driver for ectopic fat deposition? *Diabetes* **60**, 47–55 (2011).
- Bohr, C., Hasselbalch, K. & Krogh, A. Über einen in biologischer Beziehung wichtigen Einfluss, den die Kohlensäurespannung des Blutes auf dessen Sauerstoffbindung übt. *Scand. Arch. Physiol.* **16**, 402–412 (1904).
- Alemany, M. Regulation of adipose tissue energy availability through blood flow control in the metabolic syndrome. *Free Radic. Biol. Med.* **52**, 2108–2119 (2012).
- Warburg, O. On the origin of cancer cells. *Science* **132**, 309–314 (1956).
- López-Lázaro, M. The Warburg effect: Why and how do cancer cells activate glycolysis in the presence of oxygen? *Anti-Cancer Ag. Med. Chem.* **8**, 305–312 (2008).
- van der Heiden, M. G., Cantley, L. C. & Thompson, C. B. Understanding the Warburg effect: The metabolic requirements of cell proliferation. *Science* **324**, 1029–1033 (2009).
- Sabater, D., Fernández-López, J. A., Remesar, X. & Alemany, M. The use of Transwells™ improves the rates of differentiation and growth of cultured 3T3L1 cells. *Anal. Bioanal. Chem.* **405**, 5605–5610 (2013).
- Romero, M. M., Grasa, M. M., Esteve, M., Fernández-López, J. A. & Alemany, M. Semiquantitative RT -PCR measurement of gene expression in rat tissues including a correction for varying cell size and number. *Nutr. Metab.* **4**, 26 (2007).
- Everse, J. & Kaplan, N. O. Lactate dehydrogenases: structure and function. *Adv. Enzymol. Rel. Ar. Mol. Biol.* **37**, 61–133 (1973).
- DiPietro, D. L. Hexokinase of white adipose tissue. *Biochim. Biophys. Acta* **67**, 305–312 (1963).
- Si, Y. G., Shi, H. & Lee, K. B. Metabolic flux analysis of mitochondrial uncoupling in 3T3-L1 adipocytes. *PLoS One* **4**, e7000 (2009).
- Lovejoy, J., Mellen, B. & DiGirolamo, M. Lactate generation following glucose ingestion. Relation to obesity, carbohydrate tolerance and insulin sensitivity. *Int. J. Obesity* **14**, 843–855 (1990).
- van der Merwe, M. T. *et al.* Lactate and glycerol release from subcutaneous adipose tissue in black and white lean men. *J. Clin. Endocrinol. Metab.* **84**, 2888–2895 (1999).
- Märin, P., Rebiffé-Scrive, M., Smith, U. & Björntorp, P. Glucose uptake in human adipose tissue. *Metabolism* **36**, 1154–1160 (1987).
- Muñoz, S. *et al.* Chronically increased glucose uptake by adipose tissue leads to lactate production and improved insulin sensitivity rather than obesity in the mouse. *Diabetologia* **53**, 2417–2430 (2010).
- Alemany, M. The defense of adipose tissue against excess substrate-induced hyperthrophia: Immune system cell infiltration and arrested metabolic activity. *J. Clin. Endocrinol. Metab.* **96**, 66–68 (2011).
- Granata, A. L., Midrio, M. & Corsi, A. Lactate oxidation by skeletal muscle during sustained contraction in vivo. *Pflügers Arch. Eur. J. Physiol.* **366**, 247–250 (1976).
- Lopaschuk, G. D., Collins-Nakai, R. L. & Itoi, T. Developmental changes in energy substrate use by the heart. *Cardiovasc. Res.* **26**, 1172–1180 (1992).
- Radziuk, J. & Pye, S. Hepatic glucose uptake, gluconeogenesis and the regulation of glycogen synthesis. *Diabet. Metab. Res. Rev.* **17**, 250–272 (2001).
- Rognstad, R. Control of lactate gluconeogenesis by glucose in rat hepatocytes. *Arch. Biochem. Biophys.* **217**, 498–502 (1982).
- Edson, N. L. Ketogenesis-antiketogenesis. Substrate competition in liver. *Biochem. J.* **30**, 1862–1869 (1936).
- O’Hea, E. K. & Leveille, G. A. Significance of adipose tissue and liver as sites of fatty acid synthesis in the pig and the efficiency of utilization of various substrates for lipogenesis. *J. Nutr.* **99**, 338–344 (2013).



47. Randle, P. J., Garland, P. B., Hales, C. N. & Newsholme, E. A. The glucose fatty-acid cycle: its role in insulin sensitivity and the metabolic disturbances of diabetes mellitus. *Lancet* **281**, 785–789 (1963).
48. Soley, M. & Alemany, M. A rapid method for the estimation of amino acid concentration in liver tissue. *J. Biochem. Biophys. Meth.* **2**, 207–211 (1980).
49. Robert, M. & Alemany, M. Water compartments in the tissues of pentobarbital anesthetized rats. *IRCS Med. Sci.* **9**, 236–237 (1981).
50. Remesar, X., Arola, L., Palou, A. & Alemany, M. Arginase activity in the organs of fed and 24-hours fasted rats. *Horm. Metabol. Res.* **12**, 281–282 (1980).
51. Wang, C. S. & Smith, R. L. Lowry determination of protein in the presence of Triton X-100. *Anal. Biochem.* **63**, 414–417 (1975).
52. Bergmeyer, H. U. & Bernt, E. Lactate dehydrogenase UV assay with pyruvate and NADPH (eds. Bergmeyer, H. U. & Bernt, E.) 7–75 (Verlag Chemie, Weinheim, 1974).

Acknowledgments

Thanks are given to Dr. M. Riera, from the Department of Physiology, Faculty of Biology, University of Barcelona, for his help and guidance in the sampling, calibration and measuring of oxygen partial pressure in cell cultures. This study was financed in part by grants SAF2009-11739, AGL2011-23635, and SAF2012-34895, of the Plan Nacional de Investigación of the Government of Spain. CIBER Obesity and Nutrition (an initiative of the Institute of Health Carlos III of the Government of Spain) paid the salary of M.M.

Romero, S. Arriarán was recipient of a pre-doctoral grant from the Government of Catalonia. Dr. D. Sabater and S. Agnelli worked *pro bono* for most of the study.

Author contributions

D.S. did all work on cell cultures, S.Ar. and S.Ag. did the *in vivo* studies including gene expression; M.M.R. analyzed cultured cells gene expressions; X.R. and J.A.F.L. carried out the analyses of media and did the statistics; M.A. did the experimental design and wrote the draft. All Authors participated in the discussion of the results and in the final redaction.

Additional information

Supplementary information accompanies this paper at <http://www.nature.com/scientificreports/>

Competing financial interests: The authors declare no competing financial interests.

How to cite this article: Sabater, D. *et al.* Cultured 3T3L1 adipocytes dispose of excess medium glucose as lactate under abundant oxygen availability. *Sci. Rep.* **4**, 3663; DOI:10.1038/srep03663 (2014).

This work is licensed under a Creative Commons Attribution-NonCommercial-NoDerivs 3.0 Unported license. To view a copy of this license, visit <http://creativecommons.org/licenses/by-nc-nd/3.0/>

SUPPLEMENTAL MATERIALS

Cultured 3T3L1 adipocytes dispose of excess medium glucose as lactate under abundant oxygen availability

David **Sabater**, Sofía **Arriarán**, María del Mar **Romero**, Silvia **Agnelli**, Xavier **Remesar**, José Antonio **Fernández-López**, and Marià **Alemany**

SUPPLEMENTAL METHODS

Cells and transwell cell culture conditions

3T3L1 cells (ATCC-CL-173) were obtained from ATCC (Manassas, VA USA), and kept under liquid nitrogen; they were used at a passage not higher than 6. The cells were cultured in 6-well plates (Costar 3506, Corning Life Sciences, Corning, NY USA) with 24 mm polyester membrane Transwell inserts (Corning Life Sciences) under standard conditions as previously described ¹, using DMEM-GlutaMAX-I (Gibco Life Technologies, Roche Diagnostics, Indianapolis, IN USA) supplemented with 10% newborn calf serum (NBS; Gibco Life Technologies), 25 mM Hepes, 100 U/mL penicillin and 100 mg/L streptomycin (all from Sigma-Aldrich, St Louis MO USA). Two days post-confluence, the cells were differentiated to adipocytes using the same medium containing 10% fetal bovine serum instead of NBS (basal medium), supplemented with 5 mg/L insulin, 0,25 µM dexamethasone and 0,5 mM IBMX (all from Sigma-Aldrich) ². After two days this medium was switched to one supplemented only with insulin, and two more days later the cells were kept in the basal medium with no added hormones. The basal medium contained 3.5 mM L-alanyl-L-glutamine and 22 mM glucose as N and energy substrates, and was changed every 2 days for up to 1 week. Under the conditions used, pH was maintained in all cases between 7.4 and 7.8. The cells were incubated in an oven at 37 °C, ventilated with air supplemented with 5 % CO₂ which gave a theoretical pO₂ of 20 kPa (i.e. 0.2 mM dissolved O₂, almost twice the oxygen carried by blood plasma: 0.13 mM ³). The pCO₂ was 5 kPa, corresponding to 1.7 mM dissolved CO₂ (values calculated at 25°C, pH7.5) ⁴.

At the end of the experimental process, the spent medium was removed and the cells were harvested using trypsin (Sigma-Aldrich) and mechanical separation, following the protocol for trypsinization in transwell inserts established by the provider (Corning Life Sciences). Under these conditions, the cultures contained only plurivacuolar adipocytes, with nil presence of fibroblasts ¹ (Supplemental Figure 1).

Spent incubation media were immediately frozen until used for the analysis of glucose (kit 11504, Biosystems, Barcelona Spain) and L-lactate (kit 1001330 Spinreact, Sant Esteve d'en Bas, Spain) using standard enzymatic methods.

All inorganic products and solvents were purchased from Panreac (Castellar del Vallès, Spain) and biochemicals from Sigma-Aldrich unless otherwise indicated.

Cultured cell counting and size estimation

Harvested cells were suspended in fresh medium and then their number and size distribution were measured with a portable cell counter, Scepter™ Handheld Automated Cell Counter (PHCC20060 Scepter, Merck Millipore, Billerica, MA USA). The settings of the instrument were adjusted for adipocyte size ¹. The total volume of particles was considered “total biomass”, whilst that of particles within the 18-24 µm diameter range were

considered adipocytes⁵ and their total number and volume (“cell volume”) as well as mean cell volume were calculated from the Scepter count data (Supplemental Figure 2).

Measurement of medium pH and cell proton release/leakage

Direct pH measurements (using a standard pH meter) of the medium in wells containing cells were not different from those of spent medium just drained from the cells. A more precise measurement of spent medium pH was done by measuring the OD ratio of the medium at both 420 nm and 560 nm. Supplemental Figure 5(A) shows the visible light spectrum of the medium used (basically that of phenol red it contains). A shift in the height of the peaks corresponds to a change in the protonated *vs.* unprotonated form of the indicator, which allows the estimation of $[H^+]$ in the medium; Supplemental Figure 5(B) also shows the relationship between the 420 nm/560 nm OD ratios variations with pH.

Since the medium is a complex buffer system, the direct estimation of pH does not correspond directly to the amount of protons released by the cells to the medium, and cannot be directly calculated because of the interaction of proteins and superimposing buffers (including the phenol red indicator itself). In order to measure the effect of proton release upon the medium pH, fresh medium was titrated using 0.1 N HCl (actually 0.092 N after titration against a base) under continuous pH measurement. Since the addition of HCl altered the final volume, the pH was calculated in reference to the initial volume by expressing pH as $[H^+]$ and calculating the total protons’ concentration in the medium. The titration curve for medium pH *vs.* added H^+ is shown in Supplemental Figure 5(C). This curve allowed us to estimate the net emission of protons by the cells to the medium from the measurement of the spent medium pH.

Estimation of the glucose energy partition between oxidative and anaerobic pathways during 3T3L1 cell differentiation

In the differentiation experiment, calculations for 3T3L1 cells were referred to one cell in order to standardize the calculations obtained in different experiments and conditions. The main energy inputs to the system are the biomass of fibroblasts and the glucose drawn from the medium (i.e. initial glucose in fresh medium minus that found in spent medium). N metabolism has been left out of the equation because of difficulties in estimating total N in both cells and medium: the large amount of serum calf protein completely obscured any small change in this parameter; in addition, most “energy” in fibroblasts was protein, with almost nil triacylglycerols; in adipocytes, protein content is low (perhaps comparable to that of their fibroblast ancestors), but they accrue a high amount of fat. In addition, there are considerable technical difficulties in accurately measuring the actual fat content of cultured 3T3L1 cells, i.e. with the degree of precision needed for calculations.

Since mature adipocytes grew from non-fat storing fibroblasts we can safely assume that all their triacylglycerol stores were synthesized, during differentiation, from the glucose present in the medium. We calculated the new production of fat assuming (as an approximation) that the content of TAG in fibroblasts was negligible, thus the difference in total “biomass” between an adipocyte culture compared with an analogous fibroblast culture (with closely similar cell numbers) at confluence would give us an approximate value for net lipid (essentially TAG) synthesis during the whole process.

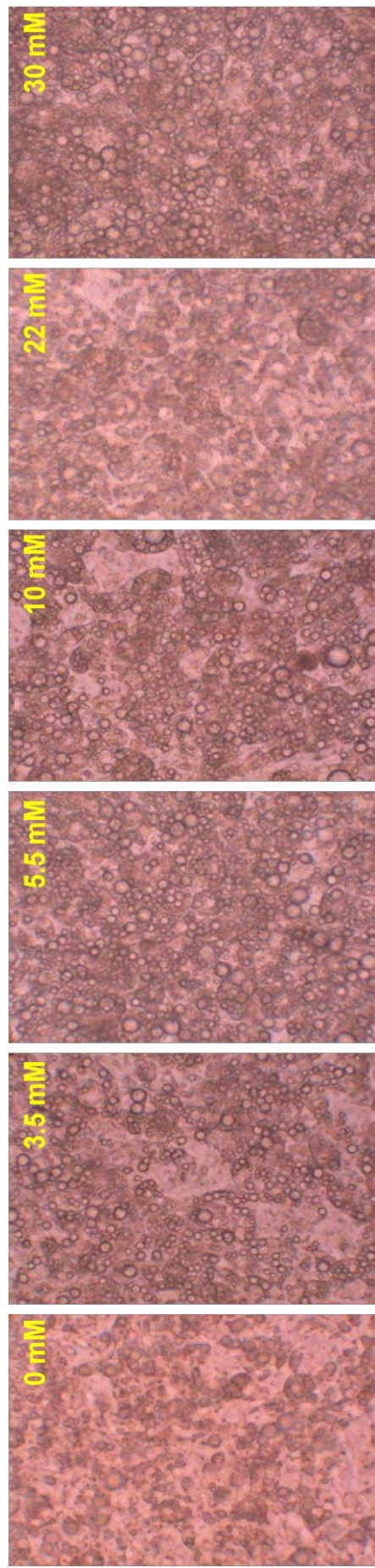
The energy outputs of cultured cells were essentially two: CO_2 from the oxidation of glucose, used for energy and the buildup of triacylglycerol reserves, as well as lactate, released in large amounts into the medium. As shown in

Supplemental Figure 3, the amount of glucose needed to synthesize 1 mmol of triacylglycerol [887 mg for *bis*-stearoyl-oleoyl-glycerol] under fully aerobic conditions are about 15.75 mmol glucose..

Cell lipid density was assumed to be 0.89 g/ml (i.e the mean of triolein, 0.915 g/ml, and tripalmitin, 0.873 g/mL), thus the volume of 1 mmol triacylglycerol corresponds to 997 µL. Since we know the total number of cells in the medium, and the total amount of glucose spent by the cells for purposes other than lactate synthesis, we can estimate the proportion of glucose used for triacylglycerol accrual to the mature adipocyte stage. Production of lactate from glucose yields only 2 ATP per mole of glucose (Supplemental Figure 4).

Supplemental Methods Reference List

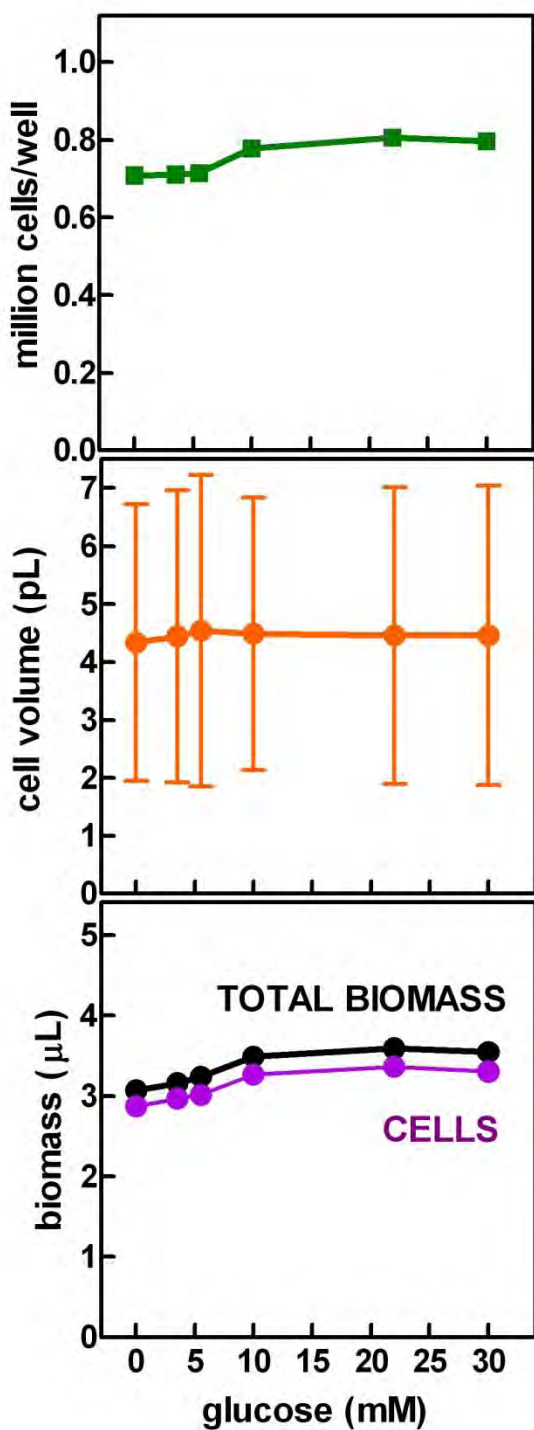
1. Sabater,D., Fernández-López,J.A., Remesar,X., & Alemany,M. The use of Transwells™ improves the rates of differentiation and growth of cultured 3T3L1 cells. *Anal. Bioanal. Chem.* **405**, 5605-5610 (2013).
2. Janssen,O.E. & Hilz,H. Differentiation of 3T3-L1 pre-adipocytes induced by inhibitors of poly(ADP-ribose) polymerase and by related noninhibitory acids. *Eur. J. Biochem.* **180**, 595-602 (1989).
3. Pitman,R.N. Oxygen transport and exchange in the microcirculation. *Microcirculation* **12**, 59-70 (2005).
4. Carroll,J.J., Sluosky,J.D., & Mather,A.E. The solubility of carbon dioxide in water at low pressure. *J. Phys. Chem. Ref. Data* **20**, 1201-1209 (1991).
5. Saiki,A. *et al.* Suppression of lipoprotein lipase expression in 3T3-L1 cells by inhibition of adipogenic differentiation through activation of the renin-angiotensin system. *Metabolism Clin. Exp.* **57**, 1093-1100 (2008).



Supplemental Figure 1

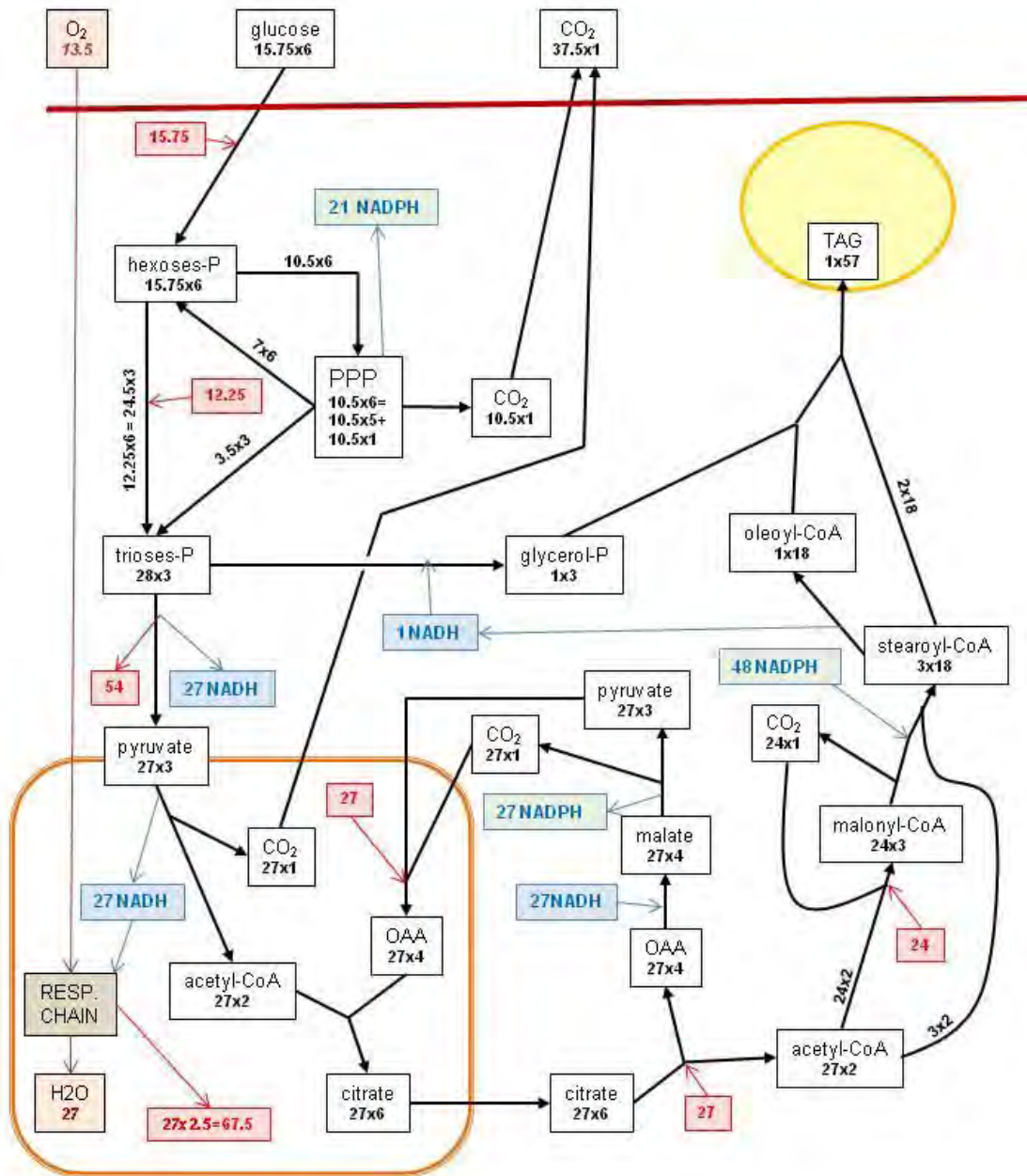
Microphotographs of mature 3T3L1 cells after 3 days of incubation on a standard medium containing glucose at the concentrations shown in each photograph.

The width of each microphotograph corresponds to 160 μm

**Supplemental Figure 2**

Cell countings, cell volume and biomass of cultured mature 3T3L1 adipocytes exposed for 3 days to a medium with variable concentrations of glucose.

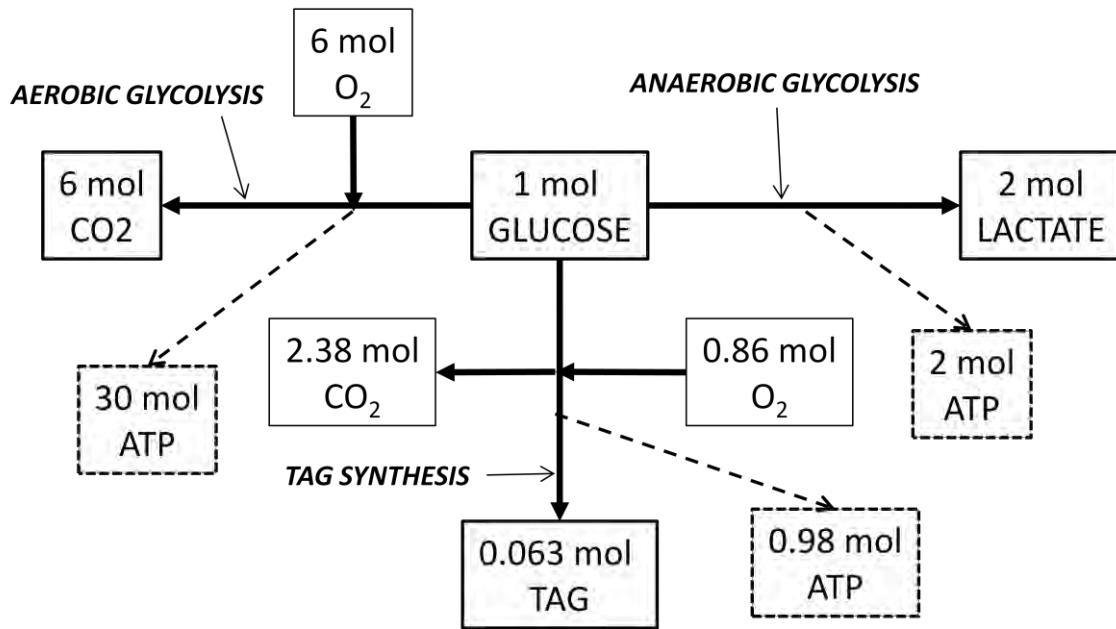
Cell counts and biomass data are presented as mean \pm SEM, but cell volume (includes thousands of individual measurements) is shown as mean \pm SD as a way to show a better representation of cell size variability.



Supplemental Figure 3

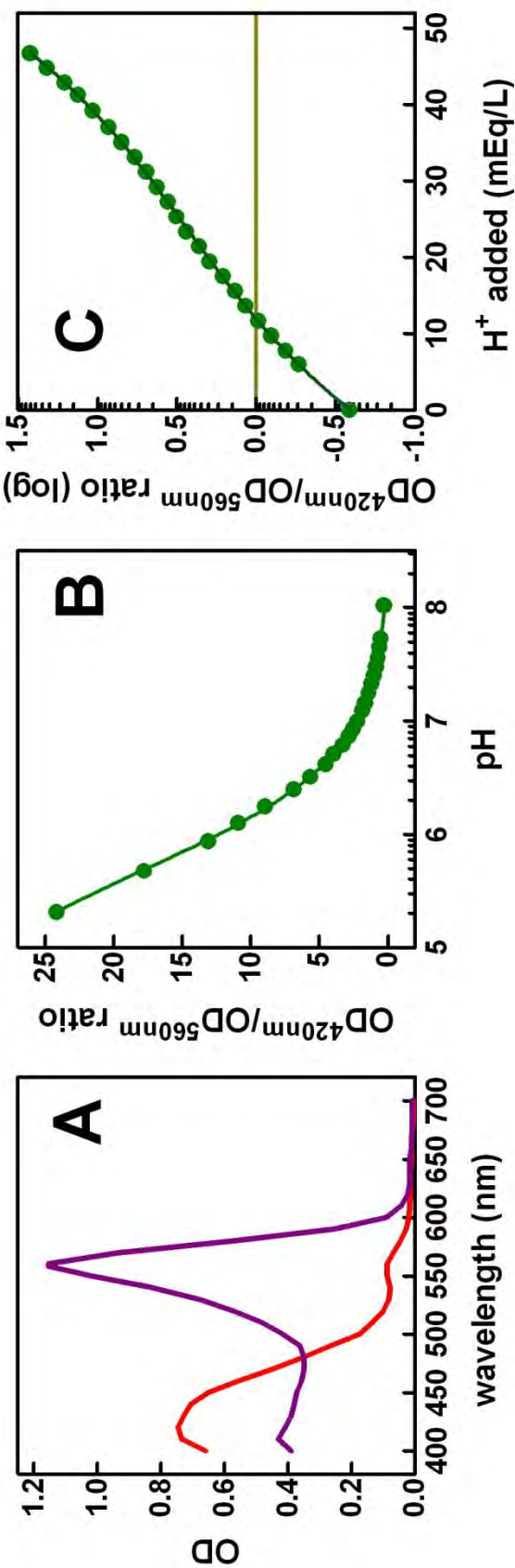
Estimation of the needs of glucose, NADPH and ATP for the synthesis of 1 mol of TAG from glucose. The figures represent the flow of C (in black); the moles of ATP produced / consumed are shown in red, and the NADH and NADPH are shown in blue.

PPP = pentose-phosphate pathway



Supplemental Figure 4

Molar relationships between glucose, triacylglycerol and lactate depending on the pathway followed for glucose utilization

**Supplemental Figure 5**

A Spectral analysis of phenol red in cultured-cell incubation medium, shown at acidic pH (red line) and at neutral pH (purple line). The acidic form of the indicator has a maximal OD response at 420 nm and 560 nm with the neutral/basic one at 560 nm.

B Relationship of the quotient of OD measured at 420 nm and 560 nm with the actual pH of the medium

C Effect of acidification of the cultured-cell incubation medium on pH or the quotient of OD at 420 nm/ OD at 560 nm.

Supplemental Table 1

Fate of the glucose taken up by mature 3T3L1 adipocytes from media with varying proportions of glucose

	units	Initial concentration of glucose in the medium (mM)					
		0	3.5	5.5	10	22	30
Glucose uptake from medium	µmol	-1.8	13.1	21.0	38.5	51.7	50.2
	% of medium	--	93.8	95.6	96.4	58.7	41.8
Glucose used for lipid synthesis	µmol	-2.24	-0.76	0.48	4.49	6.11	5.36
	% of intake	--	-5.81	2.26	11.6	11.8	10.7
Glucose used for lactate production	µmol	[4.17]	15.7	23.7	36.9	39.3	42.4
	% of intake	--	120	113	95.7	76.1	84.3
Glucose used for lactate+lipid	µmol	[1.93]	15.0	24.2	41.4	45.4	47.7
Glucose available for other uses	% of intake	[0.0]	-13.9	-15.2	-7.4	12.1	5.0

These values were calculated from the data shown in other graphs/tables, and are only a gross approximation to the actual data. Numbers between brackets indicate a non-glucose origin of the lactate found in the medium (i.e. alanine)

Supplemental Table 2 Primers used in the analysis of gene expression

Gene	Protein	Sequence 5' → 3'	Sequence 3' → 5'	size
Primers used for 3T3L1 cell gene expression analysis				
<i>Hk2</i>	hexokinase 2	CTCTCTCAACCCTGGCAAAC	GCACAATCTGCCCAAGTA	68
<i>Pfk</i>	phosphofructokinase, liver	CCAATGCTCCAGACTCAGC	AGATTCAAGCCACCACTGCTC	130
<i>Pfk</i>	phosphofructokinase, muscle	TGGTGCTGAGGAATGAGAAA	TCAAAGGGAGTTGGGCTTC	145
<i>Ldha</i>	Lactic acid dehydrogenase (muscle)	GCATCCCATTCACCAT	TCCGAGATTCCATTTGTCC	96
<i>Ldhb</i>	Lactic acid dehydrogenase (heart)	GATTACCCCCGGTCTACCA	AGCGACCTCATCGTCCTTC	136
<i>Lep</i>	leptin	AAGTCCAGGATGACACAAAC	GGTCCATCTGGACAAACTCAGAA	121
<i>AdipoQ</i>	adiponectin	GCCGTTCTTCACCTACGA	ACTTGGTCTCCCACCTCCA	92
<i>Pdk4</i>	pyruvate dehydrogenase kinase 4	ACCGCATTTCTACTCGGATG	CTTGGGTTCCCGTCTTGT	73
<i>Me1</i>	malic enzyme 1	TTCCTACGTGTTCCCTGGAG	GGCCCTTCTTGCAGGTGTTA	131
<i>Acly</i>	ATP citrate lyase	GATGAAGAAGGAGGGAAAGC	GGGAAGTGCTGTTGACGA	111
<i>Acc1</i>	acetyl-CoA carboxylase α	GGAGCCAGAACGGGACAGTAGA	CAGCCAAAGGGGATGTAAACT	92
<i>Fas</i>	fatty acid synthase	AGAGGCTTGTGCTGACTTCC	AATGTGCTTGGCTGGTAGC	59
<i>Cd36</i>	fatty acid transporter (FTO)	AGAACACAGCAGCAAAATCAAGG	ACAGTGAAGGGCTCAAAGATGG	147
<i>Ap2</i>	fatty acid binding protein 4	AACACCGAGATTTCCTT	ACACATTCCACCCAG	114

<i>Cpt1b</i>	carnitine palmitoyl-transferase 1b	CGCAGGGAGGAAGGGTAGAGT	CCAGGGTCACAAAGAAAGCA	110
<i>Lpl</i>	lipoprotein lipase	GCCAAGAGAACGAGCAAGAT	CCATCCTCAGTCCAGAAAA	101
<i>Hsl</i>	hormone sensitive lipase	CTGCTTCTCCCTCTCGTCTG	CAAATGGTCCCTCTGCCTCT	108
<i>Atgl</i>	adipose tissue triacylglycerol lipase	CAAAACAGGGCTACAGAGATGG	AAGGGTRGGTTGGTTCACT	68
<i>Pparg</i>	PPAR γ	GCAGGGAGCAGAGCAAAGAGG	CGAAACTGGCACCCCTGA	54
<i>11bhsd1</i>	11 β -hydroxysteroid dehydrogenase 1	GGACGTATTGTGACCGRTG	GGTTCACATTAGTCACTGCAT	77
<i>Pref-1</i>	Pref-1 differentiation factor	TGGAACTTGCGTGGACCT	TGGCAGGGAGAACCATGTA	117
<i>Rpl32</i>	ribosomal protein L32 (housekeeping gene)	CTGGAGGTGCTGATGT	GGGATTGGTAGCTGTGATGG	123
Primers used for rat gene analysis				
Gene	Protein	Sequence 5' → 3'	Sequence 3' → 5'	size
<i>Acc1</i>	Acetyl-CoA carboxylase 1	AGGAAGATGGTGTCCGGCTCTG	GGGGAGAGATGTGCTGGGTCA	145
<i>Ldhha</i>	Lactic acid dehydrogenase (muscle)	CACTGGTTTGAGACGATGA	GTCAGCAAGAGGGAGAGAGC	125
<i>Ldhb</i>	Lactic acid dehydrogenase (heart)	CCAGGAACCTGAACCCAGAGA	TCATAGGGCACTGTCCACCAC	131
<i>Fas</i>	Fatty acid synthase	CTTGGGTGCCGATTACAACC	GCCCTCCCGTACACTCACTC	163
<i>Pdk4</i>	Pyruvate dehydrogenase kinase 4	GTCAGGGCTATGGGACAGATGC	TTGGGATACACCAAGTCATCAGC	137
<i>Ppia</i>	Cyclophilin A (housekeeping gene)	CTGAGGCACTGGGAGAAAGGA	GAAGTCACCACCCCTGGCACA	87

Supplemental Table 3 Estimation of tissue water in plasma, liver and adipose tissues of adult male Wistar rats

tissue composition (in g/g tissue)				
parameter	liver	subcutaneous WAT	epididymal WAT	blood plasma
tissue lipid	0.041	0.576	0.809	0.011
tissue protein	0.181	0.063	0.050	0.075
tissue water	0.768	0.361	0.164	0.914

Tissue protein data were the same used for estimation of enzyme and lactate tissue concentrations. Lipid data are unpublished results obtained from animals of the same stock, age and sex than those used in this experiment. Tissue water is only an approximate value of the “lactate space” in the tissue.

RESEARCH ARTICLE

Evidences of Basal Lactate Production in the Main White Adipose Tissue Sites of Rats. Effects of Sex and a Cafeteria Diet

Sofía Arriarán¹, Silvia Agnelli¹, David Sabater^{1,3}, Xavier Remesar^{1,2,3}, José Antonio Fernández-López^{1,2,3*}, Marià Alemany^{1,2,3}

1 Department of Nutrition and Food Science, Faculty of Biology, University of Barcelona, Barcelona, Spain, **2** Institute of Biomedicine of the University of Barcelona, Barcelona, Spain, **3** CIBER Obesity and Nutrition, Barcelona, Spain

* josfernandez@ub.edu



OPEN ACCESS

Citation: Arriarán S, Agnelli S, Sabater D, Remesar X, Fernández-López JA, Alemany M (2015) Evidences of Basal Lactate Production in the Main White Adipose Tissue Sites of Rats. Effects of Sex and a Cafeteria Diet. PLoS ONE 10(3): e0119572. doi:10.1371/journal.pone.0119572

Academic Editor: Jonathan Peterson, East Tennessee State University, UNITED STATES

Received: November 14, 2014

Accepted: January 15, 2015

Published: March 5, 2015

Copyright: © 2015 Arriarán et al. This is an open access article distributed under the terms of the [Creative Commons Attribution License](#), which permits unrestricted use, distribution, and reproduction in any medium, provided the original author and source are credited.

Data Availability Statement: All relevant data are within the paper.

Funding: This study was done with the partial support of grants of the Plan Nacional de Investigación en Biomedicina (SAF2012-34895) and the Plan Nacional de Ciencia y Tecnología de los Alimentos (AGL-2011-23635) of the Government of Spain, as well as of CIBER-OBN (Institute of Health Carlos III). S. Agnelli was the recipient of a Leonardo da Vinci fellowship, and S. Arriarán a predoctoral fellowship of the Catalan Government, in both cases covering part of the time invested in this study. The

Abstract

Female and male adult Wistar rats were fed standard chow or a simplified cafeteria diet for one month. Then, the rats were killed and the white adipose tissue (WAT) in four sites: perigonadal, retroperitoneal, mesenteric and subcutaneous (inguinal) were sampled and frozen. The complete WAT weight in each site was measured. Gene expression analysis of key lipid and glucose metabolism enzymes were analyzed, as well as tissue and plasma lactate and the activity of lactate dehydrogenase. Lactate gradients between WAT and plasma were estimated. The influence of sex and diet (and indirectly WAT mass) on lactate levels and their relationships with lactate dehydrogenase activity and gene expressions were also measured. A main conclusion is the high production of lactate by WAT, practically irrespective of site, diet or sex. Lactate production is a direct correlate of lactate dehydrogenase activity in the tissue. Furthermore, lactate dehydrogenase activity is again directly correlated with the expression of the genes *Ldha* and *Ldhb* for this enzyme. In sum, the ability to produce lactate by WAT is not directly dependent of WAT metabolic state. We postulate that, in WAT, a main function of the lactate dehydrogenase path may be that of converting excess available glucose to 3C fragments, as a way to limit tissue self-utilization as substrate, to help control glycaemia and/or providing short chain substrates for use as energy source elsewhere. More information must be gathered before a conclusive role of WAT in the control of glycaemia, and the full existence of a renewed glucose-lactate-fatty acid cycle is definitely established.

Introduction

Lactate is the main by-product of peripheral organ utilization of glucose under conditions of anaerobiosis / hypoxia [1] or when used by glycolytic obligatory cells such as mammalian erythrocytes [2]. Lactate is also an acidifying factor modulating oxygen release in hypoxic tissues (Bohr effect) [3]. Lactate is one of the main splanchnic (essentially liver) organs' substrate

funders had no role in study design, data collection and analysis, decision to publish, or preparation of the manuscript.

Competing Interests: The authors have declared that no competing interests exist. Dr. Maria Alemany is an Academic Editor of PLOS ONE. This does not alter the authors' adherence to PLOS ONE Editorial policies and criteria.

for gluconeogenesis [4], and helps transfer "oxygen debt" from glycolytic muscle during exercise to the liver, completing a Cori cycle [5]. Lactate is, also, a good substrate for lipogenesis in the liver [6] and other tissues [7,8].

Lactate is a main by-product of most tumour cells, which show high rates of glycolysis [9] due to the Warburg effect [10]. In addition, lactate may be used as energy substrate by a number of tissues: heart [11], brown and white [12] adipose tissues, muscle [13], glia [14] and others, including the biota [15], because of its rapid conversion to pyruvate. Lactate is the main circulating 3C substrate, and cell (cytoplasmic) reducing power exporter, reflecting NADH status, and acting as a marker and modulator of oxygen availability and utilization [16]. These multiple roles place lactate at the centre of a critical metabolic switch. The changes in the rate of synthesis, transport in the blood and final disposal deeply modulate (and/or are the consequence of) important metabolic substrate shifts.

The main form of adipose tissue, white adipose tissue (WAT) is usually associated with energy storage in the form of an enormous vacuole containing essentially triacylglycerols. However, a significant part of body fat reserves are not found in the main WAT sites, but present in other cell types, such as myocytes or hepatocytes [17] or, more commonly, as WAT interspersed between other cell types in a number of tissues [18–21]. Curiously, all body reserves' mass changes are correlated between the macroscopic and disperse triacylglycerol depots, which, this way, show a remarkable uniformity in its physiological function as reserve organ [22], irrespective of variation in additional specialised functions [23,24].

We have recently observed that cultured 3T3L1 adipocytes, in the absence of undifferentiated fibroblasts, use glucose at extremely high rates, releasing lactate under conditions of full normoxia [25]. This is in agreement with *in vivo* lactate production by WAT [26–28] parallel to its low consumption of oxygen [29,30]. The limiting factor for lactate production under high medium glucose seems to be the availability of ADP [25]. The WAT breakup of 6C glucose to two 3C units may be directed to decrease glucose availability [25] in order to help protect the tissue from excess substrate and the damaging hypertrophy caused by excess energy substrates [31]. This defence mechanism may help restrict the supply of substrates (mainly glucose), but also that of oxygen, possibly inducing hypoxia, which has been suggested to favour the development of inflammation [32,33] and the consequent WAT immune response [34]. However, the limited needs of oxygen of adipocytes [25], and the low WAT oxygen consumption [30] suggest that the development of inflammation in WAT may not be directly related to oxygen supply.

In the present study we intended to find whether WAT lactate production *in vivo* may be in some way related to the excess energy supply of high-energy diets, but also to check whether sex [35] may also affect the WAT breakup of glucose to 3C units.

Materials and Methods

Animals, diet and experimental setup

All animal handling procedures and the experimental setup were in accordance with the animal handling guidelines of the corresponding European and Catalan Authorities. The Committee on Animal Experimentation of the University of Barcelona authorized the specific procedures used in the present study.

Nine week old female and male Wistar rats (Harlan Laboratory Models, Sant Feliu de Codines, Spain) were used. Six animals per group were housed in cages (two same-sex rats in each) with wood shreds for bedding. They had free access to water and were kept in a controlled environment (lights on from 08:00 to 20:00; 21.5–22.5°C; 50–60% humidity). Two groups of animals for each sex were selected randomly, and were fed *ad libitum*, for 30 days,

with either normal rat chow (type 2014, Harlan) or a simplified cafeteria diet as previously described [36].

The experimental setup consisted, thus, of four groups of 6 rats each: male-control, female-control, male-cafeteria and female-cafeteria. Rat weight and food consumption were measured, and we found that these parameters followed closely previous studies done using the same experimental setup [22]. Diet composition was (expressed as energy content): carbohydrate 67%, protein 20%, and lipid 13% for controls; the mean composition of the cafeteria diet ingested was: carbohydrate 47%, protein 12% and lipid 41%.

In a complementary study to analyse tissue blood flows, we used two additional groups of male rats, from the same supplier, stock, and age; they were subjected to the same feeding protocols (control or cafeteria diet) for 30 days. These animals were used exclusively for the measurement of tissue blood flow as described below.

Tissue sampling

At the end of the experiment, on day 30, the animals were anesthetized with isoflurane at the beginning of a light cycle, and blood was drawn from the exposed aorta using dry heparinized syringes, killing the animals by exsanguination. Blood was centrifuged 20 min at 2000xg, at 2–4°C. Plasma was frozen and kept at -20°C.

The rats were rapidly dissected, taking large samples of mesenteric (ME), perigonadal (periovaric in females and epididymal in males, PG), retroperitoneal (RP) and subcutaneous (inguinal fat pads, SC) WAT, which were frozen in liquid nitrogen. The samples were weighed, and stored at -80°C until processed. Later, the dissection of the dead rats continued, carefully extracting the remaining WAT in ME, PG and RP sites; the rats were skinned, and the subcutaneous WAT was dissected completely. The weights of WAT thus dissected were added to those of the frozen samples to know the mass of the four WAT sites.

WAT cellularity

Portions of frozen WAT were used for the estimation of total DNA with a classical chemical method [37]. Since a rat cell contains 5.6 pg of DNA [38], we were able to calculate the approximate number of cells per unit of WAT volume. We knew the weights and the density: ~0.9 g/mL [39] of WAT, and thus we determined the number of cells per g of tissue, and in the whole site, as well as their mean size, simply dividing the tissue volume by the number of cells.

Tissue protein content was estimated with a reliable biuret-Folin method [40]. After development of colour, turbidity was eliminated by adding to the tubes small amounts of finely powdered solid MgO, which adsorbed the suspended fat remnants, and centrifuging the tubes before reading their absorbance.

Estimation of tissue lactate

Samples of WAT tissue (in the range of 50 mg) were homogenized, still frozen, with a tissue disruptor (IKA-T10 basic Ultra-Turrax, IKA, Stauffen Germany) in 1 ml of chilled acetone: water mixture, to a final proportion (including the expected water content of the samples) of 1.25:1 [41]. The homogenate was centrifuged; all proteins removed with the precipitate, and floating lipids, not soluble in the diluted acetone, were discarded. The acetone tissue extract and plasma (10µL samples) were used for the estimation of lactate (kit 1001330 Spinreact, Sant Esteve d'en Bas, Spain), using sodium L-lactate (Sigma-Aldrich) as standard.

The proportion of lipid per g of tissue in rats treated with the same experimental setup is known [22]. By discounting the mass of fat and protein from that of tissue we were able to obtain an estimate of the amount of water present in the WAT samples (in the range of 20%).

The moles of lactate per mL of tissue or plasma and the amount of water in that same volume allowed us to calculate the molal concentrations of lactate in plasma and tissues, and to establish a molal concentrations ratio for each individual rat WAT site.

Measurement of lactate dehydrogenase activity

A modified UV method was used [42]. Frozen tissue samples were homogenized, using the tissue disruptor, in 10 volumes of chilled Krebs-Ringer bicarbonate solution, pH 7.8 containing 5 mM dithiothreitol, 0.5% bovine serum albumin, 1% dextran (MW 200,000), 0.1% Triton X-100, and 1 mM EDTA. Freshly (i.e. not later than 3 h after thawing/homogenisation in the buffer) prepared homogenates were used for all enzyme activity measurement incubations, carried out at 25°C. Homogenates were centrifuged at 4°C and 5,000xg for 10 minutes to obtain a clear intermediate phase (precipitated debris and floating lipid were discarded). The reaction mixture contained 150 μM NADH, 125 mg/L bovine serum albumin and 1 mM sodium pyruvate (all products were obtained from Sigma-Aldrich). The proportion of original tissue in each measuring well was in the range of 2.0–2.5 mg, in a volume of 0.02 mL of homogenate, diluted to the adequate proportions with homogenization medium. Absorbance at 340 nm was measured at intervals of 30 s for up to 10 min. In each case, the decrease in absorbance due to the formation of NAD⁺ was plotted, and initial (V_0) activities were determined from the course of the reaction at different times. V_0 was assumed to correspond to V_{max} under the described conditions of analysis. Protein content was measured in each of the homogenates used for enzyme activity estimation, and used for the presentation of enzyme activities, expressed in nkcat/g of protein to allow comparisons between samples with different fat content.

Gene expression analysis

Total tissue RNA was extracted from the frozen tissue samples using the Tripure reagent (Roche Applied Science, Indianapolis IN USA), and were quantified in a ND-100 spectrophotometer (Nanodrop Technologies, Wilmington DE USA). RNA samples were reverse transcribed using the MMLV reverse transcriptase (Promega, Madison, WI USA) system and oligo-dT primers.

Real-time PCR (RT-PCR) amplification was carried out using 10 μL amplification mixtures containing Power SYBR Green PCR Master Mix (Applied Biosystems, Foster City, CA USA), 4 ng of reverse-transcribed RNA and 150 nM of primers. Reactions were run on an ABI PRISM 7900 HT detection system (Applied Biosystems) using a fluorescent threshold manually set to 0.15 for all runs.

A semi-quantitative approach for the estimation of the concentration of specific gene mRNAs per unit of tissue weight was used [43]. *Rplp0* was the charge control gene [44,45]. We expressed the data as the number of transcript copies per gram of protein in order to obtain comparable data between the groups. The genes analysed and a list of primers used is presented in [Table 1](#).

Measurement of tissue blood flows

On day 27, the rats were implanted with two cannulas through the left carotid artery using Intramedic PE-10 polyethylene tubing (Becton Dickinson, Parsipanny, NJ USA), under isoflurane anaesthesia. The first carotid cannula was used to draw blood from descending aorta and the other to inject microspheres directly into the heart outflow following the instructions provided by the supplier. At 12 h intervals, the viability of the cannulas was checked (without disturbing the animals) by drawing blood up a few mm, followed by refilling with heparinized saline. On day 30 the rats were transferred to smaller individual cages, shielded from the

Table 1. Primers used for the analysis of gene expression in WAT of control and cafeteria diet-fed rats.

gene	Protein	5' > 3'	3' > 5'	bp
<i>Ldha</i>	lactic acid dehydrogenase (muscle type)	CACTGGGTTGAGACGATGA	GTCAGCAAGAGGGAGAGAGC	125
<i>Ldhb</i>	lactic acid dehydrogenase (heart type)	CCAGGAACTGAACCCAGAGA	TCATAGGCAGTGTCCACCAC	131
<i>Glut4</i>	glucose transporter 4	CTTGATGACGGTGGCTCTGC	CACAATGAACCAGGGATGG	127
<i>Hk2</i>	hexokinase 3	ATTCACCAACGGCAACCAT	GGACAAAGGGATTCAAGGCATC	113
<i>G6pd</i>	glucose-6P dehydrogenase	GACTGTGGCAAGCTCTCAA	GCTAGTGTGGCTATGGGCAGGT	77
<i>Pdk4</i>	pyruvate dehydrogenase kinase type 4	GTCAGGCTATGGACAGATGC	TTGGGATACACCAGTCATCAGC	137
<i>Pdk2</i>	pyruvate dehydrogenase kinase type 2	TCACTCTCCCTCCCATCAA	CGCCTCGGTCACTCATTT	75
<i>Nos3</i>	nitric oxide synthase (endothelial type)	CAAGTCCTACCGCCTTT	GACATCACCGCAGACAAACA	138
<i>Acc1</i>	acetyl-CoA carboxylase type 1	AGGAAGATGGTGTCCGCTCTG	GGGGAGATGTGCTGGGTCA	145
<i>Fas</i>	fatty acid synthase	CTTGGGTGCCGATTACAACC	GCCCTCCCGTACACTCACTC	163
<i>Acly</i>	ATP: citrate lyase	GACCAGAAGGGCGTGACCAT	GTTGTCAGCATCCCACCACT	96
<i>Hsl</i>	hormone-sensitive lipase	CCCATAAGACCCCCATTGCCCTG	CTGCCTCAGACACACTCTG	94
<i>Lpl</i>	lipoprotein lipase	GAAGGGGCTTGGAGATGTGG	TGCCTTGCTGGGGTTTCTT	103
<i>Atgl</i>	triacylglycerol lipase (adipose tissue)	CGGTGGATGAAGGAGCAGACA	TGGCACAGACGGCAGAGACT	138
<i>Cpt1</i>	carnitine palmitoleoyl transferase (liver)	CCGCTCATGGTCAACAGCA	CAGCAGTATGGCGTGGATGG	105
<i>Cpt2</i>	carnitine palmitoleoyl transferase (muscle)	TGTTGACGGATGTGGTTCC	GTGCTGGAGGTGGCTTGGT	152
<i>Lcad</i>	long-chain acyl-CoA dehydrogenase	ATGCCAAAAGGTCTGGGAGT	TCGACCAAAAGAGGCTAATG	148
<i>Rplp0</i>	60S acidic ribosomal protein 0	GAGCCAGCGAAGCCACACT	GATCAGCCCGAAGGAGAAGG	62

doi:10.1371/journal.pone.0119572.t001

operators. Two hours later, they were injected through the left ventricle cannula with 10^5 red latex beads (Molecular Probes, Carlsbad, CA USA) suspended in 0.1 ml of 9 g/L NaCl. At the same time, blood (about 0.2 mL) was slowly drawn (exactly during 60 s) through the other cannula. The rats were, then, anesthetized with isoflurane, and larger blood samples were obtained from the exposed aorta. Blood and tissue samples were frozen and kept at -80°C. After sacrifice the position of the cannulas was checked; no placement errors, nor cannula clotting were found. The weights of all organs analysed were measured.

Blood and tissue samples of known volume/weight were digested with 4 M KOH for 24 hours at 25°C with occasional stirring. The samples were filtered through glass-fibre filters (GF/D, 2.5 µm, Whatman, Maidstone, Kent UK) and rinsed with Tween-20 (20 g/L) followed by distilled water. Then, the fluorospheres were extracted from the filter with 2.5 ml of etoxyethyl acetate. The fluorescence at red (565 nm) excitation wavelength was measured at 598 nm emission wavelength in a spectrofluorimeter. Samples were adequately diluted and compared against tissue blanks, made with pieces of the same tissues from rats of the first experiment, which had not received fluorescent beads. At least two samples and/or extractions for each tissue were used / carried out. Samples were processed according to the bead supplier specifications. The number of beads in tissue samples was estimated from the organic extract fluorescence. The distribution of bead fluorescence equivalents vs. bead controls was used to obtain a percent distribution of blood flow between organs, since the amount of beads injected was known: a sample of the injected material was also analysed to correct for possible errors in the evaluation of injected bead numbers.

Calculation of cardiac output was done by measuring the amount of beads in the blood drawn for one minute from the artery. Bead concentration and the known amount of beads injected allowed the calculation of cardiac output. Absolute blood flows were calculated from the number of beads leaving the heart per unit of time and blood volume and the percentage of beads retained in the organs of the rats.

Table 2. Body weight, energy intake and plasma metabolites of control and cafeteria diet-fed rats.

tissue	units	male control	male cafeteria	female control	female cafeteria	P sex	i	P diet
Initial body weight	g	241±6	256±6	161±6	173±7	<0.0001	NS	
Final body weight	g	372±6	420±20	232±8	277±15	<0.0001	<0.0001	
Energy intake	MJ/30d	8.71±0.45	19.7±0.99	6.33±0.39	17.9±0.98	<0.0001	0.0121	
Plasma glucose	mM	7.80±0.32	8.25±0.33	6.60±0.26	8.78±0.24	NS	i	0.0002
Plasma triacylglycerols	mM	1.50±0.06	1.50±0.01	1.69±0.06	1.51±0.03	0.0390	NS	NS
Plasma cholesterol	mM	1.97±0.07	2.28±0.21	1.98±0.16	2.07±0.19	NS	NS	NS
Plasma urea	mM	3.90±0.17	3.82±0.20	5.13±0.25	3.78±0.20	0.0094	i	0.0025

The data are the mean ± sem of 6 different animals. Up to three significant digits are shown for each mean value. Statistical significance of the differences between groups (2-way anova): the columns show the P values for sex, diet and their interaction; a i in the interaction column indicates a significant interaction between the two factors analysed.

doi:10.1371/journal.pone.0119572.t002

Statistics

Comparisons between groups were done with two- or three-way ANOVA analyses using the Statgraphics Centurion XVI software (Warrenton, VA USA). Analyses of correlations and curve fitting (i.e. for V_0 estimation) were carried out using Prism 5 program (GraphPad Software, San Diego CA USA).

Results

The initial and final weights, energy intake, and the basic plasma parameters are shown in [Table 2](#). Body weight changes and energy data just repeat what we have previously published [\[22\]](#). Plasma glucose, triacylglycerols, total cholesterol and urea were within the normal range, showing no significant differences between groups, except for higher glucose and lower urea in cafeteria diet-fed rats.

[Table 3](#) shows the WAT site mass cellularity and protein content for female and male rats subjected to control and cafeteria diets. There were significant differences between sites for total mass, mean cell size, number of cells per unit of tissue weight and in the whole site. Sex effects were limited to SC and RP sites' mass and cell content; PG WAT also showed significant changes linked to sex for site cell and protein content. No effects attributable to sex were observed on ME WAT. With respect to the effects of diet, all sites showed significant differences for all the parameters included in [Table 3](#), except for RP WAT protein content.

Rats fed the cafeteria diet had larger WAT depots, but the relative size order was unchanged. Mean cell size followed the same pattern in all four groups, irrespective of global higher sizes in cafeteria diet-fed rats: RP>PG≈SC>ME.

Tissue lactate levels ([Table 4](#)) were lower in tissue (μmol/g) than in plasma (mM), and were not affected by sex, except for RP. Cafeteria diet decreased tissue (and plasma) lactate (significant for plasma, ME and PG). When the data were expressed in molal units, the picture was quite different ([Fig. 1](#)). The molal concentration ratios for WAT versus plasma were in all cases higher than 1, i.e. tissue lactate concentration in the water available (i.e. discounting protein and fat) was up to four-fold higher than in arterial plasma. There was a significant effect of site and of diet for PG and ME, with no effects of sex. The patterns of molal ratios between tissue and plasma lactate, however, were different in males PG>ME>SC>RP and females ME>PG>RP>SC. Cafeteria diet changed the patterns to RP>ME>PG>SC in males and ME>SC>RP>PG in females.

Table 3. White adipose tissue mass and cell size in adipose tissue sites of control and cafeteria diet-fed rats.

parameter	units	site	male control	male cafeteria	female control	female cafeteria	P-site	P sex	i	P diet
WAT site mass	g	SC	12.3±0.2	19.9±1.0	7.02±0.25	12.3±0.6	<0.0001 S>P>M≈R	<0.0001	NS	<0.0001
		ME	4.94±0.64	8.38±0.95	3.92±0.33	9.02±1.25				
		PG	7.34±0.50	12.8±1.6	4.83±0.39	11.8±1.70				
		RP	6.29±0.80	9.98±1.38	2.79±0.35	7.81±0.77				
mean cell size	nL	SC	7.72±0.88	8.34±0.49	7.15±0.39	9.89±0.25	<0.0001 R>P≈S>M	NS	i	0.0088
		ME	6.76±0.21	7.12±1.28	4.19±0.84	9.33±0.61				
		PG	7.72±0.66	9.16±0.84	8.35±0.58	11.1±0.6				
		RP	9.74±0.25	9.48±0.56	9.43±0.78	12.1±0.4				
number of cells in the whole site	10 ⁶ .cells	SC	1474±121	2556±69	1000±73	1473±213	<0.0001 S>P≈M>R	<0.0001	i	<0.0001
		ME	658±69	1392±265	906±129	959±116				
		PG	883±25	1382±85	579±31	1069±145				
		RP	681±65	1072±165	298±37	639±46				
number of cells /g tissue	10 ⁶ .cells/g	SC	122±9	122±8	142±7	101±3	0.0005 M>S≈P≈R	NS	i	0.0122
		ME	149±5	134±21	230±35	109±7				
		PG	134±10	104±7	123±8	87±4				
		RP	103±3	102±5	110±9	83.0±2.6				
protein content/g tissue	mg/g	SC	63.1±11.6	35.0±3.9	51.2±3.8	41.2±4.4	<0.0001 M>R>S≈P	NS	0.0105	NS
		ME	74.2±7.4	60.9±4.7	86.2±4.2	57.5±2.9				
		PG	44.3±1.6	35.0±2.0	54.4±2.4	47.6±2.6				
		RP	65.1±6.3	63.7±5.2	62.9±4.7	50.7±1.3				

The data are the mean ± sem of 6 different animals. Up to three significant digits are shown for each mean value. SC/S = subcutaneous inguinal; ME/M = mesenteric; PG/P = perigonadal (periovaric, epididymal), RP/R = retroperitoneal. Statistical significance of the differences between groups (2-way ANOVA): the columns show the P values for sex, diet and their interaction. A i in the interaction column indicates a significant interaction between the two factors analysed. The statistical significance of differences between sites was estimated by a 3-way-ANOVA. P values >0.05 are presented as NS; the sequences indicate overall significant differences between sites; post-hoc Duncan test: the sign > indicates significantly higher values at the left; commas are equivalent to NS.

doi:10.1371/journal.pone.0119572.t003

The levels of expression of the genes for the main lactate dehydrogenase isoenzymes in WAT (*Ldha* and *Ldhb*) are presented in Fig. 2. There was a marked difference in expression of both genes depending on WAT site. The patterns of distribution were fairly similar for both genes, with maximal expression in SC, and minimal in RP. However, there were significant

Table 4. Lactate levels in plasma and adipose tissue sites of control and cafeteria diet-fed rats.

tissue	units	male control	male cafeteria	female control	female cafeteria	P sex	i	P diet
plasma	mM	3.10±0.29	2.64±0.21	3.78±0.24	2.57±0.21	NS		0.0028
subcutaneous WAT	μmol/g	2.16±0.71	1.57±0.35	2.37±0.37	1.43±0.22	NS		NS
mesenteric WAT	μmol/g	1.98±0.33	1.80±0.37	2.87±0.17	1.04±0.13	NS	i	0.0019
perigonadal WAT	μmol/g	2.00±0.22	1.16±0.26	2.12±0.12	0.45±0.10	NS		<0.0001
retroperitoneal WAT	μmol/g	0.803±0.152	0.781±0.134	1.58±0.21	0.522±0.116	0.0026	i	NS

The data are the mean ± sem of 6 different animals. Up to three significant digits are shown for each mean value. Statistical significance of the differences between groups (2-way ANOVA): the columns show the P values for sex, diet and their interaction; a i in the interaction column indicates a significant interaction between the two factors analysed. The statistical significance of differences between sites was estimated by a 3-way-ANOVA; the P value was <0.0001; post-hoc Duncan test (same conventions as in Table 3): plasma > mesenteric, subcutaneous > perigonadal > retroperitoneal).

doi:10.1371/journal.pone.0119572.t004

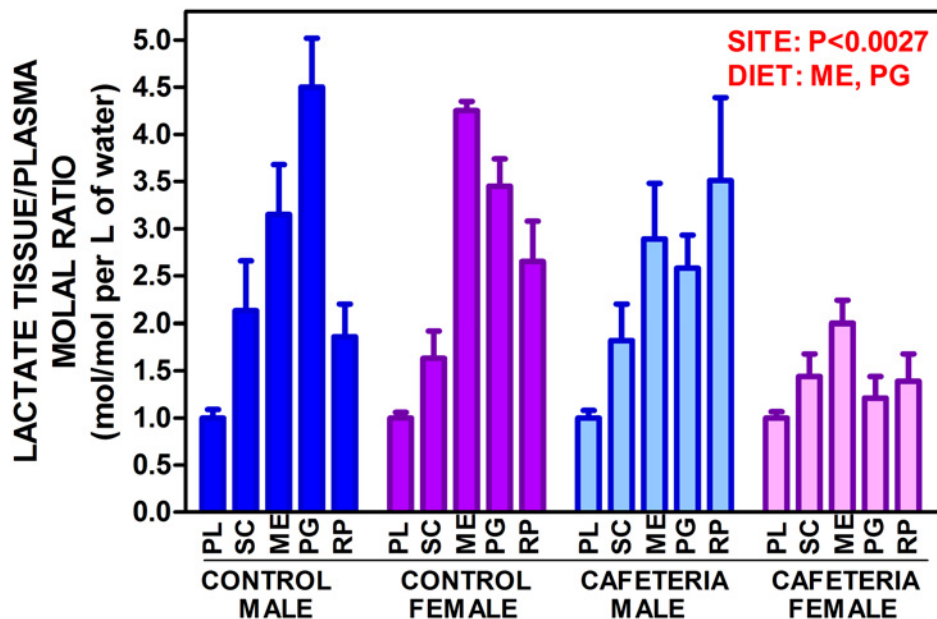


Fig 1. Lactate adipose tissue/plasma molal ratio of control- and cafeteria diet-fed male and female rats. The data are the mean \pm sem of 6 animals per group, and are expressed in moles/L of water in the tissue divided by moles/L of water in plasma. PL = plasma; SC = subcutaneous WAT; ME = mesenteric WAT; PG = perigonadal WAT; RP = retroperitoneal WAT. Statistical differences between groups: two-way anova for sex and diet and three-way anova for "site" are marked in red.

doi:10.1371/journal.pone.0119572.g001

differences induced by sex and diet. The effect of sex was less marked on *Ldhb*, which did not show significant effects of diet either, in contrast with *Ldha*. The actual tissue enzyme activities are shown in Fig 3. The patterns were comparable to those of *Ldha* and *Ldhb* expressions, but we must assume that the lactate dehydrogenase activity measured in tissue (in fact V_{max} under the conditions of measurement) was the result of the sum of both isoenzyme activities. No differences were observed for sex and only RP showed a significant effect of diet; however, the variable "site" was highly significant as in the gene expression analysis. In all groups, the patterns were comparable, but not identical, with maximal enzyme activity in SC.

The comparison of enzyme activity vs. the expression of the genes for the two isoenzymes implicated in that activity could not be done in a direct way, since gene expression of an enzyme seldom can be directly correlated with its activity in a tissue. However, we plotted (Fig. 4) the mean values for lactate dehydrogenase enzyme activity per g of tissue protein of all groups (i.e. different sex and diet) vs. the sum of the corresponding *Ldha* and *Ldhb* expressions, also referred to g of tissue protein. We obtained a significant correlation between expression and enzyme activity ($P < 0.0001$ vs. zero). When the individual rat data were plotted, we obtained a little more dispersion, but the slope of the regression line and the P values vs. zero were practically unchanged. The separate analysis of *Ldha* and *Ldhb* gave similar results (the slopes were practically halved with respect to the sum of expressions, but were superimposable for both genes). In both cases, the correlation was also significant. These data point at a direct relationship between the expression of both genes and the enzyme activity, but also that their contribution to final lactate dehydrogenase activity was similar for both isoenzymes (heart type and muscle type); thus the isozyme pattern of rat WAT is HHMM. When lactate dehydrogenase activity was plotted versus tissue lactate expressing both entities per g of protein, a significant correlation was observed between both parameters.

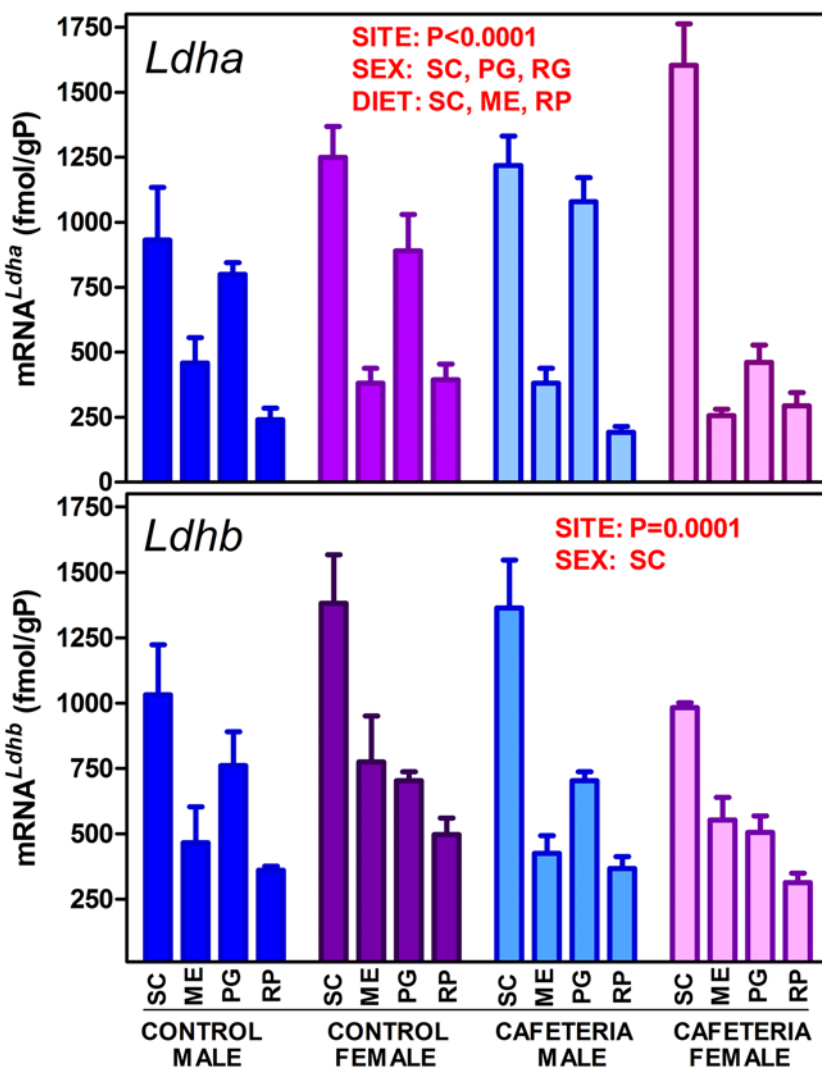


Fig 2. Lactate dehydrogenase genes (*Ldha* and *Ldhb*) expression in WAT sites of female and male rats fed control or cafeteria diet. The data are the mean ± sem of 6 animals per group, and are expressed in fmol/gP (g of tissue protein) to render the figures comparable. The conventions used are the same as in Fig. 1.

doi:10.1371/journal.pone.0119572.g002

[Table 5](#) presents the expression data for enzymes related with glucose oxidation. As observed for the lactate dehydrogenase genes, there was a marked significant effect of site in all cases. There were no effects of sex on *Glut4*, but females had higher hexokinase 2 expression, significant in ME and RP. The control of glucose entry in the cell was more affected by diet: *Glut4* and *Hk2* expressions were significantly lower for all cafeteria diet groups with the exception of SC. Glucose-6P dehydrogenase gene (*G6pd*) expression was also lowered by cafeteria diet, significantly for ME and RP, the latter with higher values in females.

The expressions of the enzymes controlling the critical step of conversion of 3C pyruvate to 2C acetyl-CoA, *Pdk4* and *Pdk2*, showed little change because of sex, with only higher male values for SC in *Pdk4* and PG in *Pdk2*, and no changes at all induced by the cafeteria diet (with only a significant decrease in ME for *Pdk2*).

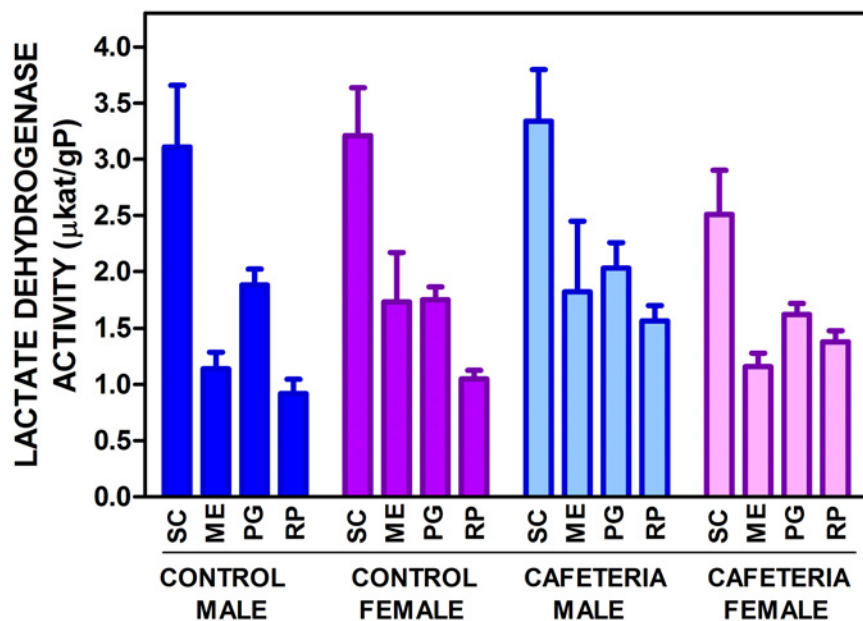


Fig 3. Total tissue lactate dehydrogenase activity in WAT sites of female and male rats fed control or cafeteria diet. The data are the mean \pm sem of 6 animals per group, and are expressed in $\mu\text{Kat/gP}$ (g of tissue protein) to render the figures comparable. The conventions used are the same as in Fig. 1.

doi:10.1371/journal.pone.0119572.g003

The expressions of the main genes controlling enzymes of lipid metabolism are presented in Table 6. The effect of "site" was significant for all genes studied with the exception of *Acly*, which was not. The differences related to sex were not evenly distributed, with higher expression values for males, the exceptions being *Acc1* (ME and RP) and *Acly* (ME) which showed

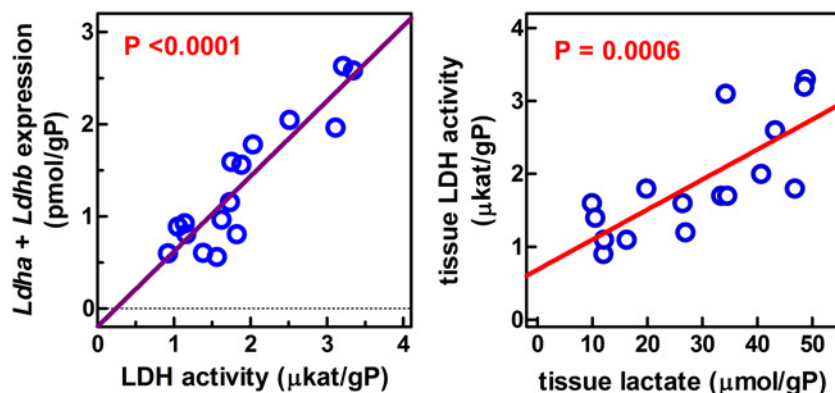


Fig 4. Linear correlation analysis of the relationship between lactate dehydrogenase activity and expression or tissue lactate content in WAT sites of male and female rats fed a control or cafeteria diet. LDH = lactate dehydrogenase; gP = g of protein. Each circle represents the mean value for one group of rats (i.e. female/male, control/cafeteria). Enzyme activities are those presented in Fig. 3; expression data are the sum of *Ldha* and *Ldhb* (Fig. 2) for the corresponding groups; tissue lactate were those shown in Table 4. Correlation between lactate dehydrogenase activity and gene expression: $r^2 = 0.828$, significantly different from zero ($P < 0.0001$). When all the individual data (i.e. all sites and groups) were plotted, the corresponding values were $r^2 = 0.380$, and $P < 0.0001$. The separate analyses of *Ldha* and *Ldhb* (using the mean values) gave similar results *Ldha* $r^2 = 0.642$, $P = 0.0002$, and *Ldhb* $r^2 = 0.840$, $P < 0.0001$. Correlation between tissue lactate dehydrogenase activity and lactate content: $r^2 = 0.583$, significantly different from zero ($P = 0.0006$). When all the individual data (i.e. all sites and groups) were plotted instead of only the means, the corresponding values were $r^2 = 0.307$, and $P < 0.0001$.

doi:10.1371/journal.pone.0119572.g004

Table 5. Gene expression in WAT of control and cafeteria diet-fed rats in fmol/g protein. I Glucose oxidation and nitric oxide synthase.

protein	gene	WAT	male control	male cafeteria	female control	female cafeteria	P site	P sex	i	P diet
glucose transporter 4	<i>Glut4</i>	SC	108±29	123±25	161±184	115±8	<0.0001	NS	NS	
		ME	31.2±8.6	15.8±3.0	116±36	12.2±0.6	S≈P>M≈R	NS	0.0189↓	
		PG	109±8	70.2±2.7	160±54	32.6±6.6		NS	0.0134↓	
		RP	44.0±6.5	25.2±3.9	119±43	26.0±5.8		NS	0.0088↓	
hexokinase 2	<i>Hk2</i>	SC	11.7±2.5	13.0±1.9	18.9±3.7	14.7±0.9	<0.0001	NS	NS	
		ME	7.9±1.2	2.7±0.5	16.8±3.2	1.5±0.2	S≈P>M≈R	0.0304 ^f	i <0.0001↓	
EC 2.7.1.1		PG	16.9±2.8	14.6±2.0	25.6±5.7	10.5±2.1		NS	0.0266↓	
		RP	4.1±0.4	2.9±0.4	13.5±4.5	3.3±0.6		0.0084 ^f	i 0.0030↓	
		SC	334±73	413±51	257±25	302±36	0.0001 S>P>M≈R	NS	NS	
glucose-6P-dehydrogenase	<i>G6pd</i>	ME	129±18	75.6±9.3	202±32	62.9±4.6		NS	i <0.0001↓	
		PG	129±12	188±23	285±51	145±16		NS	i NS	
		RP	84.2±14.2	67.0±5.7	183±35	82.0±9.3		0.0048 ^f	0.0037↓	
		SC	181±73	187±41	22.7±2.6	90.2±21.6	<0.0001	0.0113 ^m	NS	
pyruvate dehydrogenase kinase 4	<i>Pdk4</i>	ME	14.2±3.7	14.4±2.1	7.6±3.9	9.1±1.7	S>P≈M≈R	NS	NS	
		PG	14.5±5.4	20.6±3.2	8.5±3.2	11.8±2.2		NS	NS	
EC 2.7.11.2		RP	13.5±3.5	12.9±1.6	6.1±1.0	17.6±3.7		NS	NS	
		SC	263±87	167±41	146±13	302±36	<0.0001	NS	NS	
		ME	120±24	34.2±1.7	193±51	22.9±5.3	S>M≈P≈M>R	NS	0.0009↓	
		PG	91.7±12.8	90.1±11.4	86.6±16.8	41.8±3.1		0.0426 ^m	NS	
nitric oxide synthase (endothelial type)	<i>Nos3</i>	RP	48.6±7.6	27.9±3.9	63.9±10.4	31.5±6.1		NS	NS	
		SC	75.4±9.5	88.9±6.0	43.2±2.8	65.5±7.2	<0.0001	0.0009 ^m	0.0190↑	
		ME	21.6±2.6	15.3±2.3	18.5±1.0	10.4±1.5	S>P>M≈R	NS	0.0054↓	
		PG	31.6±6.3	32.9±4.6	22.6±2.4	13.3±1.9		0.0030 ^m	NS	
EC 1.14.13.39		RP	14.7±1.1	11.6±1.7	16.1±2.2	9.4±1.2		NS	0.0051↓	

The data are presented as fmol of the corresponding mRNA for g of tissue protein, and are the mean ± sem of 6 different animals. Up to three significant digits are shown for each mean value. SC/S = subcutaneous inguinal; ME/M = mesenteric; PG/P = perigonadal (periovaric, epididymal), RP/R = retroperitoneal. Statistical significance of the differences between groups (2-way ANOVA): the columns show the P values for sex, diet and their interaction. A superscript ^f represents higher (overall) values for females and ^m for males. The arrows show the direction of significant changes for diet: ↓ indicate (overall) slower values for cafeteria diet-fed rats; a i in the interaction column indicates a significant interaction between the two factors analysed. The statistical significance of differences between sites was estimated by a 3-way-ANOVA; post-hoc Duncan test (same conventions as in Table 1)

doi:10.1371/journal.pone.0119572.t005

higher specific mRNA concentrations in females. In all other cases, males showed higher mean values: *Fas* (SC and RP), *Lpl* (SC), *Atgl* (SC and PG), *Cpt1* (all sites, except ME), *Cpt2* (PG) and *Lcad* (SC).

The effects of diet resulted in all cases in either no change or decreased expression; no increased expressions were observed when comparing cafeteria diet and controls. In the case of *Acc1*, all sites showed significant effects of diet, and in *Fas*, all showed significant changes except SC. *Acly* decreased its expression with diet in ME and PG; *Hsl* showed changes only in RP, *Lpl* in PG and RP. *Atgl* also decreased its expression in RP; *Cpt1* in ME and *Cpt2* in RP and ME; there were no changes at all in *Lcad*.

The estimation of WAT blood flow in male rats fed the control or cafeteria diets is shown in Fig. 5. The data are referred to g of tissue protein for direct comparisons with the other Figures and Tables. There was a trend to show lower blood flows for the WAT sites, including the composite value of all four, MA, in cafeteria diet-fed rats but there were no statistically significant

Table 6. Gene expression in WAT of control and cafeteria diet-fed rats in fmol/g protein. II Lipid metabolism.

protein	gene	WAT	male control	male cafeteria	female control	female cafeteria	P site	P sex	i	P diet
acetyl-CoA carboxylase 1 EC 6.4.1.2	<i>Acc1</i>	SC	74.0±16.3	59±6	149±37	40.3±5.0	0.0020R>S≈M≈P	NS	0.0024↓	
		ME	30.6±4.0	14.6±1.6	165±49	9.2±2.1		0.0134 ^f	i	0.0019↓
		PG	126±12	53.4±9.5	156±66	28.0±4.6		NS	0.0064↓	
		RP	81.0±7.2	33.5±4.8	542±206	27.6±2.7		0.0087 ^f	i	0.0019↓
fatty acid synthase EC 2.3.1.85	<i>Fas</i>	SC	7620±4110	8762±1955	2447±403	540±47	<0.0001 S>M≈P≈R	0.0202 ^m	NS	
		ME	192±74	110±22	1660±536	67.3±13.9		NS	i	0.0268↓
		PG	1269±250	701±166	2106±795	319±45		NS		0.0056↓
		RP	572±85	204±28	3318±1130	190±32		0.0050 ^m	i	0.0007↓
ATP: citrate lyase EC 4.1.3.8	<i>Acly</i>	SC	167±81	174±43	186±54	71.5±7.7	NSS>M	NS	NS	
		ME	22.2±2.9	9.9±2.3	160±34	6.4±1.5		0.0020 ^f	i	0.0003↓
		PG	109±10	88.6±13.9	228±102	39.9±6.3		NS		0.0391↓
		RP	25.1±4.7	14.6±2.4	295±132	13.3±2.6		NS		NS
hormone-sensitive lipase EC 3.1.1.79	<i>Hsl</i>	SC	631±131	648±138	486±37	660±63	<0.0001 S≈P>R>M	NS	NS	
		ME	166±38	130±23	218±61	110±12		NS		NS
		PG	674±59	670±70	664±64	461±45		NS		NS
		RP	458±39	344±49	645±84	295±34		NS	i	0.0002↓
lipoprotein lipase EC 3.1.1.34	<i>Lpl</i>	SC	6300±1305	6700±1110	3790±440	4520±670	<0.0001 S>P>M≈R	0.0365 ^m	NS	
		ME	1190±38	1630±470	1100±80	1430±260		NS		NS
		PG	3970±720	3790±440	4320±290	2080±250		NS	i	0.0209↓
		RP	2610±350	1750±110	3440±820	1470±150		NS		0.0052↓
triacylglycerol lipase (adipose type) EC 3.1.1.3	<i>Atgl</i>	SC	1320±300	1680±270	701±26	1470±150	<0.0001 S, P>R>M	0.0426 ^m	NS	
		ME	429±95	412±92	338±95	403±79		NS		NS
		PG	1450±300	1790±290	1040±150	1180±90		0.0332 ^m	NS	
		RP	700±48	608±74	732±51	536±68		NS		0.0400↓
carnitine palmitoyl-transferase (liver type) EC 2.3.1.21	<i>Cpt1</i>	SC	39.6±14.8	58.9±9.0	19.4±3.9	37.9±7.3	<0.0001 P>S>M>R	0.0426 ^m	NS	
		ME	14.0±2.7	3.8±0.9	13.7±3.6	0.7±0.1		NS		0.0001↓
		PG	16.3±1.7	18.9±1.1	10.8±1.7	7.7±1.2		<0.0001 ^m	NS	
		RP	3.3±0.5	3.4±0.5	2.0±0.4	2.6±0.2		0.0200 ^m	NS	
carnitine palmitoyl-transferase (muscle type) EC 2.3.1.21	<i>Cpt2</i>	SC	10.6±3.0	17.9±2.8	17.0±1.8	13.4±12.7	<0.0001 P>S>M>R	NS	i	NS
		ME	10.7±1.5	7.8±1.0	14.9±3.6	7.5±1.3		NS		0.0214↓
		PG	25.1±4.3	20.5±1.7	19.2±3.4	11.7±1.7		0.0332 ^m	NS	
		RP	13.4±1.7	11.3±1.7	20.9±3.4	10.5±1.9		NS		0.0130↓
long-chain acyl-CoA dehydrogenase EC 1.3.8.8	<i>Lcad</i>	SC	1076±347	1370±155	365±23	733±117	<0.0001 S>P>M≈R	0.0037 ^m	NS	
		ME	166±9	196±14	298±60	179±32		NS		NS
		PG	353±72	653±99	412±91	359±37		NS		NS
		RP	204±22	379±29	302±49	207±29		NS		NS

The data are presented as fmol of the corresponding mRNA for g of tissue protein, and are the mean ± sem of 6 different animals. Up to three significant digits are shown for each mean value. SC/S = subcutaneous inguinal; ME/M = mesenteric; PG/P = perigonadal (periovaric, epididymal), RP/R = retroperitoneal. Statistical significance of the differences between groups (2-way ANOVA): the columns show the P values for sex, diet and their interaction. A superscript ^f represents higher (overall) values for females and ^m for males. The arrows show the direction of significant changes for diet: ↓ indicate (overall) slower values for cafeteria diet-fed rats; a i in the interaction column indicates a significant interaction between the two factors analysed. The statistical significance of differences between sites was estimated by a 3-way-ANOVA; post-hoc Duncan test (same conventions as in Table 3). P values >0.05 are presented as NS.

doi:10.1371/journal.pone.0119572.t006

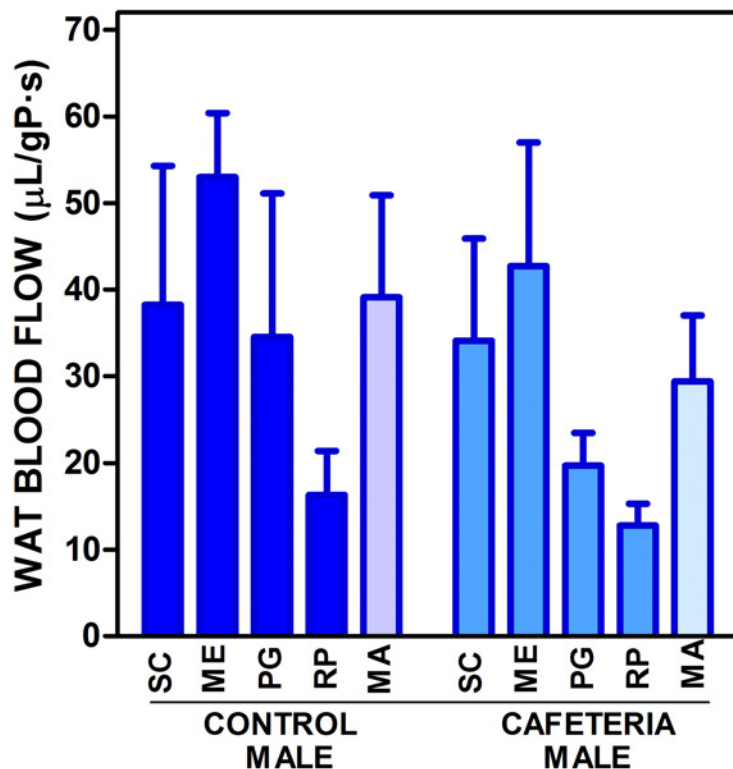


Fig 5. WAT blood flow in male rats fed control or cafeteria diets. The data are the mean \pm sem of 6 animals per group, and are expressed in $\mu\text{L}/\text{s}\cdot\text{gP}$ (g of tissue protein). The conventions used are the same as in Fig. 1; MA = mean value for SC, MS, PG and RP taking into account their combined masses.

doi:10.1371/journal.pone.0119572.g005

differences either for the four studied sites or their composite; there was no significant difference for "site" either.

Table 5 also presented the expression of the most abundant gene for an isoenzyme of nitric oxide synthase (endothelial type) *Nos3*. Sex showed significantly higher values for males in SC and PG. Feeding a cafeteria diet increased the expression of *Nos3* in SC, and decreased it in ME and RP.

Discussion

The production of lactate from glucose by WAT is well known [26–28], and is related to glucose availability [46] in a way similar to that of the Cori cycle [5] between muscle and the splanchnic bed. However, there are reports on the active use of lactate as lipogenic substrate by WAT [6,7]. The release of lactate from human and rat subcutaneous WAT has been proven *in vivo* [26,47], and we have observed, in cultured 3T3L1 adipocytes [25], that these cells produced an inordinately large amount of lactate when medium glucose concentration was high. A number of elegant studies, have found that the oxygen consumption by WAT under basal conditions is low, justifying a normal operation of the tissue even at low concentrations of oxygen [29,30,48].

The 3T3L1 adipocytes converted almost quantitatively glucose to lactate, which represents a negligible consumption of oxygen under conditions of normoxia [25]. Consequently, the hypothesis that limited blood (and thence oxygen) supply to WAT, a mechanism of defence

against excess energy substrate availability [49], may elicit inflammation because of hypoxia [50,51] should be revised, at least for adipocytes, the main component of WAT.

In this study, we found a considerable difference in the potential for lactate production between different WAT sites as shown by different levels of activity and gene expression for lactate dehydrogenase. A high enzyme activity is no proof in itself that lactate is being produced in a given tissue without using dynamic (albeit invasive) tracer studies. However, the data presented in Fig. 4 show that there is a close correlation between WAT lactate content and lactate dehydrogenase activity, regardless of site, sex and dietary treatment. These data strongly suggest that the actual lactate tissue levels are a consequence of the lactate dehydrogenase activity.

Furthermore, the plasma/tissue molal lactate ratios proved that, in all samples, lactate concentration was higher in water tissue than in plasma, i.e. the lactate in WAT could not come from plasma (uphill gradient) but was produced in WAT and released to plasma. Evidently, the main ultimate destination of this lactate is the liver, where it may be used for gluconeogenesis, lipogenesis or oxidized to supply energy. Gluconeogenesis is highly improbable under conditions of excess glucose [52]. Oxidation to CO₂ for energy is improbable too in liver and other tissues because of the availability of glucose and the induction of insulin resistance by lactate itself [53]. The large presence of fatty acids in cafeteria rats further increased insulin resistance [54]. In consequence, the most probable fate for most of the lactate produced by adipocytes will be its incorporation to the hepatic lipogenic pathway, and their final release as lipoprotein triacylglycerols.

Adipose tissue is one of the main body producers of lactate [13]. In postabsorptive state humans, whole adipose tissue releases 60–150 μmol/min; other important lactate producing tissues are the brain (with a contribution of around 50 μmol/min) and skeletal muscle. However, although skeletal muscle is a main site of lactate production during exercise [5], it also plays an important role in lactate clearance under basal conditions [13].

It is unclear why WAT contains both muscle and heart type lactate dehydrogenase isoenzymes, (HHMM) with different affinities for lactate and markedly distinct functions in different organs [55]. In the present conditions, both *Ldha* and *Ldhb* genes behaved in a similar way and both (and especially their combined expression) was closely adjusted to the total enzyme activity measured, which points to a similar (or shared) regulation *in vivo*, and also to a gene expression-linked mechanism of regulation of the enzyme activity. The similar turnover rate of the isoenzymes [55] agrees with this interpretation.

The limited changes in circulating lactate suggest that its turnover in blood was fast [56] in agreement with the high capacity of liver to take up and metabolize lactate [57] as indicated above. However, given the relatively large mass of adipose tissue, at least in the overweight cafeteria diet-fed rats, the effect of a significant breakup of glucose to produce lactate is far from being negligible and undoubtedly may help downregulate glycaemia in a significant proportion, at least under basal, i.e. non-exercise, conditions.

Intake of a hyperlipidic cafeteria diet results in a proinflammatory state [58], which is often associated with hypoxia [59,60]. However, contrary to what was expected, no increases in lactate dehydrogenase activity, neither of tissue lactate concentrations were found in the WAT of cafeteria diet-fed rats. The close correlation observed between lactate dehydrogenase activity and tissue lactate content, irrespective of site, sex and diet, suggests that hypoxia could not be a critical factor in the regulation of lactate production. This is again in agreement with the need to revise the purported relationship between hypoxia and inflammation.

There were sex-related differences in the expression of a number of key enzymes related to lipid synthesis, but the most marked effects were attributable to the exposure to cafeteria diet, providing an excess of energy. The consequence was an increased WAT mass [61], via increases in both cell numbers and cell size, as observed here and in agreement with previous

studies [62]. However, the factor "site" was markedly relevant for practically all parameters studied. The data on the expression of genes involved in lipogenesis from glucose show clearly that cafeteria diet had a marked overall influence; the entry of glucose into WAT cells was probably limited, as shown by lower *Glut4* and *Hk2* expressions. This decrease may be part of the tissue mechanism of defence against a sustained excess of energy supply and the generalized insulin resistance [63] that makes WAT the ultimate destination for excess circulating glucose [49,64]. The relative lack of changes in the expression of pyruvate dehydrogenase kinases suggest that the oxidation of pyruvate to acetyl-CoA was practically unaffected by diet, i.e. this was not, probably, an outlet for excess glucose carbon towards lipogenesis, at least in WAT. Notwithstanding, the maintenance of these expressions unchanged also hinted to a limited success of glucose transporter 4 and hexokinase decreases in gene expression to stem the flow of glucose into the cells. All the genes controlling lipogenesis, from *G6pd* role in the production of NADPH, to the cytoplasm supplier of acetate *Acly*, and to the proper lipogenic enzyme genes *Acc1*, and *Fas*, showed steady decreases in expression under the hyperlipidic cafeteria diet, as previously observed [22,65]. Lipoprotein lipase expression was also decreased, but only in RP and PG. The limitations induced in lipid metabolism by cafeteria feeding were less marked on the lipase genes *Hsl* and *Atgl*, which showed decreases only in RP.

WAT lipid utilization, thus, was also limited under cafeteria feeding, an obvious conclusion because of increases in the rat global fat mass and in all WAT sites. The expression of genes related to the transfer of acyl-CoA to the mitochondria was also limited (*Cpt1* and *Cpt2*), and those controlling the oxidation of fatty acids was unchanged (albeit maintained at low levels) as shown by the lack of effect of diet on *Lcad* expression. These data agree with those of cultured adipocytes, in which the use of glucose as substrate for lipogenesis was largely shunted to the production of 3C (lactate) fragments [25] for eventual exportation to the liver. However, the increase in WAT mass and triacylglycerol accumulation of cafeteria rats is difficult to explain with lowered WAT glucose uptake, limited lipogenesis and maintained lactate production capability, unless, incorporation of blood-borne lipids is factored in.

At first, we assumed that the contrast between lactate levels and lactate dehydrogenase activity in a given WAT site could be due to differences in blood flow. The control of blood flow is probably a key mechanism of control of substrate access to WAT [49,66,67], and its limitation under conditions of excess available energy is counterbalanced by the eventual hypoxic effects induced by this limitation [66,68]. The higher production of NOx in the obese [69] and its effects countering the vasoconstriction elicited by other factors [70,71] agrees with that interpretation. We have observed decreases in WAT expression of *Nos3*, the endothelial nitric oxide synthase gene [72], a key controller of blood flow [73], in most sites of rats fed the cafeteria diet; but it increased in subcutaneous WAT. However, the blood flow study (done only in males to limit animal lives and costs), showed a limited variability (not significant) from site to site in this parameter, which hints to a general uniform control of WAT blood flow comparable to the ability to uniformly deposit fat in all WAT sites and other organs [22] under comparable energy availability conditions.

In any case, the data on blood flow did not explain the differences in lactate and lactate dehydrogenase activity. In spite of the efforts invested, no proof has been found linking blood flow (or its control) to WAT lactate production or release. Thus, lactate production by WAT seems to be essentially unrelated to hypoxia and inflammation.

A main conclusion of this study is the production of lactate by WAT irrespective of site, diet or sex, and that this production is a direct consequence of lactate dehydrogenase activity in the tissue. Furthermore, this activity is a direct correlate of the main lactate dehydrogenase controlling genes' expression. In sum, the ability to produce lactate by WAT is not directly dependent of WAT metabolic condition. We postulate that a main function of the lactate dehydrogenase

path of WAT may be that of converting excess circulating glucose to 3C fragments as a way to control glycaemia and/or providing shorter chain substrates for use as energy source elsewhere. The higher circulating lactate levels of obese humans [27] supports this interpretation, and suggests a potential role of WAT in the control of glycaemia, at least in obese individuals.

More information must be gathered before a conclusive role of WAT in the control of glycaemia and the full existence of a renewed glucose-lactate-fatty acid cycle [74] is definitely established.

Author Contributions

Conceived and designed the experiments: XR JAFL MA. Performed the experiments: S. Arriarán S. Agnelli DS. Analyzed the data: S. Arriarán JAFL. Wrote the paper: MA.

References

1. Sahlin K. Lactate formation and tissue hypoxia. *J Appl Physiol*. 1989; 67: 2640. PMID: [2606874](#)
2. Rapoport TA, Heinrich R, Rapoport SM. The regulatory principles of glycolysis in erythrocytes in vivo and in vitro. A minimal comprehensive model describing steady states, quasi-steady states and time-dependent processes. *Biochem J*. 1976; 154: 449–469. PMID: [132930](#)
3. Bohr C, Hasselbalch K, Krogh A. Über einen in biologischer Beziehung wichtigen Einfluss, den die Kohlensäurespannung des Blutes auf dessen Sauerstoffbindung übt. *Scand Arch Physiol*. 1904; 16: 402–412.
4. Ross BD, Hems R, Krebs HA. The rate of gluconeogenesis from various precursors in the perfused rat liver. *Biochem J*. 1967; 102: 942–951. PMID: [16742514](#)
5. Cori CF. The glucose-lactic acid cycle and gluconeogenesis. *Curr Top Cell Regul*. 1981; 18: 377–387. PMID: [7273846](#)
6. O’Hea EK, Leveille GA. Significance of adipose tissue and liver as sites of fatty acid synthesis in the pig and the efficiency of utilization of various substrates for lipogenesis. *J Nutr*. 1969; 99: 338–344. PMID: [5350989](#)
7. Granata AL, Midrio M, Corsi A. Lactate oxidation by skeletal muscle during sustained contraction in vivo. *Pflügers Archiv-Eur J Physiol*. 1976; 366: 247–250.
8. Lopaschuk GD, Collinsnakai RL, Itoi T. Developmental changes in energy substrate use by the heart. *Cardiovasc Res*. 1992; 26: 1172–1180. PMID: [1288863](#)
9. López-Lázaro M. The Warburg effect: Why and how do cancer cells activate glycolysis in the presence of oxygen? *AntiCancer Agents Med Chem*. 2008; 8: 305–312. PMID: [18393789](#)
10. Warburg O. On the origin of cancer cells. *Science*. 1956; 132: 309–314.
11. Taegtmeyer H, Hems R, Krebs HA. Utilization of energy-providing substrates in the isolated working rat-heart. *Biochem J*. 1980; 186: 701–711. PMID: [6994712](#)
12. Saggesson ED, Mcallister TWJ, Baht HS. Lipogenesis in rat brown adipocytes—effects of insulin and noradrenaline, contributions from glucose and lactate as precursors and comparisons with white adipocytes. *Biochem J*. 1998; 251: 701–709.
13. van Hall G. Lactate kinetics in human tissues at rest and during exercise. *Acta Physiol*. 2010; 199: 499–508. doi: [10.1111/j.1748-1716.2010.02122.x](#) PMID: [20345411](#)
14. Dringen R, Schmoll D, Cesar M, Hamprecht B. Incorporation of radioactivity form [¹⁴C] lactate into the glycogen of cultured mouse astroglial cells- Evidence for gluconeogenesis in brain cells. *Biol Chem Hoppe-Seyler*. 1993; 374: 343–347. PMID: [8338635](#)
15. Bourriaud C, Robins RJ, Martin L, Kozlowski F, Tenailleau E, Cherbut C, et al. Lactate is mainly fermented to butyrate by human intestinal microfloras but inter-individual variation is evident. *J Appl Microbiol*. 2005; 99: 201–212. PMID: [15960680](#)
16. Tanaka K, Matsuura Y, Kumagai S, Matsuzaka A, Hirakoba K, Asano K. Relationships of anaerobic threshold and onset of blood lactate accumulation with endurance performance. *Eur J Appl Physiol*. 1983; 52: 51–56. PMID: [6686129](#)
17. Tamura Y, Tanaka Y, Sato F, Choi JB, Watada H, Niwa M, et al. Effects of diet and exercise on muscle and liver intracellular lipid contents and insulin sensitivity in type 2 diabetic patients. *J Clin Endocrinol Metab*. 2005; 90: 3191–3196. PMID: [15769987](#)
18. Gallagher D, Kuznia P, Heshka S, Albu J, Heymsfield SB, Goodpaster B, et al. Adipose tissue in muscle: a novel depot similar in size to visceral adipose tissue. *Am J Cli Nutr*. 2005; 81: 903–910.

19. Herschap B, Zakhia D, Nicolas M. Intraprostatic adipose tissue. International J Surg Pathol. 2011; 19: 190–190. doi: [10.1177/1066896910397611](https://doi.org/10.1177/1066896910397611) PMID: [21447537](https://pubmed.ncbi.nlm.nih.gov/21447537/)
20. Nadra K, Médard JJ, Quignodon L, Verheijen MHG, Desvergne B, Chrust R. Epineural adipocytes are dispensable for Schwann cell myelination. J Neurochem. 2012; 123: 662–667. doi: [10.1111/j.1471-4159.2012.07896.x](https://doi.org/10.1111/j.1471-4159.2012.07896.x) PMID: [22849425](https://pubmed.ncbi.nlm.nih.gov/22849425/)
21. Slade JM, Coe LM, Meyer RA, McCabe LR. Human bone marrow adiposity is linked with serum lipid levels not T1-diabetes. J Diabetes Complicat. 2012; 26: 1–9. doi: [10.1016/j.jdiacomp.2011.11.001](https://doi.org/10.1016/j.jdiacomp.2011.11.001) PMID: [2257906](https://pubmed.ncbi.nlm.nih.gov/2257906/)
22. Romero MM, Roy S, Pouillot K, Feito M, Esteve M, Grasa MM, et al. Treatment of rats with a self-selected hyperlipidic diet, increases the lipid content of the main adipose tissue sites in a proportion similar to that of the lipids in the rest of organs and tissues. PLOS One. 2014; 9: e90995. doi: [10.1371/journal.pone.0090995](https://doi.org/10.1371/journal.pone.0090995) PMID: [24603584](https://pubmed.ncbi.nlm.nih.gov/24603584/)
23. Alemany M, Fernández-López JA. Adipose tissue: something more than just adipocytes. Curr Nutr Food Sci. 2006; 2: 141–150.
24. Cinti S. The adipose organ. Prostag Leukot Essent Fatty Acids. 2005; 73: 9–15. PMID: [15936182](https://pubmed.ncbi.nlm.nih.gov/15936182/)
25. Sabater D, Arriarán S, Romero MM, Agnelli S, Remesar X, Fernández-López JA, et al. Cultured 3T3L1 adipocytes dispose of excess medium glucose as lactate under abundant oxygen availability. Sci Rep. 2014; 4: 3663. doi: [10.1038/srep03663](https://doi.org/10.1038/srep03663) PMID: [24413028](https://pubmed.ncbi.nlm.nih.gov/24413028/)
26. Hagström E, Arner P, Ungerstedt U, Bolinder J. Subcutaneous adipose tissue: a source of lactate production after glucose ingestion in humans. Am J Physiol. 1990; 258: E888–E893. PMID: [2333992](https://pubmed.ncbi.nlm.nih.gov/2333992/)
27. DiGirolamo M, Newby FD, Lovejoy J. Lactate production in adipose tissue: a regulated function with extra-adipose implications. FASEB J. 1992; 6: 2405–2412. PMID: [1563593](https://pubmed.ncbi.nlm.nih.gov/1563593/)
28. van der Merwe MT, Crowther NJ, Schlaphoff GP, Boyd IH, Gray IP, Joffe BI, et al. Lactate and glycerol release from the subcutaneous adipose tissue of obese urban women from South Africa; Important metabolic implications. J Clin Endocrinol Metab. 1998; 83: 4084–4091. PMID: [9814496](https://pubmed.ncbi.nlm.nih.gov/9814496/)
29. Hosogai N, Fukuhara A, Oshima K, Miyata Y, Tanaka S, Segawa K, et al. Adipose tissue hypoxia in obesity and its impact on adipocytokine dysregulation. Diabetes. 2007; 56: 901–911. PMID: [17395738](https://pubmed.ncbi.nlm.nih.gov/17395738/)
30. Hodson L, Humphreys SM, Karpe F, Frayn KN. Metabolic signatures of human adipose tissue hypoxia in obesity. Diabetes. 2013; 62: 1417–1425. doi: [10.2337/db12-1032](https://doi.org/10.2337/db12-1032) PMID: [23274888](https://pubmed.ncbi.nlm.nih.gov/23274888/)
31. Slawik M, Vidal-Puig AJ. Adipose tissue expandability and the metabolic syndrome. Genes Nutr. 2007; 2: 41–45. doi: [10.1007/s12263-007-0014-9](https://doi.org/10.1007/s12263-007-0014-9) PMID: [18850138](https://pubmed.ncbi.nlm.nih.gov/18850138/)
32. van den Borst B, Schols AMWJ, de Theije C, Boots AW, Köhler SE, Goossens GH, et al. Characterization of the inflammatory and metabolic profile of adipose tissue in a mouse model of chronic hypoxia. J Appl Physiol. 2013; 114: 1619–1628. doi: [10.1152/japplphysiol.00460.2012](https://doi.org/10.1152/japplphysiol.00460.2012) PMID: [23539316](https://pubmed.ncbi.nlm.nih.gov/23539316/)
33. Wang B, Wood IS, Trayhurn P. Dysregulation of the expression and secretion of inflammation-related adipokines by hypoxia in human adipocytes. Pflügers Archiv-Eur J Physiol. 2007; 455: 479–492.
34. Alemany M. The defense of adipose tissue against excess substrate-induced hypertrophy: Immune system cell infiltration and arrested metabolic activity. J Clin Endocrinol Metab. 2011; 96: 66–68. doi: [10.1210/jc.2010-2541](https://doi.org/10.1210/jc.2010-2541) PMID: [21209047](https://pubmed.ncbi.nlm.nih.gov/21209047/)
35. Alemany M. Steroid hormones interrelationships in the metabolic syndrome: An introduction to the ponderostat hypothesis. Hormones. 2012; 11: 272–289. PMID: [22908060](https://pubmed.ncbi.nlm.nih.gov/22908060/)
36. Ferrer-Lorente R, Cabot C, Fernández-López JA, Alemany M. Combined effects of oleoyl-estrone and a β_3 -adrenergic agonist (CL316,243) on lipid stores of diet-induced overweight male Wistar rats. Life Sci. 2005; 77: 2051–2058. PMID: [15935402](https://pubmed.ncbi.nlm.nih.gov/15935402/)
37. Vytašek R. A sensitive fluorometric assay for the determination of DNA. Anal Biochem. 1982; 120: 243–248. PMID: [6283935](https://pubmed.ncbi.nlm.nih.gov/6283935/)
38. Consortium GSP. Genome sequence of the Brown Norway rat yields insights into mammalian evolution. Nature. 2004; 428: 493–521. PMID: [15057822](https://pubmed.ncbi.nlm.nih.gov/15057822/)
39. Martin AD, Daniel MZ, Drinkwater DT, Clarys JP. Adipose tissue density, estimated adipose lipid fraction and whole body adiposity in male cadavers. Int J Obesity. 1994; 18: 79–83. PMID: [8148928](https://pubmed.ncbi.nlm.nih.gov/8148928/)
40. Lowry OH, Rosebrough RW, Farr AL, Randall RJ. Protein measurement with the Folin phenol reagent. J Biol Chem. 1951; 193: 265–275. PMID: [14907713](https://pubmed.ncbi.nlm.nih.gov/14907713/)
41. Soley M, Alemany M. A rapid method for the estimation of amino acid concentration in liver tissue. J Biochem Biophys Meth. 1980; 2: 207–211. PMID: [7419868](https://pubmed.ncbi.nlm.nih.gov/7419868/)
42. Vassault A. Lactate dehydrogenase. UV method with pyruvate and NADH⁺. Meth Enzym Anal. 1983; 3: 118–126.

43. Romero MM, Grasa MM, Esteve M, Fernández-López JA, Alemany M. Semiquantitative RT-PCR measurement of gene expression in rat tissues including a correction for varying cell size and number. *Nutr Metab.* 2007; 4: 26. PMID: [18039356](#)
44. Stern-Straeter J, Bonaterra GA, Hörmann K, Kinscherf R, Goessler UR. Identification of valid reference genes during the differentiation of human myoblasts. *BMC Mol Biol.* 2009; 10: 66. doi: [10.1186/1471-2199-10-66](#) PMID: [19573231](#)
45. Barnias G, Goukos D, Laoudi E, Balla IG, Siakavellas SI, Daikos GL, et al. Comparative study of candidate housekeeping genes for quantification of target gene messenger RNA expression by real-time PCR in patients with inflammatory bowel disease. *Inflamm Bowel Dis.* 2013; 19: 2840–2847. doi: [10.1097/MB.0000435440.22484.e8](#) PMID: [24141710](#)
46. Muñoz S, Franckhauser S, Elias I, Ferré T, Hidalgo A, Monteys AM, et al. Chronically increased glucose uptake by adipose tissue leads to lactate production and improved insulin sensitivity rather than obesity in the mouse. *Diabetologia.* 2010; 53: 2417–2430. doi: [10.1007/s00125-010-1840-7](#) PMID: [20623219](#)
47. Crandall DL, Fried SK, Francendese AA, Nickel M, DiGirolamo M. Lactate release from isolated rat adipocytes: Influence of cell size, glucose concentration; insulin and epinephrine. *Horm Metab Res.* 1983; 15: 326–329. PMID: [6350139](#)
48. Ellmerer M, Schaupp L, Sendlhofer G, Wutte A, Brunner GA, Trajanoski Z, et al. Lactate metabolism of subcutaneous adipose tissue studied by open flow microperfusion. *J Clin Endocrinol Metab.* 1998; 83: 4394–4401. PMID: [9851784](#)
49. Alemany M. Regulation of adipose tissue energy availability through blood flow control in the metabolic syndrome. *Free Radical Biol Med.* 2012; 52: 2108–2119. doi: [10.1016/j.freeradbiomed.2012.03.003](#) PMID: [22542444](#)
50. Fujisaka S, Usui I, Ikutani M, Aminuddin A, Takikawa A, Tsuneyama K, et al. Adipose tissue hypoxia induces inflammatory M1 polarity of macrophages in an HIF-1α-dependent and HIF-1α-independent manner in obese mice. *Diabetologia.* 2013; 56: 1403–1412. doi: [10.1007/s00125-013-2885-1](#) PMID: [23494472](#)
51. Taylor CT, Kent BD, Crinion SJ, McNicholas WT, Ryan S. Human adipocytes are highly sensitive to intermittent hypoxia induced NF-κappaB activity and subsequent inflammatory gene expression. *Biochem Biophys Res Commun.* 2014; 447: 660–665. doi: [10.1016/j.bbrc.2014.04.062](#) PMID: [24755071](#)
52. Rognstad R. Control of lactate gluconeogenesis by glucose in rat hepatocytes. *Arch Biochem Biophys.* 1982; 217: 498–502. PMID: [7138021](#)
53. Choi CS, Kim YB, Lee FN, Zabolotny JM, Kahn BB, Youn JH. Lactate induces insulin resistance in skeletal muscle by suppressing glycolysis and impairing insulin signaling. *Am J Physiol.* 2002; 283: E233–E240. PMID: [12110527](#)
54. Zhang LY, Keung W, Samokhvalov V, Wang W, Lopaschuk GD. Role of fatty acid uptake and fatty acid β-oxidation in mediating insulin resistance in heart and skeletal muscle. *Biochim Biophys Acta.* 2010; 1801: 1–22. doi: [10.1016/j.bbapap.2009.09.014](#) PMID: [19782765](#)
55. Nadal-Ginard B. Regulation of lactate dehydrogenase levels in the mouse. *J Biol Chem.* 1978; 253: 170–177. PMID: [618856](#)
56. Freminet A, Leclerc L, Gentil M, Poyart C. Effect of fasting on the rates of lactate turnover and oxidation in rats. *FEBS Lett.* 1975; 60: 431–434. PMID: [1227987](#)
57. Felipe A, Remesar X, Pastor-Anglada M. L-Lactate uptake by rat liver. Effect of food deprivation and substrate availability. *Biochem J.* 1991; 273: 195–198. PMID: [1989581](#)
58. de Souza CT, Araujo EP, Bordim S, Ashimine R, Zollner RL, Boschero AC, et al. Consumption of a fat-rich diet activates a proinflammatory response and induces insulin resistance in the hypothalamus. *Endocrinology.* 2005; 146: 4192–4199. PMID: [16002529](#)
59. Trayhurn P, Wood IS. Adipokines: inflammation and the pleiotropic role of white adipose tissue. *Br J Nutr.* 2004; 92: 347–355. PMID: [15469638](#)
60. O'Rourke RW, White AE, Metcalf MD, Olivas AS, Mitra P, Larison WG, et al. Hypoxia-induced inflammatory cytokine secretion in human adipose tissue stromovascular cells. *Diabetologia.* 2011; 54: 1480–1490. doi: [10.1007/s00125-011-2103-y](#) PMID: [21400042](#)
61. Sclafani A, Springer D. Dietary obesity in adult rats: Similarities to hypothalamic and human obesity syndromes. *Physiol Behav.* 1976; 17: 461–471. PMID: [1013192](#)
62. Rafecas I, Esteve M, Fernández-López JA, Remesar X, Alemany M. Deposition of dietary fatty acids in young Zucker rats fed a cafeteria diet. *Int J Obesity.* 1992; 16: 775–787. PMID: [1330957](#)
63. Davidson MB, Garvey D. Studies on mechanisms of hepatic insulin resistance in cafeteria-fed rats. *Am J Physiol.* 1993; 264: E18–E23. PMID: [8430783](#)

64. Alemany M. Adipose tissue hypoxia, a conceptual alometric view. *J Endocrinol Metab.* 2011; 1: 155–158.
65. Priego T, Sánchez J, Picó C, Palou A. Sex-differential expression of metabolism-related genes in response to a high-fat diet. *Obesity.* 2008; 16: 819–826. doi: [10.1038/oby.2007.117](https://doi.org/10.1038/oby.2007.117) PMID: [18239587](#)
66. Heinonen I, Kemppainen J, Kaskinoro K, Knuuti J, Boushel R, Kallikoski KK. Capacity and hypoxic response of subcutaneous adipose tissue blood flow in humans. *Circ J.* 2014; 78: 1501–1506. PMID: [24759795](#)
67. Andersson J, Karpe F, Sjöström LG, Riklund K, Söderberg S, Olsson T. Association of adipose tissue blood flow with fat depot sizes and adipokines in women. *Int J Obesity.* 2012; 36: 783–789. doi: [10.1038/ijo.2011.152](https://doi.org/10.1038/ijo.2011.152) PMID: [21792171](#)
68. Ardilouze JL, Fielding BA, Currie JM, Frayn KN, Karpe F. Nitric oxide and β-adrenergic stimulation are major regulators of preprandial and postprandial subcutaneous adipose tissue blood flow in humans. *Circulation.* 2004; 109: 47–52. PMID: [14662716](#)
69. Codoñer-Franch P, Tavárez-Alonso S, Murria-Estal R, Megías-Vericat J, Tortajada-Girbés M, Alonso-Iglesias E. Nitric oxide production is increased in severely obese children and related to markers of oxidative stress and inflammation. *Atherosclerosis.* 2001; 215: 475–480.
70. Mather KJ, Lteif A, Steinberg HO, Baron AD. Interactions between endothelin and nitric oxide in the regulation of vascular tone in obesity and diabetes. *Diabetes.* 2004; 53: 2060–2066. PMID: [15277386](#)
71. Toda N, Okamura T. Obesity impairs vasodilatation and blood flow increase mediated by endothelial nitric oxide: An overview. *J Clin Pharmacol.* 2013; 53:1228–1239. doi: [10.1002/jcph.179](https://doi.org/10.1002/jcph.179) PMID: [24030923](#)
72. Ribiere C, Jaubert AM, Gaudiot N, Sabourault D, Marcus ML, Boucher JL, et al. White adipose tissue nitric oxide synthase: A potential source for NO production. *Biochem Biophys Res Commun.* 1996; 222: 706–712. PMID: [8651909](#)
73. Gardiner SM, Compton AM, Bennett T, Palmer RM, Moncada S. Control of regional blood flow by endothelium-derived nitric oxide. *Hypertension.* 1990; 15: 486–492. PMID: [2332239](#)
74. Randle PJ, Garland PB, Hales CN, Newsholme EA. The glucose fatty-acid cycle: its role in insulin sensitivity and the metabolic disturbances of diabetes mellitus. *Lancet.* 1963; 281: 785–789.

3.2. Adaptación y desarrollo de métodos para la valoración de la actividad de las enzimas del ciclo de la urea en tejido adiposo blanco

* *Notas sobre el desarrollo de metodología adaptada para la valoración en el tejido adiposo blanco de la actividad de las enzimas del ciclo de la urea*

Uno de los principales objetivos de esta tesis era investigar la presencia de todas las enzimas del ciclo de la urea en el tejido adiposo blanco. Para ello tuvimos que adaptar, a nuestras necesidades y recursos, algunas de las pocas técnicas de valoración enzimática disponibles, teniendo en cuenta que las proteínas que intentábamos cuantificar se encuentran en niveles muy bajos (diluidas por la enorme cantidad de grasa de reserva) en uno de los tejidos más plásticos, dispersos, desconocidos y complejos como es el tejido adiposo blanco.

En el desarrollo de los métodos se utilizaron ratas Wistar, hembras y machos, de nueve semanas, alimentadas con pienso estándar o una dieta hiperlipídica (dieta "de cafetería") durante un mes. El estudio se realizó en cuatro localizaciones diferentes de tejido adiposo blanco: mesentérico, perigonadal, retroperitoneal y subcutáneo inguinal.

Para las valoraciones enzimáticas se prepararon homogenados utilizando la misma relación entre el peso de tejido y el volumen de homogenado (1:5 p/v). La excepción a esta proporción fue la valoración de la actividad de la carbamoil-fosfato sintetasa I (CPS-I, EC 6.3.4.16) en hígado, para la que se utilizaron diluciones en el rango de 1:10 - 1:200 p/v.

Las actividades de las dos enzimas que inician el ciclo de la urea, ornitina transcarbamila (OTC, EC 2.1.3.3) y CPS-I se cuantificaron mediante métodos radioquímicos. Así, se determinó la actividad de la OTC utilizando ^{14}C -ornitina y carbamoil-fosfato para formar ^{14}C -citrulina en presencia de MgCl_2 como cofactor. La separación de la ^{14}C -citrulina de su substrato radiactivo se realizó por cromatografía de capa fina. Una vez desarrollado el cromatograma, la banda que contenía la L-citrulina se cortaba y medía la radioactividad.

La metodología que desarrollamos para cuantificar la actividad de la CPS-I se basaba en la incorporación de ^{14}C -bicarbonato (amónico) al carbamoil-fosfato en presencia de ATP-Mg y N-acetyl-glutamato. La reacción se paró bajando el pH y la temperatura. El exceso

de bicarbonato marcado fue eliminado gaseando las muestras con una corriente continua, de CO₂ no radioactivo, con un flujo bajo pero mantenido durante el tiempo necesario para eliminar toda la marca no integrada en el carbamoil-fosfato.

La reacción enzimática era lineal hasta los 10 minutos; la actividad hepática, medida en rata control, estaba en el rango de 89 ± 8 nkat/g. En los animales que fueron alimentados con una dieta hiperproteica se observó un incremento del 40 % en la actividad de la enzima. Los análisis de expresión génica evidenciaron que el gen de la CPS-I no se expresaba en el tejido adiposo blanco, pero, por el contrario, sí se pudo medir la expresión de la CP sintetasa II (CPS-II, EC 6.3.5.5). Para cuantificar la actividad de esta enzima en tejido adiposo se adaptó el método descrito sustituyendo la mayor parte del bicarbonato amónico (pero manteniendo la marca de bicarbonato radioactivo) por glutamina (principal substrato de la CPS-II), lo que hizo innecesaria la presencia del N-acetyl glutamato.

Las actividades de las enzimas implicadas en la síntesis y escisión del arginino-succinato: arginino-succinato sintetasa (ASS, EC 6.3.4.5) y arginino-succinato liasa (ASL, EC 4.3.2.1), así como la arginasa, se cuantificaron con métodos espectrofotométricos. La actividad ASS se valoró determinando la tasa de incorporación de aspartato frente al tiempo. Para ello, se valoró el aspartato que aún contenía el medio tras la incubación de la enzima para formar arginino-succinato. El aspartato se midió mediante su transaminación a oxalacetato con aspartato transaminasa y 2-cetoglutarato, seguida de la reducción del oxalacetato a malato por la malato deshidrogenasa y NADH, cuya desaparición a 340 nm sirvió para, finalmente, cuantificar el aspartato no utilizado.

Por otro lado, la actividad de la ASL se cuantificó midiendo la arginina liberada por su actividad. La arginina se trató con arginasa para escindirla en ornitina y urea. Finalmente, la urea se valoró con un método químico colorimétrico basado en la reacción de la urea con diacetil-monoxima en medio ácido; la reacción se cuantificaba por medida de la densidad óptica a 490 nm.

La actividad de la arginasa, activada con iones Mn²⁺, se valoró midiendo la formación de urea (por el método descrito en el párrafo anterior) a partir de arginina.

Cabe resaltar, que la mayor parte de la metodología descrita en este apartado no es el resultado del desarrollo de nuevas técnicas de valoración enzimática; sino que es sólo la necesaria adaptación y mejora de técnicas preexistentes, ya publicadas, a menudo en

bibliografía antigua, a su utilización en un tejido prácticamente "virgen" por lo que respecta al estudio del metabolismo general de los aminoácidos. Otra razón de la necesidad de adaptar y modificar los métodos es la distinta disponibilidad de materiales, técnicas e instrumentos descritos previamente y aquellos a los que nuestro grupo de investigación ha tenido acceso.



A RADIOCHEMICAL METHOD FOR CARBAMOYL-PHOSPHATE SYNTHETASE-I: APPLICATION TO RATS FED A HYPERPROTEIC DIET

ARRIARÁN S.^{1,2}, AGNELLI S.^{1,2}, FERNÁNDEZ-LÓPEZ J.A.^{1,2}, REMESAR X.^{1,2} AND ALEMANY M.^{1,2*}

¹Department of Nutrition and Food Science, Faculty of Biology, University of Barcelona, Barcelona, Spain.

²CIBER Obesity and Nutrition, Institute of Health Carlos III, Spain.

*Corresponding Author: Email- malemany@ub.edu

Received: September 27, 2012; Accepted: October 04, 2012

Abstract- A method for the measurement of carbamoyl-phosphate synthetase I activity in animal tissues has been developed using the livers of rats under normal and hyperproteic diets. The method is based on the incorporation of ¹⁴C-ammonium bicarbonate to carbamoyl-phosphate in the presence of ATP-Mg and N-acetyl-glutamate. The reaction is stopped by chilling, lowering the pH and adding ethanol. Excess bicarbonate is flushed out under a gentle stream of cold CO₂. The only label remaining in the medium was that incorporated into carbamoyl-phosphate, since all ¹⁴C-CO₂ from bicarbonate was eliminated. The method is rapid and requires only a low pressure supply of CO₂ to remove the excess substrate. The reaction is linear up to 10 min using homogenate dilutions of 1:20 to 1:200 (w/v). Rat liver activity was in the range of 89±8 nkat/g. Hyperproteic diet resulted in a significant 1.4-fold increase. The design of the method allows for the processing of multiple samples at the same time, and incubation medium manipulation is unnecessary, since the plastic incubation vial and its contents are finally counted together.

Keywords- carbamoyl-phosphate synthetase I, urea cycle, hyperproteic diets

Citation: Arriarán S., et al (2012) A Radiochemical Method for Carbamoyl-Phosphate Synthetase-I: Application to Rats Fed a Hyperproteic Diet. Journal of Enzyme Research, ISSN: 0976-7657 & E-ISSN: 0976-7665, Volume 3, Issue 1, pp.-29-33.

Copyright: Copyright©2012 Arriarán S., et al. This is an open-access article distributed under the terms of the Creative Commons Attribution License, which permits unrestricted use, distribution and reproduction in any medium, provided the original author and source are credited.

Introduction

Carbamoyl-P (CP) synthetase is a critical enzyme in the control of the disposal of 2-amino N from amino acids via the urea cycle [1]. CP synthetases use either ammonia as N donor: CP-synthetase-I [2] (EC 6.3.4.16), or glutamine [3] (EC 6.3.5.5). CP-synthetase-I is found in liver mitochondria [4] and catalyzes the incorporation of CO₂ and NH₃ to form CP with the consumption of 2 moles ATP per mol of CP formed [5].

Measurement methods for CP synthetase-I have been developed using different approaches, most of them relying on the coupling of the synthesis of CP with ornithine transcarbamylase to yield citrulline [6], which is, then, estimated by radiochemical [7], or colorimetric [8] methods. The analysis of other byproducts such as ADP, coupled to dehydrogenases after a chain of added enzymes, has been also used in the past [2,9]. Usually, the key step was the separation of CP from labelled precursors [10], or, in coupled reactions, ornithine [10,11]. The problems caused by a long chain of coupled reactions, the availability of the complementary enzymes and labelled substrates and the cumbersome and time-consuming procedures of column separation are an unwanted additional source of variation and built-in error.

The marked decrease of enzyme-based amino acid metabolism studies, from a peak in the early 1980s resulted in the removal

from most scientific suppliers' catalogues of labelled substrates, reagents and enzymes needed for coupling or label-transfer reactions, which right now makes more difficult the assay of common enzymes such as CP synthetase. In addition, nowadays there is an enormous distance in knowledge between energy, glucose, and fatty acids metabolism and regulation in health and, especially, in metabolic disease with the sketchy and incomplete actualization of the role amino acids play under common metabolic challenges. In contrast, high-protein diets are widely used to fight obesity [12,13], often with limited knowledge of their potential effects.

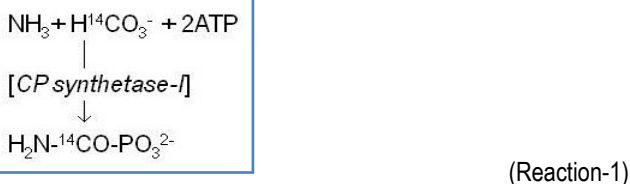
High-protein diets increase urea excretion [14], but high-energy diets lower urea synthesis [15] and increase nitrate production [16] irrespective of protein intake. We are trying to analyze how excess energy may affect so deeply amino acid catabolism, and this implies the analysis of gene expression, but primarily the direct measurement of protein levels and/or enzyme activities. The present study is centred precisely on the actualization of a method for the measurement of CP-synthetase-I in tissues, using a well established incubation medium with bicarbonate, ammonium, ATP, and N-acetyl-glutamate as activator of the reaction [17] and testing the method both in control and hyperproteic diet-fed rats. The differences with the classic procedures stem from the use of inexpensive and easily available ¹⁴C-bicarbonate, and the discrimination of the excess substrate from labelled CP at the end of the reaction by

flushing out excess bicarbonate with a stream of cold CO₂.

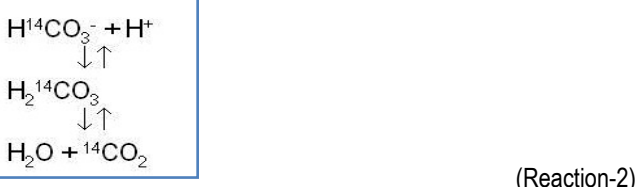
Materials and Method

Outline of the Method

Sample homogenates were incubated with ATP, ammonium ions and bicarbonate (containing ¹⁴C-bicarbonate), as well as N-acetyl-glutamate as activator. The reaction:



yields labelled carbamoyl-phosphate; but much excess labelled bicarbonate remains in the incubation medium; it is flushed out with a stream of non-labelled CO₂ in a slightly acidified medium:



The specific activity of the remaining carbonate is rapidly diluted by cold CO₂; thus after a time, the only label present in the incubation medium is that of CP. Counting the medium we can estimate the CP formation from the specific activity of the labelled bicarbonate added to the reaction mixture.

Chemicals

Inorganic chemicals, ethanol and acetic acid were purchased from Panreac (Montcada, Barcelona Spain) and all were of analytical quality. Organic compounds and albumin were obtained from Sigma (St Louis, MO USA). Labelled NaH¹⁴CO₃ (specific activity 1.48-2.22GBq/mmol) was obtained from Perkin Elmer (Bad Neuham, Germany). Plastic polyethylene tubing was purchased from Becton-Dickinson (Sparks, MD USA).

Sample Preparation

Adult (90 days old) male rats (Zucker lean) were used. Two groups of 6 animals each were randomly selected and fed during one month (i.e. from days 90 to 120) with either the standard rat chow (controls, with a protein energy content of 20%), or a hyperproteic diet (40% of protein-derived energy). On day 120, the rats were killed and liver samples were frozen in liquid nitrogen and kept at -80°C, for later use in enzyme analyses.

The protocol of animal handling was authorized by the Ethics Committee on Animal Experimentation of the University of Barcelona.

Tissue samples were homogenized in 20 volumes of chilled 50mM triethanolamine/HCl buffer pH 8.0, containing 1mM dithiothreitol and 10mM of Mg-acetate, using a cell disruptor (IKA, Stauffen, Germany). Homogenates were diluted, when needed, with homogenizing buffer. Protein content in homogenates was measured with the Lowry method [18].

There were no significant differences in enzyme activity using fresh

and frozen tissue samples under the conditions described. However, the activities measured using similarly frozen (and stored) homogenates resulted in losses of up to 50% of the enzyme activity.

Incubation

The conditions of incubation were adapted from those described in the literature for analysis of activity of the rat liver enzyme [8]. Incubations were carried out at 30°C in thin-walled 1.5ml capped polyethylene tubes (Eppendorf tubes), using a block heater. The incubation mixture (final volume 0.200mL) contained (final concentrations) 5mM ATP, 10mM Mg-acetate, 1mM dithiothreitol, 1 g/L bovine serum albumin (defatted), and 5mM disodium N-acetyl-glutamate, in 50mM triethanolamine/HCl buffer pH 8.0.

To 0.100mL of incubation medium, 0.050mL of homogenate was added. The reaction was started immediately by adding 0.050mL of 200mM ammonium bicarbonate, containing 5 kBq of NaH¹⁴CO₃, i.e. with 50 kBq/mmol specific activity. After gently shaking, the reaction was allowed to run for up to 10 minutes.

The reaction was stopped by the addition of 0.100ml of ethanol: acetic acid (20:1 v/v), shaking and leaving the uncapped tubes on ice. Zero time was established by adding (to medium and homogenate) the ethanol: acetic acid first, and then the ammonium bicarbonate. Control tubes in which the homogenate was substituted by the same volume of homogenizing buffer were also included in each series.

CO₂ Flushing and Labelled Carbamoyl-Phosphate Estimation

A series of 20 cm pieces of capillary tubing were tightly fitted in both ends with the serrated steel tubes from hypodermic needles, obtaining tubes with two steel-needle point ends. One of the extremes of the tube was stuck in a closed plastic (or rubber) tube connected to a low-pressure source of carbon dioxide. The other was introduced in the incubation mixture of the Eppendorf tubes, containing an incubated sample, or a control (no homogenate) with reagents alone. The gas was left to bubble gently through the samples for 5-10 minutes at a rate of 10-15mL/min (i.e. 4.5-6.8mMol). The tubes were maintained in a rack on ice, and the whole flushing operation was carried out in a ventilated hood, since ¹⁴CO₂ was lost.

We used advantageously a Kipp gas generator [19] (Anorsa, Barcelona Spain), producing CO₂ from HCl and marble (CaCO₃) chunks. The gas outlet was fitted to a short length of plastic/rubber tube which was capped. The only way the gas could leave the system was through the two-pronged capillary tubes stuck on this outlet tube. This setup acted as a manifold, supporting up to 20 flushing capillaries at any time. The use of a Kipp over a gas cylinder (which we also tested) has the advantage of producing low-pressure gas on demand for sustained periods of time. Pressure was an issue here, to prevent excessive evaporation or dispersion of the incubation medium, but enough to maintain the sample in turmoil and to provide enough gas in small bubbles to allow a good interchange between the sample carbonate and the gas stream.

After gas flushing, the incubation tubes were capped, held over empty 6ml scintillation counting pony vials, and then they were cut with heavy scissors. The lower part of the tube and its contents fell inside the vial; then scintillation cocktail was added and the vial

closed; after energetic shaking, the tubes were left to stand for about 10hrs. (to prevent any possible effect of chemiluminescence and to allow residual CO₂ to leave the liquid phase) and counted.

In order to determine whether part of the labelled CO₂ flushed out could come from carbamoyl-phosphate, we added unlabelled carbamoyl-phosphate (to a final concentration of 1μM) to samples after 5 min incubation. The presence of cold carbamoyl-phosphate did not alter the label countings, i.e. under the conditions of work and elimination of excess carbonate, carbamoyl-P is not broken up.

Calculations, Liver Enzyme Activity

Typically, blanks and zero-time tubes were in the range of 100-150 dpm. The zero values were discounted as background from all incubated sample counts. The amount of CP formed was derived from the net counts and the specific activity of the bicarbonate reagent. For all samples, in addition to a zero value, at least three incubation times were used, typically 2.5, 5 and 10 min; in all cases, initial velocities were calculated. This was usually made easier because there was a good linearity for up to 10 minutes in samples adequately diluted. Insufficiently diluted homogenates resulted in slightly lower Vi values and a loss of linearity. [Fig-1] shows the linear relationship between CP label found and incubation time. Repeated analyses of the same sample of liver (different homogenates) yielded practically the same enzyme activity (s.e.m. of 4.4% of the mean value, N=6).

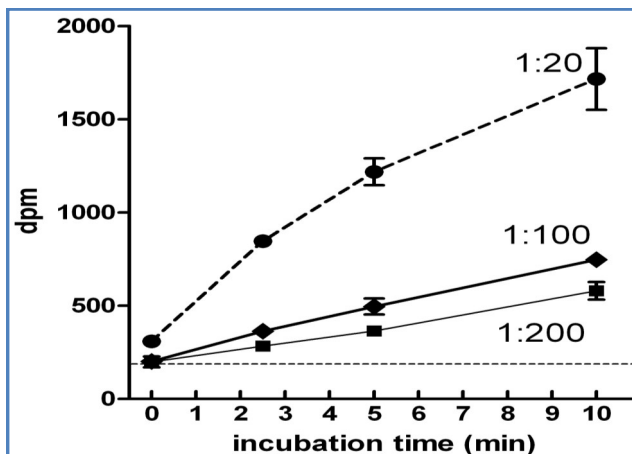


Fig. 1- Relationship between CP synthesis and time in rat liver homogenates

The data show the CP dpm obtained using the method described in the text for analysis of 0.050mL of rat liver homogenate (equivalent to about 2.5 mg of fresh tissue or 0.5 mg of protein) over time (dilution 1:20 w/v), further dilution to 1:100 and 1:200 vs. the initial tissue weight yielded more straight lines. The values are the mean ± sem of triplicate measurements. Linearity of the experimental data: 1:20 ($r=0.982$, $p=0.018$); 1:100 ($r=0.998$; $p=0.002$); 1:200 ($r=0.998$; $p=0.002$).

Results

Liver Carbamoyl-Phosphate Synthetase I Activity

Measurements in six different male rat liver samples yielded a CP synthetase-I activity of 89 ± 8 nkat/g of tissue, i.e. 444 ± 38 nkat/g protein (standard diet), and 122 ± 8 nkat/g of tissue, i.e. 704 ± 94

nkat/g protein (hyperproteic diet). The differences between groups were significant ($P<0.01$ tissue; $P<0.001$ protein; Student's *t* test).

Effectiveness of the Gas-flushing System

[Fig-2] shows the relationships between times of flushing on the bicarbonate label remaining on tubes not containing homogenate. The loss of label is rapid (depends on the flow of CO₂) and becomes practically asymptotic in a few minutes when using flow speeds of CO₂ in the range of 8-20μmol/s. The flow of gas was estimated by timing the accumulation of gas in an inverted graduated tube full of water and using one of the two-pronged capillaries to fill it up with gas.

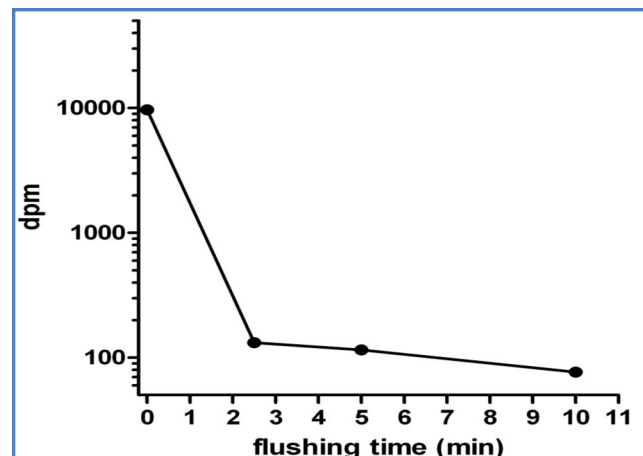


Fig. 2- Effect of CO₂ flushing on the loss of H¹⁴CO₃⁻ label in the medium used for incubations in the absence of homogenate.

The conditions for reaction stoppage and flushing are described in the text. The flow of CO₂ was 250μL/s at about 100 kPa, i.e. 12μmol/s.

We decided to use capillaries with two serrated needle extremes, since one was needed to connect to the Kipp outlet tube, and the other was had to be kept vertical within the tube; the metal needle weight and rigidity allowed it to remain in vertical position indefinitely. This way, the distribution of bubbles was uniform, and they emerged from the bottom in all incubation tubes. The use of polyethylene tubing with no attached needle resulted in a lower repetitiveness of results.

The addition of ethanol stopped effectively the reaction by decreasing the hydration envelopes of proteins, and compounded the effect of cold. Another reason why ethanol was used was its lowering of superficial tension, resulting in the practical elimination of foam from the incubation medium proteins. The absence of foam decreases the spill over of medium; CP is not soluble in ethanol [20], the amount of alcohol added (final concentration 33% by volume) may not be enough to precipitate CP, but enough to reduce its availability and limit the eventual action of phosphatases present in the medium (also inhibited by the change in pH).

The addition of acetic acid decreased the pH to 4.5, which further impeded reaction 1, and yielded enough protons to drive reaction 2 to the right, favouring the decomposition of carbonic acid and the emission of ¹⁴CO₂, helped by the diluting mass effect of the cold CO₂ stream. However, the decrease in pH was not sufficient to break up the CP in its components, especially in a medium which

contained a considerable amount of ammonium ions buffering the acetate.

When trying to establish the precise specific activity of the ammonium bicarbonate reagent, we observed that the direct estimation of radioactivity through liquid scintillation counting resulted in significant and variable losses of radioactivity. This was attributed to spontaneous decomposition of ammonium bicarbonate in equilibrium with the atmosphere. This was solved by adding 0.210mL (i.e. equivalent to the sequestering power of 1mMol of CO₂) of Carbo-Sorb E (Perkin Elmer) before the incorporation of the scintillation cocktail. This resulted in repetitive counting results and the prevention of losses. However, in the samples, part of the label was lost because of limited exchange with atmospheric (and dissolved air) CO₂; i.e., label counting of non-flushed samples (in which no acetic acid was added) was in the range of 89-95% of that expected (i.e. the amount of label added). Since the concentration of bicarbonate in the incubation medium was well in excess of that needed to sustain the reaction, and these losses did not modify the specific activity of bicarbonate, we decided to ignore this limited loss of label.

Discussion

The method presented has the advantage of simplicity; several samples can be analyzed in parallel, requires a short time of incubation, yielding a good linearity and repetitiveness, and requires minimal manipulation of the incubation medium. The main problem its utilization may pose is, perhaps, the long-term stability of homogenates (which lose activity when frozen) coupled with the necessity of previously finding the most adequate dilution of the homogenates in order to obtain the highest Vi (V_{max}) values. On the other side, the method shows considerable sensitivity, since it needs only a few mg of tissue for analysis; if needed, sensitivity can be increased simply by using less-diluted homogenates or, primarily, by increasing the specific activity of bicarbonate in the reaction mixture.

We used albumin to decrease the effect of proteases, and dithiothreitol as -SH group protector, but its presence should be removed when adapting the present method to the analysis of CP synthetase II, since its activity is inhibited by dithiothreitol [21].

The approach, and conditions of the incubation medium (and homogenization) used here are shared by other methods previously published. The main difference we introduced is, perhaps the direct measurement of CP formation without coupling this reaction to that of ornithine transcarbamylase [6] to yield citrulline, which is later measured by radioenzymatic [7] or colorimetric [8] procedures.

In fact, the true novelty of the method described here is the elimination of surplus bicarbonate/CO₂ by flushing it out under a stream of CO₂ at a mild acidic pH. This simplifies considerably the process, making it shorter, and remarkably cheaper. It also allows for the parallel analysis of multiple samples because of the simple gas supply manifold described and the small amount of sample needed. Under the conditions tested, the label in CP can be easily measured and there are no losses due to CP breakup by alkaline phosphatases [22].

The levels of activity in rat liver found using the method described here are higher than those found using the approach in which cit-

rulline formation is analyzed under conditions of excess ornithine transcarbamylase [6,23], in spite of wide variability in the actual liver enzyme activities obtained using different approaches. The rats receiving a hyperproteic diet showed a more marked CP synthetase I activity than controls, in this case, both in relation to liver weight and protein content, the activity measured was in the range of 1.4-fold increase. This is in agreement with enhanced activity of the enzyme under high protein/ammonium loads [24,25] and the increased activity of the urea cycle observed in rats receiving high protein diets [14,26]. The effect of diet on the enzyme activity measured reinforces the effectiveness of the method described for the measurement of this key urea cycle enzyme.

Acknowledgements

The study was supported by grant SAF2009-11739 from the Plan Nacional de Investigación en Biomedicina and AGL-2010-19740 from the Plan Nacional de Ciencia y Tecnología de los Alimentos of the Government of Spain. The authors declared no conflict of interest.

References

- [1] Chabas A., Grisolia S. and Silverstein R. (1972) *Eur. J. Biochem.* 29, 333-342.
- [2] Rubio V., Ramponi G. and Grisolía S. (1981) *Biochim. Biophys. Acta.*, 659, 150-160.
- [3] Mori M. and Tatibana M. (1977) *Biochim. Biophys. Acta.*, 483, 90-99.
- [4] Clarke S. (1976) *J. Biol. Chem.*, 251, 950-961.
- [5] Cohen N.S. and Rajzman L. (1980) *J. Biol. Chem.*, 255, 3352-3357.
- [6] Brown G.W. and Cohen P.P. (1959) *J. Biol. Chem.*, 234, 1769-1774.
- [7] Lof C., Wanders R.J.A. and Meijer A.J. (1982) *Eur. J. Biochem.*, 124, 89-94.
- [8] Pierson D.L. (1980) *J. Biochem. Biophys. Meth.*, 3, 31-37.
- [9] Guthörlein G. and Knappe J. (1968) *Eur. J. Biochem.*, 7, 119-127.
- [10] Christepherson R.I. and Finch L.R. (1976) *Anal. Biochem.*, 73, 342-349.
- [11] Rowe W.C., Huggins A.K. and Baldwin E. (1970) *Anal. Biochem.*, 35, 167-176.
- [12] Clifton P.M., Bastiaans K. and Keogh J.B. (2009) *Nutr. Metab. Cardiovasc. Dis.*, 19, 548-554.
- [13] Leidy H.J., Carnell N.S., Mattes R.D. and Campbell W.W. (2007) *Obesity*, 15, 421-429.
- [14] Ashida K. and Harper A.E. (1961) *Proc. Soc. Exp. Biol. Med.* 107, 151-156.
- [15] Barber T., Viña J.R., Viña J. and Cabo J. (1985) *Biochem. J.* 230, 675-681.
- [16] Green L.C., Ruiz de Luzuriaga K., Wagner D.A., Rand W., Istfan N., Young V.R. and Tannenbaum S.R. (1981) *Proc. Nat. Acad. Sci., USA*, 78, 7764-7768.
- [17] Cheung C.W. and Rajzman L. (1980) *J. Biol. Chem.*, 255, 5051-

5057.

- [18]Lowry O.H., Rosebrough R.W., Farr A.L. and Randall R.J. (1951) *J. Biol. Chem.*, 193, 265-275.
- [19]Griffin J.J. (1860) *A Popular Manual of Experimental Chemistry. Second Division: Non-metallic Elements.*, Griffin J.J. and Griffin R., London, 616-618.
- [20]Jones M.E., Spector L. and Lipmann F. (1955) *J. Am. Chem. Soc.*, 77, 819-820.
- [21]Trotta P.P., Pinkus L.M. and Meister A. (1974) *J. Biol. Chem.*, 249, 1915-1921.
- [22]Herzfeld A. and Knox W.E. (1972) *Cancer Res.*, 32, 1837-1841.
- [23]Brown T., Hug G., Lansky L., Bove K., Scheve A., Ryan M., Brown H., Schubert W.K., Partin J.C. and Lloyd-Still J. (1976) *N. Engl. J. Med.*, 294, 861-867.
- [24]Zaragozá R., Renau-Piquer J., Portolés M., Hernández-Yago J., Jordá A. and Grisolía S. (1987) *Arch. Biochem. Biophys.* 258, 426-435.
- [25]McGivan J.D., Bradford N.M. and Mendez-Mourão J. (1976) *Biochem. J.*, 154, 415-421.
- [26]Bingham S.A. (2003) *J. Nutr.*, 133, 921S-924S.

Notas sobre el desarrollo de metodología adaptada para la valoración en el tejido adiposo blanco de la actividad de las enzimas del ciclo de la urea

Sofía Arriarán¹, Silvia Agnelli¹, Xavier Remesar^{1,2,3}, José Antonio Fernández-López^{1,2,3}, Marià Alemany^{1,2,3}

1. Departamento de Nutrición y Bromatología, Facultad de Biología, Universidad de Barcelona, España.
2. Instituto de Biomedicina, Universidad de Barcelona, España.
3. CIBER Obesidad y Nutrición, Barcelona, España.

INTRODUCCIÓN

Uno de los principales objetivos de este trabajo era investigar la presencia de todas las enzimas del ciclo de la urea en tejido adiposo. Para desarrollar esta idea ha sido necesario no sólo analizar su expresión génica sino también comprobar la presencia y funcionalidad de las enzimas como proteínas. Puesto que una parte importante del trabajo de laboratorio se centró en este punto, hemos considerado conveniente incluir un capítulo en el que se describa sucintamente el proceso de ajuste, adaptación y desarrollo de la metodología necesaria para la determinación de las actividades enzimáticas del ciclo de la urea presentes en el tejido adiposo.

Una de las primeras dificultades que aparecen al intentar valorar la actividad de cualquier enzima del metabolismo de los aminoácidos, y además en el tejido adiposo, es la escasez y antigüedad de la bibliografía; la información más reciente es de los años setenta-ochenta del siglo pasado. En estos trabajos se describen métodos que utilizan técnicas que hoy día ya resultan obsoletas, con la complicación adicional de que muchos reactivos ya no se encuentran en el mercado. La práctica desaparición de estudios del metabolismo de aminoácidos analizando actividades enzimáticas, y el mayor interés actual en la investigación del funcionamiento y regulación del metabolismo lipídico y glucídico en condiciones fisiológicas y, especialmente, en enfermedades metabólicas, ha hecho que la mayor parte de proveedores de materiales para la investigación incrementen su precio, y/o descataloguen substratos radioactivos, enzimas y reactivos que son esenciales para el tipo de valoraciones que pretendíamos desarrollar. La ausencia en el mercado y/o el elevado precio de anticuerpos para medir estas enzimas como proteínas no nos permitió, por ejemplo, el desarrollo de técnicas más actuales, como el *Western blot*, aunque cabe resaltar que el *Western blot* sólo determina la presencia de la proteína, independientemente de su funcionalidad. Es decir no permite cuantificar ni su actividad

ni sus niveles, datos fundamentales para comprobar (y medir) su funcionalidad real.

Otro factor que ha dificultado el desarrollo metodológico ha sido el bajísimo nivel de financiación con el que cuenta actualmente el grupo de investigación al que pertenezco, complicado por el elevado coste de los reactivos y servicios técnicos de la propia universidad. Por ello, descartamos el uso de la cromatografía líquida de alta resolución (HPLC), sustituimos algunas técnicas radioquímicas por métodos colorimétricos, e inclusive, intentamos en algún caso la propia obtención o purificación de enzimas y reactivos.

La metodología que se detalla a continuación no es el resultado del desarrollo de técnicas nuevas de valoración enzimática; es sólo una consecuencia de la adaptación de técnicas ya publicadas en bibliografía antigua a la disponibilidad de materiales y de los instrumentos actuales en uso por nuestro grupo de investigación. Un aspecto importante que cabe reseñar, es que este trabajo representa la adaptación de técnicas, diseñadas para ser utilizadas en hígado, para la valoración de la actividad de enzimas en uno de los tejidos más plásticos, variables y desconocidos, el tejido adiposo. Este tránsito ha sido muy complicado debido a los bajos valores de actividad enzimática y al elevado contenido de lípidos del tejido, que han complicado todas las valoraciones.

ANIMALES, OBTENCIÓN DE MUESTRAS Y HOMOGENIZACIÓN

Todos los protocolos experimentales, así como los procedimientos de uso de animales de experimentación estuvieron de acuerdo con las guías de utilización animal de las Autoridades Europeas y Catalanas. El Comité de Experimentación Animal de la Universidad de Barcelona autorizó específicamente todos los procedimientos utilizados en el presente estudio. Cabe señalar que nuestro grupo de investigación tiene muy presente las normas específicas para el tratamiento adecuado de animales de

experimentación, por lo que, además de las autorizaciones pertinentes, aseguró su máximo bienestar utilizando el mínimo posible de animales y cumpliendo estrictamente las normativas que evitan el sufrimiento animal innecesario. Por todo ello, el sacrificio de los animales se hizo en condiciones no idóneas para el estudio (los animales fueron sacrificados bajo los efectos del anestésico isofluorano, que induce glucogenolisis hepática e incrementa la glucemia), pero adecuadas desde el punto de vista ético. Este enfoque ha permitido obtener resultados uniformes, haciendo posible establecer comparativas e índices con datos procedentes de un mismo animal. Se eligió este camino por razones éticas, no obstante, los resultados obtenidos han sido más homogéneos de lo previsto.

Se utilizaron ratas Wistar de 9 semanas de edad (Harlan, Sant Feliu de Codines). Los animales se separaron por sexo y por dieta, según fuesen alimentados *ad libitum*, durante 30 días, con pienso (tipo 2014, Harlan), o con una dieta de “cafetería” simplificada¹. El estudio, por consiguiente, se estructuró en cuatro grupos de 6 animales cada uno: machos-control, hembras-control, machos-cafetería y hembras-cafetería.

Al final del experimento los animales se sacrificaron y disecaron rápidamente. Se tomaron muestras de tejido adiposo mesentérico (ME), perigonadal (periovárico en las hembras y epididimal en los machos, PG), retroperitoneal (RP) y subcutáneo (cordones gramos inguinales, SC). Los fragmentos de tejido se congelaron en nitrógeno líquido, y se conservaron a -70°C para su posterior procesamiento.

El procedimiento de preparación de homogenados de tejido adiposo fue el mismo para todas las valoraciones enzimáticas. Con ello se intentó uniformizar el tratamiento de las muestras de tejido y permitir un estudio comparativo válido entre las actividades enzimáticas de diferentes localizaciones de tejido adiposo de los cuatro grupos experimentales.

Las muestras se homogeneizaron en frío, en 5 volúmenes de tampón hepes 70 mM pH 7,4, conteniendo ditioreitol 1 mM (Sigma, St Louis MO EEUU), 1g/L albúmina sérica (deslipidada) y 1g/L Triton X-100 (Sigma). La homogeneización se realizó en tres intervalos sucesivos y espaciados (enfriado) de 30 segundos cada uno, utilizando un disruptor de tejidos (Ultraturrax IKA-T10, Ika

Werke, Staufen, Alemania). La albúmina se utilizó para disminuir la posible acción de proteasas y el ditioreitol como protector de grupos sulfhidrilo. Debido a que algunas de las actividades enzimáticas del ciclo de la urea ocurren en la mitocondria, se utilizó el detergente Triton X-100 para romper las membranas y solubilizar las proteínas en el medio de homogenización. Escogimos el Triton X-100 y no otro detergente, porque ha sido descrito como el detergente no-iónico disponible que menos interacciona con las proteínas de membrana y el que interfiere menos en su funcionalidad y estructura^{2,3}.

La relación entre el peso de tejido y el volumen de homogenado se estableció a partir del estudio cinético previo de las actividades enzimáticas que se hicieron para cada uno de los componentes del ciclo de la urea. La intención era encontrar la dilución de homogenado adecuada para alcanzar los valores más elevados de velocidad inicial (*Vmax*) sin que se produjeran interferencias en la valoración por la excesiva concentración de tejido; para ello se utilizó una muestra de tejido adiposo de cada grupo experimental y se compararon tres relaciones peso/volumen (dilución 1:4, 1:5 y 1:10 p/v). La dilución 1:5 p/v resultó ser no sólo la más adecuada para alcanzar niveles máximos de actividad enzimática, sino también la que daba mejores resultados al cuantificar la actividad de las enzimas (arginino-succinato sintetasa y arginino-succinato liasa) que funcionan en rangos de actividad muy bajas en el tejido adiposo.

Al principio, y para la determinación de la actividad de la carbamoil-fosfato (CP) sintetasa I y II, se utilizó tampón de trietanolamina / HCl 50 mM pH 7,5. Puesto que diariamente se utilizaba más de un método de determinación enzimática, y que el tampón para las mediciones de las actividades restantes de las enzimas era un tampón de hepes 70 mM, decidimos intentar uniformizar el tampón de uso. Para ello, comparamos la actividad de la CP sintetasa I y II utilizando ambos tampones. Al no encontrar diferencias apreciables, pasamos a utilizar sólo el tampón hepes 70 mM también para la determinación de la actividad de las carbamoil-fosfato sintetasas.

Una vez homogeneizadas, las muestras, se centrifugaron en frío (4°C) a 5000xg durante 10 minutos para separar la grasa y los restos de tejido. Los lípidos presentes en los homogenados interfieren con el análisis enzimá-

tico, ya que en muchos casos reaccionan con los substratos y/o productos de la reacción, también interactúan con enzimas lipófilas, obstruyen filtros y columnas o placas utilizadas para la cromatografía o separación de metabolitos, y dan lugar a un efecto nefelométrico de dispersión de la luz, que afecta fuertemente las medidas espectrofotométricas⁴.

MEDIDA DE ACTIVIDADES ENZIMÁTICAS

Ornitina transcarbamila

La ornitina transcarbamila (OTC, EC 2.1.3.3) es la segunda enzima en la vía de síntesis de urea y arginina, y cataliza la conversión de ornitina y carbamoil-fosfato (CP) a citrulina y fosfato inorgánico⁵

Aproximaciones metodológicas

El ajuste metodológico para la cuantificación de la actividad de la ornitina transcarbamila se realizó en hígado y significó un arduo trabajo, realizado en su totalidad por mi compañera de doctorado, Silvia Agnelli. Por este motivo, sólo describiré brevemente los pasos que se siguieron para alcanzar la valoración de la actividad de esta enzima en tejido adiposo.

El funcionamiento de la OTC puede ser cuantificado a partir de la determinación colorimétrica o radioquímica del producto de su actividad, la citrulina. El procedimiento colorimétrico utiliza un complejo coloreado sintetizado a partir de la reacción entre L-citrulina, diacetil-monoxima, y fenazona. Este método de medición fue descartado, porque además que el complejo coloreado es relativamente sensible a la luz, la diacetil-monoxima reacciona con compuestos carbamido distintos a la citrulina, como la propia urea^{6,7}.

La metodología de elección fue radioquímica, utilizando ¹⁴C-carbamilo-fosfato o, en nuestro caso, ¹⁴C-ornitina para formar ¹⁴C-citrulina, que se separaba de su sustrato radiactivo por cromatografía de capa fina (TLC). Las regiones del cromatograma que correspondían a L-citrulina y su respectivo sustrato se cortaban y se contaba su radioactividad por centelleo líquido⁶.

Inicialmente, se pensó en adaptar el método de Goldstein *et al.*⁸, en el que se cuantifica la formación de citrulina marcada a partir de ¹⁴C-carbamilo-fosfato y ornitina. Debido al alto coste del sustrato radioactivo, intentamos sintetizar CP marcado a partir de ¹⁴C-cianato (¹⁴C-

KOCN) y KH₂PO₄. Lamentablemente, y después de un largo periodo de trabajo, comprobamos que el ¹⁴C-carbamilo-fosfato sintetizado era muy inestable en solución, razón por la que se descomponía durante la incubación de la enzima y a lo largo de la separación cromatográfica de la ¹⁴C-citrulina.

Tras comprobar la inestabilidad del ¹⁴C-carbamilo-fosfato sintetizado, decidimos utilizar ¹⁴C-ornitina como sustrato portador de la marca y proseguir con la adaptación de la metodología.

Método

Las condiciones de incubación se adaptaron a partir de la bibliografía, que describía el análisis de la actividad de la OTC en hígado humano⁶. Las incubaciones se llevaron a cabo a 37°C en tubos de polietileno de 1,5 mL (tubos eppendorf), utilizando un bloque calefactor. La mezcla de reacción (volumen final 75 µL) contenía (concentraciones finales) KCl 50 mM, MgCl₂ 7 mM, carbamoil-fosfato 9 mM, ornitina 13 mM (todos de Sigma), y ¹⁴C-ornitina 1 kBq/mL (Perkin Elmer, Bad Neuheim, Alemania) en tampón hepes 70 mM, pH 7,4.

La reacción se iniciaba añadiendo 125 µL de homogenado, preparado como se describe en el apartado de “animales, obtención de muestras y homogenización”, a 250 µL de mezcla de reacción. De esta mezcla, durante 2 minutos, a intervalos de 30 segundos se extrajeron alícuotas de 75 µL que se añadieron (en otros tubos) a 100 µL de acetona fría mantenida en hielo y agitando a continuación. El tiempo cero se estableció al añadir primero la acetona al reactivo de incubación (50 µL) y después el homogenado (25 µL). Luego los tubos se centrifugaron durante 3 minutos a 5000xg y los sobrenadantes se separaron en un concentrador centrífugo de vacío (Thermo Scientific, Waltham, MA EEUU). Los residuos secos se disolvieron en 25 µL de agua destilada y, posteriormente, se aplicaron a placas TLC de silicagel (200 µm; Macherey-Nagel, Düren, Alemania). Las placas de TLC fueron hendidas verticalmente para definir líneas independientes de 1cm de ancho, lo cual impidió la mezcla de las muestras cargadas. Se incluyó un control no marcado de ornitina y citrulina en cada placa. Las placas se desarrollaron con una fase móvil de triclorometano: metanol: ácido acético (1:2:2 por volumen). Una vez seca, y para determinar la ubicación de los aminoácidos, las zonas de

la placa cargadas con los controles se rociaron con ninhidrina y calentaron con un secador manual de cabello. La ubicación de las manchas de los controles de citrulina y ornitina permitió ajustar la localización de las zonas con los dos aminoácidos de las muestras. Así, la placa se marcó con lápiz blando en zonas horizontales dando cuadrados de aproximadamente 1 cm^2 , que fueron recortados, introducidos en viales con líquido de centelleo (Ecoscint H, National Diagnostics, Atlanta, GA EEUU) y contados en un contador (Liquid Scintillation Analyzer, Tri-Carb 2100TR, Canberra-Packard, Meriden, CT EEUU).

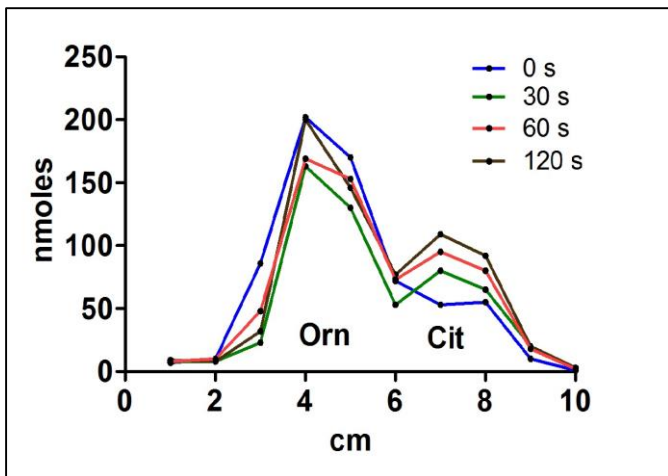


Figura 1: Separación de ^{14}C -ornitina y ^{14}C -citrulina por TLC. Separación por TLC de ^{14}C -ornitina y ^{14}C -citrulina para cada tiempo de incubación de la ornitina transcarbamila de una muestra de homogenado de tejido adiposo subcutáneo diluido en una proporción 1:5 p/v. Cada punto representa la cantidad de nanomoles de ornitina o citrulina por cm^2 del cromatograma.

Los cálculos para determinar la V_i , equiparada a V_{\max} en las condiciones estudiadas, se realizaron a partir de los resultados del marcaje de las manchas de citrulina para cada tiempo de incubación. En la figura 1 se muestra la separación de la ^{14}C -ornitina y ^{14}C -citrulina en una placa de TLC.

Antes de estudiar la actividad de la OTC en tejido adiposo, confirmamos, por análisis de expresión génica, PCR en tiempo real (rt-PCR), la expresión en dicho tejido de los transcriptos procedentes del gen que la codifica. Una vez comprobada su presencia, iniciamos las pruebas para cuantificar la actividad de la enzima. En la dilución 1:10 p/v los resultados de actividad enzimática fueron cercanos o iguales a cero nkat/g tejido. Los mayores

niveles de V_i para esta enzima fueron alcanzados con una dilución 1:5 p/v, razón por la que se utilizó dicha relación en todas las localizaciones estudiadas de tejido adiposo. La figura 2 muestra el resultado de las pruebas de cuantificación de la actividad de la OTC, utilizando dos diluciones de homogenado de tejido adiposo.

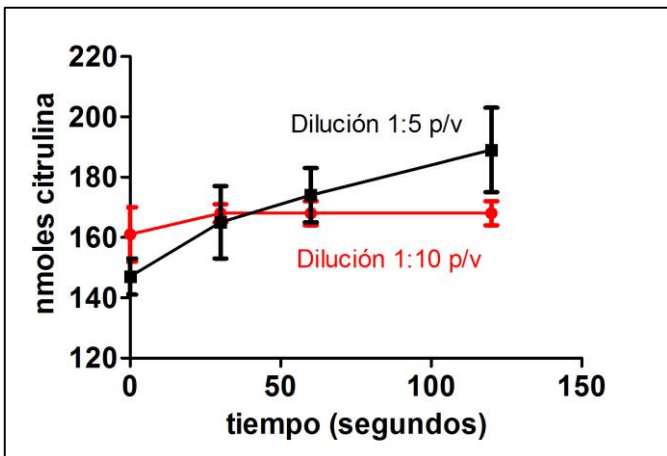


Figura 2: Actividad ornitina transcarbamila de tejido adiposo. Determinación de la aparición de ^{14}C -citrulina (nanomoles) en cada tiempo de incubación de la ornitina transcarbamila de tejido adiposo diluido en relaciones 1:5 o 1:10 p/v. Los datos son el promedio \pm sem (error estándar de la media) de cuatro localizaciones de tejido adiposo (SC, ME, PG, RP) de cuatro animales diferentes.

Carbamoil fosfato sintetasas I y II

Hay dos isoenzimas principales de la CP sintetasa; la CP sintetasa I (EC 6.3.4.16), que utiliza amonio como fuente de N, y la CP sintetasa II (EC 6.3.5.5) que utiliza glutamina⁹. Además de diferir en el sustrato que utilizan, la CP sintetasa I, principalmente hepática, funciona a nivel mitocondrial, es la encargada de incorporar el amonio al ciclo de la urea y requiere la presencia de N-acetyl-glutamato como activador, mientras que la CP-sintetasa-II es citosólica, esencial para la biosíntesis de nucleótidos, no requiere de activadores, y además de detectarse en el hígado, ha sido cuantificada en tejidos extra-hepáticos^{10,11}.

El ajuste y desarrollo de la metodología para la valoración de la actividad hepática de la CP sintetasa I dio lugar a la publicación del primer manuscrito de esta tesis⁹, por lo que sólo se presentará un resumen del citado, de

modo que se describirán principalmente las adaptaciones que se realizaron para cuantificar la actividad de la CP sintetasa II en tejido adiposo.

Aproximaciones metodológicas

El método de medición de la CP sintetasa I se basa en la cuantificación del ^{14}C -carbamoil-fosfato que se produce al incubar muestras de homogenados con una mezcla de reacción que contiene ATP, MgCl_2 , NH_4HCO_3 (marcado con $\text{NaH}^{14}\text{CO}_3$), y N-acetil-glutamato como activador necesario de la enzima.

El exceso de bicarbonato marcado se eliminaba acidificando ligeramente el medio y haciendo pasar por él un flujo constante de CO_2 no marcado. Finalmente, la radioactividad presente en el medio se atribuía al CP, que se cuantificaba por conteo y a partir de la actividad específica del bicarbonato añadido a la mezcla de reacción.

La mezcla de incubación (volumen final 200 μL) contenía (concentraciones finales): 50 mM de NH_4HCO_3 (conteniendo 5 kBq de $\text{NaH}^{14}\text{CO}_3$, Perkin Elmer), ATP 5 mM, MgCl_2 10 mM, ditioreitol 1 mM, 1g/L albúmina bovina, 1g/L Triton X-100 y N-acetil-glutamato disódico 5 mM (todos de Sigma), en 70 mM de tampón hepes pH 8. La reacción se detenía con 100 μL de etanol: ácido acético (20:1 v/v) mantenido a 0°C, agitando y colocando en hielo los tubos de reacción.

Los análisis de expresión génica en tejido adiposo evidenciaron que en dicho tejido no se expresa el gen que codifica a la CP sintetasa I (se utilizaron tres sondas específicas distintas para comprobarlo). Sin embargo, obtuvimos, y en cantidades similares a los genes de las demás enzimas del ciclo de la urea, amplicones correspondientes al gen que codifica la CP sintetasa II. A pesar de no haber encontrado la expresión del gen, y con la finalidad de confirmar la ausencia de la CP sintetasa I en tejido adiposo, realizamos pruebas de valoración enzimática utilizando una muestra por grupo experimental y localización de tejido. Los resultados confirmaron los análisis de expresión génica, al no evidenciarse actividad de la enzima durante los tiempos de incubación a los que fue sometida (0, 2,5, 5, 10 y 15 minutos). Por el contrario, las pruebas de actividad de la CP sintetasa II, realizadas con las mismas muestras y tiempos de incubación, mostraban la presencia de la enzima en tejido adiposo. Una

vez finalizadas las pruebas de comprobación, se determinó la actividad de la CP sintetasa II a partir de las adaptaciones al método de medición de la CP sintetasa I.

Método

Tras consultar la bibliografía específica ¹⁰⁻¹², y teniendo en cuenta que la principal diferencia entre los dos tipos de CP sintetasa es el sustrato que utilizan como fuente de amonio, las modificaciones que se realizaron a la metodología descrita en párrafos anteriores, para medir la actividad de la CP sintetasa II, fueron las siguientes: el NH_4HCO_3 utilizado se sustituyó por glutamina, se suprimió el N-acetil-glutamato presente en la mezcla de reacción ya que, como se ha comentado anteriormente, la CP sintetasa II no necesita de activadores para su funcionamiento y, por último, se utilizó mercaptoetanol en vez de ditioreitol, ya que éste inhibe la actividad de la CP sintetasa II ¹³. La reacción, al igual que en el caso de la CP sintetasa I, se llevó a cabo a 37°C, utilizándose, además del valor cero, tres tiempos de incubación; 2,5, 5 y 10 minutos, a partir de los cuales se calculó la velocidad inicial.

Para la determinación de la actividad de la CP sintetasa II las concentraciones de la mezcla de incubación (volumen final 200 μL) fueron las siguientes: NaHCO_3 16,7 mM (conteniendo 5kBq de $\text{NaH}^{14}\text{CO}_3$, Perkin Elmer), glutamina 2 mM, ATP 5 mM, MgCl_2 10 mM, mercaptoetanol 1 mM, 1g/L Triton X-100 y 1g/L albúmina bovina, en 70 mM de tampón hepes pH 8,0 (todos de Sigma).

Arginino-succinato sintetasa

La arginino-succinato sintetasa (ASS, L-citrulina, L-aspartato ligasa, EC 6.3.4.5) cataliza la condensación reversible, dependiente de ATP, de citrulina con aspartato para formar arginino-succinato ¹⁴. Este último es el precursor inmediato de arginina, que da lugar a la producción de urea en el hígado y de óxido nítrico (NO^\cdot) en muchos otros tejidos ¹⁵. Se ha demostrado la actividad de la ASS en muchas células y tejidos, por lo que es generalmente considerada una enzima ubicua ^{14,16}.

El desarrollo de la metodología para la cuantificación de la ASS fue uno de los retos más complicados a los que

hemos tenido que hacer frente en este estudio. Este trabajo se realizó junto con mi compañera de doctorado y se dividió en dos etapas: la primera consistió en revisar la bibliografía necesaria para adaptar las condiciones y reactivos de incubación a nuestras necesidades específicas mientras que la segunda se centró en encontrar y ajustar el procedimiento idóneo para cuantificar el arginino-succinato formado como producto de la reacción. Los problemas principales se encontraron en la segunda etapa, ya que el arginino-succinato es un compuesto químico muy inestable, sensible a los cambios de temperatura y pH. A continuación se citarán algunas de las características químicas que han hecho del arginino-succinato un compuesto difícil de cuantificar, ya sea por vía enzimática o radioquímica.

Se ha descrito que existen dos formas, probablemente cíclicas, de arginino-succinato¹⁷. Ratner *et al.* comprobaron que el arginino-succinato se modifica espontáneamente cuando permanece en solución acuosa, postulando que la nueva forma del compuesto es un anhídrido cílico¹⁸. Por ello, es conveniente mantener el arginino-succinato en forma de sal de una base fuerte, ya que como ácido libre se cicla espontáneamente cuando se encuentra en solución. El compuesto anhidro se forma principalmente bajo condiciones de temperatura elevada en medio ácido. Sin embargo, las soluciones de arginino-succinato a temperatura ambiente se ciclan, incluso en tiempos cortos, en una proporción considerable (7% por hora, durante las primeras tres horas), ya que el punto isoeléctrico de su forma libre está alrededor de pH 3,4^{17,18}.

Aproximaciones metodológicas

El primer método que se intentó adaptar para cuantificar la actividad de la ASS fue de tipo radioquímico¹⁹. Se utilizó ¹⁴C-L-aspartato (Perkin Elmer) para producir ¹⁴C-arginino-succinato en presencia de citrulina, aspartato, ATP y MgCl₂. Las condiciones de incubación se adaptaron a las descritas en la bibliografía para analizar la actividad de la enzima hepática de humanos y rata^{19,20}. La reacción se detuvo con ácido perclórico al 3%, neutralizando con KOH/KHCO₃ y centrifugando las muestras en frío a 7000xg. Los sobrenadantes se cargaron en placas de TLC para separar el ¹⁴C-arginino-succinato del aspartato radioactivo. Lamentablemente, y a pesar de varios intentos con solventes de diferentes polaridades, no se

logró una separación suficientemente clara, probablemente porque durante el proceso de incubación y desarrollo cromatográfico, el arginino-succinato se transformaba a formas cicladas, razón por la que se hacía difícil su localización en los cromatogramas como una mancha única.

Debido a que el arginino-succinato es un compuesto bastante inestable y difícil de cuantificar, optamos por transformarlo en arginina y fumarato en una reacción catalizada por la arginino-succinato liasa (ASL). Estos compuestos pueden ser posteriormente cuantificados utilizando métodos espectrofotométricos o radioquímicos. La ASL es una enzima difícil de encontrar en el mercado, y a pesar de haber contactado con varios proveedores, nacionales e internacionales, todos ellos tenían la enzima descatalogada. Al no poder adquirirla, iniciamos su aislamiento a partir de un manuscrito que describe su elevada actividad en cotiledones de guisantes germinados y en desarrollo²¹. Los cotiledones con mayor actividad ASL son los que germinan de semillas cosechadas en el periodo de antesis de la planta del guisante^{22,23}; como no encontramos ese tipo de semilla, intentamos extraer la enzima a partir de cotiledones germinados de semillas secas (de siembra) de guisantes (*Pisum sativum* L.). Las semillas se hicieron germinar en vasos con celulosa (cultivo hidropónico) y agua. Cuando las plántulas alcanzaron unos 5 cm, los cotiledones se recolectaron y se pulverizaron en un mortero: 12 g de cotiledones con 5-8 g de arena silícea fina, y 20 mL de medio de extracción, que contenía (concentración final): manitol 400 mM, tampón de ácido sulfónico-morfolino propano 50 mM (pH 7,4) y 0,25% (p/v) de bis(trimetilsilil)-acetamida (todos de Sigma). Después de pulverizar, la mezcla se filtraba con una malla de nylon y se centrifugaba a 2500xg durante 5 minutos para eliminar la arena y restos de tejido. El sobrenadante se centrifugó otra vez, a 40000xg, durante una hora, obteniéndose un precipitado. Éste se lavó en dos ocasiones y resuspendió en el medio de extracción. El extracto final tenía una actividad ASL detectable (0,874 nkat/g cotiledón) pero insuficiente (e impura) para utilizarse como enzima de acople en el método de valoración de la arginino-succinato sintetasa. Esta actividad enzimática se cuantificó, midiendo a 240 nm de longitud de onda, la aparición de fumarato tras incubar los extractos con arginino-succinato durante 15 minutos a 37°C. Es probable que la baja concentración de

la enzima se debiese al tipo de semillas de guisante que utilizamos; como se ha comentado anteriormente, los cotiledones de semillas cosechadas en períodos previos a su deshidratación natural parece que presentan una actividad ASL más elevada.

Método

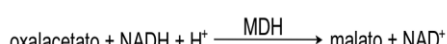
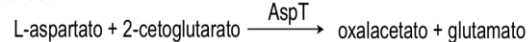
Tras intentar cuantificar, sin éxito, el arginino-succinato, decidimos dejar de lado su identificación y cuantificación, y centrarnos en valorar la tasa de utilización de sustratos de la ASS como resultado de su actividad. La ASS hace uso, además de ATP, de dos aminoácidos relativamente fáciles de medir: citrulina y aspartato. La complejidad del proceso de TLC para separar aminoácidos en presencia de arginino-succinato, nos llevó a descartar cualquier procedimiento cromatográfico (y radioquímico) de medición, y a elegir métodos espectrofotométricos. La citrulina puede cuantificarse por procedimientos colorimétricos pero, tal como se ha comentado más arriba, uno de los reactivos de medición es capaz de generar falsos positivos, razón por la que decidimos valorar la actividad de la ASS a partir del consumo de aspartato en el medio a lo largo del tiempo.

Para la valoración de aspartato se midió la desaparición de NADH, a 340 nm, como resultado de la transaminación del aspartato a oxalacetato por la aspartato transaminasa (AspT). El oxalacetato era reducido posteriormente por la malato deshidrogenasa (MDH) y NADH. La concentración de aspartato se determinaba a partir de un patrón de desaparición de NADH, realizado con concentraciones conocidas del aminoácido.

Primera fase:



Segunda fase:



Finalmente, por problemas de requerimientos de pH para favorecer ambas reacciones, se optó por utilizar un método para valorar la actividad de la ASS dividido en dos fases: la primera, de incubación de la enzima con el sustrato a diferentes tiempos, y la segunda, de cuantificación del aspartato restante en cada uno de los tiempos estudiados en la fase de incubación de la enzima.

Las condiciones de incubación fueron ajustadas a partir de estudios que describen la actividad de la ASS en levaduras (*Saccharomyces cerevisiae*) y en hígado humano o de rata^{19,20,24}. Las incubaciones se llevaron a cabo a 37°C utilizando un bloque calefactor. La mezcla de incubación (volumen final 85 µL) contenía (concentraciones finales): ATP 10 mM, MgCl₂ 5 mM, ornitina 3 mM, aspartato 2,5 mM, ditiotreitol 1 mM, 1g/L albúmina bovina y 1g/L Triton X-100 (todos de Sigma).

La reacción se iniciaba añadiendo 85 µL de L-aspartato a 340 µL de mezcla de incubación. A los 0,5, 2,5, 5 y 10 minutos de reacción se tomaban 85 µL y se mezclaban con 40 µL de 3g/L ácido perclórico. Los tubos eran luego neutralizados (pH 7,5) con una mezcla de 10 µL 60g/L de KOH y 35g/L K₂CO₃, y centrifugados a 8000xg durante 15 minutos.

Antes de iniciar la segunda fase del experimento se midió el pH de los sobrenadantes con tiras reactivas, añadiendo suficiente KOH/K₂CO₃ hasta alcanzar un valor de pH entre 7,0 y 7,5. En una placa de 96 pocillos, se añadieron 20 µL de sobrenadante y 280 µL de tampón hepes 70 mM conteniendo NADH 250 µM, 2-ceto-glutarato 200 µM, aspartato-transaminasa 20 nkatal/ml, y malato-deshidrogenasa 17 nkatal/ml (ambas enzimas de corazón cerdo y todos los reactivos de Sigma). Las placas fueron leídas en un lector de placas (Biotek, Winoosky, VT EEUU) a 340 nm a intervalos de 30 segundos durante 30 minutos. La desaparición de aspartato en cada tiempo de incubación fue utilizada para determinar la V_i de la ASS de cada muestra.

Para determinar la dilución ideal de los homogenados a utilizar en la cuantificación de la actividad de la ASS realizamos pruebas con el tejido diluido en proporción 1:5 o 1:10 (peso/volumen). Aunque ambas diluciones nos permitieron cuantificar la enzima, observamos mayores valores de Vi (y más estables) con la dilución 1:5 p/v, razón por la que se utilizó dicha relación en todas las localizaciones de tejido adiposo.

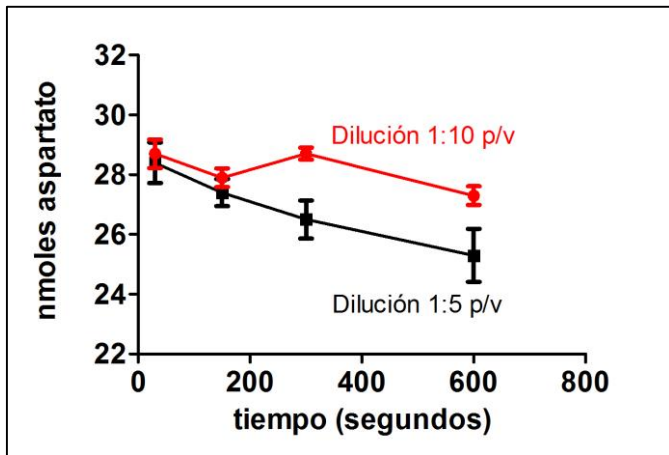


Figura 3: Actividad de la arginino-succinato sintetasa de tejido adiposo. Determinación de la desaparición de aspartato (nanomoles) en cada tiempo de incubación de la arginino-succinato sintetasa de tejido adiposo diluido en relaciones 1:5 o 1:10 p/v. Los datos son el promedio \pm sem de cuatro localizaciones de tejido adiposo (SC, ME, PG, RP) de cuatro animales diferentes.

La figura 3 muestra el resultado de las pruebas de cuantificación de la actividad de la arginino-succinato sintetasa utilizando diferentes diluciones de homogenado de tejido adiposo. Para descartar posibles falsos positivos producidos por alguna enzima distinta a la ASS, capaz de utilizar el aspartato del medio de incubación, se prepararon controles en los que se omitió la citrulina, sustituida por solución tampón. Las muestras se procesaron tal como se ha descrito más arriba. Como se puede ver en la Fig.4, no se observó ninguna actividad enzimática espuria en ausencia de citrulina, lo que permitió descartar esta posible fuente de error.

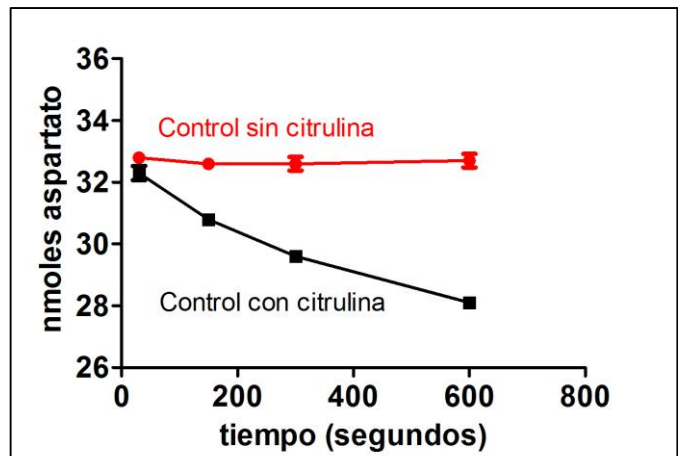


Figura 4: Actividad de la arginino-succinato sintetasa de tejido adiposo en presencia y en ausencia de citrulina. Determinación de la desaparición de aspartato (nanomoles) en muestras de tejido adiposo (dilución 1:5 p/v) incubadas en presencia y en ausencia de citrulina. Los datos son el promedio \pm sem de cuatro localizaciones de tejido adiposo (SC, ME, PG, RP) de un animal (macho) control.

Arginino-succinato liasa

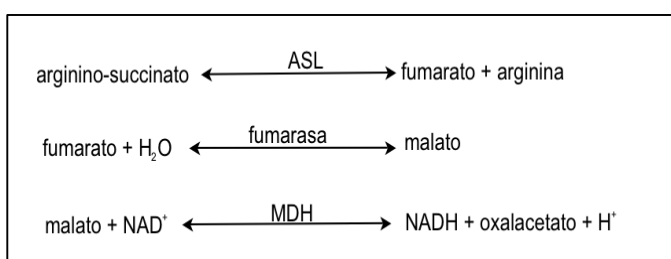
La arginino-succinato liasa (ASL, EC 4.3.2.1) es la enzima del ciclo de la urea que cataliza la ruptura del arginino-succinato, dando arginina y fumarato^{25,26}. Se ha hallado actividad de esta enzima en hígado y riñón de mamíferos²⁷, así como en los eritrocitos humanos²⁸.

Aproximaciones metodológicas

Se ha descrito toda una serie de métodos para la cuantificación de la actividad de la ASL basados en valoraciones colorimétricas, fluorimétricas o radioquímicas de la arginina liberada^{25,26}. Sin embargo, la elevada concentración de esta última en tejidos, principalmente hígado, origina elevadas lecturas de los blancos. La interferencia que genera la arginina basal llevó al desarrollo de metodología específica para valorar la actividad de esta enzima mediante la cuantificación del fumarato formado a partir de la ruptura del arginino-succinato²⁵.

A la vista de las dificultades que presentaban los distintos enfoques experimentales, decidimos cuantificar la actividad de la ASL a partir de la formación de fumarato, ya que la concentración de este último en plasma y tejidos es baja²⁹. La metodología se ajustó a partir de las medidas de la actividad de la enzima en eritrocitos y

suero humano descritas en la bibliografía²⁵. El método consiste en valorar el fumarato formado por hidratación a malato utilizando fumarasa, para luego determinar su concentración utilizando malato deshidrogenasa (MDH), y estimando por espectrofotometría (340 nm) el NADH sintetizado



La reacción se realizó en dos fases: la primera consistió en incubar los homogenados de tejido adiposo (relación p/v 1:5 o 1:10) a 37°C con arginino-succinato 2 mM (Sigma) en tampón de fosfatos 70 mM. Tras detener la reacción a los 0,5, 2,5, 5 y 10 minutos con 3,0 g/L de ácido perclórico, las muestras se neutralizaron en frío con KOH/K₂CO₃ y se centrifugaron a 8000xg durante 15 minutos a 4°C. En la segunda fase, para valorar el fumarato formado, se incubaron los sobrenadantes de la primera fase a temperatura ambiente (21-24 °C) durante 15 minutos en un medio de reacción que contenía (concentraciones finales) NAD⁺ 2 mM, fumarasa (de corazón de cerdo) 300 nkat/mL y MDH 58 nkat/mL en tampón de hidracina-glicina 50 mM pH 9,5 (todos de Sigma). La reacción de la segunda fase se inició añadiendo la fumarasa, de manera que el malato basal presente en las muestras, al oxidarse a oxalacetato, no interfiriese en la valoración final de fumarato al quedar incluido en el blanco. Antes de realizar las pruebas de dilución y la cuantificación de la actividad de la ASL de homogenados de tejido adiposo, se confirmó el funcionamiento del sistema fumarasa/ MDH con patrones de fumarato y malato a 2 mM de concentración final.

Cuando se iniciaron las pruebas para determinar la dilución ideal de homogenado a la que se cuantificaría la actividad de la ASL, detectamos que el incremento de NADH, y por ende la presencia de fumarato, no era proporcional, sino mayor que la cantidad de arginino-succinato añadido durante la incubación. Al repetir el experimento con blancos (se sustituyeron los homogenados de tejido por el tampón que se utiliza para su preparación) observamos un incremento significativo, dependiente de NADH, en la absorbancia a 340 nm. Al no haber tejido

en los blancos, y ser el argininosuccinato el único susstrato presente en los sobrenadantes, se intuyó que este último podría estar contaminado con fumarato o malato. Confirmamos la contaminación con malato al detectar la formación de NADH tras incubar el arginino-succinato con malato deshidrogenasa y NAD⁺ a pH 9,5. Para determinar el grado de contaminación se incubaron cantidades equimolares (1 µmol) de argininosuccinato y fumarato con el medio de reacción de la segunda fase del experimento; el arginino-succinato dio una absorbancia proporcional al 50% de la cantidad de fumarato añadida. Los resultados de las incubaciones de fumarato y arginino-succinato se muestran en la figura 5

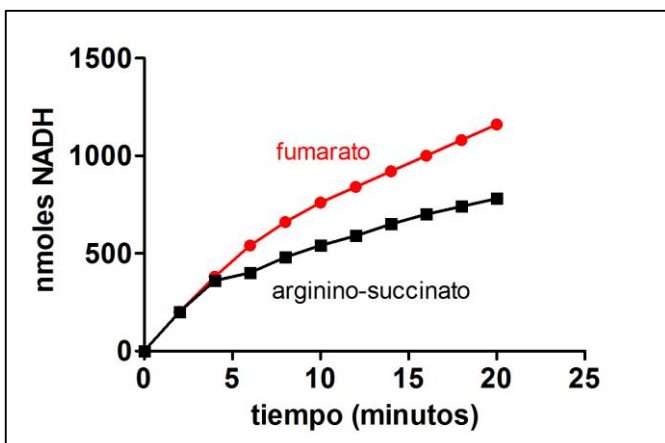


Figura 5: Contaminación con malato del reactivo de arginino-succinato. Cantidad equimolar de fumarato y arginino-succinato (1 µmol) se incubaron durante 20 minutos con malato deshidrogenasa, fumarasa para el caso del fumarato, y NAD⁺. Los resultados confirmaron que el arginino-succinato se encontraba fuertemente contaminado con malato al detectarse señal de NADH.

Al principio tratamos de restar la señal del blanco de arginino-succinato a la absorbancia producida como resultado de la actividad de la enzima; sin embargo, esta corrección no se pudo llevar a cabo, ya que la contaminación con malato era mucho más elevada que el fumarato que se podía formar a partir de la reacción catalizada por la ASS en las condiciones de ensayo. Estos problemas de cuantificación nos condujeron a intentar separar el fumarato sintetizado durante la reacción enzimática del arginino-succinato restante en los sobrenadantes. Aprovechando la insolubilidad en alcohol del arginino-succinato, se resuspendió 1 µmol de arginino-succinato o 1 µmol de

fumarato en tubos con 100 μ L de alcohol absoluto (seco con Na₂SO₄ anhidro). Ambos tubos se centrifugaron a 5000xg durante 5 minutos. Los sobrenadantes (previamente evaporados con un flujo continuo de nitrógeno gas) y los precipitados obtenidos se resuspendieron en 100 μ L de agua destilada y se midió la aparición de NADH una vez incubados con el reactivo de reacción de la segunda fase del experimento.

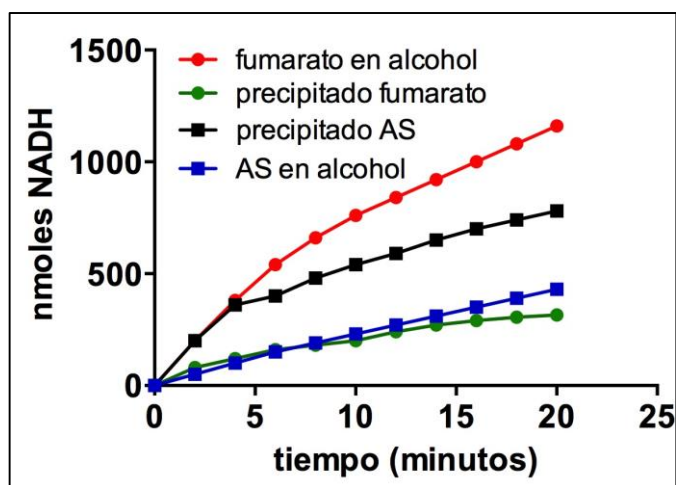


Figura 6: Separación en alcohol de argininosuccinato y fumarato. Cantidades equimolares de fumarato y arginino-succinato (1 μ mol) se resuspendieron en 100 μ L de alcohol absoluto. Tras su centrifugación, se determinó la producción de NADH de los sobrenadantes y precipitados obtenidos en presencia de MDH. Como puede observarse, una proporción significativa de arginino-succinato (AS) permaneció disuelta en alcohol, imposibilitando la separación de la señal de contaminación con malato de la del producto de la actividad de la ASL.

Lamentablemente, y como puede observarse en la figura 6, una proporción significativa (10-15% aproximadamente) de fumarato precipitó en el alcohol, mientras otra proporción similar de arginino-succinato se mantuvo disuelta en él, descartando la posibilidad de purificar suficientemente el arginino-succinato (o al menos, eliminar suficiente malato contaminante) como para poderlo utilizar en este enfoque metodológico para valorar la ASL.

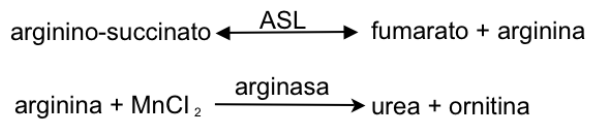
Método

Debido a la contaminación del arginino-succinato, contactamos con varios proveedores con la intención de adquirir un reactivo más puro, encontrando que todas ellas tenían el producto descatalogado. Cabe señalar que el único suministrador (caro y no siempre disponible), Sigma, nos proporcionaba un producto natural (extraído) y no sintético. No hay arginino-succinato sintético/puro disponible en el mercado. Pensamos en sintetizarlo, pero las dificultades eran enormes para nuestros medios y experiencia, por lo que nos vimos obligados a trabajar con un sustrato esencial pero impuro, de disponibilidad irregular.

Además, durante todo el periodo de desarrollo de la fase experimental del presente estudio sólo se pudo disponer de un único lote del reactivo. Por todo ello, decidimos cambiar el enfoque del método y cuantificar la actividad de la arginino-succinato liasa a partir de la arginina producida durante la reacción de escisión.

La arginina liberada como producto de la actividad de la ASL se midió a partir de su reacción con la arginasa para formar ornitina y urea. Posteriormente, la urea fue valorada utilizando un método químico sensible ³⁰.

Las condiciones y reactivos de incubación para la reacción de la ASL fueron los mismos que se describen en párrafos anteriores. El método de valoración de la arginina se ajustó a partir de la bibliografía existente, que describe la actividad de la arginasa en hígado de rata ³⁰; las principales modificaciones se centraron en la cantidad de arginasa a añadir, ya que en este caso se quería cuantificar la arginina presente, no la actividad de la enzima.



Una característica común de las argininas es el requerimiento de un pH alcalino, así como la activación con iones Mn^{2+} para medir su actividad^{31,32}. La velocidad máxima de la enzima se observa en un pH de 9,0 a 9,5. Por estas razones, se añadió $MnCl_2$ al medio de incubación, a pH 9,5.

Una vez finalizada la primera fase de la reacción, alícuotas de 100 μL de sobrenadante neutralizado se mezclaron con 50 μL de tampón hepes 70 mM pH 7,5 (alcanzándose un pH final de 9,0 con una solución de 80g/L de KOH); las concentraciones finales fueron de 7 mM $MnCl_2$ y 16,7 nkat/mL de arginasa de hígado de rata (Lee Bio-solutions, St Lous, MI EEUU). El tampón que contenía la arginasa y el Mn^{2+} fue activado previamente a su utilización manteniéndolo a 55 °C durante 5 minutos³¹. La reacción se desarrolló durante 30 minutos a 37°C, y fue detenida añadiendo 35 μL de 160 g/L ácido perclórico. Los tubos fueron posteriormente centrifugados a 8000xg durante 15 minutos a 4 °C, descartando el precipitado.

La determinación de la urea liberada por la acción de la arginasa se basa en la formación de un producto coloreado al reaccionar con una solución ácida de diacetil-monoxima³³. Dado que la diacetil-monoxima es capaz de reaccionar con algunos compuestos carbamido distintos a la urea⁶, intentamos, sin éxito, valorar esta última a partir de su transformación en amonio utilizando ureasa, hipoclorito y fenol con nitroprusiato sódico como catalizador, es decir, la clásica reacción de Berthelot³⁴. No obstante, la valoración del amonio no funcionó adecuadamente debido a que la ureasa se inhibe parcialmente en presencia de iones manganosos³⁵ presentes en los sobrenadantes de medición. Confirmamos la inhibición parcial de la ureasa al preparar patrones de urea con y sin Mn^{2+} ; la conversión de urea a amonio en presencia de Mn^{2+} no llegó al 100%.

Finalmente, para la estimación de la urea, liberada por la arginasa, alícuotas de 175 μL del sobrenadante de desproteinización con perclorato se mezclaron con 300 μL de 90g/L H_2SO_4 que contenían 270g/L de H_3PO_4 ; luego se añadieron 20 μL de 30 g/L de 1-fenil-2-oxima-1,2-propanodiona en alcohol absoluto. La reacción se llevó a cabo a 100°C en un bloque calefactor durante 30 minutos. Finalmente, se midió la densidad óptica de los tubos a 540 nm en un lector de placas. Las placas contenían

patrones de arginina y urea, así como blancos. La efectividad de la arginasa fue comprobada en cada experimento. Como se muestra en la figura 7, en todos los casos la conversión de arginina a urea fue completa.

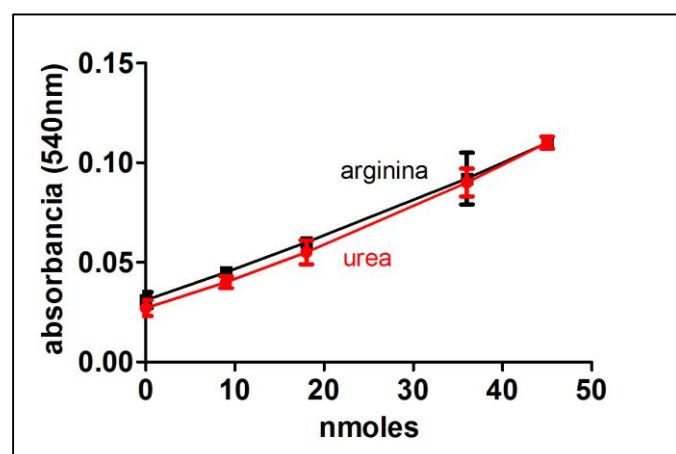


Figura 7: Efectividad de la enzima arginasa utilizada en la valoración de la ASL de tejido adiposo. Se comprobó la efectividad de la enzima arginasa utilizando cantidades equimolares de urea y arginina. Como puede observarse, la arginasa convierte a urea prácticamente el 100% de la arginina estudiada.

La presencia de arginina en tejido adiposo podría generar lecturas elevadas de blancos durante la cuantificación de la ASL²⁵, por lo que inicialmente, intentamos valorar la actividad de la enzima utilizando homogenados de tejido con una relación peso/volumen menor a las utilizadas para la cuantificación de las demás enzimas del ciclo de la urea. Puesto que los resultados de actividad enzimática con diluciones de homogenado en el rango de 1:15-1:20 peso/volumen fueron cercanos o iguales a cero nkat/g tejido, decidimos volver a probar con homogenados más concentrados. La concentración de arginina en tejido adiposo no interfirió con la cuantificación de la ASL, ya que los blancos iniciales de la valoración de la enzima se encontraban cercanos a cero a pesar de haberse utilizado homogenados que contenían una cantidad considerable de tejido (1:5 - 1:10 p/v). En la figura 8 se pueden observar los resultados de actividad de la ASL obtenidos con diferentes diluciones de homogenado de tejido adiposo. Los mayores valores de V_i para esta enzima fueron alcanzados con la dilución 1:5 p/v, razón por la que se utilizó dicha relación en todas las localizaciones estudiadas de tejido adiposo.

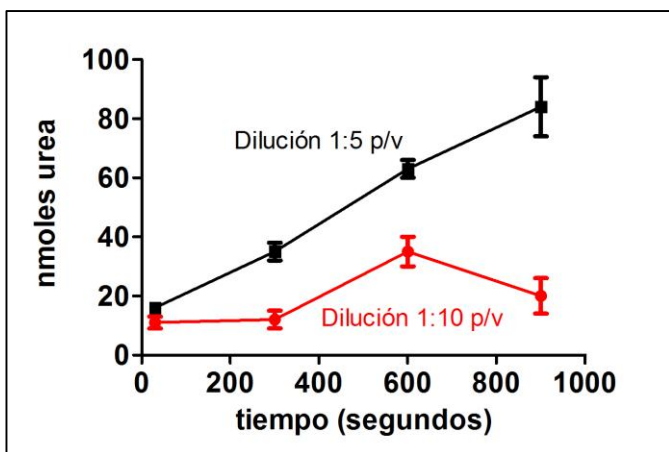


Figura 8: Actividad de la argininosuccinatilasa en tejido adiposo. Determinación de la aparición de urea (nanomoles) en cada tiempo de incubación de la enzima ASL de tejido adiposo en homogenados diluidos en relaciones 1:5 o 1:10 p/v. Los datos son el promedio \pm sem de cuatro localizaciones de tejido adiposo (SC, ME, PG, RP) de cuatro animales diferentes.

Arginasa

La arginasa (L-arginina aminohidrolasa, EC 3.5.3.1) cataliza la hidrólisis de L-arginina a L-ornitina y urea³⁶. Los mamíferos expresan dos isoenzimas de la arginasa que son codificadas por genes distintos: arginasa I, citosólica, y arginasa II, una enzima de la matriz mitocondrial^{37, 38}. La arginasa I se encuentra en el hígado como componente del ciclo de la urea³⁶, mientras que la arginasa II se expresa en otros tejidos, como próstata, riñón, intestino delgado y glándula mamaria, y está involucrada en la síntesis de poliaminas, glutamato y prolina, y en la modulación de la síntesis de óxido nítrico³⁸.

Al igual que en todos los casos anteriores de valoración enzimática, antes de realizar los estudios de la actividad de la arginasa en tejido adiposo confirmamos, mediante rt-PCR, la expresión de los genes que codifican para ambas isoenzimas. Todas las localizaciones estudiadas de tejido adiposo (SC, ME, PG y RP) expresaron el gen de la arginasa I, siendo el tejido adiposo subcutáneo el único que expresó también claramente, de modo inequívoco, el gen de la arginasa II.

Debido a la similitud en sus propiedades enzimáticas, la actividad de ambas arginasas no ha podido ser diferenciada por los métodos habituales de cuantificación, salvo

separación de las especies moleculares, algo que descartamos directamente por ser incompatible con medidas cuantitativas y por las enormes dificultades técnicas ligadas al tamaño y dilución de las muestras. Por tanto, cuando ambas isoenzimas se encuentran presentes en las muestras a estudiar los resultados de los métodos de valoración suelen representar la suma de las dos actividades³⁶.

En la bibliografía se describen una serie de métodos para la cuantificación de la actividad arginasa. Todos ellos se basan en la valoración química^{30,34} o radioquímica³⁹ de uno de los productos de su actividad, ornitina o urea.

Aproximaciones metodológicas

En un inicio intentamos ajustar un método radioquímico para la cuantificación de la arginasa, en el cual se contabiliza la ¹⁴C-urea producida por la enzima a partir de la utilización de L-(guanidino-¹⁴C) arginina como sustrato⁴⁰. Lamentablemente, y a pesar que el protocolo radioquímico presenta una mayor sensibilidad que el químico-espectrofotométrico, tuvimos que escoger este último ya que el precio del sustrato radioactivo era demasiado elevado para los recursos disponibles.

Método

El método utilizado para la cuantificación de la arginasa fue el descrito en el apartado anterior, para la segunda fase de la valoración de la ASL. No obstante, mientras que en aquel caso añadímos un exceso de arginasa para determinar la cantidad de arginina presente en la muestra, aquí se añadía en exceso el substrato, arginina, puesto que lo que nos interesaba era valorar la actividad máxima de la enzima.

La reacción se iniciaba, como se ha descrito más arriba, activando la enzima con Mn²⁺ a 55°C durante 5 minutos; para ello se mezclaron 20 μ L de homogenado con 5 μ L de MnCl₂ disuelto en agua; concentración final 10 mM. Una vez disminuyó la temperatura a 37 °C, la reacción se inició con la adición de 75 μ L de arginina disuelta en tampón hepes 70 mM, ajustando el pH a 9,7; concentración final 78 mM. Las incubaciones se llevaron a cabo durante 1, 10 y 20 minutos. La reacción se detuvo al añadir 35 μ L de una solución de 160 g/L de ácido perclórico. Los tubos se dejaron en frío y luego se centrifugaron a 8,000xg durante 15 minutos a 4°C. La urea formada se

midió tal como se ha descrito anteriormente en el método para la valoración de la arginino-succinato liasa.

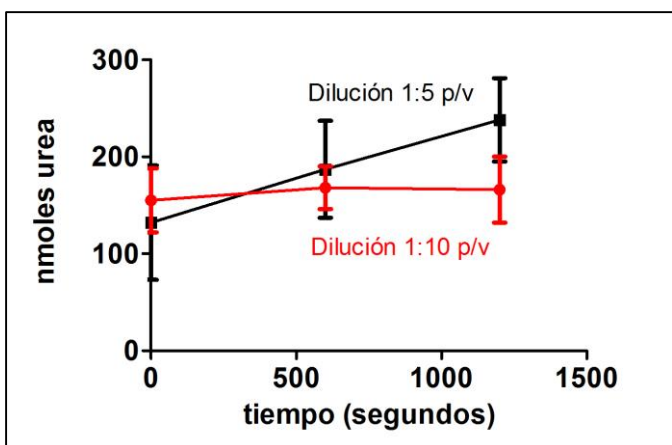


Figura 9: Actividad de la arginasa en tejido adiposo. Determinación de la aparición de urea (nanomoles) en cada tiempo de incubación de la arginasa de tejido adiposo diluido en relaciones 1:5 o 1:10 p/v. Los datos son el promedio \pm sem de cuatro localizaciones de tejido adiposo (SC, ME, PG, RP) de cuatro animales diferentes.

La expresión de los genes que codifican las arginasas I y II en tejido adiposo era relativamente baja en relación al hígado o riñón, por lo que decidimos realizar las pruebas de cuantificación enzimática con homogenados que contenían cantidades relativamente elevadas de tejido (1:10 y 1:5 p/v). Como puede observarse en la figura 9, la relación tejido: medio de homogenización 1:10 p/v mostró resultados de actividad cercanos a cero nkat/g tejido, mientras que la relación 1:5 p/v nos permitió obtener los mejores resultados de V_i , razón por la cual elegimos dicha dilución de homogenado para determinar la actividad arginasa en todas las localizaciones de tejido adiposo.

EXPRESIÓN DE LOS RESULTADOS

La metodología utilizada para determinar la funcionalidad de las proteínas involucradas en el metabolismo de los aminoácidos en el tejido adiposo blanco ha incluido no sólo el análisis de actividades enzimáticas, sino también el estudio de la expresión de sus respectivos genes utilizando la técnica de la reacción en cadena de la polimerasa en tiempo real (*real time polymerase chain reaction*, rtPCR). Los resultados de estos estudios permiten

realizar comparaciones del nivel de replicación de genes/alelos de interés entre grupos experimentales y grupos control. Comúnmente, las comparaciones se refieren a genes “constitutivos”, que no se espera que se modifiquen bajo las condiciones experimentales debido a su falta de reactividad. Los resultados son usualmente presentados como porcentajes de los controles, o expresados en unidades arbitrarias que permitan realizar comparaciones, pero en ningún caso estas pueden ser semi-cuantitativas o cuantitativas. Por ello, para expresar los resultados obtenidos a partir de los análisis génicos de las enzimas, hormonas y otros reguladores estudiados hemos utilizado un método semi-cuantitativo⁴¹, desarrollado y publicado por nuestro grupo de investigación, que permite realizar comparaciones directas (ej. como copias de ARN mensajero por g de tejido/proteína o célula) entre diferentes genes y tejidos, estableciendo el grado de abundancia de las diferentes especies moleculares investigadas.

La amplia variabilidad de tamaño, flujo sanguíneo, inervación y celularidad del tejido adiposo blanco origina problemas adicionales para comparar entre diferentes situaciones anatómicas (ej. localización del tejido), fisiológicas (ej. sexo, dieta) y patológicas (ej. obesidad). La variabilidad de las reservas lipídicas pueden generar comparaciones irrelevantes basadas en el peso; el uso de los valores de ADN o número de células da lugar a aproximaciones más precisas, pero los múltiples tipos celulares que coexisten en el tejido adiposo pueden también alterar las comparaciones directas. Con la finalidad de determinar las posibles interacciones entre las actividades enzimáticas y la expresión de sus respectivos genes, los resultados obtenidos a partir de la metodología desarrollada en el presente estudio han sido expresados según el contenido proteico de las diferentes localizaciones de tejido adiposo utilizadas. Sin embargo, probablemente la mejor manera de medir los cambios en la actividad funcional de las proteínas es a través del análisis de la expresión de sus ARN mensajeros (ARNm). Estos cambios no son paralelos a aquellos de proteína, peso o celularidad. En consecuencia, y como complemento a los análisis de actividad enzimática-expresión génica referidos al contenido proteico del tejido, hemos calculado también la relación entre las expresiones génicas y el contenido total de ARN (una cruda aproximación al ARNm) con la finalidad de comparar el efecto del sexo,

la dieta, e inclusive la localización del tejido adiposo blanco en el metabolismo del nitrógeno. Cualquier desviación significativa en la proporción de la expresión de un gen con respecto a la masa total de ARN puede implicar una modulación diferencial de su expresión.

Análisis estadístico

Los resultados obtenidos a partir del estudio génico y enzimático de las proteínas implicadas en el metabolismo de los aminoácidos se analizaron, según las variables de interés, con diferentes modelos estadísticos. Los efectos de las variables (localización del tejido adiposo, sexo del animal, y tipo de dieta) sobre el metabolismo del nitrógeno se determinaron a partir de análisis de varianza; para el estudio de una sola variable utilizamos el análisis de varianza simple (one way ANOVA), mientras que para los estudios de dos variables utilizamos el análisis de dos vías (two way ANOVA). En ambos casos, adicionalmente aplicamos pruebas de rango post-hoc (como la prueba de Tukey) para conocer las diferencias específicas de cada grupo de variables. Cabe resaltar, que para cada variable estudiada hemos estimado la media de 6 animales por grupo ($n=6$), así como errores estándar obtenidos a partir de este mismo número de animales.

La velocidad inicial (V_{max}) de las diferentes actividades enzimáticas estudiadas se obtuvo a partir de ajustes de curvas lineales y no lineales (exponentiales). Todos los datos estadísticos así como el ajuste de curvas fueron analizados con el programa Prism 5 (GraphPad Software, San Diego CA USA).

BIBLIOGRAFIA

1. Ferrer-Lorente, R., Cabot, C., Fernández-López, J.-A. & Alemany, M. Combined effects of oleoyl-estrone and a beta3-adrenergic agonist (CL316,243) on lipid stores of diet-induced overweight male Wistar rats. *Life Sciences* **77**, 2051–2058 (2005).
2. Moller, J. V. & Le Maire, M. Detergent binding as a measure of hydrophobic surface area of integral membrane proteins. *Journal of Biological Chemistry* **268**, 18659–18672 (1993).
3. Le Maire, M., Champeil, P. & Møller, J. V. Interaction of membrane proteins and lipids with solubilizing detergents. *Biochimica et Biophysica Acta* **1508**, 86–111 (2000).
4. Saibaba, K. S. S., Bhaskar, M. V., Rao, P. V. L. N. S., Ramana, G. V. & Dakshinamurti, K. V. Interferences in clinical chemistry analysis. *Indian Journal of Clinical Biochemistry* **13**, 55–62 (1998).
5. Lusty, C. J., Jilka, R. L. & Nietsch, E. H. Ornithine transcarbamylase of rat liver. Kinetic, physical, and chemical properties. *Journal of Biological Chemistry* **254**, 10030–10036 (1979).
6. McLaren, J. & Ng, W. G. Assay of ornithine carbamoyltransferase activity in human liver using carbon-labeled ornithine and thin-layer chromatography. *Clinica Chimica Acta* **81**, 193–201 (1977).
7. Masaru, O., Hiroshi, T., Yasuo, K., Kazue, O. & Ichio, H. A direct method for the estimation of ornithine carbamoyltransferase activity in serum. *Clinica Chimica Acta* **67**, 145–152 (1976).
8. Goldstein, A. S. et al. Metabolic and genetic studies of a family with ornithine transcarbamylase deficiency. *Pediatric Research* **8**, 5–12 (1974).
9. Arriarán, S., Agnelli, S., Remesar, X. & Alemany, M. A radiochemical method for carbamoyl-phosphate synthetase-I: application to rats fed a hyperproteic diet. *Journal of Enzyme Research* **3**, 29–33 (2012).
10. Deaconess, N. E. Glutamine-dependent carbamyl phosphate synthetase. *Journal of Biological Chemistry* **245**, 2199–2204 (1970).
11. Aoki, T., Morris, H. P. & Weber, G. Regulatory properties and behavior of activity of carbamoyl phosphate synthetase II (glutamine-hydrolyzing) in normal and proliferating tissues. *Journal of Biological Chemistry* **257**, 432–438 (1982).
12. Mally, M. I., Grayson, D. R. & Evans, D. R. Catalytic synergy in the multifunctional protein that initiates pyrimidine biosynthesis in Syrian hamster cells. *Journal of Biological Chemistry* **255**, 11372–11380 (1980).
13. Trotta, P. P., Pinkus, L. M. & Meister, A. Inhibition by dithiothreitol of the utilization of glutamine by carbamyl phosphate synthetase. Evidence for formation of hydrogen peroxide. *Journal of Biological Chemistry* **249**, 1915–1921 (1974).
14. Kato, H., Oyamada, I., Mizutani-Funahashi, M. & Nakagawa, H. New radioisotopic assays of argininosuccinate synthetase and argininosuccinase. *Journal of Biochemistry* **79**, 945–953 (1976).
15. Husson, A., Brasse-Lagnel, C., Fairand, A., Renouf, S. & Lavoinne, A. Argininosuccinate synthetase from the urea cycle to the citrulline-NO cycle. *European Journal of Biochemistry* **270**, 1887–1899 (2003).
16. Ratner, S. in *Advances in enzymology and related areas of molecular biology* (ed. Meister, A.) **39**, 1–90 (John Wiley & Sons, Inc., 1973).

17. Westall, R. G. Argininosuccinic aciduria: identification and reactions of the abnormal metabolite in a newly described form of mental disease, with some preliminary metabolic studies. *Biochemical Journal* **77**, 135–144 (1960).
18. Ratner, S., Petrack, B. & Rochovansky, O. Biosynthesis of urea. V. Isolation and properties of argininosuccinic acid. *Journal of Biological Chemistry* **204**, 95–113 (1953).
19. Schimke, R. T. Adaptive characteristics of urea cycle enzymes in the rat. *Journal of Biological Chemistry* **237**, 459–468 (1962).
20. O'Brien, W. E. Isolation and characterization of argininosuccinate synthetase from human liver. *Biochemistry* **18**, 5353–5356 (1979).
21. de Ruiter, H. & Kollöffel, C. Activity of enzymes of arginine metabolism in the cotyledons of developing and germinating pea seeds. *Plant Physiology* **70**, 313–315 (1982).
22. Kollöffel, C. & Stroband, H. W. J. Ornithine carbamyltransferase activity from the cotyledons of developing and germinating seeds of *Vicia faba*. *Phytochemistry* **12**, 2635–2638 (1973).
23. Kolloffel, C. & van Dijke, H. D. Mitochondrial arginase activity from cotyledons of developing and germinating seeds of *Vicia faba* L. *Plant Physiology* **55**, 507–510 (1975).
24. Hilger, F. et al. Studies on the kinetics of the enzyme sequence mediating arginine synthesis in *Saccharomyces cerevisiae*. *Journal of General Microbiology* **75**, 33–41 (1973).
25. Sherwin, J. E. & Natelson, S. Serum and erythrocyte argininosuccinate lyase assay by NADH fluorescence generated from formed fumarate. *Clinical Chemistry* **21**, 230–234 (1975).
26. Miura, T., Kashiwamura, M. & Kimura, M. An enzymatic method for the assay of serum argininosuccinate lyase. *Analytical Biochemistry* **164**, 482–487 (1987).
27. Ratner, S., Anslow, W. P. & Petrack, B. Biosynthesis of urea. VI. Enzymatic cleavage of argininosuccinic acid to arginine and fumaric acid. *Journal of Biological Chemistry* **204**, 115–125 (1953).
28. Tomlinson, S. & Westall, R. G. Argininosuccinic aciduria. Argininosuccinase and arginase in human blood cells. *Clinical Science* **26**, 261–269 (1964).
29. Nordmann, J. & Nordmann, R. in *Advances in Clinical Chemistry* (eds. Sobotka, H. & Stewart, C.) **4**, 53–120 (Elsevier, 1961).
30. Schimke, R. T. Arginase (rat liver). *Methods in Enzymology* **17**, 313–317 (1970).
31. Dismukes, G. C. Manganese enzymes with binuclear active sites. *Chemical Reviews* **96**, 2909–2926 (1996).
32. Ash, D. E. Structure and function of arginases. *Journal of Nutrition* **134**, S2760–S2764 (2004).
33. Oginsky, E. L. Isolation and determination of arginine and citrulline. *Methods in Enzymology* **3**, 639–643 (1957).
34. Fawcett, J. K. & Scott, J. E. A rapid and precise method for the determination of urea. *Journal of Clinical Pathology* **13**, 156–159 (1960).
35. Tabatabai, M. A. Effects of trace elements on urease activity in soils. *Soil Biology and Biochemistry* **9**, 9–13 (1977).
36. Kepka-Lenhart, D., Ash, D. E. & Morris, S. M. Determination of mammalian arginase activity. *Methods in Enzymology* **440**, 221–230 (2008).
37. Reddi, P. K., Knox, W. E. & Herzfeld, A. Types of arginase in rat tissues. *Enzyme* **20**, 305–314 (1975).
38. Cederbaum, S. D. et al. Arginases I and II: do their functions overlap? *Molecular Genetics and Metabolism* **81 Suppl 1**, S38–S44 (2004).
39. Klein, D. & Morris, D. R. Increased arginase activity during lymphocyte mitogenesis. *Biochemical and Biophysical Research Communications* **81**, 199–204 (1978).
40. Rüegg, U. T. & Russell, A. S. A rapid and sensitive assay for arginase. *Analytical Biochemistry* **102**, 206–212 (1980).
41. Romero, M. D. M., Grasa, M. D. M., Esteve, M., Fernández-López, J. A. & Alemany, M. Semiquantitative RT-PCR measurement of gene expression in rat tissues including a correction for varying cell size and number. *Nutrition & Metabolism* **4**, 26 (2007).

3.3. Estudio del metabolismo de los aminoácidos en el tejido adiposo blanco

* *The urea cycle of rat white adipose tissue*

* *Effects of sex and site on amino acid metabolism enzyme gene expression and activity in rat white adipose tissue*

* *Overall white adipose tissue urea cycle activity remains unchanged in female rats after one-month treatment with a hyperlipidic diet*

El tejido adiposo blanco tiene una potente maquinaria metabólica relacionada a la partición y el metabolismo de la energía. Su adaptabilidad, regulación, tamaño y variabilidad estructural coinciden con este rol de control. Sin embargo, nuestro conocimiento sobre el metabolismo del tejido adiposo blanco, especialmente en lo que respecta al metabolismo de los aminoácidos, es considerablemente limitado. En este apartado hemos analizado las principales vías del catabolismo nitrogenado del tejido adiposo blanco, centrándonos en el funcionamiento de su principal mecanismo, el ciclo de la urea.

Se utilizaron ratas Wistar de ambos性, de nueve semanas, que fueron alimentadas con pienso estándar o con una dieta simplificada “de cafetería” durante un mes. Al final del experimento, se tomaron muestras de tejido adiposo subcutáneo, mesentérico, retroperitoneal y perigonadal. En las muestras se analizaron la expresión génica y la actividad de las enzimas del ciclo de la urea, así como las de otras enzimas implicadas en el metabolismo de aminoácidos. Este estudio se complementó con el estudio de expresiones de enzimas clave del metabolismo de glúcidos y lípidos para completar una visión general de la modulación metabólica dependiente de la localización del tejido adiposo, de la dieta y, sobre todo del sexo.

Los resultados obtenidos demostraron que el ciclo de la urea está presente en todas las localizaciones estudiadas del tejido adiposo. Al analizar las expresiones génicas y actividades de las enzimas observamos un patrón muy uniforme y conservado, independiente del sexo y la dieta. Esta estabilidad contrasta con otras vías metabólicas (incluso del metabolismo nitrogenado), lo que, a nuestro juicio, constituye una evidencia de que la función del ciclo de la urea es lo suficientemente importante y bien regulada en el tejido adiposo en su conjunto como para no ser afectada por otros factores o variables

(dieta, hormonas sexuales, etc.). Dado que la dieta de cafetería aumenta significativamente la masa de los depósitos de grasa, la estabilidad del funcionamiento del ciclo de la urea se mantuvo gracias a una disminución relativa de la expresión de los genes correspondientes, junto con pequeños ajustes en las actividades enzimáticas. Por otro lado, el análisis comparativo del metabolismo de los aminoácidos mostró una marcada influencia del sexo, dependiente de la localización, con una actividad metabólica más intensa en el tejido adiposo subcutáneo de las ratas macho. La expresión de algunos genes del metabolismo de los aminoácidos era más baja, en general, que las de los genes clave que controlan el metabolismo glucídico y lipídico, aunque las diferencias fueron cuantitativamente menores de lo esperado teniendo en cuenta la bien conocida trascendencia del metabolismo hidrocarbonado en el tejido adiposo.

Los perfiles de actividad enzimática presentados sugieren, en conjunto, que (bajo condiciones basales) el ciclo de la urea es funcional en el tejido adiposo blanco. Su actividad, en la situación fisiológica analizada, probablemente se centra en el control de la disponibilidad de arginina, mediante una activa síntesis de citrulina. Esta capacidad del tejido adiposo le permitiría ser una importante fuente extra-intestinal de citrulina, con lo que ayudaría a mantener la plena disponibilidad de arginina independientemente del funcionamiento del ciclo de la urea en el eje intestino-hígado. La información aportada en el presente estudio demuestra que el tejido adiposo blanco ejerce un rol significativo en el metabolismo nitrogenado de todo el cuerpo, al disponer de un ciclo de la urea funcional y sometido a un control general centralizado que afecta al tejido como un todo. En nuestra opinión, el potencial metabólico y de control del tejido adiposo blanco en el metabolismo energético es más importante de lo que habitualmente se supone y es sólo comparable al que ejerce el hígado.



Cite this: RSC Adv., 2015, 5, 93403

The urea cycle of rat white adipose tissue

Sofía Arriarán,^a Silvia Agnelli,^a Xavier Remesar,^{abc} José-Antonio Fernández-López^{abc} and Marià Alemany^{*abc}

White adipose tissue (WAT) contains a powerful metabolic machinery related to energy metabolism and partition. The adaptive, regulatory, size and structural variety of WAT agrees with this control role. However, its nitrogen metabolism has been sparsely studied and we know close to nothing about its implication on N-related processes and homoeostasis. We have studied, and found a complete urea cycle (liver type) in four WAT sites (gene expressions and enzyme activities). We postulated a possible function of the cycle (under basal conditions) in the control of arginine handling through citrulline synthesis. In our opinion, the metabolic and control potential of WAT on energy metabolism may be second only to liver. This impression should be extended to amino acid metabolism too, WAT providing an extra-intestinal source of citrulline to maintain the body availability of arginine independently of the operation of intestine–liver urea cycle for N disposal.

Received 14th August 2015
Accepted 19th October 2015

DOI: 10.1039/c5ra16398f
www.rsc.org/advances

Introduction

Adipose tissue is one of the most versatile, adaptable and reslient tissues of the mammal's body. A number of additional functions complement the well-known energy-storage role of adipose tissue, such as protection, both physical (filling, packing, barrier action against trauma, thermal insulation) and defensive (immune organ, tissue regeneration site). White adipose tissue (WAT) plays an important role in metabolic regulation, as a paracrine and endocrine organ, but also as a key energy partition system. WAT also shows (at least in part), a thermogenic function, which is used for the elimination of unwanted excess energy as heat, and the maintenance of body temperature.

Our appreciation of adipose tissue is growing in physiological transcendence in parallel to the discovery of the full extent of its functions. A turning point has been the acknowledgment that different adipose tissue sites may carry out different functions,¹ sharing some but not all the possibilities such malleable tissue/organ possesses. Extreme differentiation resulted in the practical division of adipose tissue in at least three different types according to specialized function, cell structure, main active metabolic pathways, and anatomical placement. White (WAT), made up of large cells, usually with a single fat-filled vacuole, largely glycolytic, with low oxygen consumption and a limited number of mitochondria;² this is the most abundant adipose tissue type. Brown (BAT), formed by plurivacuolar cells; highly oxidative, with a large number of mitochondria, specialized thermogenic function, and highly vascularized and innervated.

In addition, beige or brite, sharing characteristics of brown and white, but not a transition stage between both, of independent origin, and functions also related mainly to thermogenesis.

This largely functional and morphologic division of adipose tissue affects, essentially, the functions of energy storage and thermogenesis, but there are also marked differences in location, functional adaptability and regulatory ability of WAT in different body masses and sites.^{3,4} These differences are in part a consequence of their different developmental lineage,⁵ but also of their specific function, with a critical influence of the cell environment.

This considerable variability is enhanced under conditions of metabolic derangement, as in metabolic syndrome, when most WAT sites are massively infiltrated by immune cells,⁶ to avert a possible metabolic aggression, eliciting an alarm response,⁷ which tends to become chronic, inducing generalized alterations of adipose tissue cell composition and functions.⁸

In addition to glycolysis, production of acetyl-CoA, lipogenesis, synthesis, storage and hydrolysis of triacylglycerols, WAT produces lactate⁹ and alanine¹⁰ as part of Cori and glucose-alanine cycles. WAT may use amino acids as energy (or lipogenesis) substrates,¹¹ contains active glycogen depots,¹² and converts glucose to lactate and glycerol to lower its glycemic load.¹³ BAT is capable of using almost any circulating substrate (including amino acids)¹⁴ to sustain thermogenesis.

WAT is a significant producer of nitric oxide,¹⁵ and its blood flow and metabolic activity are regulated by catecholamines and insulin.^{16,17} In sum, adipose tissues, and WAT in particular because of its size and distribution, have an enormous metabolic potential, which probably is activated on demand, depending on the needs of the particular niche/function the tissue covers. In this context, the regulatory capabilities of WAT have been explored extensively in the last years, resulting in the discovery of a sizeable number of adipokines and other regulatory agents and mechanisms.¹⁸

^aDepartment of Nutrition and Food Science, Faculty of Biology, University of Barcelona, Av. Diagonal 643, 08028 Barcelona, Spain. E-mail: malemany@ub.edu

^bInstitute of Biomedicine, University of Barcelona, 08028 Barcelona, Spain

^cCIBER-OBN Research Web, Barcelona, Spain

The study of metabolic pathways in WAT has been, so far, limited; with only a few publications dealing with issues other than glucose metabolism and lipogenesis; amino acid metabolism remains a considerably neglected field, limited to few papers from last century.^{11,19} The large relative mass of WAT and the key role that arginine plays in the control of WAT hemodynamics (*via* synthesis of nitric oxide), especially in metabolic syndrome,²⁰ made us think on the possibility that WAT implication in the control of arginine availability and metabolism²⁰ could be deeper than currently assumed. In the present work, we analyzed whether WAT can synthesize arginine through the urea cycle. We are aware that this cycle is fully complete and functional only in liver, and (at least partially) in kidney and intestine. In doing the study, we tested for a significant (and largely ignored) importance of WAT in amino acid metabolism.

Experimental

Ethics statement

All animal handling procedures and the experimental setup were in accordance with the animal handling guidelines of the corresponding European and Catalan Authorities. The Committee on Animal Experimentation of the University of Barcelona specifically authorized the procedures used in the present study.

Experimental design and animal handling

Nine week old male Wistar rats (Harlan Laboratory Models, Sant Feliu de Codines, Spain) were used. The rats ($N=6$) were housed in two-rat cages with wood shreds for bedding. They had free access to water and ate normal rat chow (type 2014, Harlan). They were kept in a controlled environment (lights on from 08:00 to 20:00; 21.5–22.5 °C; 50–60% humidity) for at least one month.

The rats were killed by exsanguination (by aortic puncture), under isoflurane anesthesia, at the beginning of a light cycle; then, were rapidly dissected, taking large samples of liver and WAT: mesenteric, epididymal, retroperitoneal and subcutaneous (inguinal fat pads). All samples were blotted and frozen in liquid nitrogen. To minimize the problems of tissue sampling for analyses, the frozen samples were weighed, and then were ground with mortar and pestle under liquid nitrogen. The coarse powder was stored at –80 °C until processed. Later, the dissection of the rats continued, extracting the remaining liver and WAT in ME, EP and RP sites; the rats were skinned, and the whole subcutaneous WAT was dissected. The weights of the recovered WAT were added to those of the frozen samples in order to determine the precise mass of the four WAT sites liver weight was determined in the same way.

Tissue homogenate preparation

Frozen tissue samples were homogenized, using a tissue disruptor (Ultraturrax IKA-T10, Ika Werke, Staufen, Germany), in 5 volumes of chilled 70 mM hepes buffer pH 7.4 containing 1 mM dithiothreitol (Sigma, St Louis MO USA), 50 mM KCl, 1 g L^{−1} Triton X-100 (Sigma) and 1 g L^{−1} lipid-free bovine serum albumin (Sigma). In homogenates to be used for carbamoyl-P synthase 2 estimation, the concentration of Triton X-100 was

halved to prevent foaming. The homogenates were centrifuged for 10 min at 5000 × *g*; the floating fat layer and gross debris precipitate were discarded. The homogenates were kept on ice, and were used for the estimation of protein and for enzymatic analyses within 2 h after their preparation. Liver homogenates were obtained using 10 volumes of chilled buffer. They were further diluted with buffer, as needed, in the reaction mixtures for the estimation of enzyme activities.

Tissue protein content was estimated with the Lowry method.²¹ After development of color, turbidity was eliminated with small amounts of finely powdered solid MgO, which adsorbed the remaining suspended fat, and centrifuging the tubes before reading the absorbance. In the measurements of homogenate protein content, homogenization buffer (containing 1 g per L albumin) was used as blank.

Enzyme activities were expressed in nkat per g protein.

Enzyme activity analyses

Carbamoyl-P synthase. Carbamoyl-P synthase was estimated from the incorporation of ¹⁴C-bicarbonate (Perkin Elmer, Bad Neuheim, Germany) into carbamoyl-P using a method previously described by us.²² Succinctly, we measured the incorporation of ¹⁴C-bicarbonate label into carbamoyl-P by the activity of the enzyme in the presence of glutamine (and/or ammonium): (carbamoyl-P synthase 2), or ammonium alone (carbamoyl-P-synthase 1), in the latter case, measured in the presence of *N*-acetyl-glutamate (Sigma) and flushing out all remaining bicarbonate label with a stream of unlabeled CO₂. The remaining label was measured with a liquid scintillation system (Tri-Carb 1500, Perkin-Elmer, Waltham MA USA), using the Ecoscint-H scintillation liquid mixture (National Diagnostics, Atlanta, GA USA). No significant carbamoyl-P 1 activity was detected (and its gene was not expressed either in WAT). Thus, only carbamoyl-P synthase 2 was measured in this tissue. In liver, the enzyme activity was measured in the presence of 1 mM final concentration of *N*-acetyl-glutamate, using ammonium bicarbonate instead of sodium bicarbonate; liver values were, thus, the sum of both carbamoyl-P synthase 1 and 2.

Ornithine carbamoyl transferase. Ornithine carbamoyl transferase was measured from the reaction of condensation of carbamoyl-P and ¹⁴C-ornithine to yield ¹⁴C-citrulline. Aliquots of 25 µL of homogenates were mixed with 50 µL of 70 mM hepes buffer pH 7.4 containing carbamoyl-P, ornithine (all from Sigma), and ¹⁴C-ornithine (Perkin-Elmer); final concentrations were 9 mM, 13 mM and 1 kBq mL^{−1}, respectively. The reaction was started with the homogenate, and was carried out at 37 °C. Aliquots of 75 µL were introduced in tubes containing 100 µL of chilled acetone, in ice, at 0, 0.5, 1 and 2 min. The tubes were later centrifuged to obtain clear supernatants; they were dried in a vacuum-centrifuge (Thermo Scientific, Waltham, MA USA). The dry residues were dissolved in 25 µL of pure water; they were applied to silicagel TLC plates (200 µm; Macherey-Nagel, Düren, Germany) with vertical lines (<1 mm) etched vertically to define 1 cm wide independent lanes; this development prevented sample intermixing. Standards of ornithine and citrulline were included in one of the lanes of each plate. The plates were developed with

a mobile phase of trichloromethane : methanol : acetic acid (1 : 2 : 2 by volume). After drying, the developed chromatograms, were sprayed (only the lane with non-labelled standards) with ninhydrin, and heated with a hair dryer. The ornithine and citrulline spots were marked and the rest of the plate penciled in horizontal 1 cm zones, which were cut and counted with the liquid scintillation system described above. The labeled areas were identified and quantified. To limit interference by size of sample and contamination, the label in the citrulline spot was expressed as a percentage of the total label counted in each TLC lane. These data allowed the calculation of newly formed citrulline at each time. The V_i value for each sample was plotted, and considered an expression of V_{max} under the conditions tested.

Arginino-succinate synthase. Arginino-succinate synthase was measured from the reaction of condensation of aspartate with citrulline in the presence of ATP to yield arginino-succinate. Aliquots of 55 μ L of homogenates were mixed with 30 μ L of 70 mM hepes buffer pH 7.4, containing ATP-Na₂, MgCl₂, citrulline, aspartate (all from Sigma); final concentrations were 10 mM, 5 mM, 3 mM, and 2.5 mM, respectively. The reaction was started with aspartate, and was carried out at 37 °C. The reaction was stopped with 40 μ L of 30 g per L perchloric acid. The tubes were vortexed and immediately neutralized (pH 7–8) with 10 μ L of 100 g per L KOH containing 62 g per L potassium bicarbonate. The tubes were vortexed again and centrifuged at 8000 \times g for 15 min and 4 °C. The aspartate remaining was measured in the supernatants by transamination to oxaloacetate, and then reduced by malate dehydrogenase and NADH. Briefly, 20 μ L of the supernatants were brought up to 300 μ L in 96-well plates, with 66 mM phosphate buffer pH 7.4 containing NADH, 2-oxoglutarate, aspartate transaminase (pig heart) and malic acid dehydrogenase (pig heart) (all from Sigma); final concentrations were, respectively, 0.25 mM, 0.2 mM, 20 nkat mL⁻¹ and 17 nkat mL⁻¹. The plates were read at 340 nm in a plate reader (Biotek, Winoosky, VT USA) at intervals of 30 s during 30 min. The fall in NADH was used to determine the levels of aspartate at each incubation time. Its disappearance (*versus* time zero levels) was used to determine the amount of aspartate incorporated into arginino-succinate by the enzyme. As in the case of ornithine carbamoyl transferase, the V_i values were plotted for each sample. In all series, a number of samples were analyzed with all reagents except citrulline: no spurious consumption of aspartate was observed.

Arginino-succinate lyase. Arginino-succinate lyase was measured from the breakup of arginino-succinate to yield fumarate and arginine. The amino acid was measured in a second reaction using arginase to form ornithine and urea, which was measured using a sensitive chemical method. We initially intended to measure the fumarate formed using fumarate and malate dehydrogenase, measuring the disappearance of NADH, but we observed many false positives with arginino-succinate (a natural extracted product) in the malate dehydrogenase reaction. Thus, we went to the arginase side, which proved to be more reliable. Aliquots of 38 μ L of homogenates were mixed with 38 μ L of 70 mM hepes buffer pH 7.4, containing arginino-succinate (Sigma), and final concentration 2 mM. Incubations were carried out at 37 °C for 0, 2.5, 5 and 10 min. The reaction was stopped by the addition of 40 μ L of 30 g per L

perchloric acid. The tubes were vortexed and brought to pH 8–9 with 10 μ L of 100 g per L KOH containing 80 g per L potassium bicarbonate. The tubes were mixed again, and centrifuged for 15 min in the cold (4 °C) at 8000 \times g. Aliquots of 100 μ L of the supernatants were mixed with 50 μ L of the reacting mixture: 70 mM hepes buffer pH 7.5 (to achieve a final pH 8.5) containing MnCl₂ and arginase (rat liver, Lee Biosolutions, St Louis, MO USA); final concentrations 7 mM and 17 nkat mL⁻¹. The buffer containing Mn and arginase was activated (heated) for 5 min at 55 °C before use. The reaction was allowed to develop for 30 min at 37 °C, and was stopped by the addition of 35 μ L 160 g per L perchloric acid. The tubes were centrifuged for 15 min at 8000 \times g and 4 °C. The acidic supernatants (175 μ L) were used for the estimation of urea. They were mixed with 300 μ L of 90 g per L H₂SO₄ containing 270 g per L H₃PO₄; then 20 μ L of 30 g per L of 1-phenyl-2-oxime-1,2-propanodione (Sigma) in absolute ethanol were added. The reaction was developed at 100 °C for 30 min in a dry block heater. The absorbance of the tubes was measured at 540 nm with a plate reader. The plates contained standards of arginine and urea as well as blanks. Arginase effectivity was tested in all batches. In all cases, conversion of arginine to urea was 100% (*i.e.* there was a full coincidence of the standard curves for both urea and arginine).

The chemical reaction using 1-phenyl-2-oxime-1,2-propanodione to measure the urea released from arginine by arginase had, in our case, the advantage of reacting also with arginine and citrulline. Thus, the values obtained from the perchloric acid supernatants at time 0 represent the sum of urea, arginine and citrulline (all reacting with the oxime²³) present in the tissue before incubation to measure the lyase activity. These values were later used for calculation of their molal concentrations in tissues (WAT sites and liver) as a composite value of its content in urea + arginine + citrulline.

Arginase. Arginase was measured through the estimation of the urea produced by the activity of the enzyme on arginine in the presence of Mn²⁺ ions. Aliquots of 20 μ L of homogenates were mixed with 5 μ L of MnCl₂ in water; final concentration 10 mM. The tubes were heated for 5 min at 55 °C to activate arginase. After the temperature was brought down to 37 °C, the reaction began with the addition of 75 μ L of arginine (Sigma); final concentration 78 mM. Incubations were carried out for 1, 10 and 20 min at 37 °C. The reaction was stopped by the addition of 35 μ L 160 g per L perchloric acid. The tubes were centrifuged at 8000 \times g and 4 °C for 15 min. The measurement of urea generated was done as described above for arginino-succinate lyase. Since the method used for arginase does not differentiate between arginases 1 and 2, we present a combined total arginase value that corresponds mostly to arginase 1 (since the expression of type 1 was much higher in both WAT and liver).

Analysis of plasma parameters

Blood plasma was deproteinized with acetone²⁴ and used for the analysis of individual amino acids using an amino acid analyzer (Biochrom 30+, Biochrom, Cambridge, UK). Plasma urea was estimated with kit #11537 (Spinreac, Sant Esteve de Bas, Spain). Plasma and tissue water contents were calculated as previously

Table 1 Enzymes and their corresponding genes analyzed in WAT sites of adult male Wistar rats^a

Enzyme	A	EC number	Gene	5' > 3'	3' > 5'	BP
Carbamoyl-phosphate synthase [ammonia], mitochondrial type 1		6.3.4.16	Cps1	ACCCATCATCCCCCTCTGACT	ACACGCCACCTCTCAGTAG	118
Glutamine-dependent carbamoyl-phosphate synthase, type 2	X	6.3.5.5	Cad	AGTTGGAGGAGGAGGCTGAG	ATTGATGGACAGGTGCTGGT	90
Ornithine carbamoyltransferase	X	2.1.3.3	Otc	CTTGGGCCTGAATGAAAGTC	ATTGGGATGGTTGCTTCCT	126
Arginino-succinate synthase 1	X	6.3.4.5	Ass1	CAAAGATGGCACTACCCACA	GTTCTCCACGATGTCATGC	100
Arginino-succinate lyase	X	4.3.2.1	Asl	CCGACCTTGCCTACTACCTG	GAGAGCCACCCCTTCATCT	104
Arginase, liver (type 1)	X	3.5.3.1	Arg1	GCAGAGACCCAGAAGAATGG	GTGAGCATCCACCCAAATG	126
Arginase-2		3.5.3.1	Arg2	GCAGCCTCTTCCCTTCTCA	CCACATCTCGTAAGCCAATG	122
N-Acetyl-glutamate synthase		2.3.1.1	Nags	GCAGCCCACCAAATCAT	CAGGTTACATTGCTCAGGA	82
Glutaminase, kidney isoform		3.5.1.2	Gls	CCGAAGGTTTGCTCTGCA	AGGGCTGTTCTGGAGTCGTA	63
Glutamate-ammonia ligase [glutamine synthetase]		6.3.1.2	Glul	AACCTCACGCCAGCATA	CTGCGATGTTTCCTCTCG	148
Adenosine monophosphate deaminase 2		3.5.4.6	Ampd2	CGGCTTCTCTCACAGGTG	CGGATTCGTTACCCCTCAG	78
Glutamate dehydrogenase 1 (NADH)		1.4.1.3	Glud1	GGACAGAATATCGGGTGCAT	TCAGGTTCAATCCCAGGTTA	122
Nitric oxide synthase 3, endothelial cell type		1.14.13.39	Nos3	CAAGTCCTCACCCCTTT	GACATCACCGCAGACAAACA	138
60S acidic ribosomal protein 0 (<i>housekeeping gene</i>)	—		Rplp0	GAGCCAGCGAAGCCACACT	GATCAGCCCAGGAGAAGG	62

^a A = activity measured in addition to the analysis of gene expression.

described¹³ for the estimation of molal concentrations of arginine, citrulline and urea.

Gene expression analysis

Total tissue RNA was extracted from the frozen tissue samples using the Tripure reagent (Roche Applied Science, Indianapolis IN USA), and was quantified in a ND-100 spectrophotometer (Nano-drop Technologies, Wilmington DE USA). These data were also used to determine the total RNA content of the tissue (per g of weight or g of protein) in order to establish comparisons between the quantitative importance of gene expressions. RNA samples were reverse transcribed using the MMLV reverse transcriptase (Promega, Madison, WI USA) system and oligo-dT primers.

Real-time PCR (RT-PCR) amplification was carried out using 10 µL amplification mixtures containing Power SYBR Green PCR Master Mix (Applied Biosystems, Foster City, CA USA), 4 ng of reverse-transcribed RNA and 150 nM of primers. Reactions were run on an ABI PRISM 7900 HT detection system (Applied Biosystems) using a fluorescent threshold manually set to 0.15 for all runs.

A semi-quantitative approach for the estimation of the concentration of specific gene mRNAs per unit of tissue/RNA or protein weight was used.²⁵ Rplp0 was the charge control gene.²⁶

We expressed the data as the number of transcript copies per gram of protein in order to obtain comparable data between the groups. The genes analyzed and a list of primers used is presented in Table 1.

The possible contamination of RNA with DNA was checked before PCR cycling by charging known RNA on a number of samples of each batch. No spurious signals were observed. All the primers used for measurement of urea-cycle enzyme gene expressions were checked by Northern blots of the PCR-synthesized cDNA. In all cases, the cDNA obtained had the expected molecular weights.

Statistics

One-way ANOVA comparisons between groups, correlations and curve fitting (including V_i estimations) were analyzed with the Prism 5 program (GraphPad Software, San Diego CA USA).

Results

Tissue distribution and analysis

The rats used weighed 373 ± 15 g. Table 2 shows the absolute and relative weights of the four WAT sites analyzed. The sum of the four WAT sites represent about 8% of *in vivo* body weight.

Table 2 Weight and protein content of the four WAT sites analyzed in adult male Wistar rats^a

	Units	SC WAT	ME WAT	EP WAT	RP WAT	ΣWAT	P
Weight	g	$12.2 \pm 0.20^{\text{A}}$	$4.94 \pm 0.49^{\text{B}}$	$7.34 \pm 0.64^{\text{C}}$	$6.29 \pm 0.79^{\text{BC}}$	30.8 ± 1.7	<0.0001
	% BW	$3.27 \pm 0.07^{\text{A}}$	$1.33 \pm 0.18^{\text{B}}$	$1.97 \pm 0.13^{\text{C}}$	$1.69 \pm 0.22^{\text{BC}}$	8.26 ± 0.47	<0.0001
Protein	mg g ⁻¹	63.1 ± 11.6	74.2 ± 7.4	44.3 ± 1.6	65.1 ± 6.3		NS
RNA	µg g ⁻¹	$248 \pm 51.1^{\text{A}}$	$880 \pm 84.3^{\text{B}}$	$94.3 \pm 6.0^{\text{AC}}$	$48.8 \pm 4.11^{\text{C}}$		<0.0001

^a All values are the mean \pm SEM of 6 different animals. Statistical significance of the differences between WAT sites were calculated using a one-way ANOVA analysis; *post hoc* Tukey test: in each row, different superscript letters represent different ($p < 0.05$) site values.

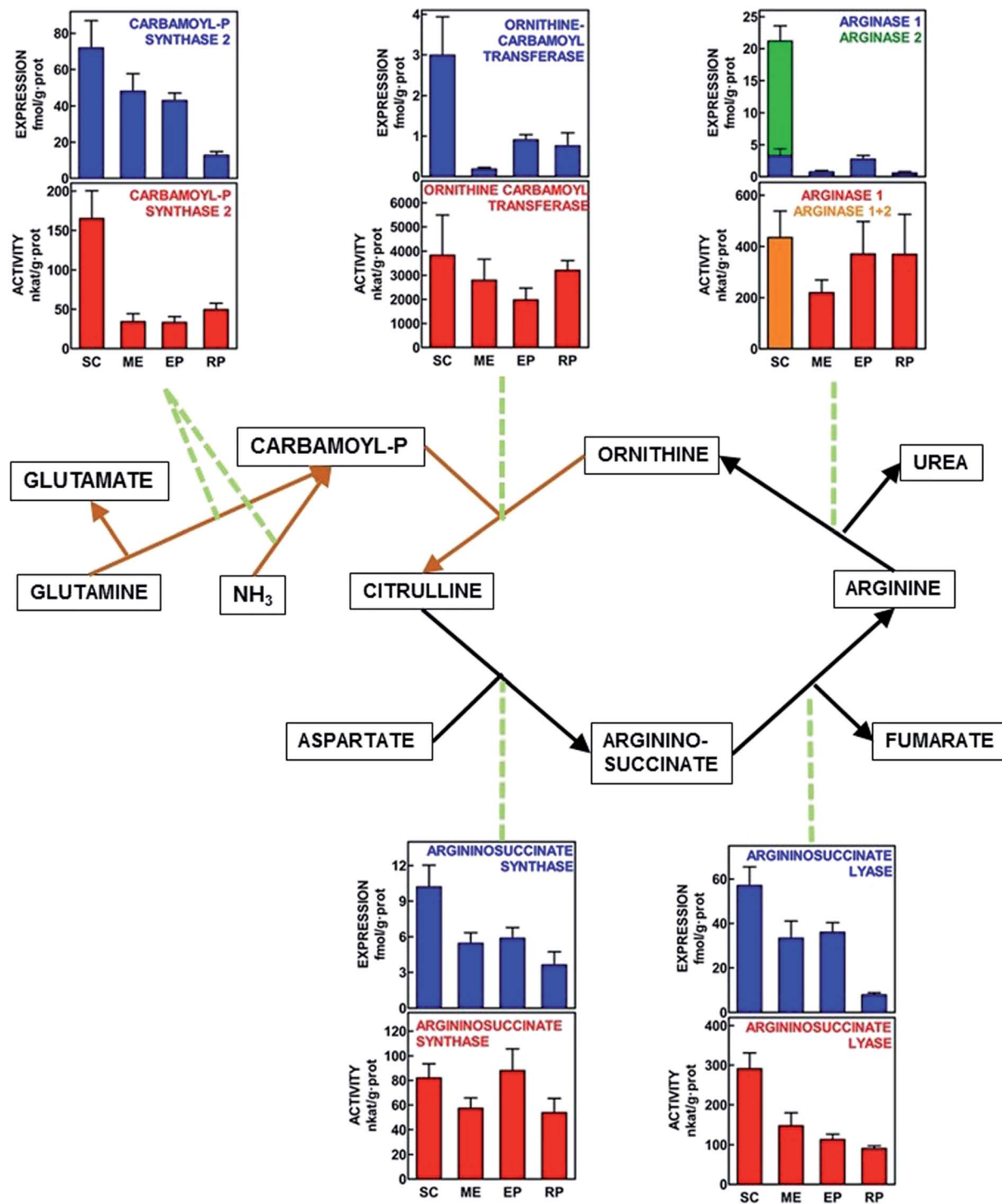


Fig. 1 Schematic representation of the urea cycle, with indication of enzyme activities and enzyme gene-expression values in four WAT sites of adult male Wistar rats. All data are presented as the mean \pm SEM of 6 different animals per group. Red columns show the enzyme activity in nkat per g protein, and blue columns depict the corresponding enzyme gene expression in fmol per g protein. In the case of subcutaneous WAT, in which both arginases 1 and 2 are expressed, and the activity is the sum; different colors have been used: orange for activity; blue for arginase 1 and green for arginase 2. Black lines represent cytosolic pathways analyzed; brown lines correspond to the mitochondrial pathways studied. SC = subcutaneous WAT; ME = mesenteric WAT; EP = epididymal WAT and RP = retroperitoneal WAT. Statistical analysis of differences between groups (one-way ANOVA applied to WAT site). Carbamoyl-P synthase 2 (activity $P = 0.0001$; expression $P = 0.0026$). Ornithine carbamoyl transferase (activity $P = \text{NS}$; expression $P = 0.0081$). Arginase (activity [total] $P = \text{NS}$; expression [arginase 1] $P = 0.0406$). Arginino-succinate synthase (activity $P = \text{NS}$; expression $P = 0.0120$). Arginino-succinate lyase (activity $P = 0.0005$; expression $P = 0.0007$).

The largest store was that of subcutaneous (SC) followed by epididymal (EP), retroperitoneal (RP) and mesenteric (ME) fat pads. Their protein content practically reversed this order, with the exception of the relatively high protein content in subcutaneous fat. The distribution of total RNA was different from that of protein, with marked differences between sites, mesenteric WAT showing 18-fold more RNA per g of tissue than retroperitoneal WAT; subcutaneous WAT RNA was only about 1/4th of mesenteric, and epididymal WAT dropped to 1/9th.

Urea-cycle enzyme activities and expressions

Fig. 1 shows a scheme of the urea cycle with the V_{max} enzyme activities measured in WAT tissue sites, as well as the expression of the genes for the same enzymes, all referred to unit of protein weight for direct comparison between different sites. The main peculiarities of this representation were the finding of arginase 1 in all WAT sites, with a robust activity in most of them. Arginase 2 was expressed only in subcutaneous WAT, where arginase activity reflected the combined action of both isoforms. The activity data suggest that, in comparison, the probable contribution of arginase 2 was lower than that of arginase 1, despite higher expression values for arginase 2. Most enzyme activities (and gene expressions) showed the maximal values for subcutaneous WAT. The presence of measurable enzyme activities, backed by the expression of the corresponding genes in all WAT sites confirm that all enzymes of urea cycle were present and active in the four WAT sites studied. The statistical analysis of differences between sites is presented in Fig. 1.

Activity/expression ratios

There were marked differences in the order of magnitude between the enzyme activities and their gene expressions, the differences being maximal for ornithine carbamoyl transferase. Thus, we calculated the quotients between enzyme activity and gene expression for each site. The data are presented in Table 3. Carbamoyl-P synthase activity/expression ratios were similar for SC and RP vs. ME and EP, with a 3–5-fold difference between both groups. The differences for ornithine carbamoyl transferase were the highest, with all sites showing similar ratios except for ME, which ratio was in the range of 3–10× that of the other sites. Arginino-succinate synthase and total arginase activity vs. arginase 1 expression ranges of ratios were rather uniform, and no significant differences between sites were observed. Arginino-succinate lyase showed similar ratios, except for RP, with values 2–3× higher. The SC ratio values for arginase were underestimated, since enzyme activity combined arginases 1 and 2.

The differences between enzymes were subjected to two additional analyses. First, using the data in Fig. 1, enzyme activities and gene expressions (both referred to g of tissue protein) were plotted and the correlation coefficients between the pairs of data were calculated for each enzyme. The results were carbamoyl-P synthase $P = 0.0003$, ornithine carbamoyl transferase $P = 0.0008$, arginino-succinate synthase $P = 0.8844$, arginino-succinate lyase $P = 0.0012$, and arginase 1, $P = 0.0430$. The only non-significant correlation between gene expression and the corresponding enzyme activity was that of arginino-succinate synthase.

The second analysis, shown in Table 4, depicts the statistical significance of the correlations between all pairs of urea cycle

Table 3 Mean values for activity/expression ratios of the urea cycle enzymes in different WAT sites of adult male Wistar rats^a

Enzyme	Units	SC WAT	ME WAT	EP WAT	RP WAT	<i>P</i>
Carbamoyl-P synthase 2	nkat fmol ⁻¹	2.65 ± 0.62 ^A	0.77 ± 0.21 ^B	0.76 ± 0.13 ^B	3.59 ± 0.46 ^A	<0.0001
Ornithine carbamoyl transferase	μkat fmol ⁻¹	1.22 ± 0.33 ^A	14.4 ± 4.4 ^B	2.28 ± 0.54 ^A	4.39 ± 0.90 ^A	<0.0001
Arginino-succinate synthase	nkat fmol ⁻¹	10.5 ± 2.8	11.4 ± 1.6	16.3 ± 3.7	16.7 ± 3.9	NS
Arginino-succinate lyase	nkat fmol ⁻¹	5.95 ± 1.26 ^A	4.45 ± 0.70 ^A	3.22 ± 0.30 ^A	10.3 ± 1.4 ^B	0.0005
Arginase 1	nkat fmol ⁻¹	232 ± 72	253 ± 35	124 ± 35	378 ± 95	NS

^a The data are the quotients of enzyme activity (in μkat per nkcat per g protein) and gene expression (fmol of the corresponding mRNA per g of protein). All values are the mean ± SEM of 6 different animals. Statistical significance of the differences between WAT sites was determined using a one-way ANOVA analysis; *post hoc* Tukey test: in each row, different superscript letters represent different ($p < 0.05$) site values.

Table 4 Correlations between the different enzyme activities (or gene expressions) of the urea cycle in different WAT sites of adult male rats^a

Ornithine carbamoyl transferase	EA: $P < 0.0001$ GE: $P = 0.0026$					
Arginino-succinate synthase	EA: NS GE: $P = 0.0079$	EA: NS GE: $P < 0.0001$				
Arginino-succinate lyase	EA: NS GE: $P < 0.0001$	EA: NS GE: NS	EA: $P = 0.0074$ GE: $P < 0.0001$			
Arginase 1	EA: $P < 0.0001$ GE: $P = 0.0059$	EA: $P = 0.0008$ GE: $P = 0.0306$	EA: $P = 0.0252$ GE: $P < 0.0001$	EA: $P = 0.0270$ GE: $P = 0.0036$		
Carbamoyl-P synthase	Ornithine carbamoyl transferase	Arginino-succinate synthase	Arginino-succinate lyase			

^a EA: P value for the correlation of paired enzyme activities for each animal and site, expressed in nkcat per g of tissue protein; GE: P value for paired enzyme gene expressions for each animal and site (corrected by RNA tissue content), expressed in fmol of the corresponding mRNA per g of tissue RNA.

enzymes, both using activities (per g of tissue protein) and gene expressions (corrected by tissue RNA content). The objective was to find whether there was a uniform mechanism (shown by a high degree of correlation) linking the enzyme activities or gene expressions of the different enzymes involved in the cycle. Most data were highly correlated (in spite of the use of different WAT sites). The most patent exceptions being ornithine carbamoyl transferase and carbamoyl-P synthase (both mitochondrial) which activities were not correlated with either of the arginino-succinate enzymes. In addition, the expression of ornithine carbamoyl transferase was not correlated with that of the lyase.

Expressions of other amino acid metabolism enzymes

In Fig. 2 the gene expressions for enzymes complementary of the urea cycle are shown. This analysis includes the main ammonium-handling enzymes (glutamine synthetase, glutaminase, glutamate dehydrogenase and AMP deaminase, which are completed by carbamoyl-P synthase 2 shown in Fig. 1). The trend towards ammonium disposal (*i.e.* mitochondrial glutamate

dehydrogenase, and cytoplasmic glutamine synthetase) showed higher expressions than glutaminase and AMP deaminase in all WAT sites, with the highest expression values for subcutaneous WAT and the lowest for retroperitoneal. *N*-Acetyl-glutamate synthase was expressed in all sites, albeit at the limit of safe expression measurement. Endothelial nitric oxide synthase was also expressed in all sites, subcutaneous WAT showing more than 2-fold expression values than the other sites, in a pattern similar to that AMP deaminase, and the glutamine enzymes.

Comparison of WAT and liver urea-cycle enzyme activities

Table 5 depicts the mean values for liver urea-cycle enzyme activities, including total carbamoyl-P synthase. These values when expressed per g of protein were close in some cases to those presented in Fig. 1 for the four main WAT sites. However, arginase, and to a lesser extent carbamoyl-P synthase and arginino-succinate synthase showed higher values in liver. When the data are presented as the total content in catalytic potential (*i.e.* nanokatals in the whole organ or tissue site), we

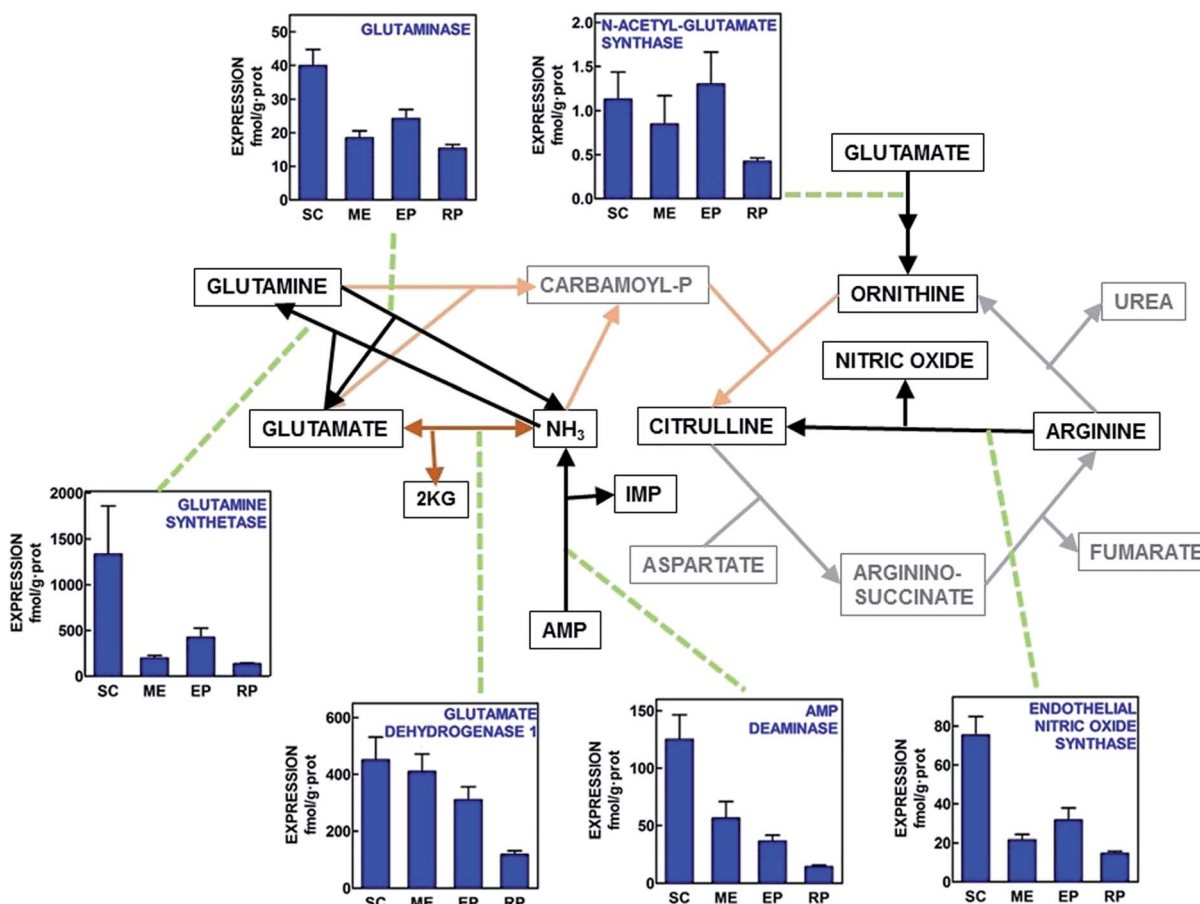


Fig. 2 Schematic representation of the placement of additional enzyme gene expressions related to the operation of the urea cycle in four WAT sites of adult male Wistar rats. All data are presented as the mean \pm SEM of 6 different animals per group. Blue columns depict the corresponding enzyme gene expression in fmol per g protein. Black lines represent cytosolic pathways analyzed; brown lines correspond to the mitochondrial pathways studied. Grey/orange lines depict the paths analyzed in Fig. 1 SC = subcutaneous WAT; ME = mesenteric WAT; EP = epididymal WAT and RP = retroperitoneal WAT. Statistical analysis of differences between groups (one-way ANOVA applied to WAT site). Glutaminase ($P < 0.0001$). N-Acetyl-glutamate synthase (NS). Glutamine synthetase ($P = 0.0098$). Glutamate dehydrogenase 1 ($P = 0.0021$). AMP deaminase ($P < 0.0001$). Endothelial nitric oxide synthase ($P < 0.001$).

Table 5 Comparison of liver and WAT urea cycle enzyme activities considered as potential catalytic capability of the whole organ/site^a

	Weight	Protein	Carbamoyl-P synthase (nkat per g P)	Ornithine carbamoyl- transferase (μkat per g P)	Arginino-succinate synthase (nkat per g P)	Arginino-succinate lyase (nkat per g P)	Arginase (μkat per g P)
Liver			509 ± 57	2.88 ± 0.44	274 ± 28	117 ± 15	227 ± 19
	Weight (g)	Protein (g)	Carbamoyl-P synthase (nkat)	Ornithine carbamoyl- transferase (nkat)	Arginino-succinate synthase (nkat)	Arginino-succinate lyase (nkat)	Arginase (nkat)
Liver	11.6 ± 0.5	2.21 ± 0.22	1110 ± 115	6183 ± 877	725 ± 78	273 ± 37	42 900 ± 3800
Sum of 4 WAT sites	30.8 ± 1.7	1.85 ± 0.14	75.0 ± 9.7	2107 ± 68	78.9 ± 7.5	134 ± 9	411 ± 61
WAT/liver ratio	2.6	0.84	0.07	0.34	0.11	0.50	0.01

^a The liver values are presented in nkat or μkat per g of tissue protein, and are the mean ± SEM of six different rats. The values for the four main WAT sites were calculated from the data of Table 2 and Fig. 1 and 2. They represent the total enzyme catalytic activity in the tissue as a whole (in nanokatals).

Table 6 Estimated molal concentration tissue/plasma ratios for arginine in WAT and liver of undisturbed adult male rats^a

	μmol per g water	Sum of urea + arginine + citrulline (μmol per g water)	Tissue/ plasma ratio
Plasma urea	4.27 ± 0.20	4.46 ± 0.19	
Plasma arginine	0.171 ± 0.019		
Plasma citrulline	0.024 ± 0.002		
SC WAT		19.7 ± 3.5	4.3 ± 0.8
ME WAT		21.8 ± 4.2	5.0 ± 1.0
EP WAT		16.2 ± 4.9	3.5 ± 0.9
RP WAT		6.48 ± 1.78	1.4 ± 0.4
Liver		39.0 ± 6.3	8.7 ± 1.4

^a The data are the mean ± SEM of 6 animals. The tissue/plasma ratio is the quotient between the (measured) tissue combined urea + arginine + citrulline values expressed in molal units divided by the composite sum of plasma urea + arginine + citrulline also in molal units. The data used for composite values and ratios were homologous (*i.e.* obtained from the same individual rats).

obtain the composite data also presented in Table 5. The direct comparison of the catalytic potential for urea cycle of liver *vs.* the combined (sum) of four main WAT sites showed an enormous difference for arginase (ratio liver/WAT in the range of 0.01). The differences were also marked for carbamoyl-P synthase and, to a lower extent, arginino-succinate synthase; however, the ratios were close to 1/3 to 1/2 of those of liver for arginino-succinate lyase and ornithine carbamoyl-transferase.

Tissue urea and guanido amino acid levels

Table 6 shows the plasma molal concentrations of urea, arginine and citrulline, as well as the combined (molal) levels of urea + arginine + citrulline in the four WAT sites studied and liver. In all cases, the combined value for tissues was higher than their sum in plasma. The molal ratios of WAT/plasma for this combined figure of urea and urea-cycle intermediary amino acids were in the range of 3.5–5.0 for subcutaneous, mesenteric and epididymal WAT, and lower ratios (higher than 1 in any case) for retroperitoneal WAT. The ratio for liver was twice that of subcutaneous WAT.

Unfortunately, the values obtained did not discriminate between arginine, citrulline and urea, but clearly showed that there must be a gradient of concentrations between any combination of these and plasma. These results seem to corroborate the hypothesis of an active urea cycle in WAT helping produce citrulline and arginine, but the wide differences with plasma, and the much higher relative levels of urea in plasma suggest that most WAT sites may produce significant amounts of urea.

Discussion

The main conclusion derived from the present study is the presence of all enzymes of the urea cycle (liver type) in WAT. The activities and their relationships were variable, depending on the site studied, but all enzymes were expressed in a degree

sufficient to allow and justify the overall operation of the cycle. This assumption was reinforced by the presence of all enzyme activities of the urea cycle in the four WAT sites studied, which are, quantitatively, the largest discrete WAT masses in the rat.

WAT nitrogen metabolism has been sparsely studied, with only a few publications dealing directly with this question;^{11,19} a small number of papers included WAT in enzyme distribution studies.^{27–29} This explains, in part, that the possible significant implication of WAT in amino acid metabolism has been seldom analyzed. Perhaps, the only clear exception is the postulated implication of WAT in the glucose–alanine cycle.¹⁰ We have recently found that WAT lactate production goes well beyond the simple limited export of 3C units under starvation.¹³ In addition, WAT contains several amino acid metabolism enzyme activities, such as glutamine synthetase,²⁸ glutaminase,²⁹ and AMP-deaminase.²⁷ Taken together, these data hint to a functional coordinated metabolism of ammonium.

Evidently, the main problems that WAT present as an “active” metabolic organ are dual: (a) its wide dispersion and function-adapted specialization, depending on the site, and (b) the limited proportion of “active tissue” with respect to tissue mass, since most of the tissue is fat. The (a) question has been widely analyzed,^{30,31} but in any case there is a substantial pattern of uniformity encompassing all sites, which act coordinately as a single energy store;⁴ WAT has been considered to act as a disperse organ.³²

With respect to the (b) question, it is true that excess tissue fat makes comparisons difficult, and needs the application of a number of methodological modifications and assumptions to allow work on it, but the non-fat and non-fiber (collagen, elastin) remaining tissue, including the non-fat part of adipocytes has a differentiated metabolic activity.³³ In fact, a number of enzyme activities or expressions, such as those we present for arginino-succinate lyase and ornithine carbamoyl transferase were in the same range (per unit of protein weight) than those of the liver. When we compare the total catalytic capability of the four main WAT sites and that of liver, the hepatic preponderance is clear. The maximal differences were observed for arginase (the liver is the main site for urea production) and carbamoyl-P synthase (again liver is a main site for detoxification of ammonium), but the differences decreased considerably for the other urea cycle enzymes, reinforcing the postulated role of extra-hepatic citrulline (and arginine) provider. However, the four main WAT sites contain about half of body WAT,⁴ which may result, in practical terms, in doubling the ratios in Table 5 when considering WAT as a whole organ, a condition that is greatly changed in obesity. In sum, the possible capabilities of WAT urea cycle may be quantitatively important and comparable only to liver. A question that needs considerable additional work to be adequately understood.

The RNA content of a tissue is, probably, a fair (albeit indirect) indicator of overall “metabolic activity”. The data for WAT sites showed wider differences than expected. However, when these data were used to compute the gene expressions, a good degree of homogeneity between WAT sites was maintained. This is an indirect indication of shared molecular (largely

genomic) regulation of urea cycle enzymes despite the specialization and diverse metabolic activity of the sites.

In spite of their expressions being correlated with those of the rest of urea cycle enzymes, the main controlling enzyme of the cycle, arginino-succinate synthase³⁴ and the accompanying lyase, show patently lower activities than the other urea cycle enzymes. The discordance between the uniform gene regulation (highly inter-correlated expressions for all enzymes) and uncorrelated gene expressions *vs.* activities for arginino-succinate enzymes agree with a possible post-transcriptional modulation of this controlling section³⁵ of the cycle. The wide differences between enzymes as to the observed ratios of activity *vs.* gene expression are a clear indication of a probably powerful additional mechanism of regulation, as is their turnover rates, which establish the real active life of the enzyme molecules. Higher activity *vs.* expression ratios, as is the case of ornithine carbamoyl transferase, suggest longer half-lives (and probably limited regulation *via* inactivation) compared with the critical controlling enzymes such as carbamoyl-P synthase and, especially arginino-succinate synthase. The isolated interpretation of either activity or gene expression alone may result in conflicting conclusions, not necessarily coincident with those we obtain from their combined analysis.

The sites for control of the urea cycle derived from the correlation analyses are: an overall genomic control of the cycle as a whole, affecting all sites, and two key control points, both well known: carbamoyl-P synthesis³⁶ and arginino-succinate synthesis.³⁴ However, the data for arginino-succinate lyase, an enzyme seldom analyzed separately, point to its activity sharing with the synthase the control of arginino-succinate, and thus the ultimate control of arginine production.³⁷ Probably, both arginino-succinate-related enzymes are subject to additional post-transcriptional regulation that breaks up the relative uniformity of the correlation data.

The finding of a complete urea cycle in WAT represents a departure of the concept of liver as the only factual regulator of N disposal. Altered urea cycle in metabolic syndrome²⁰ and decreased urea production³⁸ attest a decreasing role of liver in amino acid disposal under conditions of inflammation. This fact, so far, remains unexplained in spite of the excess energy and 2-amino N that characterizes dietary-induced metabolic syndrome.

The present study opens the question of what is the role of urea cycle in WAT. The cycle we described probably does not seem, initially, focused on the conversion of ammonia to urea. Our data show that the main ammonia producing enzymes (glutaminase, AMP deaminase) are less expressed than the enzymes using it to synthesize amino-N, amido-N or guanido-N. On the ammonia-disposing side, we find glutamate dehydrogenase, probably working mainly in the direction of glutamate synthesis,³⁹ glutamine synthetase (to produce glutamine) and carbamoyl-P synthases. The purine nucleotide cycle is probably present in adipose tissue,²⁷ and, at least in muscle, its activity is closely related to glycolysis.⁴⁰ WAT possesses a very active glycolytic capacity,¹³ which may help increase the up-regulation of the controlling enzyme, AMP deaminase.⁴¹ However, a main function of the purine nucleotide cycle is to decrease AMP

levels; and thus, affects AMPK, and WAT metabolic regulation. We do not have enough data to establish the existence of a significant flow of amino-N to ammonia-N in WAT, but a sizeable activity²⁸ and hormone-regulated expression⁴² of glutamine synthetase seems to suggest that probably the urea cycle is not, anyway, the main outlet for a significant production of ammonia in WAT under basal conditions.

The high activity of ornithine carbamoyl transferase, compared with the low arginino-succinate activity (in spite of not so different gene expressions), suggest that the main role of WAT urea cycle may not be the production of urea, but the generation of citrulline. This function seems obvious for mesenteric WAT, acting in the same way that the neighboring intestine to provide the liver (and kidney) with intermediate urea cycle substrates.⁴³ However, this function is paralleled in all four WAT sites, which suggests a higher, possibly peripheral, demand for citrulline. This amino acid plays an important role as a controller of metabolism.⁴⁴ Citrulline and arginine levels are closely related, in a way that the former is a more effective provider of arginine than arginine itself;⁴⁵ this is due, probably to the strict control of arginine levels and availability in relation to nitric oxide synthesis⁴⁶ and its implication in a number of other regulatory mechanisms.⁴⁷ Citrulline is a floating reserve of arginine for peripheral tissues. The main known body citrulline source, intestine (including mesenteric WAT) is directly connected to the liver *via* portal vein, but the liver extracts only a minor fraction of portal blood citrulline for urea synthesis.⁴⁸ The kidney takes up most of systemic blood citrulline (largely from liver efflux) into arginine⁴⁸ under standard conditions. However, kidney arginine production from citrulline exceeds liver output.⁴⁹ We postulate that WAT may justify the difference thanks to a robust ornithine carbamoyl-transferase activity sustained by the upper part of the urea cycle described here. In this respect, the difference between kidney and WAT may be the dependence of kidney of intestinal production and variable liver retention of citrulline to maintain its production of arginine. Perhaps, the immediate independence of WAT from diet as compared to the gut may justify a role for WAT to sustain the production of citrulline independently of the N-disposal function of the intestine–liver urea cycle; as well as to limit the dependence of renal-released arginine supply from this setup.

The existence of a marked gradient in WAT (and liver), for urea cycle products is not compatible with their uptake from the blood, and strongly supports that the flow of these substrates (or at least part of them) goes from WAT cells to blood. Consequently, the tissue produces them *de novo*. Additionally, the levels of enzyme activity in the tissues tested show a clear parallelism with the values of the molality ratios.

WAT has a significant potential for the generation of nitric oxide, largely thanks to the endothelial isozyme of nitric oxide synthase. The production of this key regulatory factor is tightly regulated, both through the modulation of the expression and activity of the enzyme,⁵⁰ but also controlling the supply of arginine.⁵¹ In metabolic syndrome, the low overall production of urea^{13,38} has been attributed to the preservation of arginine to fuel an increased synthesis of nitric oxide,⁵² a consequence of inflammation. The synthesis of nitric oxide also yields citrulline

as byproduct, supporting the postulated citrulline/arginine-producing role of WAT's urea cycle.

Arginase also regulates the availability of arginine to fuel nitric oxide synthesis. The widespread presence of arginases in many peripheral tissues⁵³ has been attributed to a control role through competitive arginine disposal.⁵⁴ However, in the case of WAT, we found arginase activity in all sites, but only the arginase 1 *Arg1* gene was expressed; that for arginase 2, *Arg2*, was expressed only in subcutaneous WAT (which also presented the highest arginase activity). Arginase 1 is commonly associated with the “regular” liver urea-producing cycle, thus its presence in all WAT sites could be considered, *a priori*, to be more related to breakup of arginine to yield ornithine (and urea) than to control the flow of arginine towards nitric oxide. This peculiar arginase isozyme distribution also makes WAT closer to the liver in its unique configuration of urea cycle.

In general terms, the described functions were shared by the four WAT sites studied (the correlation analyses include data from all of them), but there were marked specific differences related to location. Subcutaneous WAT showed the highest activities/expressions for most enzymes, suggesting that it is the most probable WAT site to produce urea, eventually, in significant amounts. Its location, relationship with the skin and its biota may be related to its highest expression of nitric oxide synthase and the presence of arginase 2. The role of nitric oxide within the defense system and in inflammation may be a primary justification for these differences. The also higher gene expressions of both glutamine cycle enzymes hint to an active amino acid metabolism, helped by proteolysis⁵⁵ and active branched-chain amino acid catabolism.⁵⁶ The large mass of subcutaneous adipose tissue confers a prominent position in its possible role in amino acid metabolism to this part of the adipose organ.

The data available hint at WAT acting not only locally and peripherally, but also complementing the function of the splanchnic bed organs in the regulation of – at least – arginine metabolism. We have described a complete, (mainly) expression-regulated (and coordinated), active urea cycle in the four largest WAT sites; we hinted at its possible function in the control of arginine handling through citrulline synthesis. These results, however, do not preclude the possibility of WAT to carry out a full urea cycle, eliminating excess N *via* a “peripheral” urea cycle. In our opinion, the metabolic potential and control role of energy metabolism of WAT may be second only to liver; this impression should be extended to amino acid metabolism too. The large WAT mass and widespread distribution probably compensate the deceptive low proportion of “live cytosol”. The results shown in this study correspond to a “basal” state, of male rats under a standard diet. It can be speculated that the powerful urea cycle machinery installed in WAT may play a different role under other dietary and metabolic circumstances (*i.e.* obesity, inflammation). Our study confirms that WAT contains a full urea cycle, probably fully functional, but we are yet far from knowing its possible function in such complex organ as is WAT.

Conclusions

All these considerations bring us to suggest that the urea cycle is operative (but its functionality under basal conditions remains to be proven) in all four WAT sites. The right enzymes are expressed, and show measurable activities; there is a clear coordinated regulation on their expression (and, partly, of their activities); and the key control points: ammonium availability and arginino-succinate enzymes are the obviously best controlled bottlenecks for the urea cycle operation. The data presented suggest that WAT may produce urea but its urea cycle is geared, essentially, to provide citrulline as precursor of arginine, which is probably produced too, largely for peripheral tissues utilization. In this sense, WAT, by providing urea cycle intermediaries, as the intestine does,⁴⁸ complements liver function.

Conflict of interest

The authors declare that they have no conflict of interests.

Author contributions

SAr and SAg did the entire animal handling and laboratory work. JAFL and SAr carried out the statistical analyses. XR, JAFL and MA designed the experiments and established the main conclusions. MA conceived the study and wrote the paper. All authors participated in the discussion of the results and in the preparation of the final text.

Acknowledgements

This study was done with the partial support of grants of the Plan Nacional de Investigación en Biomedicina (SAF2012-34895) and the Plan Nacional de Ciencia y Tecnología de los Alimentos (AGL-2011-23635) of the Government of Spain, as well as of the CIBER-OBN Research web. S. Agnelli was the recipient of a Leonardo da Vinci fellowship, and S. Arriarán had a predoctoral fellowship of the Catalan Government, in both cases covering part of the time invested in this study.

References

- H. Hauner, *Physiol. Behav.*, 2004, **83**, 653–658.
- C. Deveaud, B. Beauvoit, B. Salin, J. Schaeffer and M. Rigoulet, *Mol. Cell. Biochem.*, 2004, **267**, 157–166.
- P. A. Tataranni, D. E. Larson and E. Ravussin, *J. Am. Coll. Nutr.*, 1994, **13**, 569–574.
- M. M. Romero, S. Roy, K. Pouillot, M. Feito, M. Esteve, M. M. Grasa, J. A. Fernández-López, M. Alemany and X. Remesar, *PLoS One*, 2014, **9**, e90995.
- J. Sanchez-Gurmaches and D. A. Guertin, *Nat. Commun.*, 2014, **5**, 4099.
- R. Cancello, J. Tordjman, C. Poitou, G. Guilhem, J. L. Bouillot, D. Hugol, C. Coussieu, A. Basdevant, A. Bar Hen, P. Bedossa, M. Guerre-Millo and K. Clément, *Diabetes*, 2006, **55**, 1554–1561.
- M. Alemany, *J. Clin. Endocrinol. Metab.*, 2011, **96**, 66–68.
- E. Fuentes, F. Fuentes, G. Vilahur, L. Badimon and I. Palomo, *Mediators Inflammation*, 2013, **2013**, 136584.
- K. N. Frayn and S. W. Coppack, *Diabetologia*, 1990, **33**, 740.
- K. Snell and D. A. Duff, *Biochem. Biophys. Res. Commun.*, 1977, **77**, 925–931.
- T. J. Kowalski, G. Y. Wu and M. Watford, *Am. J. Physiol.*, 1997, **273**, E613–E622.
- K. R. Markan, M. J. Jurczak and M. J. Brady, *Mol. Cell. Endocrinol.*, 2010, **318**, 54–60.
- S. Arriarán, S. Agnelli, D. Sabater, X. Remesar, J. A. Fernández-López and M. Alemany, *PLoS One*, 2015, **10**, e0119572.
- F. J. López-Soriano, J. A. Fernández-López, T. Mampel, F. Villarroya, R. Iglesias and M. Alemany, *Biochem. J.*, 1988, **252**, 843–849.
- G. Pilon, P. Penfornis and A. Marette, *Horm. Metab. Res.*, 2000, **32**, 480–484.
- L. Millet, P. Barbe, M. Lafontan, M. Berlan and J. Galitzky, *J. Appl. Physiol.*, 1998, **85**, 181–188.
- F. Karpe, B. A. Fielding, J. L. Ardilouze, I. A. Macdonald and K. N. Frayn, *J. Physiol.*, 2002, **540**(3), 1087–1093.
- J. Conde, M. Scotce, R. Gómez, V. López, J. J. Gómez-Reino, F. Lago and O. Gualillo, *BioFactors*, 2011, **37**, 413–420.
- F. J. López-Soriano and M. Alemany, *Arch. Int. Physiol. Biochim.*, 1986, **94**, 121–125.
- D. Sabater, S. Agnelli, S. Arriarán, J. A. Fernández-López, M. M. Romero, M. Alemany and X. Remesar, *BioMed Res. Int.*, 2014, **2014**, 959420.
- O. H. Lowry, R. W. Rosebrough, A. L. Farr and R. J. Randall, *J. Biol. Chem.*, 1951, **193**, 265–275.
- S. Arriarán, S. Agnelli, J. A. Fernández-López, X. Remesar and M. Alemany, *J. Enzyme Res.*, 2012, **3**, 29–33.
- E. L. Oginsky, *Methods Enzymol.*, 1957, **3**, 639–643.
- L. Arola, E. Herrera and M. Alemany, *Anal. Biochem.*, 1977, **82**, 236–239.
- M. M. Romero, M. M. Grasa, M. Esteve, J. A. Fernández-López and M. Alemany, *Nutr. Metab.*, 2007, **4**, 26.
- G. Bamias, D. Goukos, E. Laouidi, I. G. Balla, S. I. Siakavellas, G. L. Daikos and S. D. Ladas, *Inflammatory Bowel Dis.*, 2013, **19**, 2840–2847.
- L. Arola, A. Palou, X. Remesar and M. Alemany, *Horm. Metab. Res.*, 1981, **13**, 264–266.
- L. Arola, A. Palou, X. Remesar and M. Alemany, *Horm. Metab. Res.*, 1981, **13**, 199–202.
- J. M. Kowalchuk, R. Curi and E. A. Newsholme, *Biochem. J.*, 1988, **249**, 705–708.
- S. Cinti, *Dis. Models & Mech.*, 2012, **5**, 588–594.
- T. Tchkonia, T. Thomou, Y. Zhu, I. Karagiannides, C. Pothoulakis, M. D. Jensen and J. L. Kirkland, *Cell Metab.*, 2013, **17**, 644–656.
- S. Cinti, *Prostaglandins, Leukotrienes Essent. Fatty Acids*, 2005, **73**, 9–15.
- J. R. Peinado, Y. Jiménez-Gómez, M. R. Pulido, M. Ortega-Bellido, C. Díaz-López, F. J. Padillo, J. López-Miranda, R. Vázquez-Martínez and M. A. M. Malagón, *Proteomics*, 2010, **10**, 3356–3366.

- 34 A. J. Meijer, C. Lof, I. C. Ramos and A. J. Verhoeven, *Eur. J. Biochem.*, 1985, **148**, 189–196.
- 35 G. Hao, L. J. Xie and S. S. Gross, *J. Biol. Chem.*, 2004, **279**, 36192–36200.
- 36 T. Saheki, T. Ohkubo and T. Katsunuma, *J. Biochem.*, 1978, **84**, 1423–1430.
- 37 R. J. Haines, L. C. Pendleton and D. C. Eichler, *Int. J. Biochem. Mol. Biol.*, 2011, **2**, 8–23.
- 38 T. Barber, J. R. Viña, J. Viña and J. Cabo, *Biochem. J.*, 1985, **230**, 675–681.
- 39 J. D. McGivan and J. B. Chappell, *FEBS Lett.*, 1975, **52**, 1–7.
- 40 K. Tornheim, *J. Theor. Biol.*, 1979, **79**, 491–541.
- 41 K. Tornheim and J. M. Lowenstein, *J. Biol. Chem.*, 1972, **247**, 162–169.
- 42 M. J. Lee, D. W. Gong, B. F. Burkey and S. K. Fried, *Am. J. Physiol.*, 2011, **300**, E571–E580.
- 43 G. Wu, A. G. Borbolla and D. A. Knabe, *J. Nutr.*, 1994, **124**, 2437–2444.
- 44 C. Breuillard, L. Cynober and C. Moinard, *Amino Acids*, 2015, **47**, 685–691.
- 45 E. Schwedhelm, R. Maas, R. Freese, D. Jung, Z. Lukacs, A. Jambrecina, W. Spickler, F. Schulze and K. H. Böger, *Br. J. Clin. Pharmacol.*, 2008, **65**, 51–59.
- 46 F. Mariotti, K. J. Petzke, D. Bonnet, I. Szezpanski, C. Bos, J. F. Huneau and H. Fouillet, *Am. J. Clin. Nutr.*, 2013, **97**, 972–979.
- 47 J. E. Huh, J. Y. Choi, Y. O. Shin, D. S. Park, J. W. Kang, D. Nam, D. Y. Choi and J. D. Lee, *Int. J. Mol. Sci.*, 2014, **15**, 13010–13029.
- 48 H. G. Windmueller and A. E. Spaeth, *Am. J. Physiol.*, 1981, **241**, E473–E480.
- 49 Y. M. Yu, J. F. Burke, R. G. Tompkins, R. Martin and V. R. Young, *Am. J. Physiol.*, 1996, **271**, E1098–E1109.
- 50 K. Kikuchi-Utsumi, B. Gao, H. Ohinata, M. Hashimoto, N. Yamamoto and A. Kuroshima, *Am. J. Physiol.*, 2001, **282**, R623–R626.
- 51 K. Velickovic, M. Markelic, I. Golic, V. Otasevic, A. Stancic, A. Jankovic, M. Vucetic, B. Buzadzic, B. Korac and A. Korac, *Eur. J. Nutr.*, 2014, **53**, 813–821.
- 52 J. G. Zhou, D. D. Kim and R. D. Peluffo, *Am. J. Physiol.*, 2010, **299**, C230–C239.
- 53 S. Y. Choi, C. N. Park, M. J. Ahn, J. H. Lee and T. K. Shin, *Acta Histochem.*, 2012, **114**, 487–494.
- 54 W. Shin, D. E. Berkovitz and S. Ryoo, *Exp. Mol. Med.*, 2012, **44**, 594–602.
- 55 B. W. Patterson, J. F. Horowitz, G. Wu, M. Watford, S. W. Coppock and S. Klein, *Am. J. Physiol.*, 2002, **282**, E931–E936.
- 56 D. E. Lackey, C. J. Lynch, K. C. Olson, R. Mostaedi, M. Ali, W. H. Smith, F. Karpe, S. Humphreys, D. H. Bedinger, T. N. Dunn, A. P. Thomas, P. J. Oort, D. A. Kieffer, R. Amin, A. Bettaieb, F. G. Haj, P. Permana, T. G. Anthony and S. H. Adams, *Am. J. Physiol.*, 2013, **304**, E1175–E1187.

Effects of sex and site on amino acid metabolism enzyme gene expression and activity in rat white adipose tissue

Sofía Arriarán¹, Silvia Agnelli¹, Xavier Remesar^{1,2,3}, José Antonio Fernández-López^{1,2,3} and Marià Alemany^{1,2,3}

¹ Department of Nutrition & Food Science, University of Barcelona, Faculty of Biology, Barcelona, Spain

² Institute of Biomedicine, University of Barcelona, Barcelona, Spain

³ CIBER OBN, Barcelona, Spain

ABSTRACT

Background and Objectives. White adipose tissue (WAT) shows marked sex- and diet-dependent differences. However, our metabolic knowledge of WAT, especially on amino acid metabolism, is considerably limited. In the present study, we compared the influence of sex on the amino acid metabolism profile of the four main WAT sites, focused on the paths related to ammonium handling and the urea cycle, as a way to estimate the extent of WAT implication on body amino-nitrogen metabolism.

Experimental Design. Adult female and male rats were maintained, undisturbed, under standard conditions for one month. After killing them under isoflurane anesthesia. WAT sites were dissected and weighed. Subcutaneous, perigonadal, retroperitoneal and mesenteric WAT were analyzed for amino acid metabolism gene expression and enzyme activities.

Results. There was a considerable stability of the urea cycle activities and expressions, irrespective of sex, and with only limited influence of site. Urea cycle was more resilient to change than other site-specialized metabolic pathways. The control of WAT urea cycle was probably related to the provision of arginine/citrulline, as deduced from the enzyme activity profiles. These data support a generalized role of WAT in overall amino-N handling. In contrast, sex markedly affected WAT ammonium-centered amino acid metabolism in a site-related way, with relatively higher emphasis in males' subcutaneous WAT.

Conclusions. We found that WAT has an active amino acid metabolism. Its gene expressions were lower than those of glucose-lipid interactions, but the differences were quantitatively less important than usually reported. The effects of sex on urea cycle enzymes expression and activity were limited, in contrast with the wider variations observed in other metabolic pathways. The results agree with a centralized control of urea cycle operation affecting the adipose organ as a whole.

Submitted 28 July 2015
Accepted 21 October 2015
Published 10 November 2015

Corresponding author
Marià Alemany, malemany@ub.edu
Academic editor
Matthew Barnett
Additional Information and
Declarations can be found on
page 18

DOI 10.7717/peerj.1399

© Copyright
2015 Arriarán et al.

Distributed under
Creative Commons CC-BY 4.0

OPEN ACCESS

Subjects Biochemistry, Nutrition, Metabolic Sciences

Keywords Adipose tissue, Urea cycle, Ammonium, Citrulline, Urea, Adipose organ, Lipogenesis

INTRODUCTION

The influence of sex on adipose tissue distribution and function, and its implication in metabolic syndrome has been known for a long time ([Mayes & Watson, 2004](#)). The

protective effects of estrogen on adipose tissue activity ([D'Eon et al., 2005](#)), and limitation of its hypertrophic growth ([Kumar et al., 2012](#)) and inflammation ([Stubbins et al., 2012](#)) are key sex-related factors, which contribute to limit the disorders elicited by metabolic syndrome ([Antonio et al., 2015](#)). The distribution of fat in gynoid and android shapes of adult humans is a consequence of the close interrelationship of adipose tissue with androgens and estrogens ([Kotani et al., 1994](#)), modulated by their different response to glucocorticoids in the aftermath of a tissue defensive response against excess nutrient loads ([Alemay, 2012a](#)).

There are clear differences between females and males in site distribution and metabolic responses ([Porter et al., 2004](#); [Demerath et al., 2007](#)), but most studies on adipose tissue are limited to a single site or isolated cells, and are usually focused on the responses to inflammation ([Revelo et al., 2014](#)).

The extensive metabolic capability of white adipose tissue (WAT) show a remarkable uniformity in metabolic function and overall regulation ([Carmean, Cohen & Brady, 2014](#); [Romero et al., 2014](#)). As a consequence, the assumed main function of WAT (i.e., triacylglycerol storage as energy reserve) ([Gallic, Oakhill & Steinberg, 2010](#); [Romacho et al., 2014](#)) is been reconsidered because of the multiple functions of this unique disperse organ ([Eringa, Bakker & Van Hinsbergh, 2012](#); [Ferrante, 2013](#); [Giordano et al., 2014](#)). However, the level of knowledge of WAT metabolism, other than the control of lipid synthesis and storage, remains remarkably insufficient, constituting a handicap for interpretation of its physiological role ([Jensen, 2007](#)).

WAT contains a complete urea cycle, as shown in the present study, which is, probably implicated in the extra-splanchnic production of citrulline, a critical factor for muscle function ([Ventura et al., 2013](#)) and inter-organ 2-amino-N transport and utilization. However, WAT is also a massive producer of 3C fragments, such as lactate ([Arriarán et al., 2015](#)), but including alanine ([Snell & Duff, 1977](#)). WAT is also a net exporter of glutamine ([Kowalski & Watford, 1994](#)), and can use branched-chain amino acids for energy and lipogenesis ([Herman et al., 2010](#)). The large combined organ size, variety of known amino acid metabolic pathways and diverse physiological functions, hint at WAT as a potentially important site for peripheral amino acid metabolism. The information available is scant, we found only a couple of earlier studies ([López-Soriano & Alemay, 1986](#); [Kowalski, Wu & Watford, 1997](#)); this is a serious limitation for a full understanding of whether amino acids should be also included in the well-established role of WAT in the management of energy, from glucose and lipids.

The little we know of WAT role in amino acid metabolism is further limited by our almost nil understanding of the role sex plays on WAT metabolism. In general terms, androgens favor protein deposition ([Griggs et al., 1989](#)), and males tend to consume spontaneously more protein than females ([Radcliffe & Webster, 1978](#)); on the other hand, estrogens lower body weight ([Bryzgalova et al., 2008](#)), in spite of females (women) having—normally—a higher body fat percentage than males (men). Young women are more resistant to obesity than men ([Meyer et al., 2011](#)); however, after menopause, this estrogenic protection wanes ([Cagnacci et al., 2007](#)).

In this study, we intended to determine whether the gross differences in WAT distribution and its resilience to change had a robust biochemical basis. Thus, we analyzed whether the WAT urea cycle and related amino acid catabolic processes of rats showed sex-modulated differences. To obtain a wider picture we studied the four main (largest) WAT sites in parallel, and we included in the analysis (for comparison) a number of gene expressions involved in the control of WAT lipogenesis from glucose and lipolysis.

MATERIALS AND METHODS

Experimental design and animal handling

All animal handling procedures and the experimental setup were in accordance with the animal handling guidelines of the corresponding European and Catalan Authorities. The Committee on Animal Experimentation of the University of Barcelona specifically authorized the procedures used in the present study (DMAH-5483).

The experimental setup consisted on keeping two groups of undisturbed rats (female and male) under standard conditions for four weeks, in order to limit the influence of factors other than sex on the parameters analyzed.

Nine week old female and male Wistar rats (Harlan Laboratory Models, Sant Feliu de Codines, Spain) were used. The rats ($N = 6$ per group) were housed in pairs (same sex) in solid-bottom cages with wood shreds for bedding. They had free access to water and ate normal rat chow (type 2014, Harlan). The rats were kept in a controlled environment (lights on from 08:00 to 20:00; 21.5–22.5 °C; 50–60% humidity) for one month.

The rats, without dietary manipulation, were killed, under isoflurane anesthesia, at the beginning of a light cycle (08:30–10:00), by aortic exsanguination, using dry-heparinized syringes; then, they were rapidly dissected, taking samples of WAT sites: mesenteric (ME), perigonadal (epididymal in males, periovaric in females, PG), retroperitoneal (RP) and subcutaneous (inguinal fat pads, SC). The samples were blotted and frozen with liquid nitrogen; after weighing, they were ground under liquid nitrogen and stored at –80 °C until processed. Later, the dissection of the rats continued, extracting the remaining WAT in ME, EP and RP sites; the rats were skinned, and the whole subcutaneous WAT was dissected. The weights of the recovered WAT were computed only to establish the total mass of each WAT site.

Blood plasma parameters

The blood obtained from the aorta was centrifuged to obtain plasma, which was frozen and kept at –80 °C until processed. Plasma samples were used to measure glucose (kit #11504), triacylglycerols (kit #11828), total cholesterol (kit #11505) and urea (kit # 11537), all from Biosystems, Barcelona Spain. Lactate was measured with another kit (ref. #1001330; Spinreact, Sant Esteve de Bas, Spain). Amino acids were analysed individually using an amino acid analyser (Pharmacia-LKB-Alpha-plus, Uppsala, Sweden) from plasma samples deproteinized with acetone (*Arola, Herrera & Alemany, 1977*). Since the method used did not provide fair analyses for glutamine (*Gowda, Gowda & Raftery, 2015*) and other amino acids (Trp, Cys, Asn), we decided to present only the partial sum of the other amino acids as a single indicative value.

Preparation of tissue homogenates

Frozen tissue samples were homogenized, using a tissue disruptor (Ultraturrax IKA-T10, Ika Werke, Staufen, Germany), in 5 volumes of chilled 70 mM hepes buffer pH 7.4 containing 1 mM dithiothreitol (Sigma, St Louis MO USA), 50 mM KCl, 1 g/L Triton X-100 (Sigma) and 1 g/L lipid-free bovine serum albumin (Sigma). In homogenates to be used for carbamoyl-P synthase 2 estimation, the concentration of Triton X-100 was halved to decrease foaming. The homogenates were centrifuged for 10 min at 5,000 × g; the floating fat layers and gross debris precipitates were discarded. The clean homogenates were kept on ice, and used for enzymatic analyses within 2 h of their preparation.

Tissue protein content was estimated with the Lowry method ([Lowry et al., 1951](#)). After development of color, fat droplet suspension-generated turbidity was eliminated with the addition of small amounts of finely powdered solid MgO before reading the absorbance. In the measurements of homogenate protein content, homogenization buffer (which contained albumin) was used as blank. Enzyme activities were expressed in nkat/g protein.

Enzyme activity analyses

Carbamoyl-P synthase was estimated from the incorporation of ¹⁴C-bicarbonate (Perkin Elmer, Bad Neuheim, Germany) into carbamoyl-P using a method previously described by us ([Arriarán et al., 2012](#)). No significant carbamoyl-P synthase 1 activity was detected (and its gene was not expressed, either, in WAT). Thus, only carbamoyl-P synthase 2 was measured.

All other enzyme activities (ornithine carbamoyl-transferase, arginino-succinate synthase, arginino-succinate lyase and arginases 1 and 2) were estimated following recently developed methods, which are presented in detail in [Supplemental Information 1](#) both to justify their adequacy and to allow others to employ a methodology developed for adipose tissue.

Gene expression analysis

Total tissue RNA was extracted from frozen tissue samples using the Tripure reagent (Roche Applied Science, Indianapolis IN USA), and was quantified in a ND-100 spectrophotometer (Nanodrop Technologies, Wilmington DE USA). These data were also used to determine the total RNA content of the tissue (per g of tissue weight or g of protein) in order to establish comparisons between the quantitative importance of gene expressions. RNA samples were reverse transcribed using the MMLV reverse transcriptase (Promega, Madison, WI USA) system and oligo-dT primers.

Real-time PCR (RT-PCR) amplification was carried out using 10 µL amplification mixtures containing Power SYBR Green PCR Master Mix (Applied Biosystems, Foster City, CA USA), 4 ng of reverse-transcribed RNA and 150 nmol of primers. Reactions were run on an ABI PRISM 7900 HT detection system (Applied Biosystems) using a fluorescent threshold manually set to 0.15 for all runs.

A semi-quantitative approach for the estimation of the concentration of specific gene mRNAs per unit of tissue/RNA or protein weight was used ([Romero et al., 2007](#)). *Rplp0* was

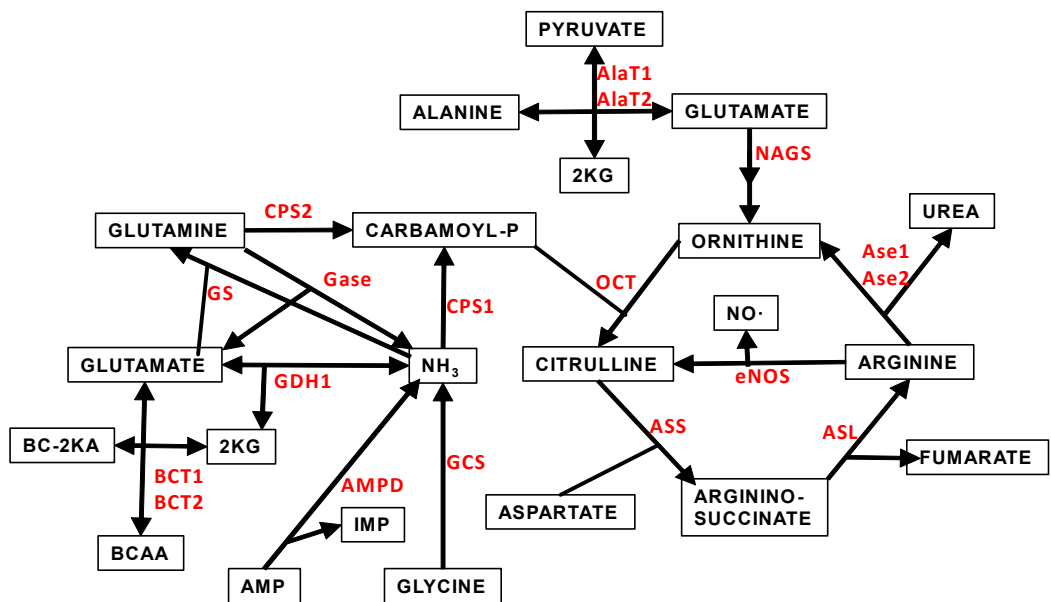


Figure 1 Scheme of the core of amino acid metabolism in WAT: urea cycle and ammonium handling. The abbreviations (marked in red) of the enzymes involved in the pathways depicted are the same described in Table 1 and throughout this study.

the charge control gene ([Eagni et al., 2013](#)). We expressed the data primarily as the number of transcript copies per gram of protein in order to obtain comparable data between the groups. The genes analyzed and a list of primers used is presented in [Table 1](#).

[Figure 1](#) depicts a scheme of the relationships between the amino acid metabolism-related enzymes which gene expressions have been analyzed in this study. This Figure also shows acronyms or abbreviations of the names of the enzyme-genes used in [Figs. 2](#) and [3](#).

Sex differences in gene expression

The ample variability of cell volume, blood flow, innervation, size of fat deposits etc. of WAT poses additional problems for comparison between different anatomical (i.e., site), physiological (i.e., sex, diet) and pathological (i.e., obesity) situations ([Caspar-Bauguil et al., 2005](#); [Prunet-Marcassus et al., 2006](#); [Gil et al., 2011](#)). The variability of lipid reserves may convert in irrelevant comparisons based on weight; the use of DNA or cell number is a better approach, but the multiple types of cells coexisting in WAT (and their widely variable numbers) may also alter direct comparisons. We used as basic comparison the protein content, largely because it has been the choice reference for enzyme activity and, by extension to gene expressions and their possible interactions. However, probably a better way to measure changes in functional activity may be the analysis of mRNA production. These changes do not parallel those of weight, protein content or cell numbers, but are a fair index of the relative importance of translation of the genes involved with respect to total protein synthesis. In fact, their use is complementary of the analysis of enzyme activity-gene expression referred to protein weight, since it includes a new variable: metabolic transcendence for the cell of the synthesis of the corresponding mRNAs. We

Table 1 Primer sequences used in the analysis of WAT gene expressions.

Protein	Gene	EC	Primer sequence 5' > 3'	Primer sequence 3' > 5'	bp
CPS2	Glutamine-dependent carbamoyl-phosphate synthase	<i>Cad</i>	6.3.5.5	AGTTGGAGGGAGGCTGAG	ATTGAIGGACAGGTGCTGGT
OTC	Ornithine carbamoyl transferase	<i>Otc</i>	2.1.3.3	CTTGGGGCTGTAATGAAAGTC	ATTGGGATGGTGTGCTTCCT
ASS	Arginino-succinate synthase	<i>Assl</i>	6.3.4.5	CAAAGATGGCACTACCCACA	GTTCTCCACGATGTCATGC
ASL	Arginino-succinate lyase	<i>Asl</i>	4.3.2.1	CGACACTTGCTACTACCTTG	GAGGCCACCCCTTCATCT
ARG1	Arginase-1	<i>Arg1</i>	3.5.3.1	GCAGAGACCCAGAAGAATGG	GTGAGCATCCACCCAAATG
ARG2	Arginase-2	<i>Arg2</i>	3.5.3.1	GCAGCCCTCTTCCTTCTCA	CCACATCTCGTAAGCCAATG
NAGS	N-acetyl-glutamate synthase	<i>Nags</i>	2.3.1.1	GCAGCCCACCAAAATCAT	CAGGTTCACATGCTCAGGA
eNOS	Nitric oxide synthase, endothelial	<i>Nos3</i>	1.14.13.39	CAAGTCCTCACGGCTTTT	GACATCACCGAGACAAACA
GS	Glutamine synthetase	<i>Glnl</i>	6.3.1.2	AACCCTCACGCCAGCATA	CTGGGATGTTTCCTCTTCG
Gase	Glutaminase kidney isoform, mitochondrial	<i>Gls</i>	3.5.1.2	CGAAAGTTGGCTCTGICA	AGGGCTGTTCTGGAGTCGTA
GDH1	Glutamate dehydrogenase 1, mitochondrial	<i>Gldl</i>	1.4.1.3	GGACAGAAATATGGGTGCAT	TCAGGTCCCAATCCCAGGTTA
GCS	Glycine cleavage system H protein, mitochondrial	<i>Gesh</i>	–	AAAGCACGAATGGTTAACAGC	TCCAAAGCACCAAACCTCC
AMPD	AMP deaminase 2	<i>Ampd2</i>	3.5.4.6	CGGCTTCTCTCACAAAGGTG	CGGATGTCGTTACCCCTCAG
AlaT1	Alanine aminotransferase 1	<i>Gpt</i>	2.6.1.2	GTATTCACGGAGCAGGAG	CACATAGCCACCAACAAACC
AlaT2	Alanine aminotransferase 2	<i>Gpt2</i>	2.6.1.2	CATTCCCTCGGATTCTCATC	GCCTTCTCGCTGTGCCAAA
BCT1	Branched-chain-amino-acid aminotransferase, cytosolic	<i>Bat1</i>	2.6.1.42	TGCCCCAGTTGCCAGTTTC	CAGTCCTCCATTCGCTCTTGA
BCT2	Branched-chain-amino-acid aminotransferase, mitochondrial	<i>Bat2</i>	2.6.1.42	AGTCTTCGGCTCAGGCACT	ATGGTAGGAATGTGGAGTTGCT
GLUT4	Solute carrier family 2 (facilitated glucose transporter), member 4	<i>Glut4</i>	–	CACAAATGAAACAGGGATG	CTTGATGACGGTGGCTCTGC
HK	Hexokinase-2	<i>Hk2</i>	2.7.1.1	ATTCACCAACGGCAACACAT	GGACAAAGGGATTCAAGGCATC
G6PDH	Glucose-6-phosphate 1-dehydrogenase	<i>G6pdx</i>	1.1.1.49	GACTGTGGCAAGCTCCCAA	GCTAGTGTGGCTATGGGCAGGT
ME	NADP-dependent malic enzyme	<i>Me1</i>	1.1.1.40	TTCTCTACGTGTTCCTGGAG	GGCCTTCTTGCAGGTGTTAA
PDHK2	Pyruvate dehydrogenase kinase 2, mitochondrial	<i>Pdk2</i>	2.7.11.2	TCACTCTCCCTCCATCAA	CGGCTTGGTTCACCTCATTT
PDHK4	Pyruvate dehydrogenase [acetyl transferring] kinase 4, mitochondrial	<i>Pdk4</i>	2.7.11.2	GTCAAGGCTATGGGACAGATGC	TTGGGATAACCCAGTCATCAGC
CATPL	ATP citrate lyase	<i>Ady</i>	2.3.3.8	GACCAGAAAGGGCTGACCAT	TTGTCAGGATCCCACCAAGT
ACoAC	Acetyl-CoA carboxylase 1	<i>Acaa</i>	6.4.1.2	AGGAAGATGGTGTGGCTCTG	GGGGAGATGTCGCTGGTCAT
FAS	Fatty acid synthase	<i>Fasn</i>	2.3.1.85	CTTGGGTGCGGATTACAACC	GCCCTCCCGTACACTCAC
PCAT1	Carnitine palmitoyltransferase 1, liver isoform	<i>Cpt1a</i>	2.3.1.21	CGCTCTATGGTCAACAGCA	CAGCACTATGGGTGGATGG
PCATm	Carnitine palmitoyltransferase 2, mitochondrial	<i>Cpt2</i>	2.3.1.21	TGCTTGACGGATGTGGCTTC	GTGCTGGAGCTGGCTTTGGT
ACADH	Long-chain acyl-CoA dehydrogenase, mitochondrial	<i>Aadl</i>	1.3.8.8	ATGCCAAAGGCTGGGAGT	TGGACCAAAAGGAGGCTAATG
ATL	Adipose triacylglycerol lipase	<i>Atgl</i>	3.1.1.3	CGTTGGATGAAGGGCAAGACA	TGGCACAGACGGCAGAGACT
HSL	Hormone-sensitive lipase	<i>Lipe</i>	3.1.1.79	CCATAAAGCCCCATTGGCTG	CTGCTCAGACACACTCC
LPL	Lipoprotein lipase	<i>Lpl</i>	3.1.1.34	GAAGGGCTTGGAGATGTGG	TGCGCTTGGGGTTCTCT
60S acidic ribosomal protein 0 (housekeeping gene)	<i>Rplp0</i>	–	GAGCCAGCGAAGCCACACT	GATCAGCCGAAGGAGAAGG	

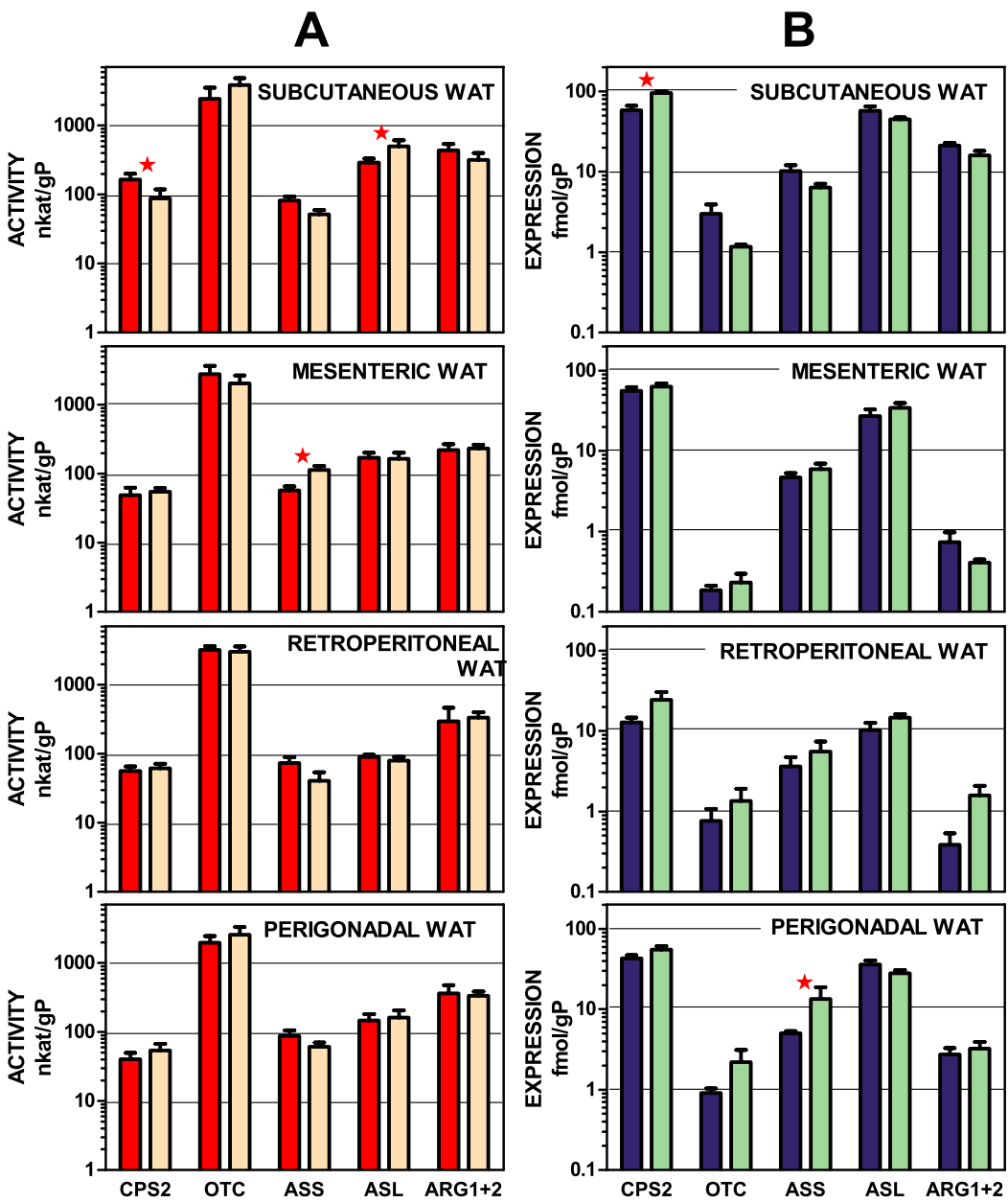


Figure 2 Urea cycle enzyme activities and expressions of their coding genes in four WAT sites of female and male rats. All data are the mean \pm sem of 6 animals, and are presented in a log scale. The numerical data are shown in Tables S1 and S2. Panels in column (A): enzyme activities, red (intense colour) columns correspond to males and orange (light colour) corresponds to female rats. (B): gene expressions, blue (intense colour) columns represent the males, and green (light colour) represents the females. CPS2, carbamoyl-P synthase 2; OTC, ornithine carbamoyl-transferase; ASS, arginino-succinate synthase; ASL, arginino-succinate lyase; ARG, arginase. Statistical analysis (2-way anova) of the differences between groups. Activity: there were no significant differences for “sex”; CPS2 and ASL showed $P < 0.0001$ for “site”. Expression: only CPS2 showed a significant ($P = 0.0002$) for “sex”: there were significant differences for “site” in CPS2 and ASL ($P < 0.0001$), OTC ($P = 0.0081$), ARG1 + 2 ($P < 0.0001$); ASS showed no significant differences. The application of post-hoc Tukey test between male/female pairs are shown in the Figure as red stars.

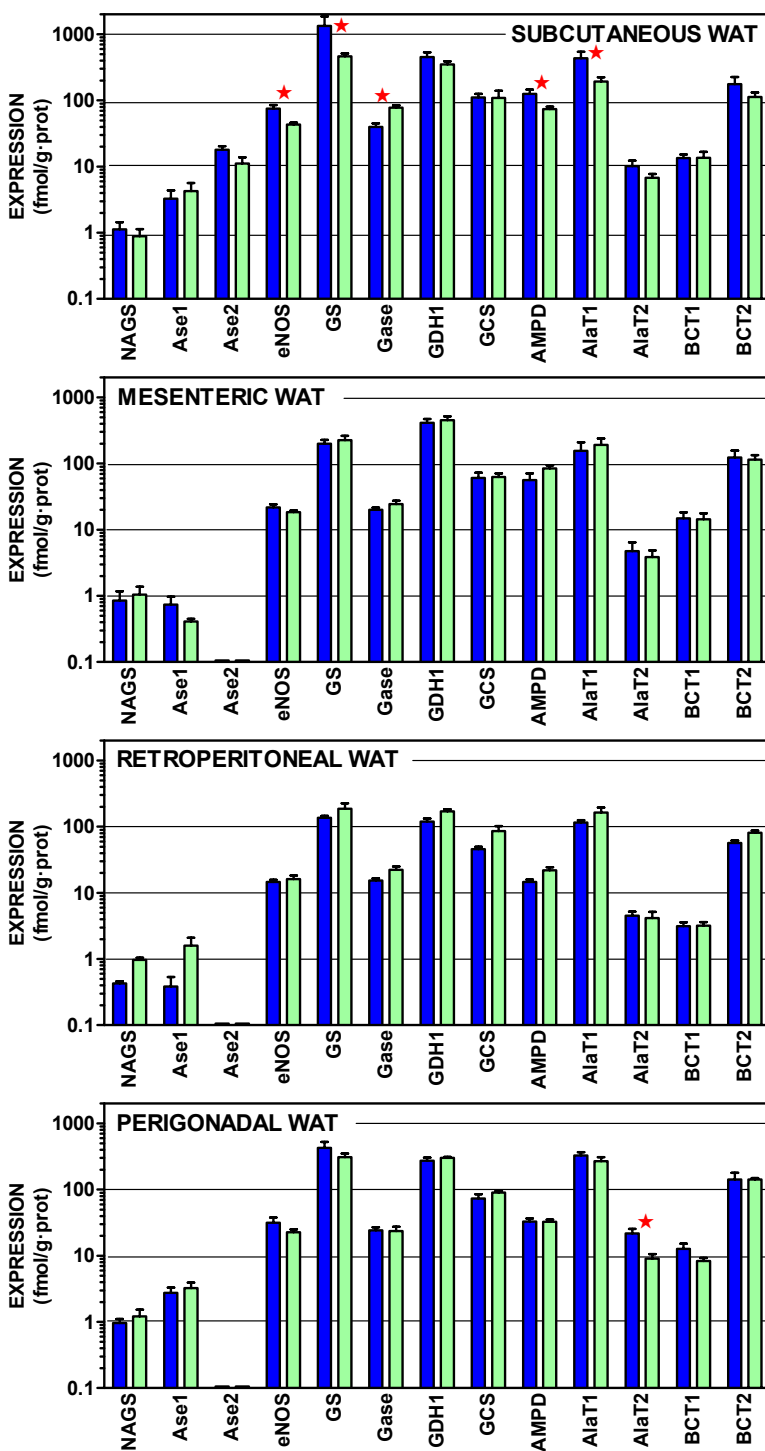


Figure 3 Expression of genes coding for enzymes of amino acid metabolism in WAT sites of male and female rats. All data are the mean \pm sem of 6 animals, and are presented in a log scale. The numerical data are shown in Table S3. Blue (dark colour) columns represent the males, and green (light colour) represents the females. NAGS, N-acetyl glutamate synthase; Ase1, arginase 1; Ase 2, Arginase 2; eNOS, endothelial nitric oxide synthase; GS, glutamine synthetase; Gase, glutaminase; GDH1, glutamate (continued on next page...)

Figure 3 (...continued)

dehydrogenase (NADPH); AMPD, AMP deaminase; AlaT1, alanine transaminase 1; AlaT2, alanine transaminase 2; BCT1, branched-chain amino acid transaminase 1; BCT2, branched-chain amino acid transaminase 2. Statistical analysis (2-way anova) of the differences between groups. The variable “sex” showed global differences for Gase ($P < 0.0001$), eNOS ($P = 0.0014$) and AlaT2 ($P = 0.0018$). The variable “site” showed significant differences for all genes ($P < 0.0001$ for eNOS, Gase, GDH1, AMPD, BCT1 and AlaT2; $P = 0.0005$ for Ase1; $P = 0.0014$ for GS; $P = 0.0023$ for AlaT1, $P = 0.024$ for BCT2, and $P = 0.039$ for GCS) except N-acetyl-glutamate synthase. The application of post-hoc Tukey test between male/female pairs are shown in the Figure as red stars between the corresponding columns.

calculated the relationships of gene expressions to total tissue RNA (a crude approximation to mRNA) only to compare the specific effect of sex on a gene expression in a given site. Any significant deviation on the proportion of a gene expression with respect to the whole RNA mass may imply a differential modulation of this expression. We included these additional data to provide further insight into the ways and means of manifestation of sex-related differences.

Statistics

Student’s *t* test (unpaired) and two-way ANOVA comparisons between groups (using the post-hoc Tukey test), correlations and curve fitting (including V_i estimations) were analyzed with the Prism 5 program (GraphPad Software, San Diego CA USA). Data were presented as mean \pm sem, and a limit of significance of $P < 0.05$ was used throughout.

RESULTS

Basic parameters

Table 2 shows the body and main adipose tissue sites weights of undisturbed female and male animals. When aged 13 weeks, female rats weighed about 62% of their male counterparts. The males accumulated more fat than females, both in individual sites and as a whole. However, the sum of the four sites analyzed showed almost identical proportions vs. body weight, c. 8%. However, there were sex-related individual site differences in relative size expressed as percentage of body weight. There were also differences in total protein and RNA proportions (per g of fresh tissue) between the different sites, but there were no global effects attributable to the variable “sex”.

The main plasma parameters studied are presented in **Table 3**. Plasma glucose levels were higher in males than in females. However, these data were influenced by isoflurane anesthesia ([Zardooz et al., 2010](#)), and are presented only as a general indication of normalcy. No differences were observed for lactate and total cholesterol. Triacylglycerol levels were significantly higher in females (albeit in the limit of statistical significance). Both plasma urea and the partial sum of amino acids were also higher in female than in male rats.

Urea cycle enzymes

Figure 2 depicts urea-cycle enzyme activities and the expression of their corresponding genes in four main WAT sites of male and female rats. In both cases, activity and gene expression, the data were presented per g of tissue protein. The data are displayed on a log

Table 2 Body and WAT site weight and composition of adult male and female Wistar rats. The data correspond to the mean \pm sem of 6 different animals. Statistical significance of the differences between groups was established with a 2-way anova; post-hoc Tukey test: an asterisk * represents $P < 0.05$ differences between sex groups. Comparison of differences between the sums of sites was done using the Student's t test.

Parameter	Unit	Site	Male	Female	p site	p sex
Body weight	g	–	373 \pm 6.1	232 \pm 8.2	–	<0.0001
		SC	12.2 \pm 0.20*	7.02 \pm 0.25		
		ME	4.94 \pm 0.49*	3.92 \pm 0.33	<0.0001	<0.0001
		PE	7.34 \pm 0.64*	4.83 \pm 0.39		
		RE	6.29 \pm 0.79*	2.79 \pm 0.35		
	% BW	Σ WAT	30.8 \pm 1.7	18.6 \pm 0.93	–	<0.0001
		SC	3.28 \pm 0.05	3.04 \pm 0.11		
		ME	1.33 \pm 0.18	1.69 \pm 0.13	<0.0001	NS
		PE	1.97 \pm 0.13	2.10 \pm 0.21		
		RE	1.69 \pm 0.22	1.22 \pm 0.17		
WAT weight	mg/g	Σ WAT	8.26 \pm 0.47	8.05 \pm 0.52	–	NS
		SC	63.1 \pm 11.6	51.8 \pm 3.3		
		ME	74.2 \pm 7.4	84.2 \pm 2.6	<0.0001	NS
		PE	44.3 \pm 1.6	54.4 \pm 2.4		
	μ g/g	RE	65.1 \pm 6.3	62.9 \pm 4.7		
		SC	248 \pm 51	219 \pm 19		
		ME	880 \pm 84	793 \pm 88	<0.0001	NS
		PE	94.3 \pm 6.0	119 \pm 10		
		RE	48.8 \pm 4.1	78.4 \pm 4.1		

Notes.

% BW, Percentage of body weight.

Table 3 Main energy plasma parameters of adult female and male Wistar rats. The data correspond to the mean \pm sem of 6 different animals. Statistical significance of the differences between groups was established with the unpaired Student's t test.

Parameter	Units	Male	Female	P sex
Glucose	mM	10.20 \pm 0.42	8.64 \pm 0.34	0.0169
Lactate	mM	3.10 \pm 0.29	3.78 \pm 0.24	NS
Total cholesterol	mM	1.97 \pm 0.07	1.98 \pm 0.16	NS
Triacylglycerols	mM	1.50 \pm 0.06	1.69 \pm 0.06	0.0491
Urea	mM	3.90 \pm 0.17	5.13 \pm 0.25	0.0029
Amino acids ^a	mM	3.34 \pm 0.08	3.96 \pm 0.18	0.0104

Notes.

^a This value does not include Gln, Asn, Trp and Cys.

scale to allow a visual comparison of the site patterns of enzyme activities and expressions. The data used in this representation are also tabulated in numeric form in Tables S1 and S2. There was a considerable coincidence in the patterns of enzyme activity distribution (and male–female similarities) in enzyme activities for all four sites. This pattern was not paralleled by that of the corresponding gene expression data, which also showed

considerable uniformity in their patterns across the WAT sites. The statistical analysis of the data in Fig. 2 showed significant differences for “site” for all enzyme expressions except for arginino-succinate synthase. The site-related differences in enzyme activities, however, were limited to arginino-succinate lyase and carbamoyl-P synthase.

Subcutaneous WAT showed more differences between sexes than other locations, affecting carbamoyl-P synthase 2 (both activity and gene expression) and arginino-succinate lyase (only activity). Arginino-succinate synthase activity showed differences between females and males in mesenteric WAT, and its higher expression was observed in periovaric WAT.

Other amino acid metabolism-related gene expressions

Figure 3 shows the gene expressions of the non-urea cycle enzymes presented in Fig. 1, as well as differentiated arginases 1 and 2, which were combined in Fig. 2. The data are depicted also on a log scale to facilitate pattern comparison; the corresponding numerical results are shown in Table S3.

In all sites, the expression of e-NOS was, at least one order of magnitude higher than arginase; subcutaneous WAT being an exception: despite showing a similar pattern of expressions, the levels of mRNA per g of tissue protein were higher for most genes, in subcutaneous WAT, than in the other three sites. There was a generalized predominance of glutamine synthetase expression over that of glutaminase. The glycine cleavage system (specifically the H protein of the complex) and AMP deaminase showed also a robust expression, at levels comparable to those of alanine transaminases. The two branched-chain amino acid transaminases were also within this range, but the expression of the form 2 was much higher.

The statistical comparisons of the data in Fig. 3 present limited effects for sex; overall only nitric oxide synthase, alanine transaminase 2 and glutaminase showed significant overall differences between female and male rats. Paired sex-related differences were concentrated in subcutaneous WAT, with higher male values in the expression of nitric oxide synthase, glutamine synthase (but female-predominant glutaminase), AMP deaminase and alanine transaminase 1. No sex-related differences were found in the other sites, except higher male values in alanine transaminase 2 of perigonadal WAT. The differences between sites, however, were more marked, affecting all genes studied except N-acetyl-glutamate synthase (low expression) and arginase 2, which was expressed only in subcutaneous WAT.

Gene expressions of proteins involved in WAT acyl-glycerol metabolism

Figure 4 presents the gene expressions of the key transporter and enzymes that regulate the lipogenic process from glucose to acetyl-CoA and from that metabolite to acyl-CoA, including the three most important WAT lipases. The data are presented in a log scale and the numerical data are shown in Table S4. In spite of a considerable uniformity in the patterns for all four sites, there were marked differences in the extent of gene expression. In general, subcutaneous WAT values were higher, than those of the other sites. Again,

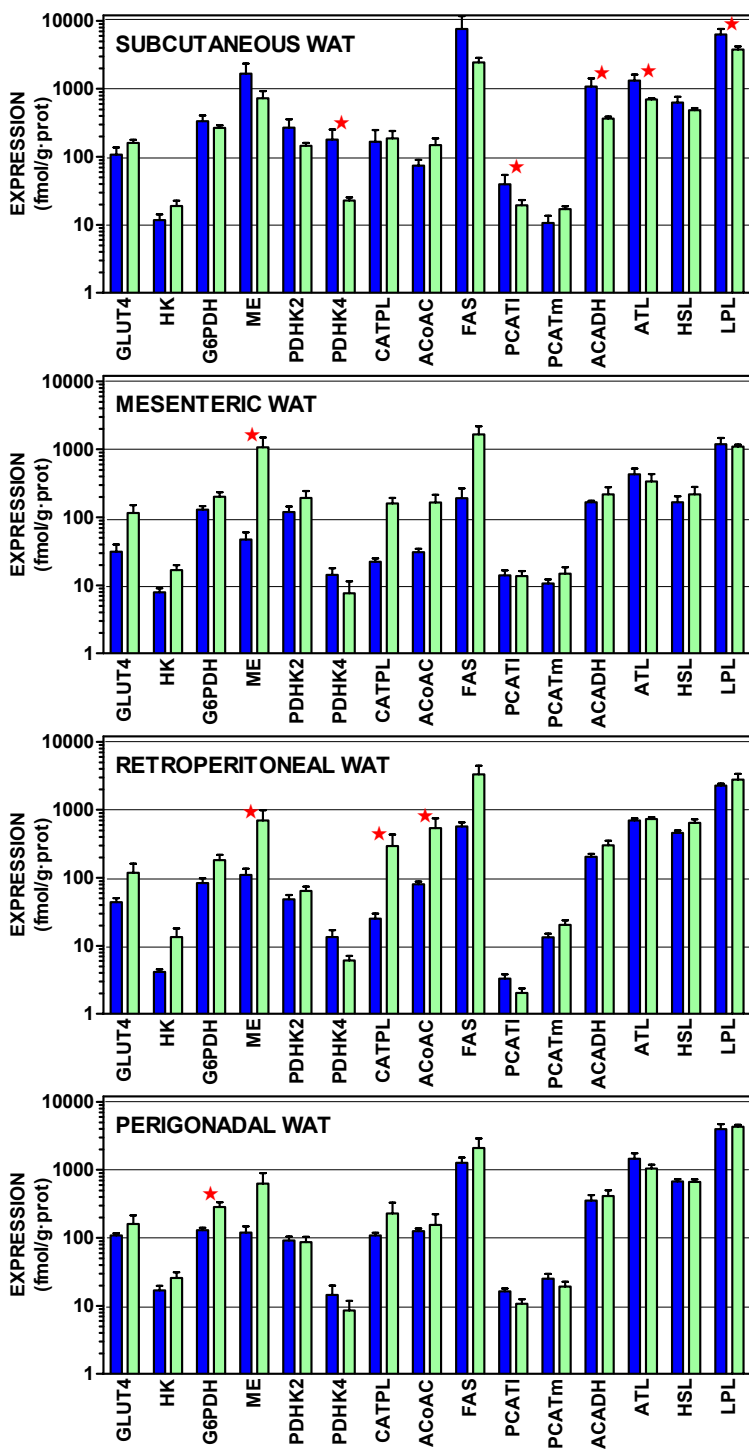


Figure 4 Expression of genes coding for transporter and enzymes related to lipogenesis from glucose and catabolism of lipid stores in WAT sites of male and female rats. All data are the mean \pm sem of 6 animals, and are presented in a log scale. The numerical data are shown in Table S4. Blue (dark colour) columns represent the males, and green (light colour) represents the females. GLUT4, glucose transpoirter 4; HK, hexokinase; G6PDH, glucose-6P dehydrogenase; ME, malic enzyme; (continued on next page...)

Figure 4 (...continued)

PDHK2, pyruvate dehydrogenase kinase 2; PDHK4, pyruvate dehydrogenase kinase 4; CATPL, citrate: ATP lyase; AcCoAC, acetyl-CoA carboxylase; FAS, fatty acid synthase; PCATl, palmitoleoyl-carnitine acyl-transferase (liver); PCATm, palmitoleoyl-carnitine acyl-transferase (muscle); AcADH, acyl-CoA dehydrogenase; ATL, adipose triacylglycerol lipase; HSL, hormone-sensitive lipase; LPL, lipoprotein lipase. Statistical analysis (2-way anova) of the differences between groups. The variable “sex” showed global differences for HK ($P = 0.0009$), AcCoAC ($P = 0.0035$), GLUT4 ($P = 0.0040$), CATPL ($P = 0.010$), G6PDH ($P = 0.020$), PHDK4 ($P = 0.020$), ME ($P = 0.024$) and ATL ($P = 0.026$). The variable “site” showed significant differences for HSL, ATL and LPL ($P < 0.0001$), PCATl ($P = 0.0004$), G6PDH ($P = 0.0005$), PDHK2 ($P = 0.0013$). PDHK4 ($P = 0.0016$), ACADH (0.0022), HK ($P = 0.0057$), PCATm ($P = 0.015$) and AcCoAC ($P = 0.0384$). The application of post-hoc Tukey test between male/female pairs are shown in the Figure as red stars ($P < 0.05$).

overall (for mesenteric, retroperitoneal and perigonadal WAT), female expression values tended to be higher than those of the males for genes coding proteins favoring glucose incorporation (GLUT4, hexokinase), generation of NADPH (glucose-6P dehydrogenase, malic enzyme), and lipogenesis (citrate: ATP lyase, and acetyl-CoA carboxylase). Regulation of pyruvate dehydrogenase by its inhibiting kinases was higher in males, suggesting a lower mitochondrial availability of acetyl-CoA. In males, mitochondrial handling of fatty acids (carnitine palmitoleoyl-transferases, acyl-CoA dehydrogenases) and lipolysis (except adipose triacylglycerol lipase) showed higher relative expressions than in females.

Subcutaneous WAT showed higher expression values for males in pyruvate dehydrogenase kinase 4, palmitoleoyl.carnitine acyl-transferase (liver), acyl-CoA dehydrogenase and both lipoprotein and adipose triacylglycerol lipases. In mesenteric WAT, the only significant difference was for higher malic enzyme expression in females. In retroperitoneal WAT, female expression values were higher for malic enzyme, citrate: ATP lyase and acetyl-CoA carboxylase. Again, in perigonadal WAT, female expression values were higher for glucose-6P dehydrogenase. The overall differences for “site” were significant for all genes investigated except for GLUT4, malic enzyme, citrate: ATP lyase and fatty acid synthase.

Comparison of female and male gene expression

Table 4 summarizes the sex-related differences in gene expression. The data are presented in two cooperative forms: expression per unit of protein and per unit of RNA weight in the tissue. The corresponding numerical data for RNA data and complete statistical analysis are shown on **Table S5**. **Table 4** shows only the cases where female–male differences were significant, and the genes are divided in four sections. In the first, corresponding to urea-cycle enzymes, only carbamoyl-P synthase 2 of subcutaneous WAT showed higher female than male values. No other differences were seen. There was a high degree of superimposition between the data obtained from protein and RNA; but the number of enzymes with statistically significant between sexes was higher in most WAT sites when the data of reference was RNA than when related to tissue protein.

Other amino acid metabolism data showed a relative predominance of higher relative expressions in males, especially affecting the transaminases. The sites with more differences

Table 4 Comparison of male-female specific expression of genes in different WAT sites with respect to tissue total protein or RNA. The data are the mean \pm sem of 6 animals per group, and are expressed as fmol of the corresponding gene mRNA per g of protein or mg of total RNA. The complete numerical data Table for RNA is presented in Table S5. Only significant differences are shown. M > F represents that male data were significantly higher than those of females; F > M represented that female data were significantly higher than those of males. Analysis of significance was done using 1- and 2-way anovas (the latter for combined sites). The data in regular font correspond to significant values in the expression of fmol/mg RNA, those in italics correspond to the data which were significant only when expressed as fmol/g protein. The data in bold correspond to differences statistically significant both when referred to tissue protein and RNA.

Parameter	WAT site				All sites P
	SC	ME	PG	RP	
<i>urea cycle enzymes</i>					
Carbamoyl-P synthase 2	F > M	—	—	—	<i>F>M</i>
Ornithine carbamoyl-transferase	—	—	—	—	—
Argininosuccinate synthase	—	—	—	—	—
Argininosuccinate lyase	—	—	—	—	—
Arginase 1	—	—	—	—	—
<i>other enzymes of amino acid metabolism</i>					
N-acetyl-glutamate synthase	<i>M>F</i>	—	—	—	—
Glutamate dehydrogenase 1	—	—	—	—	—
Glutamine synthetase	<i>M>F</i>	—	—	—	<i>M>F</i>
Glutaminase	<i>F>M</i>	<i>F>M</i>	—	—	<i>F>M</i>
AMP deaminase	M > F	—	—	—	<i>M>F</i>
Glycine cleavage system	—	—	<i>F>M</i>	—	—
Alanine transaminase 1	M > F	—	—	<i>M>F</i>	<i>M>F</i>
Alanine transaminase 2	<i>M>F</i>	—	M > F	<i>M>F</i>	M > F
Branched-chain amino acid transaminase 1	—	—	<i>M>F</i>	<i>M>F</i>	<i>M>F</i>
Branched-chain amino acid transaminase 2	—	—	—	—	—
Endothelial nitric oxide synthase	M > F	—	—	<i>M>F</i>	M > F
<i>enzymes (and transporters) related with lipogenesis from glucose</i>					
Glucose transporter 4	—	—	—	<i>F>M</i>	F > M
Hexokinase 2	—	—	<i>F>M</i>	<i>F>M</i>	F > M
Glucose-6P dehydrogenase	—	<i>F>M</i>	F>M	<i>F>M</i>	F > M
Malic enzyme	—	F > M	<i>F>M</i>	F > M	F > M
Pyruvate dehydrogenase kinase 2	<i>M>F</i>	—	—	<i>M>F</i>	<i>M>F</i>
Pyruvate dehydrogenase kinase 4	M > F	—	—	<i>M>F</i>	M > F
Citrate: ATP lyase	—	<i>F>M</i>	—	F > M	F > M
Acetyl-CoA carboxylase	<i>F>M</i>	<i>F>M</i>	—	F > M	F > M
Fatty acid synthase	—	<i>F>M</i>	<i>F>M</i>	<i>F>M</i>	<i>F>M</i>

(continued on next page)

Table 4 (continued)

Parameter	WAT site				All sites P
	SC	ME	PG	RP	
enzymes (and transporters) related with lipolysis and fatty acid oxidation					
Carnitine palmitoleyl transferase (liver)	M > F	–	M>F	M>F	M>F
Carnitine palmitoleyl transferase (muscle)	–	–	–	–	M>F
Long-chain acyl-CoA dehydrogenase	M > F	F>M	–	–	M>F
Adipose tissue triacylglycerol lipase	F > F	–	–	M>F	M > F
Hormone-sensitive lipase	–	–	–	–	M>F
Lipoprotein lipase	M > F	–	–	M>F	–

were subcutaneous and retroperitoneal WAT. In contrast, lipogenesis was more highly expressed in females, with minimal effects on subcutaneous and highest in retroperitoneal WAT. Male predominance was observed again on pyruvate dehydrogenase kinases' expressions, which increase marks a lower rate of production of acetyl-CoA as substrate for acyl-CoA synthesis. Finally, in the analysis of lipolytic and lipid oxidation-related genes, the male higher values were the norm, especially in subcutaneous and retroperitoneal WAT.

DISCUSSION

The results presented support a wide extension of amino acid metabolism in different sites of WAT, with enzyme activities and expressions following similar patterns in all four sites studied. In addition to urea cycle, AMP-deaminase ([Arola et al., 1981a](#)), glutamine synthetase ([Arola et al., 1981b](#)), glutamate dehydrogenase ([Arola et al., 1979](#)) and nitric oxide synthase ([Pilon, Penfornis & Marette, 2000](#)), we found that WAT expresses the glycine cleavage system (at least the H protein), so far not described.

The metabolic capabilities of WAT with respect to amino acid metabolism are probably more extensive than usually assumed ([Alemany, 2012b](#)), largely because it is unknown, with scant literature references to WAT amino acid metabolism ([López-Soriano & Alemany, 1986](#); [Kowalski, Wu & Watford, 1997](#); [Herman et al., 2010](#); [Lackey et al., 2013](#)). The range of expressions observed for amino acid metabolism-related enzymes in the four WAT sites studied ([Figs. 2 and 3](#)) was mostly in the 5–500 fmol/g protein. In comparison, the expressions ([Fig. 4](#)) for lipogenesis, the (assumed) main metabolic function of WAT, and other lipid metabolism-related expressions were in the range of 10–1,000 fmol/g protein. Thus, the differences between lipogenesis and amino acid metabolism-related gene expressions were not as extensive as expected from the known massive mobilization/deposition of triacylglycerols in adipocytes, compared with the relatively low level of cell proteins ([Salans & Dougherty, 1971](#)) (and cytoplasm) of WAT. This is compounded by the lack of sufficient data on WAT amino acid metabolism above indicated. The relatively elevated amino acid metabolism enzyme levels and gene expressions found hint at a potential relative importance of WAT on body amino acid metabolism.

The considerable uniformity of WAT urea cycle-enzyme activities and expressions, and their marked independence of sex can be interpreted essentially in two ways: (a) as playing a minimal metabolic role: i.e., a residual, secondary or specialized pathway. Or, alternatively, (b), it can be assumed to be a consequence of a well-established and robust homeostatic maintenance of its function. That is, a role critical enough not to be sensibly influenced by external regulatory factors such as sex hormones. The first possibility may seem the more obvious, but it is insufficient to counter a number of critical arguments: first of all, the unexpectedly high level of enzyme expressions and activities. Individual urea cycle enzymes are present in many tissues, *Emmanuel (1980)*, *Nishibe (1974)*, and *Rath et al. (2014)*. However, the mere existence of a complete urea cycle in a peripheral organ outside the splanchnic bed has not been previously described, as far as we know. A full operative urea cycle has been described only for liver (*Emmanuel, 1980*). The key question is whether this cycle is functional or not. Due to its methodological difficulties, it should be studied using other (i.e., tracer) techniques. However, the relatively high enzyme activities and gene expressions observed, and the fact that all urea cycle and related ammonium metabolism enzymes are present suggest that this distribution has a clear functional purpose. This is, consequently, a situation different from that of tissues, which contain only part of the cycle to serve other metabolic purposes. The lack of sex-related differences in WAT sites of urea cycle compared with lipogenic processes, as shown in Figs. 2–4 and the remarkable uniformity in pattern distribution between WAT sites also support the functionality of WAT urea cycle.

The varying ratios of activity/expression suggest a main post-translational control, extended to all sites. The high ornithine carbamoyl-transferase *vs.* arginino-succinate synthase activities suggest a probable implication in the peripheral (and critical) synthesis of citrulline (*Yu et al., 1996*), which may complement its conversion by the kidney (*Borsook & Dubnoff, 1941*). WAT participates in substrate cycles, including alanine synthesis (*Snell & Duff, 1977*) and glutamine release (*Kowalski & Watford, 1994*) in which amino acids are implicated. This analysis is further complicated by the quantitative importance of both activity and gene expressions compared with those of lipogenesis, the mainstay of WAT metabolism. Our understanding of these differences is complicated by the overall large size of the adipose organ (*Romero et al., 2014*), even taking into account the metabolically inert mass of fat. Taken together, these arguments support a significant role of WAT in amino acid metabolism.

Our data suggest, in any case, a clear site-sex interaction (*Lemonnier, 1972*; *Jaubert et al., 1995*) that brings up differences in the expression of several amino acid metabolism-related genes other than urea cycle, which remains uncannily undisturbed and globally uniform. In males, subcutaneous WAT shows higher expressions for genes related to transfer of acyl-CoA to the mitochondria and its oxidation than females; this is consistent with the possibility of using fatty acids as energy substrate. The higher male inhibition of pyruvate dehydrogenase, by kinases, generalized to most sites, reinforces this trend. On the other side, the expression of WAT lipogenic enzyme genes (especially when expressed with respect to total RNA) was higher in females than in males. In contrast, lipases practically

did not show differences. The different female-male specific metabolic predominance in WAT sites prove that the limited changes in urea cycle, compared with lipogenesis, could not be solely a consequence of overall lack of effects of sex on WAT; but it is, instead, a specific characteristic of WAT urea cycle as compared to other metabolic pathways.

The higher lipogenic (and lower lipolytic) gene expressions of female WAT is counter-intuitive when we think of the higher WAT mass of adult male rats (*Romero et al., 2014*). Probably, the lower male gene expressions found here mirror a less active metabolism, in conjunction with the intestine and liver. The visceral fat accumulation in adult men (*Bosch et al., 2015*) as compared with women is correlated with insulin resistance (*Pascot et al., 2000*) and other metabolic syndrome-related pathologies (*Watanabe & Tochikubo, 2003*). The discordances in sex-related control of metabolism and fat deposition between humans and rats are a critical caveat against generalization to humans of what is found using animal models, in spite of shared mechanisms and trends.

In addition to the human-rodent question, the main limitation of this study is the lack of previous data with which establish comparisons, made even more difficult by our scarce knowledge of amino acid metabolism. The extensive and interconnected net of pathways needs to be investigated. The most critical handicap, however, is the lack of a critical mass of scientists and of actualized methodology: specific protein measurement reagents (antibodies), and/or methods (and products) for the estimation of enzyme activities and metabolites of amino acid metabolism. Consequently, the data we present here should be taken as just an initial foray into a highly promising field of study.

An additional question may help explain the differences between sites (*Lemonnier, 1972*; *Rydén et al., 2014*), and the influence of sex (and sex hormones), the differences in cell populations of different WAT sites. A factor that affects the mean adipocyte size (also influenced by obesity (*Garaulet et al., 2006*)) and the presence of other types of cells, in different proportions, such as macrophages (*Králová Lesná et al., 2015*), stem cells (*Ogura et al., 2014*) and other stromal components (*Maumus et al., 2011*).

Notwithstanding these caveats, the data gathered all point to a few preliminary conclusions, which could not be yet fully proven with the data we presented, largely because no other results are available for comparison or independent confirmation. The potential for lipid handling of WAT sites was strongly modulated by sex, being considerably dependent on the site studied. This part of the study, devised to provide a background comparison for amino acid metabolism showed more extensive differences than expected, and needs to be studied more specifically and deeply before sufficiently based conclusions could be extracted.

There was a considerable stability of the urea cycle activities and expressions, irrespective of sex, and with only limited influence of site. Which we interpret as this cycle operation being more general than the specialized site metabolic peculiarities, with robust control of WAT urea cycle, probably related to a possible role as provider of arginine/ citrulline (*Beliveau Carey et al., 1993*). The resilience to change of urea cycle, in the context of a tissue characterized by its plastic adaptability, supports a generalized, probably essential, role in overall amino N handling.

In contrast, sex affected deeply WAT ammonium-centered amino N metabolism in a site-related fashion, with relatively higher levels of activity in males and in female subcutaneous WAT. The data on amino acid catabolism fit also with a role of mesenteric WAT as gatekeeper of the portal system, the hypothesis advanced for WAT glucose disposal ([Arriarán et al., 2015](#)) can be easily translated to the management of possible transient excesses of dietary amino acids.

In sum, WAT seems to play significant role in overall amino acid metabolism, including a functional urea cycle, which is not affected by sex. Contrary to lipid/glucose-related pathways, the data presented point to a centralized control of urea cycle operation affecting the adipose organ as a whole.

ADDITIONAL INFORMATION AND DECLARATIONS

Funding

This work was funded by the Plan Nacional de Ciencia y Tecnología de los Alimentos (AGL-2011-23635) of the Government of Spain and Plan Nacional de Investigación en Biomedicina (SAF2012-34895) of the Government of Spain. CIBER-OBN Research Web, Barcelona, Spain. Silvia Agnelli was the recipient of a Leonardo da Vinci fellowship. Sofía Arriarán had a predoctoral fellowship of the Catalan Government. The funders had no role in study design, data collection and analysis, decision to publish, or preparation of the manuscript.

Grant Disclosures

The following grant information was disclosed by the authors:

Plan Nacional de Ciencia y Tecnología de los Alimentos: AGL-2011-23635.

Plan Nacional de Investigación en Biomedicina: SAF2012-34895.

CIBER-OBN Research Web.

Competing Interests

The authors declare there are no competing interests.

Author Contributions

- Sofía Arriarán performed the experiments, analyzed the data, prepared figures and/or tables, reviewed drafts of the paper.
- Silvia Agnelli performed the experiments.
- Xavier Remesar analyzed the data, contributed reagents/materials/analysis tools, reviewed drafts of the paper.
- José Antonio Fernández-López analyzed the data, prepared figures and/or tables, reviewed drafts of the paper.
- Marià Alemany conceived and designed the experiments, wrote the paper, prepared figures and/or tables, reviewed drafts of the paper.

Animal Ethics

The following information was supplied relating to ethical approvals (i.e., approving body and any reference numbers):

Committee on Animal Experimentation of the University of Barcelona, Authorization: DMAH-5484

Data Availability

The following information was supplied regarding data availability:

University of Barcelona, CRAI Repository;
<http://hdl.handle.net/2445/66872>.

Supplemental Information

Supplemental information for this article can be found online at <http://dx.doi.org/10.7717/peerj.1399#supplemental-information>.

REFERENCES

- Alemany M. 2012a. Do the interactions between glucocorticoids and sex hormones regulate the development of the metabolic syndrome? *Frontiers in Endocrinology* 3 DOI 10.3389/fendo.2012.00027.
- Alemany M. 2012b. The problem of nitrogen disposal in the obese. *Nutrition Research Reviews* 25:18–28 DOI 10.1017/S0954422411000163.
- Antonio L, Wu FCW, O'Neill TW, Pye SR, Carter EL, Finn JD, Rutter MK, Laurent MR, Huhtaniemi IT, Han TS, Lean MEJ, Keevil BG, Pendleton N, Rastrelli G, Forti G, Bartfai G, Casanueva FF, Kula K, Punab M, Giwercman A, Claessens F, Decallonne B, Vanderschueren D. 2015. Associations between sex steroids and the development of metabolic syndrome: a longitudinal study in European men. *Journal of Clinical Endocrinology and Metabolism* 100:1396–1404 DOI 10.1210/jc.2014-4184.
- Arola L, Herrera E, Alemany M. 1977. A new method for deproteinization of small samples of blood plasma for amino acid determination. *Analytical Biochemistry* 82:236–239 DOI 10.1016/0003-2697(77)90153-1.
- Arola L, Palou A, Remesar X, Alemany M. 1979. NADH and NADPH dependent glutamate dehydrogenase activities in the organs of the rat. *IRCS Medical Science* 7:364–364.
- Arola L, Palou A, Remesar X, Alemany M. 1981a. Adenylate deaminase activity in the rat—effect of 24 hours of fasting. *Hormone and Metabolic Research* 13:264–266 DOI 10.1055/s-2007-1019240.
- Arola L, Palou A, Remesar X, Alemany M. 1981b. Glutamine-synthetase activity in the organs of fed and 24-hours fasted rats. *Hormone and Metabolic Research* 13:199–202 DOI 10.1055/s-2007-1019220.
- Arriarán S, Agnelli S, Fernández-López JA, Remesar X, Alemany M. 2012. A radiochemical method for carbamoyl-phosphate synthetase-I: application to rats fed a hyperproteic diet. *Journal of Enzyme Research* 3:29–33.
- Arriarán S, Agnelli S, Sabater D, Remesar X, Fernández-López JA, Alemany M. 2015. Evidences of basal lactate production in the main white adipose tissue sites of rats. Effects of sex and a cafeteria diet. *PLoS ONE* 10:e0119572 DOI 10.1371/journal.pone.0119572.

- Beliveau Carey G, Cheung CW, Cohen NS, Brusilow S, Rajzman L.** 1993. Regulation of urea and citrulline synthesis under physiological conditions. *Biochemical Journal* **292**:241–247 DOI [10.1042/bj2920241](https://doi.org/10.1042/bj2920241).
- Borsook H, Dubnoff JW.** 1941. The conversion of citrulline to arginine in kidney. *Journal of Biological Chemistry* **141**:717–738.
- Bosch TA, Steinberger J, Sinaiko AR, Moran A, Jacobs DR, Kelly AS, Dengel DR.** 2015. Identification of sex-specific thresholds for accumulation of visceral adipose tissue in adults. *Obesity* **23**:375–382 DOI [10.1002/oby.20961](https://doi.org/10.1002/oby.20961).
- Bryzgalova G, Lundholm L, Portwood N, Gustafsson JA, Khan A, Efendic S, Dahlman-Wright K.** 2008. Mechanisms of antidiabetogenic and body weight-lowering effects of estrogen in high-fat diet-fed mice. *American Journal of Physiology* **295**:E904–E912 DOI [10.1152/ajpendo.90248.2008](https://doi.org/10.1152/ajpendo.90248.2008).
- Cagnacci A, Zanin R, Cannella M, Generali M, Caretto S, Volpe A.** 2007. Menopause, estrogens, progestins, or their combination on body weight and anthropometric measures. *Fertility and Sterility* **88**:1603–1608 DOI [10.1016/j.fertnstert.2007.01.039](https://doi.org/10.1016/j.fertnstert.2007.01.039).
- Carmean CM, Cohen RN, Brady MJ.** 2014. Systemic regulation of adipose metabolism. *Biochimica et Biophysica Acta* **1842**:424–430 DOI [10.1016/j.bbadi.2013.06.004](https://doi.org/10.1016/j.bbadi.2013.06.004).
- Caspar-Bauguil S, Cousin B, Galinier A, Segafredo C, Nibbelink M, Andre A, Casteilla L, Pénicaud L.** 2005. Adipose tissues as an ancestral immune organ: site-specific change in obesity. *FEBS Letters* **579**:3487–3492 DOI [10.1016/j.febslet.2005.05.031](https://doi.org/10.1016/j.febslet.2005.05.031).
- D'Eon TM, Souza SC, Aronovitz M, Obin MS, Fried SK, Greenberg AS.** 2005. Estrogen regulation of adiposity and fuel partitioning. Evidence of genomic and non-genomic regulation of lipogenic and oxidative pathways. *Journal of Biological Chemistry* **280**:35983–35991 DOI [10.1074/jbc.M507339200](https://doi.org/10.1074/jbc.M507339200).
- Demerath EW, Sun SS, Rogers N, Lee MY, Reed D, Choh AC, Couch W, Czerwinski SA, Chumlea WC, Siervogel RM, Towne B.** 2007. Anatomical patterning of visceral adipose tissue: race, sex, and age variation. *Obesity* **15**:2984–2993 DOI [10.1038/oby.2007.356](https://doi.org/10.1038/oby.2007.356).
- Eagni E, Viganò M, Rebulla P, Giordano R, Lazzari L.** 2013. What is beyond qRT-PCR study on mesenchymal stem cell differentiation properties: how to choose the most reliable housekeeping genes. *Journal of Cellular and Molecular Medicine* **17**:168–180 DOI [10.1111/j.1582-4934.2012.01660.x](https://doi.org/10.1111/j.1582-4934.2012.01660.x).
- Emmanuel B.** 1980. Urea cycle enzymes in tissues (liver, rumen epithelium, heart, kidney, lung and spleen of sheep (*Ovis aries*). *Comparative Biochemistry and Physiology* **65B**:693–697.
- Eringa EC, Bakker W, Van Hinsbergh VWM.** 2012. Paracrine regulation of vascular tone, inflammation and insulin sensitivity by perivascular adipose tissue. *Vascular Pharmacology* **56**:204–209 DOI [10.1016/j.vph.2012.02.003](https://doi.org/10.1016/j.vph.2012.02.003).
- Ferrante AW.** 2013. The immune cells in adipose tissue. *Diabetes Obesity and Metabolism* **15**:34–38 DOI [10.1111/dom.12154](https://doi.org/10.1111/dom.12154).
- Galic S, Oakhill JS, Steinberg GR.** 2010. Adipose tissue as an endocrine organ. *Molecular and Cellular Endocrinology* **316**:129–139 DOI [10.1016/j.mce.2009.08.018](https://doi.org/10.1016/j.mce.2009.08.018).
- Garaulet M, Hernandez-Morante JJ, Lujan J, Tebar FJ, Zamora S.** 2006. Relationship between fat cell size and number and fatty acid composition in adipose tissue from different fat depots in overweight/obese humans. *International Journal of Obesity* **30**:899–905 DOI [10.1038/sj.ijo.0803219](https://doi.org/10.1038/sj.ijo.0803219).
- Gil A, Olza J, Gil-Campos M, Gomez-Llorente C, Aguilera CM.** 2011. Is adipose tissue metabolically different at different sites? *International Journal of Pediatric Obesity* **6**:13–20 DOI [10.3109/17477166.2011.604326](https://doi.org/10.3109/17477166.2011.604326).

- Giordano A, Smorlesi A, Frontini A, Barbatelli G, Cinti S.** 2014. White, brown and pink adipocytes: the extraordinary plasticity of the adipose organ. *European Journal of Endocrinology* 170:R159–R171 DOI 10.1530/EJE-13-0945.
- Gowda GAN, Gowda YN, Raftery D.** 2015. Massive glutamine cyclization to pyroglutamic acid in human serum discovered using NMR spectroscopy. *Analytical Chemistry* 87:3800–3805 DOI 10.1021/ac504435b.
- Griggs RC, Kingston W, Jozefowicz RF, Herr BE, Forbes G, Halliday D.** 1989. Effect of testosterone on muscle mass and muscle protein synthesis. *Journal of Applied Physiology* 66:498–503.
- Herman MA, She PX, Peroni OD, Lynch CJ, Kahn BB.** 2010. Adipose tissue branched chain amino acid (BCAA) metabolism modulates circulating BCAA levels. *Journal of Biological Chemistry* 285:11348–11356 DOI 10.1074/jbc.M109.075184.
- Jaubert AM, Pecquery R, Dieudonné MN, Giudicelli Y.** 1995. Estrogen binding sites in hamster white adipose tissue: sex- and site-related variations; modulation by testosterone. *General and Comparative Endocrinology* 2:179–187 DOI 10.1006/gcen.1995.1147.
- Jensen MD.** 2007. Adipose tissue metabolism—an aspect we should not neglect? *Hormone and Metabolic Research* 39:722–725 DOI 10.1055/s-2007-990274.
- Kotani K, Tokunaga K, Fujioka S, Kobatake T, Keno Y, Yoshida S, Shimomura I, Tarui S, Matsuzawa Y.** 1994. Sexual dimorphism of age-related-changes in whole-body fat distribution in the obese. *International Journal of Obesity* 18:207–212.
- Kowalski TJ, Watford M.** 1994. Production of glutamine and utilization of glutamate by rat subcutaneous adipose tissue *in vivo*. *American Journal of Physiology* 266:E151–E154.
- Kowalski TJ, Wu GY, Watford M.** 1997. Rat adipose tissue amino acid metabolism *in vivo* as assessed by microdialysis and arteriovenous techniques. *American Journal of Physiology* 273:E613–E622.
- Králová Lesná I, Poledne R, Fronek J, Králová A, Sekerková A, Thieme F, Pitha J.** 2015. Macrophage subsets in the adipose tissue could be modified by sex and the reproductive age of women. *Atherosclerosis* 241:255–258 DOI 10.1016/j.atherosclerosis.2015.03.018.
- Kumar A, Ruan M, Clifton K, Syed F, Khosla S, Oursler MJ.** 2012. TGF- β mediates suppression of adipogenesis by estradiol through connective tissue growth factor induction. *Endocrinology* 153:254–263 DOI 10.1210/en.2011-1169.
- Lackey DE, Lynch CJ, Olson KC, Mostaedi R, Ali M, Smith WH, Karpe F, Humphreys S, Bedinger DH, Dunn TN, Thomas AP, Oort PJ, Kieffer DA, Amin R, Bettaieb A, Haj FG, Permana P, Anthony TG, Adams SH.** 2013. Regulation of adipose branched-chain amino acid catabolism enzyme expression and cross-adipose amino acid flux in human obesity. *American Journal of Physiology* 304:E1175–E1187 DOI 10.1152/ajpendo.00630.2012.
- Lemonnier D.** 1972. Effect of age, sex, and site on the cellularity of the adipose tissue in mice and rats rendered obese by a high-fat diet. *Journal of Clinical Investigation* 51:2907–2915 DOI 10.1172/JCI107115.
- López-Soriano FJ, Alemany M.** 1986. Amino acid metabolism enzyme activities in rat white adipose tissue. *Archives Internationales de Physiologie et Biochimie* 94:121–125 DOI 10.3109/13813458609071409.
- Lowry OH, Rosebrough RW, Farr AL, Randall RJ.** 1951. Protein measurement with the Folin phenol reagent. *Journal of Biological Chemistry* 193:265–275.
- Maumus M, Peyrafitte JA, D'Angelo R, Fournier-Wirth C, Bouloumié A, Casteilla L, Sengenès C, Bourin P.** 2011. Native human adipose stromal cells: localization, morphology and phenotype. *International Journal of Obesity* 35:1141–1153 DOI 10.1038/ijo.2010.269.

- Mayes JS, Watson GH.** 2004. Direct effects of sex steroid hormones on adipose tissues and obesity. *Obesity Reviews* 5:197–216 DOI [10.1111/j.1467-789X.2004.00152.x](https://doi.org/10.1111/j.1467-789X.2004.00152.x).
- Meyer MR, Clegg DJ, Prossnitz ER, Barton M.** 2011. Obesity, insulin resistance and diabetes: sex differences and role of oestrogen receptors. *Acta Physiologica* 203:259–269 DOI [10.1111/j.1748-1716.2010.02237.x](https://doi.org/10.1111/j.1748-1716.2010.02237.x).
- Nishibe H.** 1974. Urea cycle enzymes in human erythrocytes. *Clinica Chimica Acta* 50:305–310 DOI [10.1016/0009-8981\(74\)90147-8](https://doi.org/10.1016/0009-8981(74)90147-8).
- Ogura F, Wakao S, Kuroda Y, Tsuchiyama K, Bagheri M, Heneidi S, Chazenbalk G, Aiba S, Dezawa M.** 2014. Human adipose tissue possesses a unique population of pluripotent stem cells with nontumorigenic and low telomerase activities: potential implications in regenerative medicine. *Stem Cells and Development* 23:717–728 DOI [10.1089/scd.2013.0473](https://doi.org/10.1089/scd.2013.0473).
- Pascot A, Després JP, Lemieux I, Bergeron J, Nadeau A, Prid'homme D, Tremblay A, Lemieux S.** 2000. Contribution of visceral obesity to the deterioration of the metabolic risk profile in men with impaired glucose tolerance. *Diabetologia* 43:1126–1135 DOI [10.1007/s001250051503](https://doi.org/10.1007/s001250051503).
- Pilon G, Penfornis P, Marette A.** 2000. Nitric oxide production by adipocytes: a role in the pathogenesis of insulin resistance? *Hormone and Metabolic Research* 32:480–484 DOI [10.1055/s-2007-978674](https://doi.org/10.1055/s-2007-978674).
- Porter MH, Fine JB, Cutchins AG, Bai YH, DiGirolamo M.** 2004. Sexual dimorphism in the response of adipose mass and cellularity to graded caloric restriction. *Obesity Research* 12:131–140 DOI [10.1038/oby.2004.18](https://doi.org/10.1038/oby.2004.18).
- Prunet-Marcassus B, Cousin B, Caton D, André M, Pénicaud L, Casteilla L.** 2006. From heterogeneity to plasticity in adipose tissues: site-specific differences. *Experimental Cell Research* 312:727–736 DOI [10.1016/j.yexcr.2005.11.021](https://doi.org/10.1016/j.yexcr.2005.11.021).
- Radcliffe JD, Webster AJF.** 1978. Sex, body composition and regulation of food intake during growth in the Zucker rat. *British Journal of Nutrition* 39:483–492 DOI [10.1079/BJN19780064](https://doi.org/10.1079/BJN19780064).
- Rath M, Muller I, Kropf P, Closs EI, Munder M.** 2014. Metabolism via arginase or nitric oxide synthase: two competing arginine pathways in macrophages. *Frontiers in Immunology* 5:Article 532 DOI [10.3389/fimmu.2014.00532](https://doi.org/10.3389/fimmu.2014.00532).
- Revelo X, Luck H, Winer S, Winer D.** 2014. Morphological and inflammatory changes in visceral adipose tissue during obesity. *Endocrine Pathology* 25:93–101 DOI [10.1007/s12022-013-9288-1](https://doi.org/10.1007/s12022-013-9288-1).
- Romacho T, Elsen M, Rohrborn D, Eckel J.** 2014. Adipose tissue and its role in organ crosstalk. *Acta Physiologica* 210:733–753 DOI [10.1111/apha.12246](https://doi.org/10.1111/apha.12246).
- Romero MM, Grasa MM, Esteve M, Fernández-López JA, Alemany M.** 2007. Semiquantitative RT -PCR measurement of gene expression in rat tissues including a correction for varying cell size and number. *Nutrition and Metabolism* 4:Article 26 DOI [10.1186/1743-7075-4-26](https://doi.org/10.1186/1743-7075-4-26).
- Romero MM, Roy S, Pouillot K, Feito M, Esteve M, Grasa MM, Fernández-López JA, Alemany M, Remesar X.** 2014. Treatment of rats with a self-selected hyperlipidic diet, increases the lipid content of the main adipose tissue sites in a proportion similar to that of the lipids in the rest of organs and tissues. *PLoS ONE* 9:e90995 DOI [10.1371/journal.pone.0090995](https://doi.org/10.1371/journal.pone.0090995).
- Rydén M, Andersson DP, Bergström IB, Arner P.** 2014. Adipose tissue and metabolic alterations: regional differences in fat cell size and number matter, but differently: a cross-sectional study. *Journal of Clinical Endocrinology and Metabolism* 99:E1870–E1876 DOI [10.1210/jc.2014-1526](https://doi.org/10.1210/jc.2014-1526).
- Salans LB, Dougherty JW.** 1971. The effect of insulin upon glucose metabolism by adipose cells of different size. Influence of cell lipid and protein content, age, and nutritional state. *Journal of Clinical Investigation* 50:1399–1410 DOI [10.1172/JCI106623](https://doi.org/10.1172/JCI106623).

- Snell K, Duff DA.** 1977. Alanine release by rat adipose tissue *in vitro*. *Biochemical and Biophysical Research Communications* **77**:925–931 DOI [10.1016/S0006-291X\(77\)80066-1](https://doi.org/10.1016/S0006-291X(77)80066-1).
- Stubbins RE, Najjar K, Holcomb VB, Hong J, Núñez NP.** 2012. Oestrogen alters adipocyte biology and protects female mice from adipocyte inflammation and insulin resistance. *Diabetes Obesity and Metabolism* **14**:58–66 DOI [10.1111/j.1463-1326.2011.01488.x](https://doi.org/10.1111/j.1463-1326.2011.01488.x).
- Ventura G, Noirez P, Breuille D, Godin JP, Pinaud S, Cleroux M, Choisy C, le Plenier S, Basic V, Neveux N, Cynober L, Moinard C.** 2013. Effect of citrulline on muscle functions during moderate dietary restriction in healthy adult rats. *Amino Acids* **45**:1123–1131 DOI [10.1007/s00726-013-1564-3](https://doi.org/10.1007/s00726-013-1564-3).
- Watanabe J, Tochikubo O.** 2003. Relationship between visceral fat accumulation and hypertension in obese men. *Clinical and Experimental Hypertension* **25**:199–208 DOI [10.1081/CEH-120019152](https://doi.org/10.1081/CEH-120019152).
- Yu YM, Burke JF, Tompkins RG, Martin R, Young VR.** 1996. Quantitative aspects of interorgan relationships among arginine and citrulline metabolism. *American Journal of Physiology* **271**:E1098–E1109.
- Zardooz H, Rostamkhani F, Zaringhalam J, Shahrivar FF.** 2010. Plasma corticosterone, insulin and glucose changes induced by brief exposure to isoflurane, diethyl ether and CO₂ in male rats. *Physiological Research* **59**:973–978.

SUPPLEMENTAL MATERIAL

SUPPLEMENTAL METHODS

Measurement of urea cycle enzyme activities

Ornithine carbamoyl transferase activity was measured from the reaction of condensation of carbamoyl-P and 14C-ornithine to yield 14C-citrulline. Aliquots of 25 µL of homogenates were mixed with 50 µL of 70 mM hepes buffer pH 7.4 containing carbamoyl-P, ornithine (all from Sigma), and 14C-ornithine (Perkin-Elmer); final concentrations were 9 mM, 13 mM and 1 kBq/mL, respectively. The reaction was started with the homogenate, and was carried out at 37°C. Aliquots of 75 µL were introduced in tubes containing 100 µL of chilled acetone, in ice, at 0, 0.5, 1 and 2 min. The tubes were later centrifuged to obtain clear supernatants; they were dried in a vacuum-centrifuge (Thermo Scientific, Waltham, MA USA). The dry residues were dissolved in 25 µL of pure water; they were applied to silicagel TLC plates (200 µm; Macherey-Nagel, Düren, Germany), etched vertically to define 1 cm wide lanes to prevent sample overlapping. Standards of ornithine and citrulline were included each plate. The plates were developed with a mobile phase of trichloromethane: methanol: acetic acid (1:2:2 by volume). After drying, the lane with non-labelled standards was sprayed with ninhydrin, and heated with a hair dryer. The ornithine and citrulline spots were marked and the plate was cut in horizontal zones, which were counted. To limit interferences, the label in the citrulline area was expressed as a percentage of the total label counted in each TLC lane. These data allowed the calculation of newly formed citrulline; the Vi value for each sample was plotted, and considered to be an expression of V_{max} under the conditions tested.

Arginino-succinate synthase activity was measured from the condensation of aspartate with citrulline in the presence of ATP to yield argininosuccinate. Aliquots of 55 µL of homogenates were mixed with 30 µL of 70 mM hepes buffer pH 7.4, containing ATP-Na₂, MgCl₂, citrulline, aspartate (all from Sigma); final concentrations were 10 mM, 5 mM, 3 mM, and 2.5 mM, respectively. The reaction was started with aspartate, and was carried out at 37°C. The reaction was stopped with 40 µL of 30 g/L perchloric acid. The tubes were vortexed and immediately neutralized (pH 7-8) with 10 µL of 100 g/L KOH containing 62 g/L potassium bicarbonate. The tubes were vortexed again and centrifuged at 8,000xg for 15 min and 4°C. The aspartate remaining in the supernatants was measured (by transamination to oxaloacetate, and then reduced by malate dehydrogenase and NADH). Briefly, 20 µL of the supernatants were brought up to 300 µL in 96-well plates, with 66 mM phosphate buffer pH 7.4 containing NADH, 2-oxoglutarate, aspartate transaminase (pig heart) and malic acid dehydrogenase (pig heart) (all from Sigma); final concentrations were, respectively, 0.25 mM, 0.2 mM, 20 nkatal/ml and 17 nkatal/ml. The samples were read at 340 nM in a plate reader (Biotek, Winoosky, VT USA) for 30 min at intervals of 30 s. The fall in NADH was used to determine the levels of aspartate at each incubation time. Its disappearance

(versus time zero levels) was used to determine the amount of aspartate incorporated into argininosuccinate. As in the case of ornithine carbamoyl transferase, the Vi values were plotted for each sample. In all series, a number of samples were analyzed with all reagents except citrulline: No spurious consumption of aspartate was observed

The activity of argininosuccinate synthase was measured from the breakup of argininosuccinate to yield fumarate and arginine. This amino acid was measured in a second reaction using arginase to form ornithine and urea, which was analyzed using a chemical method. Aliquots of 38 µL of homogenates were mixed with 38 µL of 70 mM hepes buffer pH 7.4, containing argininosuccinate (Sigma); final concentration 2 mM. Incubations were carried out at 37°C for 0, 2.5, 5 and 10 min. The reaction was stopped by the addition of 40 µL of 30 g/L perchloric acid. The tubes were vortexed and brought to pH 8-9 with 10 µL of 100 g/L KOH containing 80 g/L potassium bicarbonate. The tubes were mixed again, and centrifuged for 15 min in the cold (4°C) at 8,000xg. Aliquots of 100 µL of the supernatants were mixed with 50 µL of the reacting mixture: 70 mM hepes buffer pH 7.5 (to achieve a final pH 8.5) containing MnCl₂ and arginase (rat liver, Lee Biosolutions, St Louis, MO USA); final concentrations 7 mM and 17 nkatal/ml. The buffer containing Mn and arginase was activated (heated) for 5 min at 55°C before use. The reaction was allowed to develop for 30 min at 37°C, and was stopped by the addition of 35 µL 160 g/L perchloric acid. The tubes were centrifuged for 15 min at 8,000xg and 4°C. The acidic supernatants (175 µL) were used for the estimation of urea. They were mixed with 300 µL of 90 g/L H₂SO₄ containing 270 g/L H₃PO₄; then 20 µL of 30 g/L of 1-phenyl-2-oxime-1,2-propanodione (Sigma) in absolute ethanol were added (MC). The reaction was developed at 100°C for 30 min in a dry block heater. The absorbance of the tubes was measured at 540 nm using a plate reader, including standards of arginine and urea as well as blanks. Under these conditions, conversion of arginine to urea was complete.

Total arginase activity was measured through the estimation of the urea produced from arginine in the presence of Mn²⁺ (MG). Aliquots of 20 µL of homogenates were mixed with 5 µL of 50 mM MnCl₂. The tubes were heated for 5 min at 55°C to activate arginase (MH). Then, the temperature was brought down to 37°C. The reaction began with the addition of 75 µL of arginine (Sigma); final concentration 78 mM. Incubations were carried out for 1, 10 and 20 min at 37°C. The reaction was stopped by the addition of 35 µL 160 g/L perchloric acid. The tubes were centrifuged at 8,000xg and 4°C for 15 min. The measurement of urea generated was done as described above for argininosuccinate lyase. Since the method used for arginase does not differentiate between arginases 1 and 2, we present a combined total arginase value that corresponds mostly to arginase 1 (expressed in all WAT sites, whilst arginase 2 was expressed only in SC WAT).

SUPPLEMENTAL TABLES

Supplemental Table 1 Urea cycle enzyme activities in WAT sites of female and male Wistar rats

enzyme	units	sex	SC	ME	RP	PG	P (site)	P (sex)
glutamine-dependent carbamoyl-phosphate synthase	M	165 ± 35*	49.0 ± 13.7	56.5 ± 9.2	40.4 ± 9.3	<0.0001	NS	
	F	88.0 ± 30.8	55.3 ± 6.7	61.6 ± 9.9	53.8 ± 13.3			
ornithine carbamoyl transferase	M	2434 ± 1108	2792 ± 872	3206 ± 403	1975 ± 496	NS	NS	
	F	3871 ± 981	2051 ± 598	3015 ± 579	2585 ± 727			
argininosuccinate synthase	M	82 ± 11.4	57.3 ± 8.5	73.8 ± 15.3	87.8 ± 17.7	NS	NS	
	F	51.7 ± 7.5	114 ± 15.4*	40.7 ± 13.1	61.2 ± 9.0			
argininosuccinate lyase	M	291 ± 40	170 ± 33	90.1 ± 6.7	147 ± 35	<0.0001	NS	
	F	501 ± 108*	166 ± 37	79.8 ± 10.3	162 ± 42.3			
arginase (total)	M	435 ± 103	220 ± 50	297 ± 168	361 ± 117	NS	NS	
	F	316 ± 82	232 ± 32	335 ± 64	337 ± 51			

The data are the mean ± sem of 6 animals per group. Statistical significance of the differences between groups was established with a 2-way anova; post-hoc Tukey test: different superscript letters represent P<0.05 differences

Supplemental Table 2 Urea cycle enzyme gene expressions in WAT sites of female and male Wistar rats

enzyme (gene)	units	sex	SC	ME	RP	PG	P (site)	P (sex)
glutamine-dependent carbamoyl-phosphate synthase, type 2 (<i>Cad</i>)	M	58.3 ± 7.9	56.3 ± 6.3	12.8 ± 1.9	43.0 ± 4.2	<0.0001	0.0002	
	F	95.6 ± 4.7*	63.4 ± 6.1	24.5 ± 5.9	55.0 ± 5.9			
ornithine carbamoyltransferase (<i>Otc</i>)	M	2.99 ± 0.95	0.19 ± 0.02	0.76 ± 0.32	0.91 ± 0.13	0.008	NS	
	F	1.17 ± 0.07	0.23 ± 0.07	1.35 ± 0.57	2.19 ± 0.94			
argininosuccinate synthase 1(<i>Ass1</i>)	M	10.2 ± 1.8	4.68 ± 0.61	3.62 ± 1.12	5.02 ± 0.35	NS	NS	
	F	6.39 ± 0.71	5.96 ± 1.01	5.58 ± 1.84	13.4 ± 5.4*			
argininosuccinate lyase (<i>As</i>)	M	57.1 ± 8.4	27.3 ± 5.7	10.3 ± 2.4	36.0 ± 4.4	<0.0001	NS	
	F	44.9 ± 2.4	34.5 ± 4.9	14.8 ± 1.5	28.0 ± 2.8			
arginase (<i>Arg1 + Arg2</i>)	M	21.2 ± 1.7*	0.74 ± 0.24	0.39 ± 0.15	2.74 ± 0.56	<0.0001	NS	
	F	16.1 ± 2.1	0.41 ± 0.04	1.59 ± 0.50	3.23 ± 0.67			

The data are the mean ± sem of 6 animals per group. Statistical significance of the differences between groups was established with a 2-way anova; post-hoc Tukey test: different superscript letters represent P<0.05 differences: "Total" arginase is the composite value of the sums of expressions of the genes for arginases 1 and 2, affecting only SC data, since in the other sites, only arginase 1 was detected. The separate data for arginases is shown in Supplemental Table 3.

Supplemental Table 3 Amino acid metabolism enzyme gene expressions in WAT sites of female and male Wistar rats

enzyme (gene)		sex	SC	ME	RP	PG	P (site)	P (sex)
N-acetylglutamate synthase (<i>Nags</i>)		M	1.13 ± 0.31	0.85 ± 0.32	0.43 ± 0.04	0.96 ± 0.15	NS	NS
arginase-1 (<i>Arg1</i>)		F	0.88 ± 0.25	1.04 ± 0.33	0.97 ± 0.08	1.21 ± 0.32		
arginase-2, mitochondrial (<i>Arg2</i>)		M	3.29 ± 1.08	0.74 ± 0.24	0.39 ± 0.15	2.74 ± 0.56	0.0042	NS
nitric oxide synthase, endothelial (<i>Nos3</i>)		F	4.25 ± 1.38	0.41 ± 0.04	1.59 ± 0.50	3.23 ± 0.67		
glutamine synthetase (<i>GluL</i>)		M	17.9 ± 2.4	--	--	--	<0.0001	0.0031
glutaminase kidney isoform, mitochondrial (<i>Gls</i>)		F	11.1 ± 2.7	--	--	--	<0.0001	0.0031
glutamate dehydrogenase 1, mitochondrial (<i>Glud1</i>)		M	75.4 ± 9.5*	21.6 ± 2.6	14.6 ± 1.1	31.6 ± 6.3	<0.0001	0.0031
glycine cleavage system H protein, mitochondrial (<i>GcsH</i>)		F	43.2 ± 2.8	18.5 ± 1.0	16.1 ± 2.2	22.6 ± 2.4		
AMP deaminase 2 (<i>Ampd2</i>)		M	1336 ± 523*	198 ± 29	136 ± 9	426 ± 99	0.0005	NS
alanine aminotransferase 1 (<i>Gpt2</i>)		F	461 ± 49	225 ± 38	186 ± 39	308 ± 42		
branched-chain-amino-acid aminotransferase, cytosolic (<i>Bcat1</i>)		M	39.9 ± 4.8	20.1 ± 1.5	15.4 ± 1.1	24.2 ± 2.7	<0.0001	<0.0001
branched-chain-amino-acid aminotransferase, mitochondrial (<i>Bcat2</i>)		F	77.5 ± 6.4*	24.4 ± 2.9	22.2 ± 2.7	23.6 ± 3.6		
		M	451 ± 80	410 ± 62	119 ± 13	272 ± 32	<0.0001	NS
		F	350 ± 37	454 ± 62	170 ± 13	300 ± 11		
		M	110 ± 15	60.6 ± 11.8	45.8 ± 3.9	72.9 ± 12.2	NS	NS
		F	109 ± 31	62.8 ± 7.8	86.1 ± 15.2	90.1 ± 5.2		
		M	125 ± 21*	56.4 ± 14.6	14.5 ± 1.3	32.9 ± 3.6	<0.0001	NS
		F	73.5 ± 6.7	83.9 ± 9.9	22.0 ± 2.4	32.4 ± 2.7		
		M	434 ± 104*	156 ± 53	115 ± 10	325 ± 41	0.0033	NS
		F	193 ± 31	191 ± 49	163 ± 31	268 ± 39		
		M	10.1 ± 2.2	4.76 ± 1.68	4.52 ± 0.69	21.7 ± 3.7*	<0.0001	0.0018
		F	6.72 ± 1.02	3.86 ± 0.97	4.15 ± 1.00	9.03 ± 1.59		
		M	13.5 ± 1.8	14.9 ± 0.9	3.15 ± 0.43	12.7 ± 2.5	<0.0001	NS
		F	13.6 ± 3.0	14.4 ± 3.3	3.20 ± 0.42	8.31 ± 0.95		
		M	176 ± 49	132 ± 33	56.7 ± 5.0	142 ± 37	0.0344	NS
		F	113 ± 18	114 ± 20	80.5 ± 6.3	142 ± 7		

The data are the mean ± sem of 6 animals per group, and are expressed as fmol/g of protein. Statistical significance of the differences between groups was established with a 2-way ANOVA; post-hoc Tukey test: different superscript letters represent P<0.05 differences. The data for arginase 2 were compared with an 1-way ANOVA test and pos

Supplemental Table 4 Lipid metabolism-related protein gene expressions in WAT sites of female and male Wistar rats

protein (gene)	sex	SC	ME	RP	PG	P (site)	P (sex)
solute carrier family 2 (facilitated glucose transporter), member 4	M	108 ± 29	31.2 ± 8.6	44.0 ± 6.5	109 ± 8.1	NS	0.0040
	F	160 ± 18	116 ± 36	119 ± 43	160 ± 54		
hexokinase-2 (<i>Hk2</i>)	M	11.7 ± 2.5	7.89 ± 1.18	4.12 ± 0.39	16.9 ± 2.8	0.0057	0.0009
	F	18.9 ± 3.7	16.8 ± 3.2	13.5 ± 4.5	25.6 ± 5.7		
glucose-6-phosphate 1- dehydrogenase (G6pdx)	M	334 ± 73	129 ± 18	84.2 ± 14.2	129 ± 12	0.0005	0.0196
	F	267 ± 25	202 ± 32	183 ± 35	285 ± 51*		
NADP-dependent malic enzyme (<i>Me1</i>)	M	1672 ± 684	47.3 ± 13	110 ± 27	120 ± 28	NS	0.0244
	F	725 ± 200	1251 ± 379*	1361 ± 307*	721 ± 255		
pyruvate dehydrogenase kinase 2, mitochondrial (<i>Pdk2</i>)	M	269 ± 87	120 ± 24	48.6 ± 7.6	91.7 ± 12.8	0.0013	NS
	F	146 ± 13	193 ± 51	63.9 ± 10.4	86.8 ± 16.8		
pyruvate dehydrogenase [acetyl transferring] kinase 4, mitochondrial (<i>Pdk4</i>)	M	180 ± 73*	14.2 ± 3.7	13.5 ± 3.5	14.5 ± 5.4	0.0016	0.0203
	F	22.7 ± 2.6	7.64 ± 3.86	6.10 ± 1.00	8.52 ± 3.29		
ATP citrate lyase (Acly)	M	167 ± 81	22.2 ± 2.9	25.1 ± 4.7	109 ± 10	NS	0.0100
	F	186 ± 54	160 ± 34	295 ± 140*	228 ± 102		
acetyl-CoA carboxylase 1 (Acaca)	M	74.0 ± 16.3	30.6 ± 3.9	81.0 ± 7.2	126 ± 12	0.0038	0.0035
	F	149 ± 37	165 ± 49	54.2 ± 206*	156 ± 66		
fatty acid synthase (Fasn)	M	7620 ± 4114	191 ± 74	572 ± 85	1269 ± 250	NS	NS
	F	2447 ± 403	1657 ± 536	3318 ± 1130	2106 ± 795		
carnitine palmitoyltransferase 1, liver isoform (Cpt1a)	M	39.6 ± 14.8*	14.0 ± 2.7	3.31 ± 0.51	16.3 ± 1.7	0.0002	NS
	F	19.4 ± 3.9	13.7 ± 3.6	2.02 ± 0.36	10.8 ± 1.7		
carnitine palmitoyltransferase 2, mitochondrial (Cpt2)	M	10.6 ± 3.0	10.7 ± 1.5	13.4 ± 1.7	25.1 ± 4.3	0.0150	NS
	F	17.0 ± 1.8	14.9 ± 3.6	20.3 ± 3.4	19.2 ± 3.4		
long-chain acyl-CoA dehydrogenase, mitochondrial (Acad)	M	1076 ± 347*	166 ± 9	204 ± 22	353 ± 72	0.022	NS
	F	365 ± 23	298 ± 60	302 ± 49	412 ± 91		
adipose triglyceride lipase (Atgl)	M	1322 ± 297*	429 ± 95	700 ± 48	1453 ± 296	0.0002	0.0425
	F	701 ± 26	338 ± 95	732 ± 51	1044 ± 149		
hormone-sensitive lipase (Lipe)	M	631 ± 131	166 ± 38	458 ± 39	674 ± 59	<0.0001	NS
	F	486 ± 37	218 ± 61	645 ± 84	664 ± 64		
lipoprotein lipase (Lpl)	M	6299 ± 1305*	1192 ± 279	2283 ± 139	3969 ± 719	<0.0001	NS
	F	3788 ± 444	1097 ± 80	2783 ± 588	4316 ± 294		

The data are the mean ± sem of 6 animals per group, and are expressed as fmol/g of protein . Statistical significance of the differences between groups was established with a 2-way anova; post-hoc Tukey test: different superscript letters represent differences P<0.05

Supplemental Table 5 Comparison of male-female specific expression of genes in different WAT sites with respect to tissue total RNA.

gene	sex	SC fmol/mgRNA	P	ME fmol/mgRNA	P	PG fmol/mgRNA	P	RP fmol/mgRNA	P	all-sites P value
urea cycle enzymes										
ornithine carbamoyl-transferase	M	0.61 ± 0.16	NS	0.020 ± 0.003	NS	0.42 ± 0.05	NS	1.08 ± 0.46	NS	NS
	F	0.27 ± 0.01		0.031 ± 0.007		1.03 ± 0.43		1.24 ± 0.54		
carbamoyl-P synthase 2	M	17.0 ± 2.0		6.19 ± 0.27	NS	16.8 ± 2.7	NS	16.4 ± 1.4	NS	NS
	F	24.0 ± 1.6	0.0220	5.87 ± 0.54		17.3 ± 2.4		18.4 ± 3.2		
arginino-succinate synthase	M	1.94 ± 0.19	NS	0.51 ± 0.04	NS	2.69 ± 0.21	NS	3.67 ± 1.11	NS	NS
	F	1.51 ± 0.18		0.62 ± 0.11		6.31 ± 2.45		4.31 ± 1.51		
arginino-succinate lyase	M	13.8 ± 1.2	NS	3.07 ± 0.45	NS	18.5 ± 3.2	NS	11.2 ± 1.1	NS	NS
	F	10.6 ± 0.7		3.65 ± 0.37		15.1 ± 2.0		12.1 ± 1.4		
arginase 1	M	0.56 ± 0.12	NS	0.065 ± 0.018	NS	1.28 ± 0.25	NS	0.50 ± 0.17	NS	NS
	F	0.93 ± 0.28		0.045 ± 0.010		1.60 ± 0.38		1.43 ± 0.61		
Other enzymes of amino acid metabolism										
N-acetyl-glutamate synthase	M	0.44 ± 0.095	0.0197	0.11 ± 0.035	NS	0.60 ± 0.18	NS	0.59 ± 0.05	NS	NS
	F	0.12 ± 0.01		0.12 ± 0.037		0.62 ± 0.15		0.72 ± 0.14		
glutamate dehydrogenase 1	M	112 ± 17	NS	38.9 ± 3.6	NS	142 ± 11	NS	155 ± 9	NS	NS
	F	82.9 ± 10		48.4 ± 6.1		157 ± 14		134 ± 16		
glutamine synthetase	M	291 ± 74	NS	19.0 ± 2.0	NS	166 ± 9.9	NS	178 ± 5	NS	0.0035
	F	109 ± 11		20.0 ± 1.3		139 ± 15		139 ± 19		
glutaminase	M	10.5 ± 1.9	NS	1.81 ± 0.22	0.0292	12.0 ± 1.0	NS	20.4 ± 0.8	NS	NS
	F	16.4 ± 2.5		2.62 ± 0.23		10.8 ± 1.5		17.2 ± 1.6		
AMP deaminase	M	25.6 ± 2.3	0.0109	9.05 ± 0.79	NS	16.9 ± 1.2	NS	19.1 ± 1.2	NS	0.0048
	F	16.8 ± 1.4		8.87 ± 0.41		16.0 ± 0.9		17.8 ± 1.5		
glycine cleavage system	M	26.8 ± 4.0	NS	7.08 ± 1.22	NS	32.8 ± 3.2	0.0128	61.3 ± 5.4	NS	NS
	F	18.4 ± 3.0		6.64 ± 0.82		45.7 ± 2.8		65.2 ± 6.4		
alanine transaminase 1	M	91.7 ± 6.3	0.0007	16.5 ± 5.1	NS	150 ± 9		152 ± 10	0.0409 <0.0001	
	F	45.3 ± 7.1		16.3 ± 3.6		121 ± 15		114 ± 13		
alanine transaminase 2	M	2.87 ± 0.27	0.0104	0.49 ± 0.15	NS	9.90 ± 1.22	0.0034	6.00 ± 0.68	0.0057	
	F	1.58 ± 0.21		0.56 ± 0.18		3.99 ± 0.46		3.05 ± 0.42		
branched-chain amino acid transaminase 1	M	3.07 ± 0.41	NS	1.62 ± 0.13	NS	4.90 ± 0.25	0.0419	4.04 ± 0.37	0.0087	0.0110
	F	3.15 ± 0.59		1.50 ± 0.20		3.82 ± 0.42		2.54 ± 0.25		
branched-chain amino acid transaminase 2	M	36.5 ± 9.8	NS	15.6 ± 3.0	NS	53.5 ± 5.8	NS	74.9 ± 6.0	NS	NS
	F	26.1 ± 3.6		14.6 ± 2.4		66.0 ± 4.7		65.5 ± 4.3		
endothelial nitric oxide synthase	M	22.8 ± 4.1	0.0382	2.13 ± 0.28	NS	14.3 ± 1.9	NS	19.7 ± 1.9	0.0102	0.0001
	F	11.4 ± 1.5		2.18 ± 0.29		10.4 ± 1.1		12.4 ± 1.0		

(Continues in next page)

Supplemental Table 5 (conclusion)

gene	sex	SC fmol/mgRNA	P	ME fmol/mgRNA	P	PG fmol/mgRNA	P	RP fmol/mgRNA	P	all-sites P value
enzymes (and transporters) related with lipogenesis from glucose										
glucose transporter 4	M	36.1 ± 7.9	NS	4.31 ± 1.43	NS	47.3 ± 6.8	NS	56.8 ± 5.6	101 ± 16	0.0432 0.0115
	F	46.7 ± 9.5		9.34 ± 2.48		69.6 ± 21.2				
hexokinase 2	M	3.02 ± 0.18	NS	1.36 ± 0.31	NS	7.07 ± 1.05	0.0365	5.49 ± 0.56	11.5 ± 2.2	0.0392 0.0001
	F	4.45 ± 0.79		2.26 ± 0.46		12.8 ± 2.0				
glucose-6P dehydrogenase	M	72.7 ± 4.0	NS	13.1 ± 2.3	0.0458	61.9 ± 7.8	0.0192	108 ± 10	197 ± 27	0.0198 0.0001
	F	63.8 ± 6.7		21.6 ± 2.9		128 ± 20				
malic enzyme	M	344 ± 103	NS	5.15 ± 1.02	0.0485	65.5 ± 14.0	0.0476	147 ± 24	1022 ± 267	0.0218 0.0018
	F	170 ± 43		81.7 ± 29.5		313 ± 95				
pyruvate dehydrogenase kinase 2	M	52.7 ± 7.1	0.0450	14.4 ± 2.6	NS	39.3 ± 4.4	NS	56.2 ± 2.9	47.8 ± 2.3	0.0458 0.0319
	F	33.9 ± 2.1		15.6 ± 3.0		38.7 ± 6.3				
pyruvate dehydrogenase kinase 4	M	37.2 ± 9.0	0.0164	1.49 ± 0.30	NS	6.49 ± 1.48	NS	18.8 ± 5.2	5.10 ± 1.09	0.0458 <0.0001
	F	5.35 ± 0.72		0.93 ± 0.36		3.89 ± 1.24				
citrate: ATP lyase	M	33.4 ± 10.6	NS	4.58 ± 1.07	0.0045	48.5 ± 9.8	NS	36.3 ± 8.5	290 ± 91	0.0384 0.0016
	F	46.0 ± 12.3		28.0 ± 4.9		107 ± 43				
acetyl-CoA carboxylase	M	21.2 ± 3.6	0.0442	3.39 ± 0.51	0.0242	55.0 ± 10.3	NS	112 ± 5	466 ± 88	<0.0001 0.0100
	F	58.2 ± 13.9		24.1 ± 6.5		120 ± 39				
fatty acid synthase	M	936 ± 234	NS	39.5 ± 14.7	0.0143	496 ± 98	0.0483	789 ± 85	2286 ± 523	0.0348 0.0018
	F	696 ± 134		157 ± 33		1553 ± 408				
enzymes (and transporters) related with lipolysis and fatty acid oxidation										
carnitine palmitoleoyl transferase (liver)	M	11.7 ± 2.8	0.0491	1.88 ± 0.23	NS	8.90 ± 1.09	0.0137	4.23 ± 0.43	1.68 ± 0.33	0.001 <0.0001
	F	4.55 ± 0.83		1.33 ± 0.18		4.92 ± 0.66				
carnitine palmitoleoyl transferase (muscle)	M	3.75 ± 0.91	NS	1.18 ± 0.17	NS	11.7 ± 1.9	NS	19.9 ± 2.1	15.2 ± 1.2	NS 0.0350
	F	3.49 ± 0.60		1.55 ± 0.35		8.67 ± 1.18				
long-chain acyl-CoA dehydrogenase	M	210 ± 38	0.0214	18.5 ± 1.8	0.0462	168 ± 24	NS	271 ± 26	229 ± 16	NS 0.0460
	F	86.0 ± 5.5		30.9 ± 4.7		185 ± 37				
adipose tissue triacylglycerol lipase	M	337 ± 73	0.0460	43.2 ± 9.7	NS	667 ± 105	NS	929 ± 61	577 ± 56	0.0017 <0.0001
	F	145 ± 22		34.3 ± 7.2		477 ± 66				
hormone-sensitive lipase	M	168 ± 37	NS	16.7 ± 3.9	NS	379 ± 48	NS	603 ± 32	499 ± 46	NS 0.0131
	F	114 ± 8		17.5 ± 4.0		306 ± 31				
lipoprotein lipase	M	1553 ± 68	0.0324	154 ± 41	NS	1796 ± 211	NS	3458 ± 372	2275 ± 354	0.0440 NS
	F	1038 ± 177		132 ± 28		2269 ± 263				

The data are the mean ± sem of 6 animals per group, and are expressed as fmol of the corresponding mRNA per mg of total RNA. Statistical significance of the differences between groups was established with 1- and 2-way anova; NS = P>0.05.

1

2

3 **Overall white adipose tissue urea cycle activity remains unchanged in female rats after
4 one-month treatment with a hyperlipidic diet**

5 Sofia Arriarán, Silvia Agnelli, Xavier Remesar, Marià Alemany and José Antonio Fernández-
6 López

7 Department of Nutrition and Food Science, Faculty of Biology, University of Barcelona,
8 Barcelona, Spain

9 Institute of Biomedicine, University of Barcelona, Barcelona, Spain

10 CIBER-OBN Research web, Barcelona, Spain

11

12 Corresponding Author:

13 Dr. José Antonio Fernández-López; Department of Nutrition and Food Science, Faculty of
14 Biology, University of Barcelona. Av. Diagonal, 643; 08028 Barcelona, Spain. Tel: 93
15 4021546; fax: 34934037064; E-mail: josfernandez@ub.edu.

16

17 Short title: rat adipose tissue urea cycle and diet

18

19 Key words: urea cycle, amino acid metabolism, white adipose tissue, adipose organ,
20 cafeteria diet.

21

22 ABSTRACT

23 Under high-energy diets, amino acid N is difficult to dispose of, consequence of the
24 availability of alternative substrates. We found, recently, that WAT contains a complete
25 functional urea cycle, we analyzed the possible overall changes in WAT urea cycle (and
26 other-related amino acid metabolism gene expressions) in rats subjected to a cafeteria diet.
27 Adult female Wistar rats were fed control or simplified cafeteria diets. Samples of WAT sites:
28 mesenteric, periovaric, retroperitoneal and subcutaneous, were obtained, and all urea cycle
29 enzyme activities and gene expressions were estimated. Other key amino acid metabolism
30 gene expressions, and lactate dehydrogenase were also measured. Subcutaneous WAT
31 showed a differentiated amino acid metabolism profile, since its cumulative (whole site)
32 activity for most enzymes was higher than the activities of the other sites studied. After one
33 month of eating an energy-rich cafeteria diet, and in spite of doubling the size of WAT, the
34 transforming capacity of most amino acid metabolism enzymes in WAT remained practically
35 unchanged. This was a consequence of limited changes in the overall enzyme activity, but
36 also because of a relative decrease in the expression of the corresponding genes. Overall, the
37 results of this study give support to the consideration of WAT as an organ, disperse but under
38 uniform control. The metabolic peculiarities between its different sites, and their ability to
39 adapt to different energy availability conditions only add to the variable nature of adipose
40 tissue. We have presented additional evidence of the significant role of WAT in amino acid
41 metabolism.

42

43

44 INTRODUCTION

45 The most characteristic trait of white adipose tissue (WAT) is its inordinate growth
46 when experimental animals are exposed to energy-rich, mainly hyperlipidic, diets as are the
47 self-selected "cafeteria" diets^(1, 2). These diets are widely used as model of human obesity,
48 largely attributed to the consumption of hyper-energetic/ hyperlipidic diets^(1, 3), which elicit
49 the development of inflammation⁽⁴⁾. Inordinate WAT growth has been intensely studied,
50 along with the development of other pathologies related to inflammation in the context of
51 metabolic syndrome^(5, 6). Inflamed WAT reacts to the aggression provoked by excess nutrient
52 availability by reducing its blood flow⁽⁷⁾ to diminish excessive availability of nutrients to fuel
53 its storage of fat, and releasing a number of adipokines⁽⁸⁾, which tend to help activate the

54 defense systems and metabolic adaptations to face off the problem of disposal of excess
55 available energy⁽⁹⁾.

56 The key point is the largely glucose-fueled lipogenesis, since WAT insulin response is
57 better maintained, under conditions of generalized insulin resistance, than in other peripheral
58 organs and the liver⁽¹⁰⁾. Thus, the adipocyte could not fully prevent the uptake of high
59 circulating glucose other than decreasing blood flow⁽⁷⁾, which may elicit hypoxia⁽¹¹⁾, or a
60 decrease in the synthesis of acyl-glycerols. We have found recently that both cultured 3T3-L1
61 adipocytes⁽¹²⁾, and rat WAT *in vivo*⁽¹³⁾, break up inordinate amounts of glucose to release 3C
62 units, largely lactate⁽¹²⁻¹⁴⁾. This is a consequence of diversion of pyruvate towards lactate
63 instead of entering the mitochondria and producing acetyl-CoA, the key building block of
64 acyl-CoA. Reduced oxidative metabolism facilitates the process; *in vivo* studies in humans
65 and rats have shown low oxygen levels in WAT without signs of hypoxia^(15, 16). This "normal
66 hypoxia" is coupled to a low WAT oxygen consumption *in vivo*⁽¹⁶⁾. Evidently, these data
67 contrast with the obvious hypertrophic and hyperplastic growth of WAT when the adipocyte is
68 exposed to abundant glucose. Curiously, in cultured adipocytes, differentiation from
69 fibroblast and massive accumulation of fat, at high medium glucose levels, is continued by a
70 massive breakup to lactate of this same glucose when the cells are mature and their fat stores
71 (sufficiently?) large⁽¹³⁾. Therefore, lipogenesis and the potential resistance to hypoxia run in
72 parallel, i.e. hypertrophic WAT response to excess glucose and oxygen needs should be
73 markedly different from a basal or starved state, when lipogenesis is highly stimulated.

74 Amino acid metabolism is not generally included in overall energy metabolism
75 analyses, in part because of its complexity, usually limited provision of energy, and its direct
76 implication with a number of biosynthetic paths, of which protein synthesis is paramount for
77 survival. However, all cells have a significant amino acid metabolism, despite the key role of
78 liver and other organs of the splanchnic bed^(17, 18), since it takes the double role of controlling
79 the dietary supply of amino acids and is the main site for the final conversion to ammonium,
80 and then urea of 2-amino N.

81 The mechanisms of preservation of 2-amino N have evolved to powerful fail-safe
82 mechanisms, which prevent the loss of hard-to-obtain amino acids^(19, 20). However, high-
83 energy high-quality protein diets tend to create havoc in the mechanisms of regulation of
84 amino acid metabolism: cafeteria diets decrease the excretion of urea N in spite of maintained
85 (or increased) N intake⁽²¹⁾; the form of excretion of the excess N –which is not significantly
86 stored—is unknown^(22, 23). In this context the role of WAT is, usually, not even considered, in

87 part because of the perceived low metabolic activity of the tissue and our superficial
88 knowledge of amino acid metabolism in WAT²⁴. We have found, recently, that WAT
89 contains a complete and functional urea cycle (unpublished results), which makes our
90 assumptions of how 2-amino N is disposed of even more complicated, especially under
91 conditions of obesity/ inflammation, since an increase in WAT mass may result in a parallel
92 increase in its ability to dispose of 2-amino N. In the present study, we have analyzed in detail
93 the possible overall changes in WAT urea cycle (and other-related amino acid metabolism
94 gene expressions) in female rats subjected to a cafeteria diet compared with controls. The
95 comparisons have been done essentially by comparing the whole WAT site enzyme activity
96 (or gene expression) of control and cafeteria diet-fed rats to better understand their possible
97 influence on the whole body amino acid handling capability.

98

99 MATERIALS AND METHODS

100 *Experimental design and animal handling*

101 All animal handling procedures and the experimental setup were in accordance with the
102 animal handling guidelines of the corresponding European and Catalan Authorities. The
103 Committee on Animal Experimentation of the University of Barcelona specifically authorized
104 the procedures used in the present study.

105 Nine week old female Wistar rats (Harlan Laboratory Models, Sant Feliu de Codines,
106 Spain) were used. Six animals per group were housed in two-rat cages and had free access to
107 water. The animals were kept in a controlled environment (lights on from 08:00 to 20:00;
108 21.5-22.5°C; 50-60% humidity). Two groups were randomly selected and were fed *ad libitum*,
109 for 30 days, with either normal rat chow (Harlan #2014) or a simplified cafeteria diet⁽²⁵⁾.
110 Chow pellets, plain cookies, with liver pâté, bacon, whole milk with 300 g/L sucrose and a
111 mineral and vitamin supplement. We used the procedures for food intake estimation and
112 analysis described previously⁽²⁶⁾. Estimated diet intake composition was (expressed as energy
113 content): carbohydrate 67%, protein 20%, and lipid 13% for controls. That of rats fed the
114 cafeteria diet (i.e. food ingested) was: carbohydrate 47%, protein 12% and lipid 41% (energy
115 content). This diet induced a significant increase in body fat and has been used for a long time
116 in comparative studies on metabolic syndrome^(25, 27).

117 The rats were killed, under isoflurane anesthesia, at the beginning of a light cycle by
118 aortic exsanguination, using dry-heparinized syringes; then, were rapidly dissected, taking

119 samples of WAT sites: mesenteric (ME), periovaric (PO), retroperitoneal (RP) and
120 subcutaneous (SC, inguinal fat pads). The samples were blotted, and frozen with liquid
121 nitrogen. After weighing, they were ground under liquid nitrogen; they were stored at -80°C
122 until processed. Later, the dissection of the rats continued, extracting the remaining WAT in
123 ME, EP and RP sites; the rats were skinned, and the whole subcutaneous WAT was dissected.
124 The weights of the recovered WAT were added to obtain the total mass of each WAT site.

125 *Blood plasma parameters*

126 The blood obtained from the aorta was centrifuged to obtain plasma, which was frozen
127 and kept at -80 °C until processed. Plasma samples were used to measure glucose (kit
128 #11504), triacylglycerols (kit #11828), total cholesterol (kit #11505) and urea (kit # 11537),
129 all from Biosystems, Barcelona Spain). Lactate was measured with kit #1001330 (Spinreact,
130 Sant Esteve de Bas, Spain). Amino acids were analyzed individually using an amino acid
131 analyzer (Pharmacia-LKB-Alpha-plus, Uppsala, Sweden) from plasma samples deproteinized
132 with acetone⁽²⁸⁾. Since the method used did not provide fair analyses for glutamine and other
133 amino acids (Trp, Cys, Asn), we decided to present only the partial sum of the other amino
134 acids as a single indicative value.

135 *Preparation of tissue homogenates*

136 Frozen tissue samples were homogenized, using a tissue disruptor (Ultraturrax IKA-
137 T10, Ika Werke, Staufen, Germany), in 5 volumes of chilled 70 mM hepes buffer pH 7.4
138 containing 1 mM dithiothreitol (Sigma-Aldrich, St Louis MO USA), 50 mM KCl, 1g/L Triton
139 X-100 (Sigma) and 1 g/L lipid-free bovine serum albumin (Sigma-Aldrich). In homogenates
140 to be used for carbamoyl-P synthase 2 estimation, the concentration of Triton X-100 was
141 reduced 50% to decrease foaming. The homogenates were centrifuged for 10 min at 5,000xg;
142 the floating fat layers and gross debris precipitates were discarded. The clean homogenates
143 were kept on ice, and used for enzyme analyses within 2 h.

144 Tissue protein was estimated with the Lowry method⁽²⁹⁾, using finely powdered inert
145 MgO to eliminate the remaining fat-generated turbidity after development of color.
146 Homogenization buffer (which contained albumin) was used as blank. Enzyme activities were
147 initially expressed in nkat/g protein.

148 *Enzyme activity analyses*

149 Carbamoyl-P synthase was estimated from the incorporation of ^{14}C -bicarbonate (Perkin
150 Elmer, Bad Neuheim, Germany) into carbamoyl-P using a method previously described by
151 us⁽³⁰⁾.

152 All other urea cycle enzyme activities (ornithine carbamoyl-transferase, arginino-
153 succinate synthase, arginino-succinate lyase and arginase) were estimated following our
154 recently developed methods which are presented with detail in the Supplemental Methods.

155 A modified UV method was used for lactate dehydrogenase activity⁽³¹⁾. The reaction
156 mixture contained 150 μM NADH, 125 mg/L bovine serum albumin and 1 mM sodium
157 pyruvate (Sigma-Aldrich). The proportion of original tissue in each measuring well was in the
158 range of 2.0-2.5 mg, in a volume of 0.02 mL of homogenate, diluted to the adequate
159 proportions with homogenization medium. Absorbance at 340 nm was measured at intervals
160 of 30 s for up to 10 min. In each case, the decrease in absorbance, due to the formation of
161 NAD^+ , was plotted, and initial (V_0) activities were determined from the course of the reaction
162 at different times.

163 *Gene expression analysis*

164 Total tissue RNA was extracted from frozen tissue samples using the Tripure reagent
165 (Roche Applied Science, Indianapolis IN USA), and was quantified in a ND-100
166 spectrophotometer (Nanodrop Technologies, Wilmington DE USA). RNA samples were
167 reverse transcribed using the MMLV reverse transcriptase (Promega, Madison, WI USA)
168 system and oligo-dT primers. These data were also used to determine the total RNA content
169 of the tissue (per g of tissue weight).

170 Real-time PCR (RT-PCR) amplification was carried out using 10 μL amplification
171 mixtures containing Power SYBR Green PCR Master Mix (Applied Biosystems, Foster City,
172 CA USA), 4 ng of reverse-transcribed RNA and 150 nmol of primers. Reactions were run on
173 an ABI PRISM 7900 HT detection system (Applied Biosystems) using a fluorescent threshold
174 manually set to 0.15 for all runs.

175 A semi-quantitative approach for the estimation of the concentration of specific gene
176 mRNAs per unit of tissue/ RNA or protein weight was used⁽³²⁾. *Rplp0* was the charge control
177 gene⁽³³⁾. We expressed the data as the number of transcript copies per gram of protein in order
178 to obtain comparable data between the groups. The genes analyzed and a list of primers used
179 is presented in Table 1.

180 *Statistics*

181 One- and two-way ANOVA comparisons between groups and curve fitting (e.g. Vi
182 estimations) were analyzed with the Prism 5 program (GraphPad Software, San Diego CA
183 USA).

184

185 RESULTS

186 Table 2 shows the rat weights, and those of the four WAT sites studied, as well as the
187 levels of protein and RNA per g of adipose tissue. In spite of cafeteria-fed rats weighing
188 slightly more than controls, the differences were not significant. However, both the
189 differences for site and diet were statistically significant. Control rats combined WAT weight
190 for all four WAT sites was 8.1 % of body weight, against 15.2 % for cafeteria rats. The
191 difference in body weight minus the sum of WAT sites was minimal for both dietary groups
192 (213 g controls, 226 g cafeteria), suggesting that WAT was, precisely, the main factor
193 affecting the small differences in body weight. The differences induced by diet and those on
194 WAT sites were also significant for protein content and total RNA. Both protein and RNA
195 tended to decrease in cafeteria rats when expressed per g of tissue. The RNA/protein ratio
196 decreased considerably in all WAT sites under the cafeteria diet; mesenteric ratio showing the
197 highest, and subcutaneous WAT the lowest values.

198 Plasma parameters were all within the expected range and were similar to previously
199 published data^(25, 34). They are presented in Supplemental Table 1.

200 Figure 1 depicts the data in Table 1 but now, in addition to WAT site weight, the protein
201 and RNA are presented as total amount in the whole site, for direct comparison on eventual
202 changes induced by the diet. The clear significance in the weight differences of cafeteria *vs.*
203 controls were less marked for protein, with no differences for subcutaneous WAT, and the
204 loss of significance of the differences between sites. When analyzing RNA, the differences
205 were even less patent; cafeteria diet-feeding resulted in a marked difference between sites, but
206 there were no overall effects of diet. In fact, the only site showing a marked difference
207 between diet groups was mesenteric, in which the total RNA content of the tissue was reduced
208 to roughly one third with cafeteria diet.

209 Figure 2 presents the urea cycle enzyme activities present in the whole site (nkat or
210 μ kat), and the expressions of the corresponding genes (i.e. in nmol or μ mol of the specific
211 gene mRNA), also expressed with respect to the whole site. The arginase value for activity
212 corresponds to the sum of arginases 1 and 2; the latter being expressed only in subcutaneous

213 WAT. The corresponding value for gene expression reflects also the sum of *Arg1* and *Arg2*.
214 There were clear discordances between the total enzyme activities and the mRNA content for
215 their coding genes in different sites. In all cases (activities and expressions), there was a
216 significant difference between WAT sites. However, the overall effects of diet were minimal,
217 only for ornithine carbamoyl-transferase activity and the expressions of arginase and
218 carbamoyl-P synthase. In general, subcutaneous WAT showed higher activities for
219 carbamoyl-P synthase 2, arginino-succinate lyase and arginase activities (and expressions).
220 Cafeteria diet induced a marked increase in ornithine carbamoyl-transferase activity and
221 decrease in arginino-succinate synthase activity in mesenteric WAT. This diet increased
222 ornithine carbamoyl-transferase, arginino-succinate lyase and arginases expressions in
223 subcutaneous WAT, and decreased the expression of carbamoyl-P synthase in mesenteric
224 WAT and arginino-succinate synthase in periovaric WAT. In spite of punctual variations, and
225 the marked differences between sites, the general trend was to maintain the same amount of
226 active enzyme and specific gene mRNA in the WAT sites, with only limited changes, despite
227 their different mass and dietary treatment

228 Figure 3 shows the expressions of genes coding for proteins related to ammonia/ 2-
229 amino N metabolism in four sites of WAT in control or cafeteria diet-fed female rats. All
230 genes showed significant differences in expression between sites, but the overall effects of
231 diet were limited to *Glul*, glutamine synthetase. *Glud1*, glutamate dehydrogenase NADP⁺;
232 *Gls*, glutaminase; *Gcsh*, h protein of the glycine cleavage system; and *Bcat2*, branched-chain
233 amino acid aminotransferase mitochondrial. In addition to these generalized changes, specific
234 sites showed significant changes with cafeteria diet feeding: increases in subcutaneous WAT
235 for all genes except *Ala1* and *Ala2*. On the other side, mesenteric WAT also showed
236 significant decreases for *Amp2*, and *Bcat1*, and *Glul*, increased in periovaric WAT.

237 In the way of comparison, Figure 4 depicts the WAT site lactate dehydrogenase activity
238 (μ kat in the whole tissue mass) and the corresponding values for both genes coding for lactate
239 dehydrogenases, a and b (*Ldha*, *Ldhb*). In addition to a significant difference for site, both
240 lactate dehydrogenase activity and *Ldha* changed significantly with diet. Periovaric WAT
241 activity was higher in cafeteria diet-fed rats, whereas the expression of *Ldha* and *Ldhb* were
242 lower in subcutaneous WAT under the hyperlipidic diet.

243 The data of Figures 2-4 are also presented in the more usual form of activity/expression
244 per unit of protein weight in the Supplemental Tables 2-5.

245

246 DISCUSSION

247 The main result derived from the present study has been rather surprising, since, in spite
248 of doubling the size of WAT because of one month of eating an energy-rich cafeteria diet, the
249 actual transforming capacity of most amino acid metabolism enzymes in WAT remained
250 practically unchanged with respect to the whole body. This was a consequence of limited
251 changes in the overall enzyme activity, but also because of a generalized decrease in the
252 expression of the corresponding genes when related to tissue weight. The considerable
253 increase in size of WAT was mainly due to accumulation of fat, but protein followed suit. The
254 most marked differences were in RNA content, which actually decreased in most sites, largely
255 compensating the disproportion in size.

256 The remarkable stability of urea cycle enzyme activities observed here contrasts with
257 the decreases observed in liver⁽²¹⁾. However, one can wonder whether the actual importance of
258 the changes in liver function would be appreciated as so deep if the activity/expression were
259 corrected by the actual size (and, better, including blood flow)⁽¹³⁾ of the organ. The enormous
260 change that WAT experiences when challenged with an excess of nutrients, however, is not
261 comparable to any other "regular" organ. We speculated whether part of the problems derived
262 from an enlarged (in fact engorged) WAT would be a consequence of the disproportion of its
263 mass with respect to all other tissues; however, what we found experimentally was a clear
264 downregulation of enzyme activities that practically compensated the increase in tissue mass.

265 Lowered blood flow⁽³⁵⁾ may be –also— part of the homoeostatic adjustment to
266 increased WAT mass, since lower blood flow is consistent with decreased metabolic activity
267 (as the low total RNA data show). In addition, excess "inert" triacylglycerol stores reduce
268 considerably the active tissue mass. In any case, the maintenance of most enzyme activities/
269 gene expressions seem to be a consequence of a generalized homoeostatic adjustment
270 preventing the eventual loss of balance between organ (size) and function. We are aware that
271 the form of expression we used here must be complemented with other, more common, forms
272 of data representation (presented in the Supplemental Tables 2-5). The results obtained made
273 us suggest that the analysis we carried out on key aspects of amino acid metabolism should be
274 applied to the most critical aspects of glucose handling and lipogenesis too, to check whether
275 the increased WAT size is countered by a generalized diminution of its metabolic activity.
276 Our own data suggest that diet has only limited (if any) effect on lactate metabolism *in*
277 *vivo*⁽¹³⁾. The results presented here corroborate the conclusions obtained from tissue lactate
278 levels and enzyme activities⁽¹³⁾. Lactate dehydrogenase (and lactate metabolism) is

279 diminished in adipocytes of obese animals^(13, 36), but the overall handling capacity is
280 maintained as we have shown here.

281 The results presented highlight a differential, protagonist, role for subcutaneous WAT,
282 at least for amino acid metabolism, since its cumulative activity for most enzymes was higher
283 than the combined activities of the other three sites studied. The widely known metabolic
284 difference between subcutaneous and "visceral"^(37, 38), in this case represented by mesenteric
285 WAT, was in part confirmed by a loss of amino acid metabolizing activity in this site in rats
286 fed a cafeteria diet; this effect was largely compensated by an increase in subcutaneous WAT
287 activity. This shift of main role from the splanchnic bed to peripheral tissues agrees with the
288 loss of energy substrate control of the liver (and intestine?) in obesity^(39, 40). It is also in
289 agreement with the predominant role of peripheral tissues as suppliers of substrates under
290 starvation: muscle exports 3C units⁽⁴¹⁾, and WAT fatty acids⁽⁴²⁾ (and 3C units too⁽¹⁴⁾) after the
291 liver exhausted its glycogen reserves and the intestine cannot supply dietary-derived
292 nutrients⁽⁴³⁾. It has been postulated that high availability of circulating fatty acids spurns
293 insulin resistance as a way to save glucose, and this effort is counterproductive when the fatty
294 acids come from the diet (together with glucose) and not from peripheral lipolysis⁽⁴⁴⁾. Under
295 these overfeeding conditions, thus, the problem of disposing of excess glucose becomes a
296 priority. Moreover, since 2-amino N preservation is critical for survival (an evolutionary
297 fiat)⁽¹⁹⁾, consequently, amino acids become even more difficult to dispose of⁽⁴⁵⁾.

298 The lowered amino acid disposal capacity observed in cafeteria-diet fed rats^(21, 46) stems
299 from a lowered or unfocussed function of liver (in fact liver-intestine as a unit), and is
300 reflected in lower levels and excretion of urea^(21, 46). We wanted to check whether the newly
301 found WAT urea cycle could somehow compensate the disorders caused in liver by metabolic
302 syndrome, perhaps through activation of peripheral amino acid catabolism. The surprising
303 lack of changes in peripheral urea cycle suggests a maintenance of its function in spite of
304 lowered activity / gene expression per g of tissue. Since the combined activity of WAT in
305 both dietary groups was higher for most enzyme activities than those of liver (data not
306 published), we must assume that, at least in part, the production of urea may be taken up by
307 WAT in the obese. The peculiar increase in enzyme activities observed in subcutaneous WAT
308 suggests that this site (the most "peripheral" of those studied here) may play a role more
309 important than usually assumed in amino acid handling. High *Nags* expression may indicate
310 an activation of the synthesis of ornithine⁽⁴⁷⁾, in agreement with the role of WAT as postulated

311 peripheral producer of citrulline (unpublished results). This increase may help compensate the
312 alteration of citrulline synthesis by intestine⁽⁴⁸⁾ in obesity.

313 *Glul* increased expression in subcutaneous WAT of rats fed a cafeteria diet, suggests
314 that part of the ammonium probably produced by the increased expression of *Amp2* and the
315 glycine cleavage system, but also *Gls* (to a lower extent), is not driven towards the urea cycle,
316 but maintained as glutamine or glutamate (increased expression of *Glud1*). However, there is
317 a clear role of subcutaneous WAT in the catabolism of 2-amino N as clearly shown by the
318 considerable increases in the expression of *Bcat1* and *Bcat2*, marking this site as a probably
319 significant place for the catabolism of branched-chain amino acids, as previously
320 suggested⁽⁴⁹⁾. This contrasts with the lack of changes in *Gpt* and *Gpt2*, in spite of the known
321 release of alanine by adipocytes⁽⁵⁰⁾.

322 We can summarize our findings by stating that increased WAT mass produced by
323 cafeteria diet feeding does not translate into higher overall WAT metabolic activity, but to its
324 maintenance: the enzyme activities and RNA are diluted in a reversed proportion to the
325 increase in mass of the tissue. This is logical from a homoeostatic point of view, since, under
326 this assumption, the only significant difference in WAT function from lean to obese would be
327 the storage of fat. This question needs further metabolic analyses to check whether lipid
328 metabolism follows this same trend, and, further, what are the key differences between the
329 initial phases of WAT engorgement and a relative steady state as that observed here.

330 The other key point is the remarkable constancy of the WAT urea cycle under high
331 energy availability and under the pressure of excess 2-amino N availability and the need to
332 dispose of it and the powerful mechanisms of preservation of amino acids. The only clear
333 trend observed was the shift from abdominal WAT, mainly mesenteric, to an acquired
334 metabolic predominance of subcutaneous WAT in amino acid metabolism, in line with the
335 displacement of metabolic activity from the splanchnic bed to peripheral tissues typical of
336 starvation and, contrastingly, of the excess of nutrient availability.

337 Overall, the results of this study give support to the consideration of WAT as an
338 organ⁽⁵¹⁾, albeit dispersed⁽⁵²⁾ but under uniform control⁽³⁴⁾. The metabolic peculiarities
339 between its different sites⁽⁵³⁻⁵⁵⁾, and their ability to adapt to different energy availability
340 conditions only add to the protean nature of the adipose tissue. Last, but not least, we have
341 presented additional evidence on the role of WAT in amino acid metabolism, a question
342 difficult to discuss because of the absence of sufficient studies with which to compare and
343 check our results.

344

345 **Acknowledgements**

346 This study was done with the partial support of grants of the Plan Nacional de Investigación
347 en Biomedicina (SAF2012-34895) and the Plan Nacional de Ciencia y Tecnología de los
348 Alimentos (AGL-2011-23635) of the Government of Spain, as well as of CIBER-OBN
349 (Institute of Health Carlos III). S. Agnelli was the recipient of a Leonardo da Vinci
350 fellowship, and S. Arriarán a predoctoral fellowship of the Catalan Government, in both cases
351 covering part of the time invested in this study.

352 Authors' contributions: X.R, M.A and J.A.F.L designed the study; S.Ar and S.Ag carried out
353 the experiments; S.Ar and J.A.F.L calculated the data and carried out statistical analyses;
354 J.A.F.L wrote the first manuscript draft. All authors discussed the text and contributed to the
355 final version.

356

357 **Conflict of interests**

358 The Authors declare that they have no conflict of interests.

359

360 REFERENCES

361

362 1. Sclafani A, Springer D (1976) Dietary obesity in adult rats: Similarities to
363 hypothalamic and human obesity syndromes. *Physiol Behav* **17**: 461-471.

364

365 2. Rafecas I, Esteve M, Fernández-López JA *et al.* (1994) The effect of cafeteria feeding
366 on energy balance in lean and obese Zucker rats. *Nutr Res* **14**: 1077-1088.

367

368 3. Sampey BP, Vanhoose AM, Winfield HM *et al.* (2011) Cafeteria diet is a robust
369 model of human metabolic syndrome with liver and adipose inflammation:
370 comparison to high-fat diet. *Obesity* **19**: 1109-1117.

371

372 4. Zimmermann MB, Aeberli I (2008) Dietary determinants of subclinical inflammation,
373 dyslipidemia and components of the metabolic syndrome in overweight children: a
374 review. *Int J Obesity* **32**(Suppl.6): S11-S18.

375

376 5. Monteiro R, Azevedo I (2010) Chronic inflammation in obesity and the metabolic
377 syndrome. *Mediators Inflamm.* Published online: 14 july 2010. doi:
378 10.1155/2010/289645

379

380 6. Motie M, Evangelista LS, Horwitz T *et al.* (2014) Association between inflammatory
381 biomarkers and adiposity in obese patients with heart failure and metabolic syndrome.
382 *Exp Ther Med* **8**: 181-186.

383

384 7. West DB, Francendese AA, Greenwood MRC *et al.* (1987) Adipocyte blood flow is
385 decreased in obese Zucker rats. *Am J Physiol* **253**: R228-R233.

386

387 8. Cao HM (2014) Adipocytokines in obesity and metabolic disease. *J Endocrinol* **220**:
388 T47-T59.

389

390 9. Alemany M (2011) The defense of adipose tissue against excess substrate-induced
391 hyperthrophia: Immune system cell infiltration and arrested metabolic activity. *J Clin
392 Endocrinol Metab* **96**: 66-68.

- 393
- 394 10. Frayn KN (2001) Adipose tissue and the insulin resistance syndrome. *Proc Nutr Soc*
395 **60:** 375-380.
- 396
- 397 11. Trayhurn P, Wang B, Wood IS (2008) Hypoxia in adipose tissue: a basis for the
398 dysregulation of tissue function in obesity? *Br J Nutr* **100:** 227-235.
- 399
- 400 12. Sabater D, Arriarán S, Romero MM *et al.* (2014) Cultured 3T3L1 adipocytes dispose
401 of excess medium glucose as lactate under abundant oxygen availability. *Sci Rep.*
402 Published online: 13 January 2014. doi: 10.1038/srep03663.
- 403
- 404 13. Arriarán S, Agnelli S, Sabater D *et al.* (2015) Evidences of basal lactate production in
405 the main white adipose tissue sites of rats. Effects of sex and a cafeteria diet. *PLoS*
406 *One* 2015. Published online: 5 March 2015. doi: 10.1371/journal.pone.0119572.
- 407
- 408 14. van der Merwe MT, Crowther NJ, Schlaphoff GP *et al.* (1998) Lactate and glycerol
409 release from the subcutaneous adipose tissue of obese urban women from South
410 Africa; Important metabolic implications. *J Clin Endocrinol Metab* **83:** 4084-4091.
- 411
- 412 15. Goossens GH, Blaak EE (2012) Adipose tissue oxygen tension: implications for
413 chronic metabolic and inflammatory diseases. *Curr Opin Clin Nutr Metab Care* **15:**
414 539-546.
- 415
- 416 16. Hodson L, Humphreys SM, Karpe F *et al.* (2013) Metabolic signatures of human
417 adipose tissue hypoxia in obesity. *Diabetes* **62:** 1417-1425.
- 418
- 419 17. de Blaauw I, Deutz NEP, von Meyenfeldt MF (1996) In vivo amino acid metabolism
420 of gut and liver during short and prolonged starvation. *Am J Physiol* **270:** G298-G306.
- 421
- 422 18. Aikawa T, Matsutaka H, Yamamoto H *et al.* (1973) Gluconeogenesis and amino acid
423 metabolism. II. Interorganal relations and roles of glutamine and alanine in the amino
424 acid metabolism of fasted rats. *J Biochem* **74:** 1003-1017.
- 425

- 426 19. Felig P, Owen OE, Wahren J *et al.* (1969) Amino acid metabolism during prolonged
427 starvation. *J Clin Invest* **48**: 584-594.
- 428
- 429 20. Tessari P, Barazzoni R, Zanetti M *et al.* (1996) The role of substrates in the regulation
430 of protein metabolism. *Baillière's Clin Endocrinol Metab* **10**: 511-532.
- 431
- 432 21. Barber T, Viña JR, Viña J *et al.* (1985) Decreased urea synthesis in cafeteria-diet-
433 induced obesity in the rat. *Biochem J* **230**: 675-681.
- 434
- 435 22. Esteve M, Rafecas I, Remesar X *et al.* (1991) Nitrogen balances of lean and obese
436 Zucker rats subjected to a cafeteria diet. *Int J Obesity* **16**: 237-244.
- 437
- 438 23. Esteve M, Rafecas I, Fernández-López JA *et al.* (1993) Dietary amino acid balances in
439 young Wistar rats fed a cafeteria diet. *Biochem Mol Biol Int* **29**: 1069-1081.
- 440
- 441 24. López-Soriano FJ, Alemany M (1986) Amino acid metabolism enzyme activities in rat
442 white adipose tissue. *Arch Int Physiol Biochim* **94**: 121-125.
- 443
- 444 25. Ferrer-Lorente R, Cabot C, Fernández-López JA *et al.* (2005) Combined effects of
445 oleoyl-estrone and a β_3 -adrenergic agonist (CL316,243) on lipid stores of diet-induced
446 overweight male Wistar rats. *Life Sci* **77**: 2051-2058.
- 447
- 448 26. Prats E, Monfar M, Iglesias R *et al.* (1989) Energy intake of rats fed a cafeteria diet.
449 *Physiol Behav* **45**: 263-272.
- 450
- 451 27. Rafecas I, Esteve M, Fernández-López JA *et al.* (1992) Deposition of dietary fatty
452 acids in young Zucker rats fed a cafeteria diet. *Int J Obesity* **16**: 775-787.
- 453
- 454 28. Arola L, Herrera E, Alemany M. (1977) A new method for deproteinization of small
455 samples of blood plasma for amino acid determination. *Anal Biochem* **82**: 236-239.
- 456
- 457 29. Lowry OH, Rosebrough RW, Farr AL *et al.* (1951) Protein measurement with the
458 Folin phenol reagent. *J Biol Chem* **193**: 265-275.
- 459

- 460 30. Arriarán S, Agnelli S, Fernández-López JA *et al.* (2012) A radiochemical method for
461 carbamoyl-phosphate synthetase-I: Application to rats fed a hyperproteic diet. *J
462 Enzyme Res* **3**: 29-33.
- 463
- 464 31. Vassault A (1983) Lactate dehydrogenase. UV method with pyruvate and NADH⁺.
465 *Methods Enzymatic Analysis* **3**: 118-126.
- 466
- 467 32. Romero MM, Grasa MM, Esteve M *et al.* (2007) Semiquantitative RT -PCR
468 measurement of gene expression in rat tissues including a correction for varying cell
469 size and number. *Nutr Metab*. Published online: 26 November 2007. doi:
470 10.1186/1743-7075-4-26.
- 471
- 472 33. Bamias G, Goukos D, Laoudi E *et al.* (2013) Comparative study of candidate
473 housekeeping genes for quantification of target gene messenhgAR RNA expression by
474 real-time PCR in patients with inflammatory bowel disease. *Inflamm Bowel Dis* **19**:
475 2840-2847.
- 476
- 477 34. Romero MM, Roy S, Pouillot K *et al.* (2014) Treatment of rats with a self-selected
478 hyperlipidic diet, increases the lipid content of the main adipose tissue sites in a
479 proportion similar to that of the lipids in the rest of organs and tissues. *PLoS One*.
480 Published online: 6 March 2014. doi: 10.1371/journal.pone.0090995.
- 481
- 482 35. Frayn KN, Karpe F (2014) Regulation of human subcutaneous adipose tissue blood
483 flow. *Int J Obesity* **38**: 1019-1026.
- 484
- 485 36. Rotondo F, Romero MM, Fernández-López JA *et al.* (2015) Adipose tissue site-
486 related differences in lactate production from glucose by isolated adipocytes. *Obesity
487 Facts* **8**(Suppl. 1): 170.
- 488
- 489 37. Bertile F, Criscuolo F, Oudart H *et al.* (2003) Differences in the expression of
490 lipolytic-related genes in rat white adipose tissues. *Biochem Biophys Res Commun*
491 **307**: 540-546.
- 492

- 493 38. Zahorska-Markiewicz B (2006) Metabolic effects associated with adipose tissue
494 distribution. *Adv Med Sci* **51**: 111-114.
- 495
- 496 39. Wasada T, Kasahara T, Wada J *et al.* (2008) Hepatic steatosis rather than visceral
497 adiposity is more closely associated with insulin resistance in the early stage of
498 obesity. *Metab Clin Exp* **57**: 980-985.
- 499
- 500 40. Ndumele CE, Nasir K, Conceição RD *et al.* (2011) Hepatic steatosis, obesity, and the
501 metabolic syndrome are independently and additively associated with increased
502 systemic inflammation. *Arterioscl Thromb Vasc Biol* **31**: 1927-1932.
- 503
- 504 41. Cori CF (1981) The glucose-lactic acid cycle and gluconeogenesis. *Curr Top Cell
Regul* **18**: 377-387.
- 506
- 507 42. Randle PJ, Garland PB, Hales CN *et al.* (1963) The glucose fatty-acid cycle: its role in
508 insulin sensitivity and the metabolic disturbances of diabetes mellitus. *Lancet* **281**:
509 785-789.
- 510
- 511 43. Alemany M (2013) Adjustment to dietary energy availability: from starvation to
512 overnutrition. *RSC Advances* **3**: 1636-1651.
- 513
- 514 44. Cahill GF (2006) Fuel metabolism in starvation. *Annu Rev Nutr* **26**: 1-22.
- 515
- 516 45. Alemany M (2012) The problem of nitrogen disposal in the obese. *Nutr Res Rev* **25**:
517 18-28.
- 518
- 519 46. Sabater D, Agnelli S, Arriarán S *et al.* (2014) Altered nitrogen balance and decreased
520 urea excretion in male rats fed cafeteria diet are related to arginine availability.
521 *BioMed Res Int* epub ahead of print 24 February 2014; doi: 10.1155/2014/959420.
- 522
- 523 47. Tujioka K, Lyou S, Hirano E *et al.* (2002) Role of N-acetylglutamate concentration
524 and ornithine transport into mitochondria in urea synthesis of rats given proteins of
525 different quality. *J Agric Food Chem* **50**: 7467-7471.
- 526

- 527 48. Henslee JG, Jones ME (1982) Ornithine synthesis from glutamate in rat small
528 intestinal mucosa. *Arch Biochem Biophys* **219**: 186-197.
- 529
- 530 49. Herman MA, She PX, Peroni OD *et al.* (2010) Adipose tissue branched chain amino
531 acid (BCAA) metabolism modulates circulating BCAA levels. *J Biol Chem* **285**:
532 11348-11356.
- 533
- 534 50. Snell K, Duff DA (1977) Alanine release by rat adipose tissue *in vitro*. *Biochem
535 Biophys Res Commun* **77**: 925-931.
- 536
- 537 51. Cinti S (2005) The adipose organ. *Prostaglandins Leukotrienes Essent Fatty Acids* **73**:
538 9-15.
- 539
- 540 52. Giordano A, Smorlesi A, Frontini A *et al.* (2014) White, brown and pink adipocytes:
541 the extraordinary plasticity of the adipose organ. *Eur J Endocrinol* **170**: R159-R171.
- 542
- 543 53. Boivin A, Brochu G, Marceau S *et al.* (2007) Regional differences in adipose tissue
544 metabolism in obese men. *Metab Clin Exp* **56**: 533-540.
- 545
- 546 54. Tchernof A, Bélanger C, Morisset AS *et al.* (2006) Regional differences in adipose
547 tissue metabolism in women. Minor effect of obesity and body fat distribution.
548 *Diabetes* **55**: 1353-1360.
- 549
- 550 55. Östman J, Arner P, Engfeldt P *et al.* (1979) Regional differences in the control of
551 lipolysis in human adipose tissue. *Metabolism* **28**: 1198-1205.
- 552
- 553
- 554
- 555
- 556
- 557
- 558

TABLE 1. Primer sequences used in the analysis of WAT gene expressions

gene	Protein	EC	primer sequence 5' > 3'	primer sequence 3' > 5'	bp
<i>Cad</i>	glutamine-dependent carbamoyl-phosphate synthase	6.3.5.5	AGTTGGAGGAGGAGGCTTGAG	ATTGATGGACAGGGTGTGGT	90
<i>Otc</i>	ornithine carbamoyl transferase	2.1.3.3	CTTGGGGCTGAATGAAAGTC	ATTTGGATGGTGTGGCTTCCT	126
<i>AssJ</i>	arginino-succinate synthase	6.3.4.5	CAAAGATGGCACTACCCACA	GTTCTCCACGAATGCAATGC	100
<i>Asl</i>	arginino-succinate lyase	4.3.2.1	CCGACACTGGCTACTACCTG	GAGAGCCACCCCTTCATCT	104
<i>ArgJ</i>	arginase-1	3.5.3.1	GCAGAGACCCAGAAGAAATGG	GTGAGCATCCACCCAAATG	126
<i>Arg2</i>	arginase-2	3.5.3.1	GCAGGCCCTTTCCTTCTCA	CCACATCTCGTAAGCCAATG	122
<i>Nags</i>	N-acetyl-l-glutamate synthase	2.3.1.1	GCAGGCCACCAAAATCAT	CAGGTTCACATTCCTCAGGA	82
<i>Nos3</i>	nitric oxide synthase, endothelial	1.14.13.39	CAAGTCCTCACCCCTTT	GACATCACCGCAGAACACA	138
<i>Ghl</i>	glutamine synthetase	6.3.1.2	AACCTCACGCCAGCATA	CTGGATGTTTCTCTCG	148
<i>Gls</i>	glutaminase kidney isoform, mitochondrial	3.5.1.2	CCGAAGGTTGGCTCTGTCA	AGGGCTGTTCTGGATGCTGA	63
<i>GluD1</i>	glutamate dehydrogenase 1, mitochondrial	1.4.1.3	GGACAGAAATATGGGTGCA	TCAGGTCCAATCCAGGTTA	122
<i>Gesh</i>	glycine cleavage system H protein, mitochondrial	--	AAGCACGAATGGGTAAACAGC	TCCAAGGACCAAAACTCCIC	146
<i>Ampd2</i>	AMP deaminase 2	3.5.4.6	CGGCTCTCTCACAAAGGTG	CGGATGTCGTTACCCCTCAG	78
<i>Gpt</i>	alanine aminotransferase 1	2.6.1.2	GTATTCCACGCAGCAGGAG	CACATAGCCACCGAAAACC	85
<i>Gpt2</i>	alanine aminotransferase 2	2.6.1.2	CATTCCCTGGATTCATC	GCTCTCTCGCTGTCAAA	146
<i>Bcat1</i>	branched-chain-amino-acid aminotransferase, cytosolic	2.6.1.42	TGCCCAGTGGCAGTATTTC	CAGTGTCCATTCGCTCTGTA	138
<i>Bcat2</i>	branched-chain-amino-acid aminotransferase, mitochondrial	2.6.1.42	AGTCCTGGCTCAGGCACT	ATGGTAGGAATGGAGTTGCT	84
<i>LdhA</i>	lactic acid dehydrogenase muscle type (a)	1.1.1.27	CACTGGTTTGAGACGATGA	GTCAGCAAAGGGAGAGAGC	125
<i>LdhB</i>	lactic acid dehydrogenase heart type (b)	1.1.1.27	CCAGGAACATGAAACCCAGAGA	TCATAGGCACITGTCACCAC	131
<i>Rplp0</i>	60S acidic ribosomal protein 0 (housekeeping gene)	--	GAGCCAGCGAAGGCCACACT	GATCAGCCGAAAGGAGAAAGG	62

TABLE 2

WAT weight, protein and RNA content of female Wistar rats fed for 30 d with a cafeteria diet

parameter	site	unit	control	cafeteria	P diet	P site
body weight	--	g	232 ± 8	267 ± 16	NS	-
WAT weight	SC	g	7.02 ± 0.25	12.3 ± 0.3	<0.0001	<0.0001
	ME		3.92 ± 0.33	9.02 ± 1.25		
	PO		4.83 ± 0.39	11.8 ± 1.7		
	RE		2.79 ± 0.35	7.81 ± 0.77		
	Σ WAT	g	18.6 ± 0.93	41.0 ± 3.5	0.0001	-
		% BW	8.05 ± 0.52	15.2 ± 0.5	<0.0001	-
protein	SC	mg/g	51.8 ± 3.3	41.2 ± 4.3	0.0010	<0.0001
	ME		84.2 ± 2.6	77.4 ± 5.8		
	PO		54.4 ± 2.4	47.6 ± 2.6		
	RE		62.9 ± 4.7	50.7 ± 1.3		
RNA	SC	µg/g	219 ± 19	154 ± 15	<0.0001	<0.0001
	ME		793 ± 88	92.0 ± 5.5		
	PO		119 ± 10	57.6 ± 4.1		
	RE		78.4 ± 8.8	38.4 ± 6.2		
RNA/protein ratio	SC	mg/g	4.25 ± 0.13	4.77 ± 0.86	<0.0001	<0.0001
	ME		9.49 ± 1.13	1.87 ± 0.68		
	PO		2.19 ± 0.16	1.24 ± 0.14		
	RE		1.26 ± 0.12	0.75 ± 0.11		

The data are the mean ± sem of 6 different animals per group. Statistical significance of the differences between groups (two-way ANOVA: diet and WAT site). NS P>0.05. BW = body weight. SC = subcutaneous WAT; ME = mesenteric WAT; PO = periovaric WAT; RE = retroperitoneal WAT. The sum of these four sites is indicated as Σ WAT.

LEGENDS TO FIGURES

FIGURE 1

Comparison of the weights, protein and RNA content of the four main WAT sites of female rats fed control or cafeteria diets.

The data are the mean \pm sem of 6 different animals. Dotted columns: control diet; dashed columns: cafeteria diet. WAT sites: SC = subcutaneous, ME = mesenteric, PO = periovaric; RP = retroperitoneal.

Statistical significance of the differences between groups (Two-way anova). S represents the P value for "site" and D that for "diet". Only significant results have been shown. Individual site differences (diet) are marked with an asterisk * ($P<0.05$, post-hoc Tukey test)

FIGURE 2

Total activity and gene expression of urea cycle enzymes present in the mass of WAT tissue sites of female rats fed control or cafeteria diets.

The data are the mean \pm sem of 6 different animals. Left, enzyme activities: grey columns: control diet; grey and dashed columns: cafeteria diet. Right, gene expressions: white columns: control diet; dashed columns: cafeteria diet. WAT sites: SC = subcutaneous, ME = mesenteric, PO = periovaric; RP = retroperitoneal.

The expression data for arginase are the sum of *Arg1* and *Arg2* for subcutaneous WAT, and of *Arg1* for all other sites.

Statistical significance of the differences between groups (Two-way anova). S represents the P value for "site" and D that for "diet". Only significant results have been shown. Individual site differences (diet) are marked with an asterisk * ($P<0.05$, post-hoc Tukey test)

FIGURE 3

Total expression (i.e. specific mRNA content) of amino acid metabolism enzyme genes present in the mass of WAT tissue sites of female rats fed control or cafeteria diets.

The data are the mean \pm sem of 6 different animals. White columns: control diet; dashed columns: cafeteria diet. WAT sites: SC = subcutaneous, ME = mesenteric, PO = periovaric; RP = retroperitoneal.

Statistical significance of the differences between groups (Two-way anova). S represents the P value for "site" and D that for "diet". Only significant results have been shown. Individual site differences (diet) are marked with an asterisk * (P<0.05, post-hoc Tuckey test).

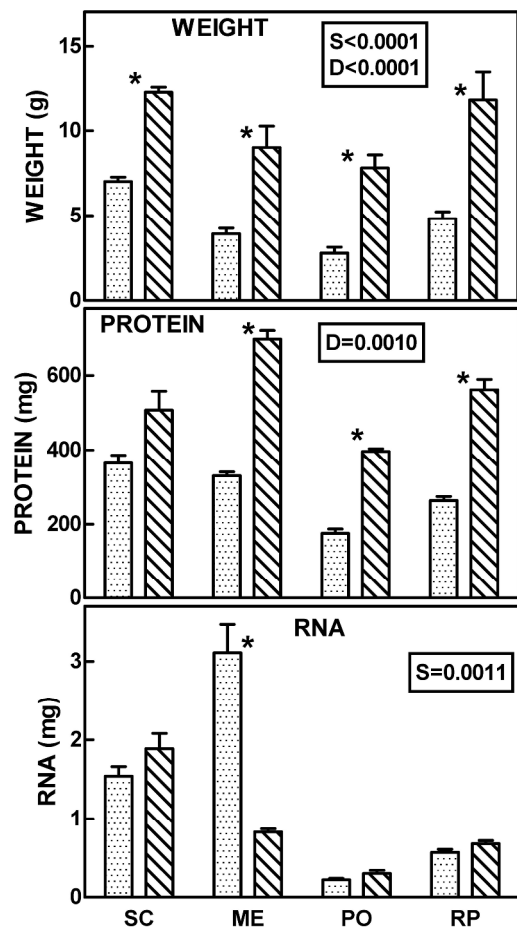
FIGURE 4

Total activity and expression of lactate dehydrogenase genes present in the mass of WAT tissue sites of female rats fed control or cafeteria diets.

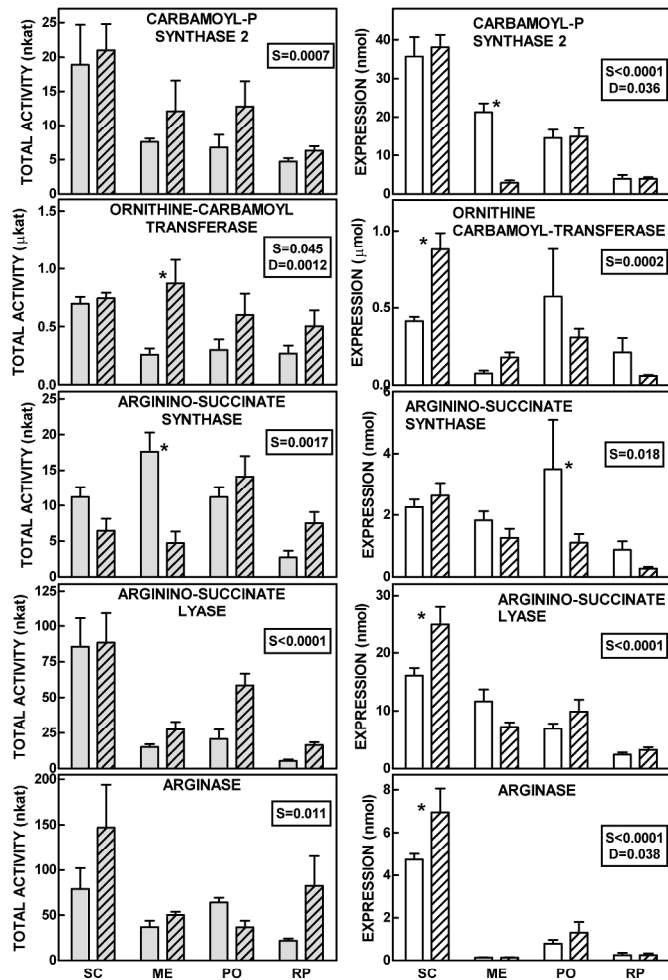
The data are the mean \pm sem of 6 different animals.

Activity: grey columns: control diet; grey and dashed columns: cafeteria diet. Expressions: white columns: control diet; dashed columns: cafeteria diet. WAT sites: SC = subcutaneous, ME = mesenteric, PO = periovaric; RP = retroperitoneal.

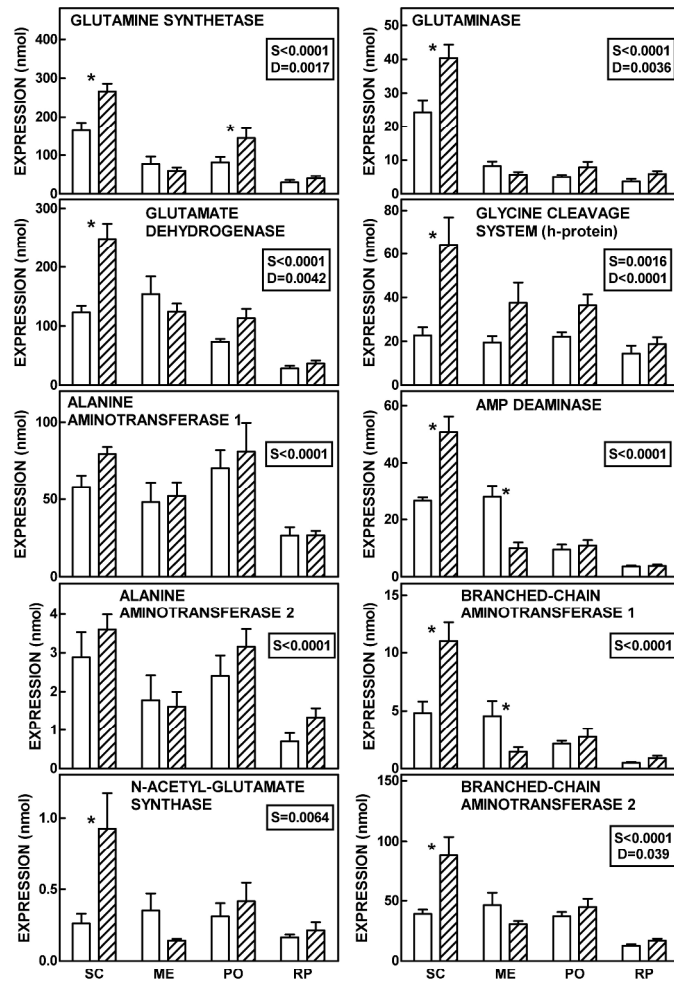
Statistical significance of the differences between groups (Two-way anova). S represents the P value for "site" and D that for "diet". Only significant results have been shown. Individual site differences (diet) are marked with an asterisk * (P<0.05, post-hoc Tuckey test)



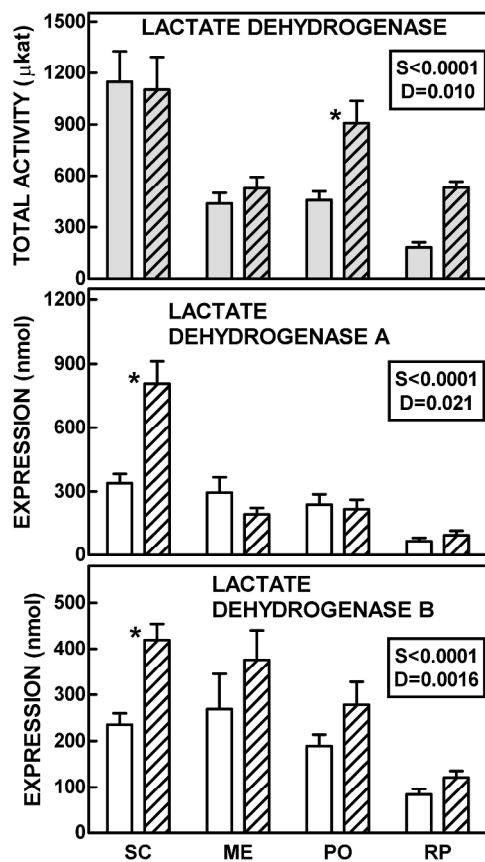
287x414mm (300 x 300 DPI)



287x414mm (300 x 300 DPI)



287x414mm (300 x 300 DPI)



287x414mm (300 x 300 DPI)

SUPPLEMENTAL MATERIAL

SUPPLEMENTAL METHODS

Measurement of urea cycle enzyme activities

Ornithine carbamoyl transferase activity was measured from the reaction of condensation of carbamoyl-P and 14C-ornithine to yield 14C-citrulline. Aliquots of 25 µL of homogenates were mixed with 50 µL of 70 mM hepes buffer pH 7.4 containing carbamoyl-P, ornithine (all from Sigma), and 14C-ornithine (Perkin-Elmer); final concentrations were 9 mM, 13 mM and 1 kBq/mL, respectively. The reaction was started with the homogenate, and was carried out at 37°C. Aliquots of 75 µL were introduced in tubes containing 100 µL of chilled acetone, in ice, at 0, 0.5, 1 and 2 min. The tubes were later centrifuged to obtain clear supernatants; they were dried in a vacuum-centrifuge (Thermo Scientific, Waltham, MA USA). The dry residues were dissolved in 25 µL of pure water; they were applied to silicagel TLC plates (200 µm; Macherey-Nagel, Düren, Germany), etched vertically to define 1 cm wide lanes to prevent sample overlapping. Standards of ornithine and citrulline were included each plate. The plates were developed with a mobile phase of trichloromethane: methanol: acetic acid (1:2:2 by volume). After drying, the lane with non-labelled standards was sprayed with ninhydrin, and heated with a hair dryer. The ornithine and citrulline spots were marked and the plate was cut in horizontal zones, which were counted. To limit interferences, the label in the citrulline area was expressed as a percentage of the total label counted in each TLC lane. These data allowed the calculation of newly formed citrulline; the Vi value for each sample was plotted, and considered to be an expression of V_{max} under the conditions tested.

Arginino-succinate synthase activity was measured from the condensation of aspartate with citrulline in the presence of ATP to yield argininosuccinate. Aliquots of 55 µL of homogenates were mixed with 30 µL of 70 mM hepes buffer pH 7.4, containing ATP-Na₂, MgCl₂, citrulline, aspartate (all from Sigma); final concentrations were 10 mM, 5 mM, 3 mM, and 2.5 mM, respectively. The reaction was started with aspartate, and was carried out at 37°C. The reaction was stopped with 40 µL of 30 g/L perchloric acid. The tubes were vortexed and immediately neutralized (pH 7-8) with 10 µL of 100 g/L KOH containing 62 g/L potassium bicarbonate. The tubes were vortexed again and centrifuged at 8,000xg for 15 min and 4°C. The aspartate remaining in the supernatants was measured (by transamination to oxaloacetate, and then reduced by malate dehydrogenase and NADH). Briefly, 20 µL of the supernatants were brought up to 300 µL in 96-well plates, with 66 mM phosphate buffer pH 7.4 containing NADH, 2-oxoglutarate, aspartate transaminase (pig heart) and malic acid dehydrogenase (pig heart) (all from Sigma); final concentrations were, respectively, 0.25 mM, 0.2 mM, 20 nkat/ml and 17 nkat/ml. The samples were read at 340 nM in a plate reader (Biotek, Winoosky, VT USA) for 30 min at intervals of 30 s. The fall in NADH was used to determine the levels of aspartate at each incubation time. Its disappearance (versus time zero levels) was used to determine the amount of aspartate incorporated into argininosuccinate. As in the case of ornithine carbamoyl transferase, the Vi values were plotted for each sample. In all series, a number of samples were analyzed with all reagents except citrulline: No spurious consumption of aspartate was observed.

The activity of argininosuccinate synthase was measured from the breakup of argininosuccinate to yield fumarate and arginine. This amino acid was measured in a second reaction using arginase to form ornithine and urea, which was analyzed using a chemical method. Aliquots of 38 µL of homogenates were mixed with 38 µL of 70 mM hepes buffer pH 7.4, containing argininosuccinate (Sigma); final concentration 2 mM. Incubations were carried out at 37°C for 0, 2.5, 5 and 10 min. The reaction was stopped by the addition of 40 µL of 30 g/L perchloric acid. The tubes were vortexed and brought to pH 8-9 with 10 µL of 100 g/L KOH containing 80 g/L potassium bicarbonate. The tubes were mixed again, and centrifuged for 15 min in the cold (4°C) at 8,000xg. Aliquots of 100 µL of the supernatants were mixed with 50 µL of the reacting mixture: 70 mM hepes buffer pH 7.5 (to achieve a final pH 8.5) containing MnCl₂ and arginase (rat liver, Lee Biosolutions, St Louis, MO USA); final concentrations 7 mM and 17 nkat/mL. The buffer containing Mn and arginase was activated (heated) for 5 min at 55°C before use. The reaction was allowed to develop for 30 min at 37°C, and was stopped by the addition of 35 µL 160 g/L perchloric acid. The tubes were centrifuged for 15 min at 8,000xg and 4°C. The

acidic supernatants (175 µL) were used for the estimation of urea. They were mixed with 300 µL of 90 g/L H₂SO₄ containing 270 g/L H₃PO₄; then 20 µL of 30 g/L of 1-phenyl-2-oxime-1,2-propanodione (Sigma) in absolute ethanol were added. The reaction was developed at 100°C for 30 min in a dry block heater. The absorbance of the tubes was measured at 540 nm using a plate reader, including standards of arginine and urea as well as blanks. Under these conditions, conversion of arginine to urea was complete.

Total arginase activity was measured through the estimation of the urea produced from arginine in the presence of Mn²⁺. Aliquots of 20 µL of homogenates were mixed with 5 µL of 50 mM MnCl₂. The tubes were heated for 5 min at 55°C to activate arginase. Then, the temperature was brought down to 37°C. The reaction began with the addition of 75 µL of arginine (Sigma); final concentration 78 mM. Incubations were carried out for 1, 10 and 20 min at 37°C. The reaction was stopped by the addition of 35 µL 160 g/L perchloric acid. The tubes were centrifuged at 8,000xg and 4°C for 15 min. The measurement of urea generated was done as described above for argininosuccinate lyase. Since the method used for arginase does not differentiate between arginases 1 and 2, we present a combined total arginase value that corresponds mostly to arginase 1 (expressed in all WAT sites, whilst arginase 2 was expressed only in SC WAT).

SUPPLEMENTAL TABLES

SUPPLEMENTAL TABLE 1 Plasma parameters of female Wistar rats fed for 30 d with a cafeteria diet

parameter	control	cafeteria	P diet
glucose *	8.64 ± 0.34	11.5 ± 0.3	<0.0001
lactate	3.78 ± 0.24	2.57 ± 0.21	0.0035
cholesterol	1.98 ± 0.16	2.07 ± 0.19	NS
triacylglycerols	1.69 ± 0.06	1.51 ± 0.03	0.0230
urea	5.13 ± 0.25	3.78 ± 0.20	0.0018
amino acids	3.96 ± 0.18	4.07 ± 0.12	NS

The data are the mean ± sem of 6 different animals per group, and are expressed in mM. Statistical significance of the differences between groups (one-way ANOVA). NS P>0.05.

* The values were obtained from rats anesthetized with isoflurane.

SUPPLEMENTAL TABLE 2 Urea cycle enzyme activities in WAT sites of female Wistar rats fed control or cafeteria diets

enzyme	diet	SC	ME	RP	PG	P (site)	P (diet)
Gln-dependent carbamoyl-P synthase	control	103±33	55.3±6.7	61.6±9.9	53.8±13.3	0.0248	0.0482
	cafeteria	71.4±12.6	51.5±15.4	29.7±7.2	31.3±9.2		
ornithine carbamoyl transferase	control	3871±981	2051±598	3015±579	2585±727	NS	NS
	cafeteria	2432±251	4126±472	2938±718	1793±634		
arginino-succinate synthase	control	51.7±7.5	114±15	38.3±11.0	58.5±9.2	0.0053	<0.0001
	cafeteria	17.1±5.7*	9.8±3.4*	23.5±5.9	33.6±81		
arginino-succinate lyase	control	501±108	166±37	79.8±10.3	229±75	<0.0001	NS
	cafeteria	299±72*	155±18	79.6±13.8	163±18		
arginase (total)	control	316±82	232±32	334±64	337±51	NS	NS
	cafeteria	535±218	150±23	396±187	85±23		

The data are the mean ± sem of 6 animals per group, and are presented in nkat/g of protein. Statistical significance of the differences between groups was established with a 2-way anova; post-hoc Tukey test: an * represent P<0.05 differences between diets.

SUPPLEMENTAL TABLE 3 Urea cycle enzyme gene expressions in WAT sites of female Wistar rats fed control or cafeteria diets

enzyme (gene)	diet	SC	ME	RP	PG	P (site)	P (diet)
Gln-dependent carbamoyl-P synthase, type 2 (<i>Cad</i>)	control	95.6±4.7	63.4±6.1	3.88±1.06	55.0±5.9	<0.0001	>0.0001
	cafeteria	80.0±9.9	4.10±0.95*	3.89±0.46	29.8±2.5*		
ornithine carbamoyl-transferase (<i>Otc</i>)	control	1.17±0.07	0.232±0.065	1.35±0.57	2.19±0.94	0.0061	NS
	cafeteria	0.232±0.065	0.272±0.059	0.167±0.029	0.577±0.060*		
arginino-succinate synthase 1(<i>Ass1</i>)	control	6.39±0.71	5.96±1.01	5.58±1.84	13.4±5.42	NS	0.0008
	cafeteria	5.49±0.95	1.69±0.22	0.709±0.151	1.98±0.26*		
arginino-succinate lyase (<i>Asl</i>)	control	44.9±2.4	34.5±4.9	14.8±1.45	28.0±2.82	<0.0001	<0.0001
	cafeteria	45.6±3.2	11.1±1.51*	8.39±1.25	21.1±2.55		
arginase (<i>Arg1 + Arg2</i>)	control	12.3±1.3	0.409±0.038	1.59±0.50	3.23±0.67	<0.0001	NS
	cafeteria	15.3±2.3	0.279±0.059	0.597±0.144	1.32±0.155		

The data are the mean ± sem of 6 animals per group and are expressed as fmol of the corresponding mRNA per g of protein. Statistical significance of the differences between groups was established with a 2-way anova; post-hoc Tukey test: an * represent P<0.05 differences between diets. "Total" arginase is the composite value of the sums of expressions of the genes for arginases 1 and 2, affecting only SC data, since in the other sites, only arginase 1 was detected. The separate data for arginases is shown in Supplemental Table 3.

SUPPLEMENTAL TABLE 4 Amino acid metabolism enzyme gene expressions in WAT sites of female Wistar rats fed control or cafeteria diets

enzyme (gene)	diet	SC	ME	RP	PG	P (site)	P (diet)
N-acetylglutamate synthase (<i>Nags</i>)	control	0.883±0.253	1.04±0.33	0.967±0.078	1.21±0.320	NS	0.0029
	cafeteria	0.895±0.224	0.258±0.029*	0.473±0.140	0.549±0.076		
arginase-1 (<i>Arg1</i>)	control	2.78±0.82	0.409±0.038	1.59±0.50	3.23±0.67	<0.0001	NS
	cafeteria	3.67±0.80	0.279±0.059	0.597±0.144	1.32±0.155*		
arginase-2, mitochondrial (<i>Arg2</i>)	control	11.8±2.7	--	--	--	--	--
	cafeteria	23.9±8.0	--	--	--	--	--
glutamine synthetase (<i>GluI</i>)	control	461±49	225±38	186±39	308±42	<0.0001	0.0467
	cafeteria	545±26	92.0±14.6*	105±14	249±15		
glutaminase kidney isoform, mitochondrial (<i>Gls</i>)	control	77.5±6.4	24.4±2.88	22.2±2.6	23.6±3.6	<0.0001	NS
	cafeteria	83.6±9.9	8.39±0.95	15.5±2.2	14.9±0.7		
glutamate dehydrogenase 1, mitochondrial (<i>Gld1</i>)	control	350±37	454±62	170±13	300±11	<0.0001	0.0032
	cafeteria	525±26*	195±29*	95.0±13.6	191±9		
glycine cleavage system H protein, mitochondrial (<i>Gch1</i>)	control	109±31	62.8±7.8	86.1±15.2	90.1±5.2	<0.0001	NS
	cafeteria	112±18	43.8±10.3	48.1±8.3	66.5±5.8		
AMP deaminase 2 (<i>Ampd2</i>)	control	73.5±6.7	83.9±10.0	22.0±2.4	32.4±2.7	<0.0001	0.0005
	cafeteria	75.2±13.2	16.8±5.3*	11.7±2.1	20.9±1.0		
alanine aminotransferase 1 (<i>Gpt</i>)	control	193±31	191±49	163±31	268±39	0.0116	0.0001
	cafeteria	181±12	87.7±13.2*	67.8±5.4	139±16*		
alanine aminotransferase 2 (<i>Gpt2</i>)	control	6.72±1.02	3.86±0.97	4.15±1.00	9.03±1.59	<0.0001	NS
	cafeteria	3.86±0.97	2.43±0.57	3.43±0.58	5.71±0.38*		
branched-chain-amino-acid aminotransferase, cytosolic (<i>Bcat1</i>)	control	13.6±2.9	14.4±3.3	3.20±0.42	8.31±0.95	<0.0001	NS
	cafeteria	23.0±3.6*	1.50±0.14*	2.20±0.29	4.58±0.68		
branched-chain-amino-acid aminotransferase, mitochondrial (<i>Bcat2</i>)	control	113±18	115±20	80.5±6.3	142±7	0.0001	NS
	cafeteria	180±38*	47.6±5.9*	43.8±4.7	82.4±9.6		

The data are the mean ± sem of 6 animals per group and are expressed as fmol of the corresponding mRNA per g of protein. Statistical significance of the differences between groups was established with a 2-way anova; post-hoc Tukey test: an * represent P<0.05 differences between diets.

SUPPLEMENTAL TABLE 5 Lactate dehydrogenase activity and gene expressions in WAT sites of female Wistar rats fed control or cafeteria diets

	diet	SC	ME	RP	PG	P (site)	P (diet)
lactate dehydrogenase activity (μ kat/g protein)	control	3.21 \pm 0.43	1.73 \pm 0.44	1.05 \pm 0.08	1.75 \pm 0.11	<0.0001	NS
	cafeteria	2.51 \pm 0.39	1.16 \pm 0.12	1.38 \pm 0.10	1.62 \pm 0.10		
lactate dehydrogenase a (muscle) gene expression (fmol/g protein)	control	1249 \pm 119	727 \pm 94	394 \pm 61	890 \pm 140	<0.0001	0.0178
	cafeteria	1604 \pm 160	257 \pm 24*	240 \pm 51	462 \pm 66*		
lactate dehydrogenase b (heart) gene expression (fmol/g protein)	control	750 \pm 58	774 \pm 177	496 \pm 64	719 \pm 59	<0.0001	NS
	cafeteria	983 \pm 18	552 \pm 87	313 \pm 36	505 \pm 62		

The data are the mean \pm sem of 6 animals per group. Statistical significance of the differences between groups was established with a 2-way anova; post-hoc Tukey test: different superscript letters represent P<0.05 differences.

DISCUSIÓN GENERAL

4. Discusión General

4.1. Producción basal de lactato en el tejido adiposo blanco

En la primera parte de esta tesis analizamos la producción basal de lactato en el tejido adiposo blanco. Para ello, realizamos estudios *in vitro* utilizando células 3T3L1 e *in vivo*, analizando cuatro localizaciones de tejido adiposo blanco de rata. Como antecedente contamos con varios estudios que han demostrado la capacidad de este tejido para convertir glucosa en lactato^{182,183}, y la asociación existente, similar al ciclo de Cori⁶⁸ entre el músculo y el lecho esplácnico, con la disponibilidad de glucosa¹⁸⁹.

El estudio *in vitro* tuvo como objetivo determinar la capacidad de producir lactato de los adipocitos en condiciones de normoxia. Para ello, cultivamos las células 3T3L1 (a partir de fibroblastos y también como adipocitos maduros) en condiciones estándar, en medios conteniendo concentraciones variables de glucosa (de 0 a 30 mM). Este enfoque nos permitió demostrar que los adipocitos 3T3L1 producen lactato, en condiciones de plena normoxia, desde su diferenciación como fibroblastos hasta su desarrollo como adipocitos maduros. Durante el proceso de diferenciación y desarrollo celular, comprobamos que la mayor parte de la glucosa disponible se convirtió en lactato mediante glucolisis anaerobia, con sólo una mínima proporción utilizada para la síntesis de reservas lipídicas (triacilgliceroles). Cabe resaltar que las mediciones directas de la pO₂ en el medio confirmaron que las células cultivadas tenían, de hecho, una mayor disponibilidad de oxígeno que las células de la sangre *in vivo*. Debido a la similitud del comportamiento de los adipocitos 3T3L1 con las células cancerígenas en lo que se refiere a la síntesis de lactato, nos interesamos por analizar si los adipocitos simplemente mostraban un efecto Warburg debido a una fuerte necesidad de ATP citosólico para tareas de síntesis¹⁹⁰. Los datos obtenidos descartaron que en los adipocitos se diese un efecto Warburg, ya que la capacidad de producción de lactato de los adipocitos tenía lugar en paralelo a su diferenciación celular y también a la acumulación de lípidos. Además, no se observaron indicios de proliferación celular (no incrementó el número de células; los adipocitos solo crecieron en tamaño), otro factor característico de la glucolisis activa en presencia de oxígeno¹⁹¹. Los resultados de este estudio demostraron también que los adipocitos 3T3L1 producen lactato en presencia de concentraciones variables de glucosa, lo que sugiere que el adipocito es probablemente una célula obligatoriamente glucolítica. De hecho, los adipocitos maduros fueron

inclusive capaces de sintetizar lactato con concentraciones de glucosa de 0 mM (probablemente a partir de la alanina y/o de la poca glucosa remanente del cambio de medios de cultivo previos).

En lo que respecta al análisis de la expresión de los principales genes que controlan el metabolismo glucídico y lipídico de los adipocitos, la concentración de glucosa del medio de cultivo no afectó la expresión de las enzimas implicadas en la síntesis de lípidos, pero modificó, en cambio, la expresión de las enzimas implicadas en la lipólisis e incorporación de ácidos grasos exógenos. Al parecer, bajo las condiciones estudiadas, el punto clave de control metabólico se encontraría en la entrada y eliminación del carbono de la glucosa; la baja expresión de los genes de las enzimas que regulan estos procesos (hexoquinasa *Hk2* y lactato deshidrogenasa *Ldh*), principalmente en los adipocitos sometidos a elevadas concentraciones de glucosa, podrían justificar esta hipótesis. A pesar de la expresión génica limitada de la lactato deshidrogenasa, la tasa de síntesis de lactato se mantuvo elevada incluso en los adipocitos cultivados con concentraciones de glucosa muy altas (22 y 30 mM). Por otro lado, la estabilidad de la pO_2 en los medios de cultivo frente a concentraciones variables de glucosa confirmó que no había relación entre la disponibilidad del principal substrato de los adipocitos y el metabolismo oxidativo.

La información que nos aporta este estudio sugiere que los adipocitos 3T3L1 son esencialmente anaeróbicos, incluso durante la lipogénesis y almacenamiento de triacilgliceroles. Sin embargo, no debe perderse de vista que el tejido adiposo blanco contiene, además de adipocitos, otros tipos celulares que en principio son esencialmente aeróbicos (estroma), y por ende el tejido adiposo blanco como un todo podría ser más susceptible a la hipoxia que su principal constituyente, el adipocito.

La segunda fase de este estudio, realizada *in vivo*, se centró en definir la influencia de la localización del tejido adiposo, el sexo y la dieta en la capacidad del tejido adiposo para producir lactato. Utilizamos cuatro localizaciones de tejido adiposo blanco (subcutáneo, mesentérico, retroperitoneal y perigonadal) de ratas Wistar adultas, hembras y machos, sometidas durante 30 días a una dieta control o hiperlipídica ("de cafetería"). Los datos obtenidos mostraron una diferencia considerable en el potencial de síntesis de lactato entre las diversas localizaciones de tejido adiposo blanco, tal y como indican las diferencias de expresión génica y de actividad de la lactato deshidrogenasa. Al analizar en profundidad los resultados, encontramos una relación directa, independiente de la

localización, sexo y dieta, entre la actividad de la enzima y la presencia de lactato en las diferentes masas de tejido adiposo investigadas. Al calcular las relación entre la molalidad de lactato del tejido adiposo y la del plasma pudimos constatar que en todas las localizaciones estudiadas la concentración de lactato era mayor en el agua del tejido que en la del plasma. Por consiguiente, el lactato del tejido adiposo blanco, debido a la existencia de un marcado gradiente en contra, no podía provenir del plasma, por lo que necesariamente ha tenido que ser sintetizado en el propio tejido adiposo. Evidentemente, el exceso de lactato producido es liberado al plasma (siguiendo el gradiente) y captado por el hígado¹⁹² donde se oxida a piruvato que luego se incorpora al metabolismo hepático. Bajo condiciones de exceso de glucosa y ácidos grasos (como las que genera la dieta de cafetería), la gluconeogénesis hepática deviene un destino improbable¹⁹³, igual que la cetogénesis, que se inhibe por la presencia de glucosa¹⁹⁴. Prácticamente el único camino abierto para utilizar el piruvato es la lipogénesis, que es plenamente operativa en el hígado a partir de lactato¹⁹⁵. En consecuencia, el destino más probable del lactato generado por el tejido adiposo, que como hemos comprobado se sintetiza en grandes proporciones tanto en adipocitos *in vitro* como en el tejido adiposo blanco *in vivo*, es su incorporación a la lipogénesis hepática, que da lugar, finalmente, a su exportación como triacilgliceroles de lipoproteínas. El tejido adiposo ha podido evitar la incorporación de un exceso de glucosa a sus reservas grasas mediante su conversión a lactato y bloqueo efectivo de la lipogénesis, pero no puede evitar incorporar los ácidos grasos transportados por las lipoproteínas (y que proceden de la misma glucosa-lactato) a sus reservas de triacilgliceroles gracias a la lipoproteína lipasa y las proteínas transportadoras de ácidos grasos. El lípido del tejido adiposo procede del exceso de glucosa, pero la lipogénesis es hepática.

La ingesta prolongada de una dieta hiperlipídica (“de cafetería”) conduce a un estado proinflamatorio¹⁹⁶, que generalmente se asocia a hipoxia¹⁹⁷. Sin embargo, contrariamente a lo que esperábamos, no encontramos incrementos ni en la actividad lactato deshidrogenasa ni en el contenido de lactato del tejido adiposo de las ratas alimentadas con dieta de cafetería en comparación con los controles. La relación directa entre la actividad de la lactato deshidrogenasa y la capacidad, observada *in vitro*, del adipocito de producir lactato en condiciones de normoxia, sugieren que el factor crítico de la producción de lactato no es la hipoxia. Estos resultados resaltan la necesidad de revisar en profundidad la relación propuesta entre la inflamación y la hipoxia en el

síndrome metabólico.

El análisis de la expresión de los genes más relevantes del metabolismo glucídico y lipídico mostraron algunas diferencias asociadas al sexo, pero los efectos más destacados fueron los debidos a la exposición a una dieta “de cafetería”. La consecuencia fue el incremento de la masa de tejido adiposo blanco, representada por un mayor número y tamaño de los adipocitos. Estos resultados están de acuerdo con los publicados en otros estudios ¹⁹⁸. Cabe resaltar que la expresión de algunos genes asociados a la captación y utilización de glucosa (*Glut4*, hexoquinasa 2, lactato deshidrogenasas y piruvato deshidrogenasa quinasa 4) fueron similares en el tejido adiposo de las ratas alimentadas con una dieta “de cafetería” y en los adipocitos 3T3L1 cultivados con concentraciones elevadas de glucosa. En ambos casos, la entrada de glucosa a las células probablemente estaba limitada, tal y como muestran las bajas expresiones de *Glut4* y hexoquinasa 2. Este perfil de expresión génica puede ser parte de un mecanismo de defensa del tejido adiposo ante el exceso sostenido de disponibilidad de energía ¹⁹⁹ que convierte a este tejido en el último destino del exceso de glucosa circulante ²⁰⁰. Sin embargo, y a pesar de la baja expresión del gen de la lactato deshidrogenasa, las concentraciones de lactato tisular y la estabilidad en la expresión del gen de la piruvato deshidrogenasa quinasa 4 apuntan a una efectividad limitada de la caída de la expresión de los genes del *Glut4* y de la hexoquinasa en cuanto a frenar el flujo de entrada de glucosa a la célula, y con ello su ulterior conversión a lactato. Como se ha evidenciado en otras publicaciones ^{51, 201}, la dieta hiperlipídica “de cafetería” también inhibe la expresión de los genes lipogénicos, y, una vez mas, la glucosa disponible intracelular es derivada mayoritariamente hacia la producción de lactato.

La principal conclusión de este primera parte de la tesis es que el tejido adiposo blanco, en especial los adipocitos, producen lactato en condiciones de oxigenación normal, es decir, en ausencia de hipoxia, independientemente de su localización, del sexo o del carácter de la dieta consumida. Esta producción es una consecuencia inmediata de una importante actividad de la lactato deshidrogenasa. Creemos que la principal función de esta vía de la lactato deshidrogenasa en el tejido adiposo blanco es la de convertir el exceso de glucosa en fragmentos de 3 carbonos como una manera de ayudar a controlar la glucemia y/o proveer substratos de cadena corta, fácilmente metabolizables, a otros tejidos. Los elevados niveles circulantes de lactato observados en personas

obesas²³ apoyan indirectamente esta interpretación, y sugieren un nuevo rol del tejido adiposo en el control de la glucemia.

4.2. Estudio del metabolismo de los aminoácidos en el tejido adiposo blanco

Desde el descubrimiento de la leptina se ha investigado mucho sobre las funciones paracrinas, endocrinas y de regulador metabólico del tejido adiposo⁷⁸. Sin embargo, nuestro conocimiento sobre el metabolismo del tejido adiposo blanco, especialmente en lo que respecta al metabolismo nitrogenado, sigue siendo considerablemente limitado, tal y como lo demuestran las escasas publicaciones que tratan sobre este tema^{104, 130}. El tejido adiposo blanco tiene enzimas del metabolismo del amonio plenamente funcionales, como la glutamina sintetasa¹¹⁶, la glutaminasa¹¹⁷, y la AMP desaminasa¹¹⁹, pero, a pesar de disponer de datos aislados, no se han estudiado a fondo los procesos metabólicos que afectan a los aminoácidos en este tejido, olvidando, sobre todo, la posible implicación e importancia cuantitativa de estas vías en el contexto del metabolismo global de los aminoácidos.

En este apartado, hemos analizado las principales bases bioquímicas del metabolismo de los aminoácidos en el tejido adiposo blanco, centrados en el funcionamiento de la principal vía catabólica, el ciclo de la urea. Estudiamos cuatro localizaciones distintas de tejido adiposo blanco (subcutáneo, mesentérico, retroperitoneal y perigonadal) de ratas Wistar adultas, hembras y machos, sometidas durante 30 días a una dieta control o hiperlipídica (“de cafetería”). Los resultados obtenidos mostraron claramente la presencia de todas las enzimas del ciclo de la urea en el tejido adiposo blanco. La magnitud de sus actividades variaron según la localización estudiada, pero todas las enzimas se expresaron en grado suficiente como para justificar el funcionamiento del ciclo. Esta información se reforzó con la detección de todas las actividades enzimáticas del ciclo de la urea en las cuatro localizaciones estudiadas, que constituyen, desde un punto de vista cuantitativo, una importante proporción del total del tejido y las masas con mayor tamaño en la rata.

Cuando analizamos las expresiones génicas y las actividades de las enzimas del ciclo de la urea encontramos un alto grado de uniformidad entre las localizaciones de tejido adiposo estudiadas, en buena medida independientes del sexo y la dieta. Esta

estabilidad contrasta con otras vías metabólicas (como la lipogénesis y otros aspectos del propio metabolismo de los aminoácidos), lo que, a nuestro juicio, evidencia de que la función del ciclo de la urea debe ser lo suficientemente importante (y bien regulada en el tejido adiposo en su conjunto) como para no ser afectada por otros factores o variables (dieta, hormonas sexuales, etc.). Dado que la dieta de cafetería aumenta significativamente los depósitos de grasa, la estabilidad del ciclo de la urea se pudo mantener gracias a una disminución relativa (de hecho, coordinada) de la expresión de los genes correspondientes, junto con pequeños ajustes en las actividades enzimáticas. Cabe resaltar, que la marcada estabilidad del ciclo de la urea en el tejido adiposo de las ratas sometidas a dieta de cafetería contrasta con la fuerte caída de su actividad global en el hígado ²⁰², por lo que creemos que en la obesidad podría producirse urea, al menos en parte, en el tejido adiposo blanco.

Las expresiones de las enzimas del ciclo de la urea estaban claramente interrelacionadas, con la notable excepción de la arginino-succinato sintetasa, enzima controladora del ciclo ²⁰³, y la liasa que la acompaña y complementa en la síntesis de arginina; ambas mostraron también actividades más bajas que las demás enzimas del ciclo de la urea. Esta discordancia, frente a la uniformidad global de la regulación génica, unida a la falta de correlación entre dicha expresión y la actividad de las enzimas del arginino-succinato sugieren una posible modulación post-transcripcional ²⁰⁴ de esta sección del ciclo. Las grandes diferencias observadas entre las enzimas en lo que respecta a las ratios de actividad/ expresión génica sugieren la existencia de un probable mecanismo adicional de regulación por inactivación/ activación o regulación de su recambio, modulando así la vida activa real de las enzimas. Una ratio de actividad/ expresión mayor, como es el caso de la ornitina transcarbamila, podría corresponder a una mayor vida media (o una menor tasa de recambio) en comparación con las enzimas de control como la carbamoil-fosfato sintetasa y, especialmente, la arginino-succinato sintetasa. En resumen, el ciclo de la urea del tejido adiposo presenta un control génico global, que afecta a todas las localizaciones estudiadas, combinado con la regulación específica de dos puntos clave ya conocidos: las síntesis del carbamoil-fosfato ²⁰⁵ y la de arginino-succinato ²⁰⁴.

A pesar de la gran cantidad de grasa que contiene el tejido adiposo blanco, es importante señalar que los adipocitos y la fracción estromal-vascular presentan una considerable actividad metabólica ²⁰⁶, regulada en cada una de las localizaciones

mediante un patrón substancialmente uniforme⁵¹, lo que permite actuar al tejido como un único órgano disperso²⁰⁷. De hecho, las expresiones y actividades de las enzimas del ciclo de la urea encontradas en este estudio, especialmente las de la arginino-succinato liasa y la ornitina transcarbamila, estaban en el mismo rango (por unidad de proteína tisular) que las del hígado. Cuando comparamos la capacidad catalítica conjunta de las cuatro principales localizaciones del tejido adiposo y la del hígado, la capacidad global del hígado era patente. Sin embargo, estos cuatro depósitos grasos contienen en promedio la mitad del tejido adiposo blanco de la rata, lo que podría, teóricamente, rebajar a la mitad las diferencias con el hígado al considerar el tejido adiposo como un órgano único. Asimismo, estas comparaciones se modifican notablemente en la obesidad. En suma, la posible capacidad del ciclo de la urea del tejido adiposo blanco podría ser cuantitativamente importante y en este sentido sólo comparable al hígado.

La elevada actividad de la ornitina transcarbamila, comparada con la baja actividad de la arginino-succinato sintetasa, probablemente indican que el rol principal del ciclo de la urea del tejido adiposo blanco sea la síntesis de citrulina, más que la producción de urea. Este enfoque se observó en las cuatro localizaciones de tejido adiposo, lo que estaría de acuerdo con una elevada demanda periférica de citrulina. Este aminoácido es un importante regulador del metabolismo²⁰⁸, y sus niveles se encuentran íntimamente relacionados con los de arginina²⁰⁹, siendo la citrulina un proveedor más efectivo de arginina que la arginina misma²¹⁰; la citrulina se sintetiza principalmente en el intestino²¹¹ (incluyendo el tejido adiposo mesentérico), pero es el riñón quien la utiliza preferentemente en condiciones basales para convertirla en arginina, aunque se ha observado que la producción renal de arginina a partir de citrulina es mayor que la capacidad de síntesis intestinal²¹². A partir de estos datos, postulamos que el tejido adiposo blanco podría justificar esta diferencia gracias a la importante actividad de la ornitina transcarbamila descrita en este estudio. En el caso de esta enzima, la diferencia entre el tejido adiposo y el riñón en cuanto al mantenimiento de la producción de arginina estribaría en la dependencia renal de la producción intestinal de citrulina, así como de su posible retención por el hígado. Quizás, al contrario que en el intestino, la capacidad de generación de citrulina y arginina por el tejido adiposo blanco es más independiente de la dieta por lo que su producción no estaría relacionada con la disponibilidad de nitrógeno amínico que regula el funcionamiento del ciclo de la urea en

el eje intestino-hígado.

Tanto el tejido adiposo blanco como el hígado, mostraron un marcado gradiente molal plasma/ tejido para los productos del ciclo de la urea, que resulta incompatible con su posible captación a partir de la sangre. Este gradiente indica claramente que el flujo de citrulina, arginina y urea va de las células del tejido adiposo hacia el plasma y no viceversa. Es decir, hay una síntesis neta de intermediarios o productos del ciclo en el tejido adiposo. Adicionalmente, las actividades enzimáticas de los tejidos evaluados mostraron un claro paralelismo con las molalidades medidas de dichos productos.

Nuestros resultados también demostraron que el metabolismo de los aminoácidos en las diferentes localizaciones de tejido adiposo blanco presentaba tanto niveles de actividad enzimática como expresiones génicas muy por encima de lo que cabría esperar por su aparente mínima importancia en dicho metabolismo. La marcada influencia del sexo y la dieta, dependiente de la localización, refuerzan esta asunción, y nos muestra otra faceta, la de la variabilidad de su orientación como parte de su postulado papel regulador global. Las expresiones observadas para las enzimas relacionadas al metabolismo de los aminoácidos estaban en el rango de 5-500 fmol por g de proteína en las cuatro localizaciones de tejido adiposo blanco estudiadas. En comparación, el número de tránscritos relacionados con la lipogénesis, y otras expresiones asociadas al metabolismo de los lípidos se encontraban en el rango de 10-1000 fmol por g de proteína. Por ende, las diferencias entre las expresiones de la lipogénesis y de los genes asociados al metabolismo de aminoácidos no fueron tan amplias como esperábamos, teniendo en cuenta la función básica de depósito y movilización de triacilgliceroles de los adipocitos, el bajo nivel de proteínas celulares²¹³ y la relativamente pequeña masa de citoplasma del tejido adiposo blanco.

Nuestros datos sugieren que la expresión de algunos genes de las enzimas del metabolismo de los aminoácidos, lípidos y glúcidos muestran una marcada interacción de los factores localización-sexo-dieta que da lugar a claras diferencias entre los grupos. Así, en comparación con otras localizaciones, el tejido adiposo subcutáneo mostró una mayor actividad (y/o expresión génica) de las enzimas del metabolismo de aminoácidos, más marcada en las ratas macho. Debido a su localización, y relación con la piel²¹⁴ y su biota²¹⁵, estos resultados podrían relacionarse con la mayor expresión de la óxido nítrico sintasa y la arginasa 2. Los mayores niveles de expresión génica de las enzimas relacionadas con la glutamina, y de las transaminasas de cadena ramificada¹⁵⁰ indican,

también, un intenso metabolismo de los aminoácidos. El gran tamaño global del tejido adiposo le puede conferir, además, un papel importante en este metabolismo. Asimismo, los animales sometidos a una dieta “de cafetería” mostraron actividades del metabolismo de aminoácidos en el tejido adiposo mesentérico relativamente más bajas que en otras localizaciones, que se compensó en parte por la mayor actividad del tejido adiposo subcutáneo. Estas modificaciones del protagonismo del lecho esplácnico hacia los tejidos periféricos está de acuerdo con la pérdida del control de los substratos energéticos por parte del hígado ^{216, 217} (y quizás del intestino) en el síndrome metabólico.

Por lo que respecta al metabolismo glucídico y al lipídico, la expresión de las enzimas lipogénicas y de aquellos genes que favorecen la incorporación de la glucosa (*Glut4* y hexoquinasa 2) al tejido fue más elevada en el tejido adiposo blanco de las hembras que en los machos. En contraposición a esta situación, el tejido adiposo subcutáneo de los machos contenía una mayor cantidad de tránscritos para los genes relacionados a la oxidación de lípidos que el de las hembras, lo que podría indicar una tendencia hacia la utilización de ácidos grasos como fuente de energía. La probable mayor inhibición de la piruvato deshidrogenasa en los machos, generalizada en la mayoría de localizaciones de tejido adiposo, refuerza esta hipótesis. El análisis del metabolismo glucídico y lipídico que hemos incluido en nuestro estudio se realizó para obtener datos con los que comparar el metabolismo de aminoácidos debido a la limitada información disponible sobre éste último. Sin embargo, se han observado diferencias mayores de las esperadas, por lo que esta parte requiere ser estudiada más a fondo, y con un enfoque más globalizado para poder extraer conclusiones claras al integrar en el análisis el metabolismo de los aminoácidos en sus dos vertientes, el nitrógeno amínico y el esqueleto hidro-carbonado.

La información aportada en el presente estudio demuestra, por primera vez, que el tejido adiposo blanco presenta un ciclo de la urea completo y funcional sometido a un control centralizado, independiente de factores externos como la localización de sus depósitos, el sexo (las hormonas sexuales) y la dieta (su contenido lipídico/ energético), que afecta al tejido como un todo, lo que refuerza la idea de que nos encontramos ante un único órgano disperso que funciona de modo coordinado. Es probable que la principal función de este ciclo sea la de controlar la disponibilidad de arginina mediante la síntesis activa de citrulina. Esta capacidad del tejido adiposo le permitiría comportarse como una

importante fuente extra-intestinal de citrulina, con lo que su papel sería el de ayudar a mantener una plena disponibilidad de arginina, en buena medida independiente del aporte alimentario y del funcionamiento esplácnico del ciclo de la urea. Asimismo, los resultados obtenidos en este apartado han mostrado que el tejido adiposo blanco tiene una importante participación en el metabolismo de los aminoácidos, mostrando diferencias asociadas con la dieta, pero especialmente con el sexo, por lo que respecta a la producción y destoxicificación del amonio.

En nuestra opinión, el potencial metabólico y de control del tejido adiposo blanco dentro del contexto global del metabolismo energético es más importante de lo que habitualmente se supone, de modo que probablemente sólo sea comparable al del hígado.

CONCLUSIONES

5. Conclusiones

1. El tejido adiposo blanco participa en el mantenimiento de la glucemia al metabolizar la glucosa a lactato en grandes cantidades mediante la vía glucolítica. Hemos observado que esta actividad es proporcional a la disponibilidad de glucosa, en condiciones de normoxia, sin que se produzca una síntesis significativa de lípidos; en condiciones normales, por tanto, el tejido adiposo blanco (adipocitos) es esencialmente anaerobio.
2. Las diferentes masas de tejido adiposo blanco responden a procesos de regulación uniformes a pesar de sus amplias diferencias en cuanto a su composición, funcionalidad, distribución anatómica y nivel de actividad metabólica, reforzando la idea de que nos encontramos ante un único órgano disperso que funciona de modo coordinado.
3. Se ha comprobado que el tejido adiposo blanco tiene una importante implicación en el metabolismo de los aminoácidos, mostrando diferencias asociadas a la dieta, pero especialmente al sexo, en lo que respecta a la producción y destoxicificación del amonio.
4. Se ha hallado, por primera vez, un ciclo de la urea extrahepático completo, activo y funcional en todas las localizaciones de tejido adiposo blanco estudiadas, y cuya actividad global sería sólo comparable a la del hígado. Es probable que este ciclo funcione a demanda, aunque su principal objetivo podría ser la de controlar la disponibilidad de arginina.

BIBLIOGRAFÍA

6. Bibliografía citada

1. O'Rahilly, S. Science, medicine, and the future. Non-insulin dependent diabetes mellitus: the gathering storm. *British Medical Journal* **314**, 955–959 (1997).
2. WHO | Obesity and overweight. (2015). at <<http://www.who.int/mediacentre/factsheets/fs311/en/>>
3. Alemany, M. Metabolic syndrome: a multifaceted disease of affluence. *Journal of Endocrinology and Metabolism* **2**, 155–165 (2012).
4. Sorrentino, M. J. Implications of the metabolic syndrome: the new epidemic. *American Journal of Cardiology* **96**, E3–E7 (2005).
5. Oda, E. Metabolic syndrome: its history, mechanisms, and limitations. *Acta Diabetologica* **49**, 89–95 (2012).
6. Desroches, S. & Lamarche, B. The evolving definitions and increasing prevalence of the metabolic syndrome. *Applied Physiology, Nutrition, and Metabolism* **32**, 23–32 (2007).
7. Bruce, K. D. & Byrne, C. D. The metabolic syndrome: common origins of a multifactorial disorder. *Postgraduate Medical Journal* **85**, 614–621 (2009).
8. Alemany, M. Adjustment to dietary energy availability: from starvation to overnutrition. *RSC Advances* **3**, 1636–1651 (2013).
9. Alemany, M. The defense of adipose tissue against excess substrate-induced hyperthrophia: immune system cell infiltration and arrested metabolic activity. *Journal of Clinical Endocrinology and Metabolism* **96**, 66–68 (2011).
10. Taylor, P. D. et al. Impaired glucose homeostasis and mitochondrial abnormalities in offspring of rats fed a fat-rich diet in pregnancy. *American Journal of Physiology* **288**, R134–R139 (2005).
11. Ingvorsen, C., Brix, S., Ozanne, S. E. & Hellgren, L. I. The effect of maternal inflammation on fetal programming of metabolic disease. *Acta Physiologica* **214**, 440–449 (2015).
12. Leibel, N. I., Baumann, E. E., Kocherginsky, M. & Rosenfield, R. L. Relationship of adolescent polycystic ovary syndrome to parental metabolic syndrome. *Journal of Clinical Endocrinology and Metabolism* **91**, 1275–1283 (2006).
13. Wang, J. et al. Nutrition, epigenetics, and metabolic syndrome. *Antioxidants & Redox Signaling* **17**, 282–301 (2012).
14. Tremblay, A. Nutritional determinants of the insulin resistance syndrome. *International Journal of Obesity* **19 Suppl 1**, S60–S68 (1995).
15. Dandona, P., Aljada, A., Chaudhuri, A., Mohanty, P. & Garg, R. Metabolic syndrome: a comprehensive perspective based on interactions between obesity, diabetes, and inflammation. *Circulation* **111**, 1448–1454 (2005).
16. Alemany, M. Utilization of dietary glucose in the metabolic syndrome. *Nutrition & Metabolism* **8**, 74 (2011).

17. Reaven, G. M. Hypothesis: muscle insulin resistance is the ('not so') thrifty genotype. *Diabetologia* **41**, 482–484 (1998).
18. O'Connell, R. C., Morgan, A. P., Aoki, T. T., Ball, M. R. & Moore, F. D. Nitrogen conservation in starvation: graded responses to intravenous glucose. *Journal of Clinical Endocrinology and Metabolism* **39**, 555–563 (1974).
19. Shimomura, I., Bashmakov, Y. & Horton, J. D. Increased levels of nuclear SREBP-1c associated with fatty livers in two mouse models of diabetes mellitus. *Journal of Biological Chemistry* **274**, 30028–30032 (1999).
20. Gauthier, M.-S., Favier, R. & Lavoie, J.-M. Time course of the development of non-alcoholic hepatic steatosis in response to high-fat diet-induced obesity in rats. *British Journal of Nutrition* **95**, 273 (2007).
21. Strömlad, G. & Björntorp, P. Reduced hepatic insulin clearance in rats with dietary-induced obesity. *Metabolism: Clinical and Experimental* **35**, 323–327 (1986).
22. Sethi, J. K. & Vidal-Puig, A. J. Thematic review series: adipocyte biology. Adipose tissue function and plasticity orchestrate nutritional adaptation. *Journal of Lipid Research* **48**, 1253–1262 (2007).
23. DiGirolamo, M., Newby, F. D. & Lovejoy, J. Lactate production in adipose tissue: a regulated function with extra-adipose implications. *FASEB Journal* **6**, 2405–2412 (1992).
24. Apovian, C. M. & Mechanick, J. I. Obesity IS a disease! *Current Opinion in Endocrinology, Diabetes, and Obesity* **20**, 367–368 (2013).
25. Pingali, P. L. Green revolution: impacts, limits, and the path ahead. *Proceedings of the National Academy of Sciences of the United States of America* **109**, 12302–12308 (2012).
26. Schmidhuber, J. & Shetty, P. The nutrition transition to 2030. Why developing countries are likely to bear the major burden. *Food Economics* **2**, 150–166 (2005).
27. Depner, C. M., Stothard, E. R. & Wright, K. P. Metabolic consequences of sleep and circadian disorders. *Current Diabetes Reports* **14**, 507 (2014).
28. Hill, P. L., Weston, S. J. & Jackson, J. J. Connecting social environment variables to the onset of major specific health outcomes. *Psychology & Health* **29**, 753–767 (2014).
29. Bray, G. A. Obesity is a chronic, relapsing neurochemical disease. *International Journal of Obesity* **28**, 34–38 (2004).
30. Bray, G. A. Obesity: the disease. *Journal of Medicinal Chemistry* **49**, 4001–4007 (2006).
31. Dabelea, D. *et al.* Birth weight, type 2 diabetes, and insulin resistance in Pima Indian children and young adults. *Diabetes Care* **22**, 944–950 (1999).
32. Bhargava, S. K. *et al.* Relation of serial changes in childhood body-mass index to impaired glucose tolerance in young adulthood. *New England Journal of Medicine* **350**, 865–875 (2004).
33. Owen, C. G. Effect of infant feeding on the risk of obesity across the life course: a quantitative review of published evidence. *Pediatrics* **115**, 1367–1377 (2005).

34. Loos, R. J. F. Recent progress in the genetics of common obesity. *British Journal of Clinical Pharmacology* **68**, 811–829 (2009).
35. van Dijk, S. J., Molloy, P. L., Varinli, H., Morrison, J. L. & Muhlhausler, B. S. Epigenetics and human obesity. *International Journal of Obesity* **39**, 85–97 (2015).
36. Rankinen, T. *et al.* The human obesity gene map: the 2005 update. *Obesity* **14**, 529–644 (2006).
37. Halaas, J. *et al.* Weight-reducing effects of the plasma protein encoded by the obese gene. *Science* **269**, 543–546 (1995).
38. Li, S. *et al.* Cumulative effects and predictive value of common obesity-susceptibility variants identified by genome-wide association studies. *American Journal of Clinical Nutrition* **91**, 184–190 (2009).
39. Frayling, T. M. *et al.* A common variant in the FTO gene is associated with body mass index and predisposes to childhood and adult obesity. *Science* **316**, 889–894 (2007).
40. Hervey, G. R. Regulation of energy balance. *Nature* **222**, 629–631 (1969).
41. Alemany, M. Steroid hormones interrelationships in the metabolic syndrome: an introduction to the ponderostat hypothesis. *Hormones* **11**, 272–289
42. Mayer, J. Glucostatic mechanism of regulation of food intake. *New England Journal of Medicine* **249**, 13–16 (1953).
43. Jacques, L. M., Michel, D., Jean-Pierre, G., Jeanine, L.-S. & Suzanne, T. Role of lipostatic mechanism in regulation by feeding of energy balance in rats. *Journal of Comparative Physiological Psychology* **84**, 1–23 (1973).
44. Zhang, Y. *et al.* Positional cloning of the mouse obese gene and its human homologue. *Nature* **372**, 425–432 (1994).
45. Remesar, X. *et al.* Oral oleoyl-estrone induces the rapid loss of body fat in Zucker lean rats fed a hyperlipidic diet. *International Journal of Obesity* **24**, 1405–1412 (2000).
46. Keesey, R. E. & Hirvonen, M. D. Body weight set-points: determination and adjustment. *Journal of Nutrition* **127**, S1875–1883 (1997).
47. Faust, I., Johnson, P., Stern, J. & Hirsch, J. Diet-induced adipocyte number increase in adult rats: a new model of obesity. *American Journal of Physiology* **235**, E279–E286 (1978).
48. Schwartz, M. W., Woods, S. C., Porte, D., Seeley, R. J. & Baskin, D. G. Central nervous system control of food intake. *Nature* **404**, 661–671 (2000).
49. Cinti, S. The adipose organ at a glance. *Disease Models & Mechanisms* **5**, 588–594 (2012).
50. Cinti, S. The adipose organ: morphological perspectives of adipose tissues. *Proceedings of the Nutrition Society* **60**, 319–328 (2001).

51. Romero, M. D. M. *et al.* Treatment of rats with a self-selected hyperlipidic diet, increases the lipid content of the main adipose tissue sites in a proportion similar to that of the lipids in the rest of organs and tissues. *PLoS ONE* **9**, e90995 (2014).
52. Klaus, S. & Keijer, J. Gene expression profiling of adipose tissue: individual, depot-dependent, and sex-dependent variabilities. *Nutrition* **20**, 115–120 (2004).
53. Giordano, A., Smorlesi, A., Frontini, A., Barbatelli, G. & Cint, S. White, brown and pink adipocytes: the extraordinary plasticity of the adipose organ. *European Journal of Endocrinology* **170**, R159–R171 (2014).
54. Granneman, J. G., Li, P., Zhu, Z. & Lu, Y. Metabolic and cellular plasticity in white adipose tissue I: effects of beta3-adrenergic receptor activation. *American Journal of Physiology* **289**, E608–E616 (2005).
55. Wu, J. *et al.* Beige adipocytes are a distinct type of thermogenic fat cell in mouse and human. *Cell* **150**, 366–376 (2012).
56. Nedergaard, J., Bengtsson, T. & Cannon, B. New powers of brown fat: fighting the metabolic syndrome. *Cell Metabolism* **13**, 238–240 (2011).
57. Seale, P. *et al.* PRDM16 controls a brown fat/skeletal muscle switch. *Nature* **454**, 961–967 (2008).
58. Richert, M. M., Schwertfeger, K. L., Ryder, J. W. & Anderson, S. M. An atlas of mouse mammary gland development. *Journal of Mammary Gland Biology and Neoplasia* **5**, 227–241 (2000).
59. Morroni, M. *et al.* Reversible transdifferentiation of secretory epithelial cells into adipocytes in the mammary gland. *Proceedings of the National Academy of Sciences of the United States of America* **101**, 16801–16806 (2004).
60. Crandall, D. L., Hausman, G. J. & Kral, J. G. A review of the microcirculation of adipose tissue: anatomic, metabolic, and angiogenic perspectives. *Microcirculation* **4**, 211–232 (1997).
61. Alemany, M. & Fernandez-Lopez, J. Adipose tissue: something more than just adipocytes. *Current Nutrition & Food Science* **2**, 141–150 (2006).
62. Hausaman, G. in *New perspectives in adipose tissue: structure, function and development*. (eds. Cryer, A. & Van, R.) 1–21 (Butterworths, 1985).
63. Tang, W. *et al.* White fat progenitor cells reside in the adipose vasculature. *Science* **322**, 583–586 (2008).
64. Sanchez-Gurmaches, J. & Guertin, D. A. Adipocyte lineages: tracing back the origins of fat. *Biochimica et Biophysica Acta* **1842**, 340–351 (2014).
65. Rutkowski, J. M., Stern, J. H. & Scherer, P. E. The cell biology of fat expansion. *Journal of Cell Biology* **208**, 501–512 (2015).
66. Nielsen, T. S., Jessen, N., Jørgensen, J. O. L., Møller, N. & Lund, S. Dissecting adipose tissue lipolysis: molecular regulation and implications for metabolic disease. *Journal of Molecular Endocrinology* **52**, R199–R222 (2014).

67. Hauner, H. The new concept of adipose tissue function. *Physiology & Behavior* **83**, 653–658 (2004).
68. Cori, C. F. The glucose-lactic acid cycle and gluconeogenesis. *Current Topics in Cellular Regulation* **18**, 377–387 (1981).
69. Felig, P. The glucose-alanine cycle. *Metabolism: Clinical and Experimental* **22**, 179–207 (1973).
70. Randle, P. J., Garland, P. B., Hales, C. N. & Newsholme, E. A. The glucose fatty acid-cycle its role in insulin sensitivity and the metabolic disturbance of diabetes mellitus. *Lancet* **281**, 785–789 (1963).
71. Frayn, K. N. in *Metabolic regulation. A human perspective*. (ed. Frayn, K. N.) 151–189 (Blackwell Publishing, 2003).
72. Kowalski, T. J., Wu, G. & Watford, M. Rat adipose tissue amino acid metabolism in vivo as assessed by microdialysis and arteriovenous techniques. *American Journal of Physiology* **273**, E613–E622 (1997).
73. López-Soriano, F. J. & Alemany, M. Activities of enzymes of amino acid metabolism in rat brown adipose tissue. *Biochemistry International* **12**, 471–478 (1986).
74. Arriarán, S. et al. Evidences of basal lactate production in the main white adipose tissue sites of rats. Effects of sex and a cafeteria diet. *PLoS ONE* **10**, e0119572 (2015).
75. Wang, P., Mariman, E., Renes, J. & Keijer, J. The secretory function of adipocytes in the physiology of white adipose tissue. *Journal of Cellular Physiology* **216**, 3–13 (2008).
76. Caspar-Bauguil, S. et al. Adipose tissues as an ancestral immune organ: site-specific change in obesity. *FEBS Letters* **579**, 3487–3492 (2005).
77. Patrick, C. W. Tissue engineering strategies for adipose tissue repair. *The Anatomical Record* **263**, 361–366 (2001).
78. Kershaw, E. E. & Flie, J. S. Adipose tissue as an endocrine organ. *Journal of Clinical Endocrinology and Metabolism* **89**, 2548–2556 (2004).
79. Trayhurn, P. & Beattie, J. H. Physiological role of adipose tissue: white adipose tissue as an endocrine and secretory organ. *Proceedings of the Nutrition Society* **60**, 329–339 (2001).
80. Fraser, J. K., Wulur, I., Alfonso, Z. & Hedrick, M. H. Fat tissue: an underappreciated source of stem cells for biotechnology. *Trends in Biotechnology* **24**, 150–154 (2006).
81. Rondinone, C. M. Adipocyte-derived hormones, cytokines, and mediators. *Endocrine* **29**, 81–90 (2006).
82. Yang, W. S. et al. Weight reduction increases plasma levels of an adipose-derived anti-inflammatory protein, adiponectin. *Journal of Clinical Endocrinology and Metabolism* **86**, 3815–3819 (2001).
83. Strissel, K. J. et al. Adipocyte death, adipose tissue remodeling, and obesity complications. *Diabetes* **56**, 2910–2918 (2007).

84. Karlsson, C. *et al.* Human adipose tissue expresses angiotensinogen and enzymes required for its conversion to angiotensin II. *Journal of Clinical Endocrinology and Metabolism* **83**, 3925–3929 (1998).
85. Gude, M. F. *et al.* The production and regulation of IGF and IGFBPs in human adipose tissue cultures. *Growth Hormone & IGF Research* **22**, 200–205 (2012).
86. Jo, J. *et al.* Hypertrophy and/or hyperplasia: dynamics of adipose tissue growth. *PLoS Computational Biology* **5**, e1000324 (2009).
87. Yin, J. *et al.* Role of hypoxia in obesity-induced disorders of glucose and lipid metabolism in adipose tissue. *American Journal of Physiology* **296**, E333–E342 (2009).
88. Catalán, V., Gómez-Ambrosi, J., Rodríguez, A. & Frühbeck, G. Role of extracellular matrix remodelling in adipose tissue pathophysiology: relevance in the development of obesity. *Histology and Histopathology* **27**, 1515–1528 (2012).
89. Sun, K., Kusminski, C. M. & Scherer, P. E. Adipose tissue remodeling and obesity. *Journal of Clinical Investigation* **121**, 2094–2101 (2011).
90. Sam, S. & Mazzone, T. Adipose tissue changes in obesity and the impact on metabolic function. *Translational Research* **164**, 284–292 (2014).
91. Apovian, C. M. *et al.* Adipose macrophage infiltration is associated with insulin resistance and vascular endothelial dysfunction in obese subjects. *Arteriosclerosis, Thrombosis, and Vascular Biology* **28**, 1654–1659 (2008).
92. Hotamisligil, G. S. & Erbay, E. Nutrient sensing and inflammation in metabolic diseases. *Nature Reviews Immunology* **8**, 923–934 (2008).
93. Mraz, M. & Haluzik, M. The role of adipose tissue immune cells in obesity and low-grade inflammation. *Journal of Endocrinology* **222**, R113–R127 (2014).
94. Cildir, G., Akincilar, S. C. & Tergaonkar, V. Chronic adipose tissue inflammation: all immune cells on the stage. *Trends in Molecular Medicine* **19**, 487–500 (2013).
95. Lumeng, C. N., Bodzin, J. L. & Saltiel, A. R. Obesity induces a phenotypic switch in adipose tissue macrophage polarization. *Journal of Clinical Investigation* **117**, 175–184 (2007).
96. Gordon, S. & Taylor, P. R. Monocyte and macrophage heterogeneity. *Nature Reviews Immunology* **5**, 953–964 (2005).
97. Shoelson, S. E., Herrero, L. & Naaz, A. Obesity, inflammation, and insulin resistance. *Gastroenterology* **132**, 2169–2180 (2007).
98. Gregor, M. F. & Hotamisligil, G. S. Thematic review series: adipocyte biology adipocyte stress: the endoplasmic reticulum and metabolic disease. *Journal of Lipid Research* **48**, 1905–1914 (2007).
99. Chang, T.-L. *et al.* The roles of ubiquitin and 26S proteasome in human obesity. *Metabolism: Clinical and Experimental* **58**, 1643–1648 (2009).
100. Cnop, M., Foufelle, F. & Velloso, L. A. Endoplasmic reticulum stress, obesity and diabetes. *Trends in Molecular Medicine* **18**, 59–68 (2012).

101. Olefsky, J. M. Insensitivity of large rat adipocytes to the antilipolytic effects of insulin. *Journal of Lipid Research* **18**, 459–464 (1977).
102. Lelliott, C. & Vidal-Puig, A. J. Lipotoxicity, an imbalance between lipogenesis de novo and fatty acid oxidation. *International Journal of Obesity and Related Metabolic Disorders* **28 Suppl 4**, S22–S28 (2004).
103. Festa, A. *et al.* The relation of body fat mass and distribution to markers of chronic inflammation. *International Journal of Obesity and Related Metabolic Disorders* **25**, 1407–1415 (2001).
104. López Soriano, F. J. & Alemany, M. Amino acid metabolism enzyme activities in rat white adipose tissue. *Archives Internationales de Physiologie et de Biochimie* **94**, 121–125 (1986).
105. Salway, J. G. in *Metabolism at a glance* (ed. Wiley) 84–86 (Blackwell Publishing, 2004).
106. Frayn, K. N. in *Metabolic regulation. A human perspective*. (ed. Frayn, K. N.) 82–129 (Blackwell Publishing, 2003).
107. Jensen, M. D., Haymond, M. W., Gerich, J. E., Cryer, P. E. & Miles, J. M. Lipolysis during fasting. Decreased suppression by insulin and increased stimulation by epinephrine. *Journal of Clinical Investigation* **79**, 207–213 (1987).
108. Jansson, P. A., Smith, U. & Lönnroth, P. Evidence for lactate production by human adipose tissue in vivo. *Diabetologia* **33**, 253–256 (1990).
109. Dimitriadis, G., Mitrou, P., Lambadiari, V., Maratou, E. & Raptis, S. A. Insulin effects in muscle and adipose tissue. *Diabetes Research and Clinical Practice* **93 Suppl 1**, S52–S59 (2011).
110. Frayn, K. N., Arner, P. & Yki-Järvinen, H. Fatty acid metabolism in adipose tissue, muscle and liver in health and disease. *Essays in Biochemistry* **42**, 89–103 (2006).
111. Buchalter, S. E., Crain, M. R. & Kreisberg, R. Regulation of lactate metabolism in vivo. *Diabetes / Metabolism Reviews* **5**, 379–391 (1989).
112. Stanley, W. & Connett, R. Regulation of muscle carbohydrate metabolism during exercise. *FASEB Journal* **5**, 2155–2159 (1991).
113. Newgard, C. B., Hirsch, L. J., Foster, D. W. & McGarry, J. D. Studies on the mechanism by which exogenous glucose is converted into liver glycogen in the rat. A direct or an indirect pathway? *Journal of Biological Chemistry* **258**, 8046–8052 (1983).
114. Thacker, S. V., Nickel, M. & DiGirolamo, M. Effects of food restriction on lactate production from glucose by rat adipocytes. *American Journal of Physiology* **253**, E336–E342 (1987).
115. Alemany, M. The problem of nitrogen disposal in the obese. *Nutrition Research Reviews* **25**, 18–28 (2012).
116. Arola, L., Palou, A., Remesar, X. & Alemany, M. Glutamine synthetase activity in the organs of fed and 24-hours fasted rats. *Hormone and Metabolic Research* **13**, 199–202 (1981).

117. Kowalchuk, J. M., Curi, R. & Newsholme, E. A. Glutamine metabolism in isolated incubated adipocytes of the rat. *Biochemical Journal* **249**, 705–708 (1988).
118. Herman, M. A., She, P., Peroni, O. D., Lynch, C. J. & Kahn, B. B. Adipose tissue branched chain amino acid (BCAA) metabolism modulates circulating BCAA levels. *Journal of Biological Chemistry* **285**, 11348–11356 (2010).
119. Arola, L., Palou, A., Remesar, X. & Alemany, M. Adenylate deaminase activity in the rat. Effect of 24 hours of fasting. *Hormone and Metabolic Research* **13**, 264–266 (1981).
120. Longo, V. D. & Mattson, M. P. Fasting: molecular mechanisms and clinical applications. *Cell Metabolism* **19**, 181–92 (2014).
121. Mallet, L. E., Exton, J. H. & Park, C. R. Control of gluconeogenesis from amino acids in the perfused rat liver. *Journal of Biological Chemistry* **244**, 5713–5723 (1969).
122. Hagström-Toft, E., Enoksson, S., Moberg, E., Bolinder, J. & Arner, P. Absolute concentrations of glycerol and lactate in human skeletal muscle, adipose tissue, and blood. *American Journal of Physiology* **273**, E584–E592 (1997).
123. Rui, L. Energy metabolism in the liver. *Comprehensive Physiology* **4**, 177–197 (2014).
124. Coppack, S. W., Persson, M., Judd, R. L. & Miles, J. M. Glycerol and nonesterified fatty acid metabolism in human muscle and adipose tissue in vivo. *American Journal of Physiology* **276**, E233–E240 (1999).
125. Rennie, M. J., Bohé, J., Smith, K., Wackerhage, H. & Greenhaff, P. Branched-chain amino acids as fuels and anabolic signals in human muscle. *Journal of Nutrition* **136**, S264–S268 (2006).
126. Consoli, A., Nurjhan, N., Reilly, J. J., Bier, D. M. & Gerich, J. E. Contribution of liver and skeletal muscle to alanine and lactate metabolism in humans. *American Journal of Physiology* **259**, E677–E684 (1990).
127. Kim, J. Y., Tillison, K., Lee, J.-H., Rearick, D. A. & Smas, C. M. The adipose tissue triglyceride lipase ATGL/PNPLA2 is downregulated by insulin and TNF-alpha in 3T3-L1 adipocytes and is a target for transactivation by PPAR gamma. *American Journal of Physiology* **291**, E115–E127 (2006).
128. Garber, A. J., Menzel, P. H., Boden, G. & Owen, O. E. Hepatic ketogenesis and gluconeogenesis in humans. *Journal of Clinical Investigation* **54**, 981–989 (1974).
129. Foster, D. W. & McGarry, J. D. The regulation of ketogenesis. *Ciba Foundation Symposium* **87**, 120–131 (1982).
130. Serra, F., Bonet, L. & Palou, A. Amino acid enzyme activities in brown and white adipose tissues and in the liver of cafeteria rats. Effects of 24 hours starving. *Archives Internationales de Physiologie et de Biochimie* **95**, 263–268 (1987).
131. Palou, A., Remesar, X., Arola, L., Herrera, E. & Alemany, M. Metabolic effects of short term food deprivation in the rat. *Hormone and Metabolic Research* **13**, 326–330 (1981).
132. López-Soriano, F. J. *et al.* Amino acid and glucose uptake by rat brown adipose tissue. Effect of cold-exposure and acclimation. *Biochemical Journal* **252**, 843–849 (1988).

133. Baba, H., Zhang, X. J. & Wolfe, R. R. Glycerol gluconeogenesis in fasting humans. *Nutrition* **11**, 149–53 (1995).
134. Goldberg, I. J. et al. Localization of lipoprotein lipase mRNA in selected rat tissues. *Journal of Lipid Research* **30**, 1569–1577 (1989).
135. Viscarra, J. A. & Ortiz, R. M. Cellular mechanisms regulating fuel metabolism in mammals: role of adipose tissue and lipids during prolonged food deprivation. *Metabolism: Clinical and Experimental* **62**, 889–897 (2013).
136. Frühbeck, G., Méndez-Giménez, L., Fernández-Formoso, J.-A., Fernández, S. & Rodríguez, A. Regulation of adipocyte lipolysis. *Nutrition Research Reviews* **27**, 63–93 (2014).
137. Zimmermann, R. et al. Fat mobilization in adipose tissue is promoted by adipose triglyceride lipase. *Science* **306**, 1383–1386 (2004).
138. Fredrikson, G., Tornqvist, H. & Belfrage, P. Hormone-sensitive lipase and monoacylglycerol lipase are both required for complete degradation of adipocyte triacylglycerol. *Biochimica et Biophysica Acta* **876**, 288–293 (1986).
139. Nørrelund, H. et al. The decisive role of free fatty acids for protein conservation during fasting in humans with and without growth hormone. *Journal of Clinical Endocrinology and Metabolism* **88**, 4371–4378 (2003).
140. Lafontan, M. An unsuspected metabolic role for atrial natriuretic peptides: the control of lipolysis, lipid mobilization, and systemic nonesterified fatty Acids levels in humans. *Arteriosclerosis, Thrombosis, and Vascular Biology* **25**, 2032–2042 (2005).
141. Xu, C. et al. Direct effect of glucocorticoids on lipolysis in adipocytes. *Molecular Endocrinology* **23**, 1161–1170 (2009).
142. Ryden, M. et al. Mapping of early signaling events in tumor necrosis factor- α -mediated lipolysis in human fat cells. *Journal of Biological Chemistry* **277**, 1085–1091 (2001).
143. Crandall, D. L., Fried, S. K., Francendese, A. A., Nickel, M. & DiGirolamo, M. Lactate release from isolated rat adipocytes: influence of cell size, glucose concentration, insulin and epinephrine. *Hormone and Metabolic Research* **15**, 326–329 (1983).
144. Doar, J. W. H., Wynn, V. & Cramp, D. G. Blood pyruvate and plasma glucose levels during oral and intravenous glucose tolerance tests in obese and non-obese women. *Metabolism* **17**, 690–701 (1968).
145. Molnár, D., Varga, P., Rubecz, I., Hamar, A. & Mestyán, J. Food-induced thermogenesis in obese children. *European Journal of Pediatrics* **144**, 27–31 (1985).
146. Lovejoy, J., Newby, F. D., Gebhart, S. S. & DiGirolamo, M. Insulin resistance in obesity is associated with elevated basal lactate levels and diminished lactate appearance following intravenous glucose and insulin. *Metabolism: Clinical and Experimental* **41**, 22–27 (1992).
147. Newby, F. D., Sykes, M. N. & DiGirolamo, M. Regional differences in adipocyte lactate production from glucose. *American Journal of Physiology* **255**, E716–E722 (1988).
148. Newby, F. D., Wilson, L. K., Thacker, S. V. & DiGirolamo, M. Adipocyte lactate production remains elevated during refeeding after fasting. *American Journal of Physiology* **259**, E865–E871 (1990).

149. Tischler, M. E., Ost, A. H., Spina, B., Cook, P. H. & Coffman, J. Regulation of protein turnover by glucose, insulin, and amino acids in adipose tissue. *American Journal of Physiology* **247**, C228–C233 (1984).
150. Lackey, D. E. et al. Regulation of adipose branched-chain amino acid catabolism enzyme expression and cross-adipose amino acid flux in human obesity. *American Journal of Physiology* **304**, E1175–E1187 (2013).
151. Badoud, F. et al. Serum and adipose tissue amino acid homeostasis in the metabolically healthy obese. *Journal of Proteome Research* **13**, 3455–3466 (2014).
152. Rous, S., Bas, S. & Sengupta, S. Contribution of leucine in the fatty acid synthesis and ketogenesis in mice adipose tissue. *International Journal of Biochemistry* **11**, 337–340 (1980).
153. Odessey, R. & Goldberg, A. Oxidation of leucine by rat skeletal muscle. *American Journal of Physiology* **223**, 1376–1383 (1972).
154. Tischler, M. E. & Goldberg, a. L. Leucine degradation and release of glutamine and alanine by adipose tissue. *Journal of Biological Chemistry* **255**, 8074–8081 (1980).
155. Odessey, R. in *Problems and potentials of branched chain amino acids in physiology and medicine*. (ed. Odessey, R.) 49–79 (Elsevier, 1986).
156. Goodman, H. & Frick, G. in *Problems and potential of branched chain amino acids in physiology and medicine* (ed. Odessey, R.) 173–198 (Elsevier, 1986).
157. Zierler, K. Whole body glucose metabolism. *American Journal of Physiology* **276**, E409–E426 (1999).
158. Chakrabarti, P. et al. Insulin inhibits lipolysis in adipocytes via the evolutionarily conserved mTORC1-Egr1-ATGL-mediated pathway. *Molecular and Cellular Biology* **33**, 3659–3666 (2013).
159. Rosenthal, J., Angel, A. & Farkas, J. Metabolic fate of leucine: a significant sterol precursor in adipose tissue and muscle. *American Journal of Physiology* **226**, 411–418 (1974).
160. Snell, K. & Duff, D. A. Alanine release by rat adipose tissue in vitro. *Biochemical and Biophysical Research Communications* **77**, 925–931 (1977).
161. Lowenstein, J. M. Ammonia production in muscle and other tissues: the purine nucleotide cycle. *Physiological Reviews* **52**, 382–414 (1972).
162. Kowalski, T. J. & Watford, M. Production of glutamine and utilization of glutamate by rat subcutaneous adipose tissue in vivo. *American Journal of Physiology* **266**, E151–E154 (1994).
163. Demerath, E. W. et al. Anatomical patterning of visceral adipose tissue: race, sex, and age variation. *Obesity* **15**, 2984–2993 (2007).
164. Ameer, F., Scanduzzi, L., Hasnain, S., Kalbacher, H. & Zaidi, N. De novo lipogenesis in health and disease. *Metabolism: Clinical and Experimental* **63**, 895–902 (2014).

165. Diraison, F. *et al.* Differences in the regulation of adipose tissue and liver lipogenesis by carbohydrates in humans. *Journal of Lipid Research* **44**, 846–853 (2003).
166. Sjöström, L. Fatty acid synthesis de novo in adipose tissue from obese subjects on a hypercaloric high-carbohydrate diet. *Scandinavian Journal of Clinical and Laboratory Investigation* **32**, 339–349 (1973).
167. Strawford, A. Adipose tissue triglyceride turnover, de novo lipogenesis, and cell proliferation in humans measured with $^{2}\text{H}_2\text{O}$. *American Journal of Physiology* **286**, E577–E588 (2004).
168. Coleman, R. Enzymes of triacylglycerol synthesis and their regulation. *Progress in Lipid Research* **43**, 134–176 (2004).
169. Nakajima, K. *et al.* Postprandial lipoprotein metabolism: VLDL vs chylomicrons. *Clinica Chimica Acta* **412**, 1306–1318 (2011).
170. Gibbons, G. F. Assembly and secretion of hepatic very-low-density lipoprotein. *Biochemical Journal* **268**, 1–13 (1990).
171. Kersten, S. Physiological regulation of lipoprotein lipase. *Biochimica et Biophysica Acta* **1841**, 919–933 (2014).
172. Stahl, A. A current review of fatty acid transport proteins (SLC27). *European Journal of Physiology* **447**, 722–727 (2004).
173. Greenberg, A. S. *et al.* Perilipin, a major hormonally regulated adipocyte-specific phosphoprotein associated with the periphery of lipid storage droplets. *Journal of Biological Chemistry* **266**, 11341–11346 (1991).
174. Brasaemle, D. L. *et al.* Adipose differentiation-related protein is an ubiquitously expressed lipid storage droplet-associated protein. *Journal of Lipid Research* **38**, 2249–2263 (1997).
175. Nye, C., Kim, J., Kalhan, S. C. & Hanson, R. W. Reassessing triglyceride synthesis in adipose tissue. *Trends in Endocrinology and Metabolism* **19**, 356–361 (2008).
176. Memon, R. A. *et al.* Regulation of putative fatty acid transporters and Acyl-CoA synthetase in liver and adipose tissue in ob/ob mice. *Diabetes* **48**, 121–127 (1999).
177. Aarsland, A., Chinkes, D. & Wolfe, R. Hepatic and whole-body fat synthesis in humans during carbohydrate overfeeding. *American Journal of Clinical Nutrition* **65**, 1774–1782 (1997).
178. Assimacopoulos-Jeannet, F., Brichard, S., Rencurel, F., Cusin, I. & Jeanrenaud, B. In vivo effects of hyperinsulinemia on lipogenic enzymes and glucose transporter expression in rat liver and adipose tissues. *Metabolism* **44**, 228–233 (1995).
179. Gondret, F., Ferré, P. & Dugail, I. ADD-1/SREBP-1 is a major determinant of tissue differential lipogenic capacity in mammalian and avian species. *Journal of Lipid Research* **42**, 106–113 (2001).
180. Flatt, J. P. & Ball, E. G. Studies on the metabolism of adipose tissue. XV. An evaluation of the major pathways of glucose catabolism as influenced by insulin and epinephrine. *Journal of Biological Chemistry* **239**, 675–685 (1964).

181. DiGirolamo, M., Howe, M. D., Esposito, J., Thurman, L. & Owens, J. L. Metabolic patterns and insulin responsiveness of enlarging fat cells. *Journal of Lipid Research* **15**, 332–338 (1974).
182. Hagstrom, E., Arner, P., Ungerstedt, U. & Bolinder, J. Subcutaneous adipose tissue: a source of lactate production after glucose ingestion in humans. *American Journal of Physiology* **258**, E888–E893 (1990).
183. van der Merwe, M. T. *et al.* Lactate and glycerol release from the subcutaneous adipose tissue of obese urban women from South Africa; important metabolic implications. *Journal of Clinical Endocrinology and Metabolism* **83**, 4084–4091 (1998).
184. Lovejoy, J., Mellen, B. & Digirolamo, M. Lactate generation following glucose ingestion: relation to obesity, carbohydrate tolerance and insulin sensitivity. *International Journal of Obesity* **14**, 843–855 (1990).
185. Bernstein, R. S., Zimmerman, K. S. & Carney, A. L. Absence of impaired glucose utilization in adipocytes from rats fed a carbohydrate-free, high protein diet. *Journal of Nutrition* **111**, 237–243 (1981).
186. Frick, G. P. & Goodman, H. M. Insulin regulation of branched chain alpha-keto acid dehydrogenase in adipose tissue. *Journal of Biological Chemistry* **255**, 6186–6192 (1980).
187. Chang, T. W. & Goldberg, A. L. Leucine inhibits oxidation of glucose and pyruvate in skeletal muscles during fasting. *Journal of Biological Chemistry* **253**, 3696–3701 (1978).
188. Evans, M. A. & Shrouts, E. P. Intestinal fuels: glutamine, short-chain fatty acids, and dietary fiber. *Journal of the American Dietetic Association* **92**, 1239–1246 (1992).
189. Muñoz, S. *et al.* Chronically increased glucose uptake by adipose tissue leads to lactate production and improved insulin sensitivity rather than obesity in the mouse. *Diabetologia* **53**, 2417–2430 (2010).
190. Warburg, O. On the origin of cancer cells. *Science* **123**, 309–314 (1956).
191. Vander Heiden, M. G., Cantley, L. C. & Thompson, C. B. Understanding the Warburg effect: the metabolic requirements of cell proliferation. *Science* **324**, 1029–1033 (2009).
192. Radziuk, J. & Pye, S. Hepatic glucose uptake, gluconeogenesis and the regulation of glycogen synthesis. *Diabetes/Metabolism Research and Reviews* **17**, 250–272 (2001).
193. Rognstad, R. Control of lactate gluconeogenesis by glucose in rat hepatocytes. *Archives of Biochemistry and Biophysics* **217**, 498–502 (1982).
194. Edson, N. L. Ketogenesis-antiketogenesis: substrate competition in liver. *Biochemical Journal* **30**, 1862–1869 (1936).
195. Clark, D. G., Rognstad, R. & Katz, J. Lipogenesis in rat hepatocytes. *Journal of Biological Chemistry* **249**, 2028–2036 (1974).
196. De Souza, C. T. *et al.* Consumption of a fat-rich diet activates a proinflammatory response and induces insulin resistance in the hypothalamus. *Endocrinology* **146**, 4192–4199 (2005).

197. Trayhurn, P. & Wood, I. S. Adipokines: inflammation and the pleiotropic role of white adipose tissue. *British Journal of Nutrition* **92**, 347–355 (2004).
198. Rafecas, I., Esteve, M., Fernández-López, J. A., Remesar, X. & Alemany, M. Deposition of dietary fatty acids in young Zucker rats fed a cafeteria diet. *International Journal of Obesity* **16**, 775–787 (1992).
199. Alemany, M. Regulation of adipose tissue energy availability through blood flow control in the metabolic syndrome. *Free Radical Biology & Medicine* **52**, 2108–2119 (2012).
200. Alemany, M. Adipose tissue hypoxia, a conceptual allometric view. *Journal of Endocrinology and Metabolism* **1**, 155–158 (2011).
201. Priego, T., Sánchez, J., Picó, C. & Palou, A. Sex-differential expression of metabolism-related genes in response to a high-fat diet. *Obesity* **16**, 819–826 (2008).
202. Barber, T., Viña, J. R., Viña, J. & Cabo, J. Decreased urea synthesis in cafeteria-diet-induced obesity in the rat. *Biochemical Journal* **230**, 675–681 (1985).
203. Meijer, A. J., Lof, C., Ramos, I. C. & Verhoeven, A. J. Control of ureogenesis. *European Journal of Biochemistry* **148**, 189–196 (1985).
204. Hao, G., Xie, L. & Gross, S. S. Argininosuccinate synthetase is reversibly inactivated by S-nitrosylation in vitro and in vivo. *Journal of Biological Chemistry* **279**, 36192–36200 (2004).
205. Saheki, T., Ohkubo, T. & Katsunuma, T. Regulation of Urea Synthesis in Rat Liver: Increase in the Concentrations of Ornithine and Acetylglutamate in Rat Liver in Response to Urea Synthesis Stimulated by the Injection of an Ammonium Salt. *Journal of Biochemistry* **84**, 1423–1430 (1978).
206. Peinado, J. R. et al. The stromal-vascular fraction of adipose tissue contributes to major differences between subcutaneous and visceral fat depots. *Proteomics* **10**, 3356–3366 (2010).
207. Cinti, S. The adipose organ. *Prostaglandins, Leukotrienes, and Essential Fatty Acids* **73**, 9–15 (2005).
208. Breuillard, C., Cynober, L. & Moinard, C. Citrulline and nitrogen homeostasis: an overview. *Amino Acids* **47**, 685–91 (2015).
209. van de Poll, M. C. G. et al. Intestinal and hepatic metabolism of glutamine and citrulline in humans. *Journal of Physiology* **581**, 819–827 (2007).
210. Schwedhelm, E. et al. Pharmacokinetic and pharmacodynamic properties of oral L-citrulline and L-arginine: impact on nitric oxide metabolism. *British Journal of Clinical Pharmacology* **65**, 51–59 (2008).
211. Curis, E., Crenn, P. & Cynober, L. Citrulline and the gut. *Current Opinion in Clinical Nutrition and Metabolic Care* **10**, 620–626 (2007).
212. Windmueller, H. G. & Spaeth, A. E. Source and fate of circulating citrulline. *American Journal of Physiology* **241**, E473–E480 (1981).

213. Salans, L. B. & Dougherty, J. W. The effect of insulin upon glucose metabolism by adipose cells of different size. Influence of cell lipid and protein content, age, and nutritional state. *Journal of Clinical Investigation* **50**, 1399–1410 (1971).
214. Driskell, R. R., Jahoda, C. A. B., Chuong, C.-M., Watt, F. M. & Horsley, V. Defining dermal adipose tissue. *Experimental Dermatology* **23**, 629–631 (2014).
215. Nakatsuji, T. *et al.* The microbiome extends to subepidermal compartments of normal skin. *Nature Communications* **4**, 1431 (2013).
216. Wasada, T. *et al.* Hepatic steatosis rather than visceral adiposity is more closely associated with insulin resistance in the early stage of obesity. *Metabolism: Clinical and Experimental* **57**, 980–985 (2008).
217. Ndumele, C. E. *et al.* Hepatic steatosis, obesity, and the metabolic syndrome are independently and additively associated with increased systemic inflammation. *Arteriosclerosis, Thrombosis, and Vascular Biology* **31**, 1927–1932 (2011).